

EXPERIMENTAL AND EPIDEMIOLOGICAL APPROACHES TO *CAMPYLOBACTER*  
*JEJUNI*-ASSOCIATED GUILLAIN BARRÉ SYNDROME

By

Jessica L. St. Charles

A DISSERTATION

Submitted to  
Michigan State University  
in partial fulfillment of the requirements  
for the degree of

Comparative Medicine and Integrative Biology – Doctor of Philosophy

2013

## ABSTRACT

### EXPERIMENTAL AND EPIDEMIOLOGICAL APPROACHES TO *CAMPYLOBACTER JEJUNI*-ASSOCIATED GUILLAIN BARRÉ SYNDROME

By

Jessica L. St. Charles

Guillain Barré Syndrome (GBS), an immune-mediated acute polyneuropathy of the peripheral nerves, is the leading cause of acute autoimmune neuromuscular paralysis in the Western world. Approximately two-thirds of patients report a prior respiratory or gastrointestinal infection; *Campylobacter jejuni* is the most commonly reported antecedent infection. *C. jejuni* is the leading cause of foodborne bacterial gastrointestinal infection; transmission is by ingestion of contaminated water, milk, and poultry. The proposed mechanism of GBS is similarity of the lipo-oligosaccharide (LOS) on the outer surface of some *C. jejuni* strains to gangliosides, glycolipid structures found in the nervous system. This molecular mimicry results in an immune response directed at both the LOS and gangliosides. Current data surrounding molecular mimicry are conflicting, therefore suggesting that other surface structures of *C. jejuni* are involved in GBS pathogenesis. Epidemiological studies on isolates collected from patients that presented with either enteritis or neuropathy to define potential genetic relationships of GBS to the highly variable *C. jejuni* flagellar and major outer membrane proteins have given inconclusive and contradictory results. Therefore additional work is needed to improve molecular typing of *C. jejuni* isolates.

The work reported here took two complementary directions: development of a murine model of GBS using *C. jejuni* strains of an LOS type known to be associated with GBS in humans and an epidemiological study of *C. jejuni* isolates from the U.S. with a focus in Michigan, in which the LOS biosynthetic locus, the flagellar protein, and the major outer membrane protein were all characterized in addition to standard multilocus sequence typing.

To understand the role of the genetic factors of *C. jejuni* and potential host factors in the pathogenesis of GBS more *in vivo* studies are needed. However, current animal models to study GBS employ immunization of rabbits with purified LOS or mice with bovine myelin to initiate an immune response similar to that in GBS patients. These are not natural models of GBS following *C. jejuni* infection. In a more natural model in chickens, birds given GBS-associated strains of *C. jejuni* develop both clinical signs and immunological responses similar to those seen in GBS patients. However, chickens are anatomically and physiologically different from humans. The goal of the first half of my studies was development of a murine model secondary to *C. jejuni* infection; we found a strain of mouse that has the potential to be such a model, but more work must be done.

The goal of the second half of my studies was to examine possible epidemiological relationships between other variable surface components of *C. jejuni* and LOS types associated with GBS. In epidemiological studies using molecular typing of both variable and conserved genes, we found that both human *C. jejuni* isolates from a limited collection from the U.S. with focus in Michigan and from calves on a Michigan dairy farm that had a *C. jejuni* outbreak had LOS biosynthetic loci characteristic of GBS-associated strains.

Copyright by  
JESSICA LYNN ST. CHARLES  
2013

Dedicated in Loving Memory to Neil T. St. Charles

## ACKNOWLEDGMENTS

First and foremost I would like to thank my family and loved ones for their love and endless support throughout my time here at MSU. A very special thanks to my better half, Ben Dunn, for the love, unconditional support, and encouragement he has provided me continuously day and night as I worked to complete my degree.

I'd like to thank my wonderful advisor, Dr. Linda S. Mansfield, for her support, knowledge, and guidance throughout my studies. She was my advisor as an undergraduate and is the reason I considered graduate school in the first place, so without her I wouldn't be here today and for that I am grateful. I would also like to sincerely thank my committee members Dr. Bill Atchison, Dr. Katheryn Meek, Dr. John Linz, and Dr. Jon Patterson for their guidance and support.

In addition, I thank Dr. Julia Bell for her support and guidance; she taught me all the basic laboratory skills a scientist needs to succeed when I was an undergraduate in the lab. I would also like to thank Dr. Shannon Manning for the knowledge and support she shared with me.

Many thanks to the members of the Comparative Enteric Disease Laboratory who created a wonderful laboratory environment to work in. I had the pleasure to work with Andy Flies, JP Jerome, Ankit Malik, Barbie Gadsden, and Phillip Brooks who I will miss and wish them the best of luck with their studies. I have also had the pleasure to work with past members of the lab that include Alice Murphy, Vijay Rathinam, Eric Smith, Melisa Bailey, Anthony Brooks, Allison Zaleski, Laura Krzykowski, Jenna

Gettings, Jamie Kopper, and Amanda Stanton. I also thank Rebekah Mosci, Samantha Wengert, and Amber “Cody” Springman from Dr. Manning’s lab.

Thank you to Dr. Vilma Yuzbasiyan-Gurkan, Victoria Hoelzer-Maddox, and the Comparative Medicine and Integrative Biology program for support and encouragement throughout my studies. And thank you to the Microbiology Research Unit (MRU) and Enteric Research Investigative Network (ERIN) both funded by the National Institute of Health for the financial support of my research.

I would also like to thank the great people at the MSU University Research Containment Facility that helped with maintenance of my mice. I want to thank the great people at the MSU Investigative Histopathology Laboratory and the MSU Genomic Research Technology Facility for their help and knowledge in the analysis of data.

## TABLE OF CONTENTS

LIST OF TABLES.....	xiii
LIST OF FIGURES.....	xiv
CHAPTER 1: Introduction .....	1
Guillain Barré Syndrome .....	2
Subtypes of GBS .....	7
Acute Inflammatory Demyelinating Polyneuropathy .....	7
Acute Motor Axonal Neuropathy (and Acute Sensory Motor Axonal Neuropathy).....	8
Miller Fisher Syndrome.....	9
<i>Campylobacter jejuni</i> .....	11
Lipo-oligosaccharides (LOS) .....	12
Molecular Typing of <i>C. jejuni</i> .....	15
Animal Models .....	19
Rationale .....	23
CHAPTER 2: Non-Obese Diabetic (NOD) mice as working models of Guillain Barré Syndrome following <i>Campylobacter jejuni</i> infection.....	25
Abstract .....	26
Introduction.....	28
Materials and Methods .....	34
Animals.....	34
<i>Campylobacter jejuni</i> .....	35
Experimental Design.....	35
Experiment 1: Screening mice of various NOD genotypes for GBS following <i>C. jejuni</i> infection.....	36
Experiment 2: Screening larger group sizes of NOD WT and NOD B7-2 <sup>-/-</sup> mice for GBS.....	36
Experiment 3: Examination of NOD IL-10 <sup>-/-</sup> mice using antibiotics to treat enteritis .....	37
Neurological Phenotype Testing.....	37
Open field testing.....	38
Hang testing .....	38
Rotarod testing .....	39
Footprinting.....	39
DigiGait™ testing.....	39
Enzyme-Linked Immunosorbent Assays (ELISAs) .....	41

Assessment of Clinical Signs.....	42
Necropsy Methods and Assessment of Gross Pathology.....	42
Culture for Presence of <i>C. jejuni</i> , DNA Extraction and PCR Assays ..	43
Histopathological Scoring of the Gastrointestinal Tract .....	43
Histopathological Scoring of the Sciatic Nerve .....	43
Nerve Histology Criteria.....	45
Immunohistochemical Staining (IHC) .....	46
Statistical Analyses.....	47
Results .....	49
Selection of Mice for Analysis.....	49
Experiment 1: Screening mice of various NOD genotypes for GBS following <i>C. jejuni</i> infection .....	50
Experimental screen for GI disease with GBS-associated <i>C. jejuni</i> strains .....	50
Detection of anti-ganglioside antibodies .....	51
Neurological phenotype testing .....	53
NOD WT mice.....	54
NOD IL-10 <sup>-/-</sup> mice .....	55
NOD B7-2 <sup>-/-</sup> mice.....	56
Experiment 2: Screening larger groups sizes of NOD WT and NOD B7-2 <sup>-/-</sup> mice for GBS.....	57
Experimental screen for GI disease with GBS-associated <i>C. jejuni</i> strains .....	57
Detection of anti-ganglioside antibodies .....	58
Neurological phenotype testing .....	59
NOD WT mice.....	60
NOD B7-2 <sup>-/-</sup> mice.....	61
Presence of nerve lesions and detection of cellular infiltrates ..	62
Experiment 3: Examination of NOD IL-10 <sup>-/-</sup> mice using antibiotics to treat enteritis.....	64
Experimental screen for GI disease with GBS-associated <i>C. jejuni</i> 260.94.....	64
Detection of anti-ganglioside antibodies .....	65
Neurological phenotype testing .....	67
Rotarod .....	68
DigiGait™ .....	68
Stride Length and Hind Base Width.....	68
Clinical Analysis .....	69
Presence of nerve lesions and detection of cellular infiltrates ..	70
Detection of macrophages in nerves .....	70
Discussion .....	72
Comparison of NOD mouse genotypes .....	73
Difficulties encountered and their resolutions .....	76
Future work.....	77

Acknowledgements .....	79
Tables.....	80
Figures .....	83
CHAPTER 3: Examination of Miller Fisher Syndrome in NOD WT and C57BL/6 WT mice subsequent to <i>Campylobacter jejuni</i> CF93-6 infection .....	103
Abstract .....	104
Introduction.....	106
Materials and Methods .....	110
Animals.....	110
<i>Campylobacter jejuni</i> .....	111
Experimental Design.....	111
Neurological Testing.....	112
Open field testing.....	112
Rotarod testing .....	113
Footprinting and tracking .....	113
Enzyme-Linked Immunosorbent Assays (ELISAs) .....	114
Assessment of Clinical Signs.....	115
Necropsy Procedure and Assessment of Gross Pathological Features .....	115
Assessment of Enteric Disease .....	116
Histopathological Scoring for the GI Tract and Sciatic Nerve .....	117
Gastrointestinal tract.....	117
Sciatic nerve .....	117
Statistical Methods .....	118
Results .....	119
Screening for Enteric Disease with GBS-associated and MFS-associated <i>C. jejuni</i> Strains.....	119
Detection of Anti-Ganglioside Antibodies with ELISA Assays.....	120
Neurological Testing.....	121
Rotarod.....	122
Open Field Test.....	122
Footprint Measurements.....	123
Presence of Nerve Lesions.....	124
Discussion .....	126
Table .....	129
Figures .....	130
CHAPTER 4: Multiple molecular typing schemes applied to define genetic relationships among <i>C. jejuni</i> isolates that share the same LOS classification .....	139
Abstract .....	140
Introduction.....	142
Materials and Methods .....	147
<i>Campylobacter jejuni</i> Strains and Growth Conditions.....	147
Preparation of Genomic DNA .....	148

Determination of <i>Campylobacter</i> spp. ....	149
Classification of LOS Classes by PCR .....	149
DNA Sequencing and Allele Assignment.....	150
Multi-locus sequence typing (MLST).....	150
<i>flaA</i> SVR.....	150
<i>porA</i> .....	150
Sequence Analysis .....	151
Statistical Analysis.....	152
Results .....	153
LOS Classification .....	153
MLST Analysis.....	154
<i>porA</i> Typing .....	155
<i>flaA</i> SVR Sequence Types .....	156
Comparison of Isolates with All Molecular Typing Methods.....	156
Discussion .....	158
Table .....	163
Figures .....	168

CHAPTER 5: *Campylobacter jejuni* isolates from calves have A, B, and C lipooligosaccharide (LOS) biosynthetic locus classes similar to human Guillain Barré Syndrome associated strains .....

.....	173
Abstract .....	174
Introduction.....	176
Materials and Methods .....	179
Case Study.....	179
<i>Campylobacter jejuni</i> Isolation.....	179
Preparation of Genomic DNA and Confirmation of <i>Campylobacter</i> spp.....	180
Classification of LOS Biosynthesis Loci.....	181
Multi-locus Sequence Typing (MLST).....	181
<i>porA</i> Allele Typing and <i>flaA</i> SVR Sequence Typing .....	182
Sequence Analysis .....	183
Statistical Analysis .....	183
Results .....	185
Verification of <i>C. jejuni</i> .....	185
LOS Classification .....	185
MLST Analysis.....	185
<i>porA</i> Allele Typing and <i>flaA</i> SVR Sequence Typing .....	186
Composite Profiles .....	188
Discussion .....	189
Zoonotic Transmission Between the Calves and Family Members ....	189
Examination of Genetic Relationships Among Calf Isolates with LOS Locus Classes A–C .....	190
Table .....	192
Figures .....	193

CHAPTER 6: Conclusions.....	196
Summary.....	197
Chapter 2 Summary: Non-Obese Diabetic (NOD) mice as working models of Guillain Barre Syndrome following <i>Campylobacter jejuni</i> infection.....	200
Chapter 3 Summary: Examination of Miller Fisher Syndrome in NOD WT and C57BL/6 WT mice subsequent to <i>Campylobacter jejuni</i> CF93-6 infection.....	204
Chapter 4 Summary: Multiple molecular typing schemes applied to define genetic relationships among <i>C. jejuni</i> isolates that share the same LOS classification.....	205
Chapter 5 Summary: <i>Campylobacter jejuni</i> isolates from calves have A, B, and C lipo-oligosaccharide (LOS) biosynthetic locus classes similar to human Guillain Barre Syndrome associated strains.....	207
Future Directions.....	210
Defining the NOD WT mouse as a natural model of GBS.....	210
Potential for the NOD IL-10 <sup>-/-</sup> mouse as a natural model of GBS.....	211
Examination of other factors contributing to the pathogenesis of GBS.....	213
 APPENDICES.....	 216
Appendix A: Chapter 2 Experiment 1.....	217
Appendix B: Chapter 2 Experiment 2.....	230
Appendix C: Chapter 2 Experiment 3.....	243
Appendix D: Chapter 2 Rotarod Controls.....	250
 REFERENCES.....	 252

## LIST OF TABLES

<b>Table 2.1:</b> Clinical Assessment for DigiGait™ videos.....	80
<b>Table 2.2:</b> Statistical results for change within treatment groups over the course of the experimental time. ....	81
<b>Table 2.3:</b> P values for ELISA assays for ELISA assays for all 3 experiments.....	82
<b>Table 3.1:</b> P values for ELISA assays.....	129
<b>Table 4.1:</b> Summary of <i>C. jejuni</i> Isolates and their assigned allele types .....	163
<b>Table 5.1:</b> Summary of Molecular Typing .....	192

## LIST OF FIGURES

<b>Figure 2.1:</b> Experiment 1 Data Summary .....	83
<b>Figure 2.2:</b> Experiment 2 Data Overview.....	86
<b>Figure 2.3:</b> Examination of Peripheral Nerves.....	91
<b>Figure 2.4:</b> Immunohistochemical Data for Experiment 2.....	92
<b>Figure 2.5:</b> Macrophage infiltration of NOD WT mice.....	93
<b>Figure 2.6:</b> Experiment 3 Data Summary .....	95
<b>Figure 2.7:</b> Heat Map of Clinical Neurological Assessment.....	99
<b>Figure 2.8:</b> Infiltration of macrophages in the nerve root .....	101
<b>Figure 3.1:</b> Examination of GI disease .....	130
<b>Figure 3.2:</b> ELISA data.....	132
<b>Figure 3.3:</b> Assessment of Clinical Neurological Signs with Phenotype Tests .....	134
<b>Figure 4.1:</b> Dendrogram of the LOS biosynthetic loci .....	168
<b>Figure 4.2:</b> Comparison of LOS classes to MLST Clonal Complexes .....	170
<b>Figure 4.3:</b> Phylogenic tree of the <i>porA</i> based on DNA sequences .....	171
<b>Figure 5.1:</b> SplitsTree diagram based on MLST alleles.....	193

<b>Figure 5.2:</b> Dendograms of <i>porA</i> and <i>flaA</i> SVR DNA sequences .....	194
<b>Figure 5.3:</b> SplitsTree analysis of combined allelic profiles of 7 MLST loci, <i>porA</i> alleles, and <i>flaA</i> SVR sequence types .....	195
<b>Figure A-1:</b> Examination of enteric disease from <i>C. jejuni</i> infection in Experiment 1. ....	218
<b>Figure A-2:</b> Experiment 1 ELISA assay data .....	219
<b>Figure A-3:</b> Phenotypic data for Experiment 1 .....	225
<b>Figure B-1:</b> Examination of enteric disease caused by <i>C. jejuni</i> infection in Experiment 2. ....	231
<b>Figure B-2:</b> ELISA assay data for days 0 and 14 P.I. ....	232
<b>Figure B-3:</b> Experiment 2 Phenotype Data .....	238
<b>Figure B-4:</b> Presence of nerve lesions in Experiment 2 .....	242
<b>Figure C-1:</b> Evidence of enteric disease in Experiment 3 .....	244
<b>Figure C-2:</b> ELISA assay data for Experiment 3 .....	246
<b>Figure D-1:</b> Rotarod Control Experiment with C57/BL6 mice .....	251

# CHAPTER 1

## Introduction

## **GUILLAIN BARRÉ SYNDROME**

Guillain Barré Syndrome (GBS) was first described in 1916 during World War I, when G. Guillain, J. A. Barré, and A. Strohl examined two soldiers who had symptoms of a rapid and progressive motor neuropathy that involved loss of reflexes and spontaneously recovered (7, 153). In these patients they also described an elevated protein level in the cerebrospinal fluid (CSF) without an increase in white blood cells (9, 82, 153). Today, the disease is clinically characterized as progressive weakness with a symmetrical ascending flaccid paralysis, areflexia, and increased CSF protein level (9, 67, 129).

The annual incidence rate of GBS worldwide is approximately 0.6–4.0 per 100,000 population (7, 55, 63, 72, 116, 141, 157). In Europe, incidence rates are 1.2–1.9 annually per 100,000 persons (116). In Western countries, the annual incidence rate ranges from 0.89–1.89 cases per 100,000 persons (163). With the near eradication of polio, GBS is the leading cause of acute flaccid paralysis in the Western world (7, 63, 67, 140, 150, 157, 160, 162, 165). Incidence rates are lower in children than adults and are highest in the elderly (72). The occurrence of GBS can increase with age, a rate of 1.0 per 100,000 persons below the age of 30 increases to 4.0 cases per 100,000 persons in people older than 75 years of age (116). Men are more commonly affected than women with a rate of 1.25–1.5 men to 1.0 women, which is an unusual occurrence in autoimmune diseases (72, 116, 148, 157).

GBS is typically a monophasic disease with symptoms most severe at weeks 2–4 and then plateauing. However, 7% of GBS patients have had 2 or more occurrences (7,

72, 163). Symptomatic patients present with overall weakness that frequently involves muscles served by the motor, sensory, and autonomic nerves associated with the limbs and may involve the respiratory muscles and muscles served by facial and ocular motor nerves as well (7, 72, 116). Patients report the first onset of symptoms to include numbness, tingling sensation, weakness, and pain in the limbs (116, 163). The average stay in the hospital is 7 days; nearly 25% of patients require mechanical ventilation (72, 148, 163). Ten to twenty percent of patients have lifelong severe disability and mortality rates range from 3–10% (7, 72, 148, 163).

Two-thirds of GBS patients report a preceding infection prior to developing GBS (17, 63, 147, 148, 160, 162, 163). Prior infections include *Campylobacter jejuni*, *Mycoplasma pneumonia*, *Haemophilus influenza*, cytomegalovirus, and Epstein-Barr virus (EBV) (7, 163). *C. jejuni* is the most common antecedent infection in GBS patients (63, 140, 160, 162, 163). It is estimated that 0.25–0.65 per 1000 cases of *C. jejuni* infections go on to develop GBS (163). A study by Kuroki *et al.* (1993) determined that 41% of GBS patients were infected with *C. jejuni* prior to development of GBS (92). Another study, which was performed in England between April, 2000, and March, 2001, was performed to identify the number of GBS cases reported that were associated with *C. jejuni* infection. The results indicated that 15% of all GBS cases in England during this time period were the result of *C. jejuni* infection (140). A separate and larger study of 229 GBS patients showed that 23% (53/229) of GBS patients had a prior *C. jejuni* infection (58). Eight percent and 2% of patients had cytomegalovirus and EBV respectively (58).

Other less common causes of GBS include surgery, head injury, and vaccinations (26, 148). One study demonstrated that a patient presented with clinical features of GBS one week after a serious head injury. Pathological studies showed peripheral nerve demyelination, confirming that the patient had GBS (142). Other reports of GBS following head injury have been cited in the medical literature; patients commonly present with increased levels of antibodies reactive to myelin proteins (37, 95, 142). GBS has also been shown to develop after administration of vaccines (147). A meta-analysis was performed for the 2009 H1N1 flu vaccination and association of developing GBS. There was a 1.6 per 1 million rate of vaccinated individuals developing GBS (129).

The mechanism of GBS is thought to be molecular mimicry between antibodies that are produced during a preceding infection and neural epitopes (7, 63, 148). Specifically, it is thought that the lipo-oligosaccharides (LOS) on the surface of *C. jejuni* cross react with gangliosides localized in the nervous tissue (7, 77). The terminal glycan portion of the *C. jejuni* LOS is highly variable and is thought to be the region of the bacterium that mimics gangliosides (63). Gangliosides are sialylated glycosphingolipids highly enriched in the nervous tissue (7, 15, 16, 84, 162). They are made up of a ceramide tail inserted into the phospholipid bilayer and a highly variable sialylated oligosaccharide tail that is exposed extracellularly (7, 84, 160). Over 100 different gangliosides have been identified to date; they play many roles in cell growth and differentiation and maintenance of stability of paranodal junctions (7, 160).

Association of anti-ganglioside antibodies with GBS was first reported in 1988 by Ilyas *et al.* in 5/26 patients who presented with anti-ganglioside antibodies (74). Anti-

ganglioside antibodies are highly associated with GBS in patients; approximately 60% of patients present with anti-ganglioside antibodies during the acute phase of the disease (84, 157, 168). Antibodies reactive to gangliosides GM1 and GD1a have been shown to disrupt the axons, lipid raft, and ion channels along the peripheral nerves (160). It has also been shown in multiple *in vivo* studies that anti-GQ1b antibody binds to the neuromuscular junction in patients resulting in complement activation (117, 151, 152). One study examined the association of the complement system and its role in damage to the nerves by exposing neuromuscular junctions (NMJ) of the diaphragm to anti-disialoside antibody, antibody that binds to portions of gangliosides GQ1b and GT1a. The study saw deposits of antibody on the NMJ that resulted in injury that was observed histologically (62). They also observed a correlation with nerve damage and the presence of the membrane attack complex of the complement system, but showed no nerve damage occurred in mice that lacked the complement system therefore reinforcing its role in nerve damage (62).

A set of criteria has been established to verify that molecular mimicry is the mechanism producing an autoimmune disease (7). Thus, the criteria for molecular mimicry in GBS include: 1) establishment of an epidemiological association between the immune-mediated disease and an infectious agent, 2) identification of T cells or antibodies directed against host tissue, 3) identification of a component of the infectious agent mimicking the target antigen, and 4) reproduction of the disease in an animal model (7, 160). It has been shown by Ang *et al.* (2004) that GBS fulfills these criteria and therefore occurs as a result of molecular mimicry (160).

Patients can spontaneously recover from GBS or may need treatment; treatment options include plasma exchange (PE), intravenous immune globulin (IVIG), and complement inhibitors (7, 72). PE was first used as a treatment in 1978 on a GBS patient and was successful in alleviating the symptoms. In 1985 PE became the primary treatment method for GBS (134). The success of PE is thought to be a result of removing anti-ganglioside antibodies that attack the nerves from the plasma of patients (116, 134). IVIG has also been successful in the treatment of GBS patients. It is thought that IVIG neutralizes the IgG autoantibodies that are produced during the disease (116, 134). Complement inhibitors have also been examined as a possible treatment. It has been demonstrated that the membrane attack complex (MAC) formed during complement cascade activation plays a role in the damage seen in nerve tissue (116). Markers for the MAC have been identified in the sera of GBS patients and have been found in the affected neurons with its associated Schwann cells (116). Inhibitors of components of the complement cascade may become a treatment option in the future. Steroids have also been examined as a treatment option but were found to be unsuccessful (116).

## SUBTYPES OF GBS

### **Acute Inflammatory Demyelinating Polyneuropathy**

Acute inflammatory demyelinating polyneuropathy (AIDP) is the most common subtype of GBS in the Western world; Europe and North America have 69–90% of AIDP cases (17, 72, 134, 147, 157, 163). AIDP patients present clinically with flaccid paralysis and areflexia that progress for 2–4 weeks with mild sensory changes (134, 147, 148, 157). Patients with AIDP more commonly have autonomic nerves affected, experience facial weakness (71% of patients), and need mechanical ventilation (134, 147, 148). Anti-ganglioside antibodies are not commonly associated with AIDP, but antibodies to ganglioside GD2 have been linked with this syndrome (116, 153). The pathogenesis of this subtype includes inflammatory infiltrates in nervous tissue, primarily macrophages and T cells associated with peripheral nerve demyelination. In AIDP, axons are generally not affected (17, 116, 147, 150, 163). Complement activation has also been shown to play a role (116, 163). Histopathological studies using human specimens have shown that complement activation in the Schwann cell membrane is important in the development of GBS (60). Three patients that suffered from this subtype of GBS were autopsied, nerves removed, and immunohistochemistry was performed. It was observed in all autopsies that markers for the complement cascade were localized along the outer surface of the Schwann cells, therefore suggesting complement is activated by antibody bound to the nerve and results in damage to the myelin (60). Nerve conduction studies showed that demyelination occurs but re-myelination can occur as well as the disease

wanes. Furthermore, Schwann cells have been observed to migrate to the site of the lesions to initiate re-myelination of neurons (134, 150).

### **Acute Motor Axonal Neuropathy (and Acute Motor Sensory Axonal Neuropathy)**

Acute motor axonal neuropathy (AMAN) is a subtype of GBS prevalent in China, Japan, South and Central America, and India; 38–65% of GBS cases in these regions are AMAN and 22–46% are classified as AIDP (134, 147, 157, 163). In North America, approximately 10–15% of GBS cases are classified as AMAN variants (17, 147, 148, 157). *C. jejuni* is the leading antecedent infection associated with AMAN (116, 147). AMAN presents clinically with abrupt motor weakness that can progress. Recovery begins within 2–3 weeks and complete recovery is often achieved. Also, nerve conduction studies showed that recovery from AMAN is quicker than recovery from AIDP (17, 134). Antibodies to gangliosides GM1, GM1b, GD1a, and GalNAc-GD1a are all highly associated with AMAN with reactivity to GM1 and GD1a the most commonly associated antibodies (77, 134, 153). The pathogenesis of this subtype is an immune attack on the axon of the neuron rather than the Schwann cells and myelin (17, 154, 157). Complement and IgG bind to the axolemma of the motor nerves at the nodes of Ranvier which results in MAC formation and subsequent axonal damage; demyelination rarely occurs (163). Using a rabbit model that has been immunized with a ganglioside mixture including ganglioside GM1, it was shown that immunoglobulins were deposited on the axons of the anterior roots (167). Moran *et al.* demonstrated that anti-GM1 antibodies induced from *C. jejuni* LOS bind to the nodes of Ranvier in humans, disrupting Na<sup>+</sup> and K<sup>+</sup> channels and resulting in poor nerve conduction (103).

A GBS subtype similar to AMAN is acute motor sensory axonal neuropathy (AMSAN), in which damage involves both motor and sensory peripheral nerves (17). Onset is abrupt, as in AMAN, and many patients require mechanical ventilation within days of onset (17). Incidence of AMSAN is less than 10% of all AMAN cases, making it the most uncommon subtype of GBS (154, 157).

### **Miller Fisher Syndrome**

Miller Fisher Syndrome (MFS) is commonly found in East Asia, where 20–25% of cases present as MFS, compared to 1–5% in Western countries (134, 163). MFS was first described in 1956 by C. Miller Fisher, who examined patients who had symptoms similar to those seen with GBS but also presented with ophthalmoplegia, ataxia, and areflexia (153). Today, MFS is clinically characterized by this triad of symptoms: areflexia, ataxia, and ophthalmoplegia, though not all symptoms may present (17, 93, 134, 137, 157, 162). Unlike GBS, MFS presents as a descending paralysis that affects both the central and peripheral nervous system (17, 139). The disease usually progresses for 1 week after the first onset of symptoms, and improvement begins within 2 weeks. The average time for full recovery is 1–3 months in most patients (163). Reactivity against ganglioside GQ1b is strongly associated with MFS; 83–100% of MFS patients present with anti-GQ1b antibodies (17, 72, 77, 93, 137, 157). Immunostaining assays have shown that ganglioside GQ1b is highly enriched in the human cranial nerves that control the extrinsic eye muscles, including the 3<sup>rd</sup> (oculomotor), 4<sup>th</sup> (trochlear), and 6<sup>th</sup> (abducens) cranial nerves (93, 116, 153, 154). Presence of anti-

GQ1b is a good diagnostic marker for MFS because very few of these patients lack these antibodies (93).

## **CAMPYLOBACTER JEJUNI**

In the 1970's *Campylobacter jejuni* was identified as a foodborne pathogen (68). *C. jejuni* is a gram negative curved rod bacterium with a unipolar or bipolar flagella (7, 75, 91). It is the leading cause of foodborne bacterial gastroenteritis in the developing world (7, 31, 63, 75, 162). In the United States the annual incidence of *C. jejuni* infection is approximately 1–2.4 million infections (44, 68, 91, 131). Symptoms of *C. jejuni* infection include fatigue, abdominal cramps, nausea, watery diarrhea and bloody diarrhea (102). Mortality rates are low for campylobacteriosis in the United States; it is estimated that approximately 124 deaths result annually (44). Studies have shown that infection of *C. jejuni* is the highest during early Fall and that all age groups can be affected (91). In some instances *C. jejuni* infection can also be associated with post-infectious syndromes such as Guillain Barré Syndrome, Reiter's Syndrome, Inflammatory Bowel Disease, and Irritable Bowel Syndrome (44, 68, 75, 87, 125). *C. jejuni* can colonize the gastrointestinal tracts of both wild and domesticated animals, but rarely cause clinical disease in food animals (pigs, cows, chicken, etc) (68). Therefore, routes of infection with *C. jejuni* include contaminated meat (mainly poultry), contaminated water, and unpasteurized milk (75, 112, 156).

It is well recognized that *C. jejuni* is highly associated with the development of GBS, specifically the AMAN subtype. However, only select strains of *C. jejuni* have the ability to mimic gangliosides (38). The genes involved in LOS biosynthesis have been identified in many sequenced strains and strains not sequenced (47, 112). The genetic mechanisms that result in the highly variable LOS have also been identified (47, 112).

GBS patients can be co-infected with multiple strains of *C. jejuni* but only one of the strains may have the ability to mimic gangliosides (38). Some strains have a higher frequency of association with the development of GBS as a result of the presence or absence of certain genes in the LOS biosynthesis loci (7). Other genetic factors such as the flagella or major outer membrane protein have been examined to identify a genetic relationship of *C. jejuni* strains associated with GBS, but have yielded contradicting results (27, 35, 36).

### **Lipo-oligosaccharides (LOS)**

The LOS is a surface molecule found on some gram negative bacteria in place of the larger lipopolysaccharide (LPS) structures found on such organisms such as *Salmonella* (112, 125). LOS is anchored to the bacterial outer membrane by insertion of the lipid A tail into the membrane, with the highly variable region—the oligosaccharide portion—extending into the extracellular space (112). Variability of this outer membrane component is a result of the diverse monosaccharide components and linkages between them that make up the structure of the LOS (112). Mechanisms that result in the high variability of the LOS include: 1) lateral gene transfer, 2) phase variation due to homopolymeric tracts, and 3) gene inactivation, deletion, duplication, or fusion (31, 51, 125).

The LOS has been classified into 23 different classes (A–W) based on gene content and organization in the complex LOS biosynthesis locus; in *C. jejuni* 11168, this locus occupies the open reading frames (ORFs) from Cj1131 to Cj1151 (46, 47, 63). Initially the LOS was classified into 3 classes (A–C), class B was interpreted as an

evolutionary intermediate between class A and C (47). Classes A and B may also be further classified by allele type (A1/B1 or A2/B2) based on presence the *cgtA* (orf5abl) and *cgtB* (orf6ab) genes (112). Parker *et al.* (2005) further organized the LOS biosynthesis loci, resulting in 8 classes (A–H) and eventually identified an additional 11 classes (A–S) (63, 111, 112). Classes T–W have also been identified recently by Stanhope and colleagues (125). In the most recent organization, classes A, B, C, M, R, and V all have the necessary genes needed to synthesize a ganglioside mimicking LOS (51, 63, 111). These LOS classes all have the genes *neuBCA* that encode for the biosynthesis of sialic acid and the *cst* gene (*cstII* for classes A, B, M, and R; *cstIII* for class C), that encodes sialyltransferase needed to sialylate the LOS (63, 111, 112, 124, 125). All other classes of the LOS lack the genes necessary for an LOS structure that may mimic gangliosides; they lack the sialic acid biosynthesis genes and a sialyltransferase.

LOS class A *C. jejuni* strains are more commonly associated with GBS while *C. jejuni* strains with class B LOS are more common in MFS patients (47, 63, 124). A study by Parker *et al.* (2005) examined the LOS biosynthesis loci of 16 GBS isolates and concluded that 14/16 were classified as LOS class A1 and 2/16 as LOS class allele A2 (112). Another study by Godschalk *et al.* (2004) focused on examining the LOS loci of 17 GBS strains and found that 53% of these *C. jejuni* GBS associated strains had class A LOS and 18% belonged to a class unable to mimic gangliosides (49). They postulated that this observation could be the result of a unique sialyltransferase that allows the LOS structure to mimic gangliosides or that these GBS patients were co-infected with multiple strains of *C. jejuni*, some having the ability to mimic gangliosides and others

not, but culture only resulted in the isolation of a single strain (49). Godschalk and Parker in two different studies determined that 62% and 64%, respectively, of the *C. jejuni* strains that only caused enteritis were classified as LOS classes A–C. This result suggests that presence of ganglioside mimicking epitopes on the LOS of *C. jejuni* may be advantageous to the bacterium in gastrointestinal colonization and infection (49, 111). Contradictory to this suggestion, an *in vitro* study by Guerry *et al.* (2002) showed *C. jejuni* strains that lacked the *cgtA* gene (*N*-acetylgalactosaminyl (GalNAc) transferase) had a higher rate of invasion in intestinal epithelial cells (56).

An example of variation within the LOS is a polymorphism that occurs on the gene that encodes a sialyltransferase, *csfII* (134). Of the 291 amino acids in the gene, amino acid 51 determines its enzymatic activity (134). If the amino acid is threonine (Thr51) then the enzyme encodes a mono-functional  $\alpha$ -2,3, sialyltransferase which commonly results in gangliosides associated with GBS (90). If the amino acid produced is asparagine (Asn51) the *csfII* is bi-functional, encoding an enzyme with both  $\alpha$ -2,3, sialyltransferase and  $\alpha$ -2,8, sialyltransferase activity, resulting in a LOS structure that more commonly mimics the GQ1b ganglioside associated with MFS (63, 90).

Recently, work has been performed with C-Dps, which is a protein produced by *C. jejuni* in response to levels of nutritional or oxidative stress (114, 115). Two studies by Piao *et al.* (2010 and 2011) have shown that C-Dps binds to sulfatide, a neutrophil glycosphingolipid that is needed for paranodal junction formation and maintenance of ion channels along the axons. Once bound it results in demyelination of the myelin sheath and axonal degeneration (114, 115). Using immunohistochemistry, he was able to demonstrate both *in vitro* and *in vivo* that C-Dps binds to the nodes of Ranvier, outer

most portion of the myelin sheath and basement membranes of the peripheral nerves (115). Using cell culture, he was able to show further binding of C-Dps to the anterior horn cells in the spinal cord grey matter and to myelin sheath in the white matter (114). These findings suggest that C-Dps should be analyzed further in its role in the pathogenesis of GBS.

### **Molecular Typing of *C. jejuni***

The most common approach used to classify *C. jejuni* strains is multi-locus sequence typing (MLST), which is based on partial sequences of seven housekeeping genes. MLST has been used to characterize the source of *C. jejuni* infections (124). There is an accessible website that allows assignment of sequence types and examination of the different clonal complexes based on sequence of their MLST alleles (<http://pubmlst.org/campylobacter>). Studies have shown that clonal complexes (CC) CC 21 and CC 45 are the most common assigned to *C. jejuni* isolates (124). A study was done to examine 335 *C. jejuni* strains that included human, bovine, and poultry isolates for correlation of their clonal complex assigned based on MLST and their LOS class (A–H) (124). Results showed that LOS class A1 was highly associated with CC 22 (27/27), CC 508 (2/2), CC 1034 (1/1) and CC 1332 (4/4) while LOS class A2 was associated with CC 61 (7/7). Two of two LOS locus class B1 strains were in the CC 42, while two of two B2 strains were in the CC 58 and 14/15 B2 strains were in CC 48. In this study, the LOS class E, which is not sialylated, was completely associated with complexes CC 677 and CC 283 (124). Therefore, these results suggest that the combination of MLST and LOS classification may be useful approach for predicting disease outcomes.

Other typing schemes used to classify and analyze GBS-associated *C. jejuni* strains involve examination of the major outer membrane protein, *porA*, and the major flagella protein, *flaA*. It has been demonstrated that a highly variable region termed, short variable region (SVR) in the *flaA* of *C. jejuni* is a molecular typing tool useful to compare *C. jejuni* isolates (101, 102). The SVR is only 321 base pairs in length and therefore provides a quick and reliable typing scheme (102). Comparisons of the SVR in *C. jejuni* strains are commonly used to examine the different *C. jejuni* strains in a population (102). One study in Curacao performed multiple molecular typing methods to identify the spread of clonal *C. jejuni* including MLST and sequencing of the *flaA* SVR (36). The study examined 234 isolates of *C. jejuni* from patients that presented with gastroenteritis, 2 of which also developed GBS. It was performed from March, 1999, to March, 2000, and based on the *flaA* SVR 11 different types were identified; MLST identified 29 sequence types (ST). The 2 *C. jejuni* isolates from the GBS patients were in two different sequence types for both MLST and *flaA* SVR. There was a poor correlation of the MLST typing with the *flaA* SVR typing together; each ST identified with MLST had *flaA* SVR sequence with variation, thus supporting the high variability in the *flaA* (36). A study by Tsang *et al.* (2001) proposed that a *flaA* SVR sequence type was highly associated with patients that developed GBS (144). They compared their isolates to GenBank®, and based on their results concluded that isolates of *C. jejuni* that result in neuropathy do cluster together based on their *flaA* SVR sequence types (144). They also identified that 3 isolates from their study were identical in *flaA* SVR type and found it unusual since each isolate was from a different geographical part of the world (Japan,

Chile, and America). Based on these data, the authors suggested that this specific *flaA* SVR sequence type could be a marker for GBS (144).

Dingle *et al.* (2001) examined the typing of 25 *C. jejuni* isolates from both GBS and MFS patients with MLST and *flaA* SVR typing; they also wanted to examine the rate of the proposed *flaA* SVR sequence type described above in his isolates (35). They found 20 different sequence types that were able to group into 13 different clonal complexes, though they did note that the second most common clonal complex of *C. jejuni*, CC 45, was not present in any of the 25 isolates suggesting that isolates associated with CC 45 are less likely to develop neuropathy. The sequencing of the *flaA* SVR identified 20 distinct sequences and only 4 of the isolates had the *flaA* SVR sequence that was a proposed marker for GBS (35). The lack of the proposed *flaA* SVR sequence to the GBS isolates conflicts with the results of Tsang *et al.* and therefore more work would need to be done to understand this discrepancy.

The other proposed typing scheme involves using the porin that is the major *C. jejuni* outer membrane protein as a target for rapid classification of strains. This porin is a hypervariable region of *C. jejuni* (27). Clark *et al.* (2007) sequenced the *porA* gene of 105 *C. jejuni* isolates to examine if any correlation of the *porA* sequence was present during development of GBS. Based on their sequence results they identified 3 different sequence types but no correlation to development of GBS was noted with any of the sequences (27).

Both the *flaA* SVR and *porA* have been isolated and sequenced from *C. jejuni* from patients who presented with either enteritis only or enteritis and neuropathy, and based on findings there is contradicting evidence of whether molecular typing of the *flaA*

SVR or *porA* show any association with the development of GBS (35, 144). Therefore, we hypothesized that assigning *C. jejuni* strains based on MLST, *porA* sequence, and *flaA* SVR sequence together could result in correlations between GBS-associated strains and *C. jejuni* associated with enteritis only based on LOS classification.

## ANIMAL MODELS

Currently there are few animal models used to study the natural development of GBS. Rabbits provide the current model of the GBS subtype, AMAN. Previously, Yuki *et al.* provided proof for a rabbit model by immunizing rabbits subcutaneously with either 2.5 mg of a mixture of gangliosides or 1 mg of GM1 isolated from bovine brain. At 3 week intervals, rabbits were injected intraperitoneally with the same cocktail until limb weakness was observed; if no limb weakness occurred, rabbits were observed for 6 months and euthanized (167). All of the rabbits given the mixture of gangliosides developed flaccid paralysis within 35–57 days and antibodies to GM1 were observed 2–3 weeks after the first injection. Studies of the sciatic nerves from these rabbits showed mild to severe Wallerian-like degeneration with infiltration of macrophages. Nine of eleven rabbits given isolated GM1 extracted from bovine brain developed flaccid paralysis and had presence of anti-GM1 antibodies as determined by enzyme-linked immunosorbent assays (167). Sciatic nerves from these rabbits showed mild to severe Wallerian-like degeneration with no presence of lymphocytes (167).

More recently, Yuki *et al.* immunized two groups of rabbits with *C. jejuni* LOS known to mimic ganglioside GM1; this LOS preparation was from a *C. jejuni* isolate of a GBS patient that presented with antibodies to ganglioside GM1 (165, 166). Group 1 had rabbits immunized at 3 week intervals with 2.5 mg of *C. jejuni* LOS and group 2 rabbits were immunized at the same time points but received 10 mg of LOS (165). After immunization, the rabbits in both groups 1 and 2 exhibited clinical, electrophysiological, and histopathological features that are common in AMAN. The rabbits in group 1 began

to develop flaccid paralysis between 133 to 329 days after the first inoculation. Group 2 of rabbits developed tetraparesis 40 to 227 days after the initial inoculation of LOS. Rabbits in both groups 1 and 2 developed anti-GM1 IgM and anti-GM1 IgG antibodies 2–4 weeks and 4–6 weeks, respectively, after inoculation (165). Histological studies showed macrophage infiltration in the nerve roots of all rabbits that exhibited any type of paralysis. In the sciatic nerve, Yuki observed Wallerian-like degeneration with little to no demyelination. He also observed no T cell infiltration but did see IgG bound to the axons (165). Thus, despite documenting some new observations, these rabbit models are not a natural model of the pathogenesis of GBS.

Another model is experimental autoimmune neuritis (EAN), which is a T cell-mediated demyelinating disease in the peripheral nervous system that resembles GBS. Peripheral nerve myelin, purified myelin protein P2 or T cell transfers (T cells are from stimulated lymph node cells *in vitro* with P2) are used to immunize SJL/J mice to elicit an anti-myelin response (20, 126). The clinical and histological presentations in these mice are very similar to those of GBS (8, 163). Some mice given these preparations developed lesions of the sciatic nerve that peaked at 40 days with infiltration of T cells in the nerves observed. The mice display clinical and pathological features that resemble the GBS subtype, AIDP (52, 126, 163). Lewis rats have also been used as an EAN model; myelin proteins P0 or P2 along with Freund's complete adjuvant are used to immunize Lewis rats which have been shown to have T cell infiltration and macrophage-mediated demyelination that is similar to that seen in GBS (20, 61). These EAN models do not make a good GBS model however, because there is not conclusive evidence to show that T cells occur in GBS patients (134, 163).

The only true model of GBS following *C. jejuni* infection is the chicken. To initiate disease, chickens were inoculated by oral gavage with 5 ml of a *C. jejuni* isolate taken from a boy who developed GBS (94). After inoculation, chickens were observed for neurological signs and at endpoint, the sciatic nerves from both control and infected chickens were removed for pathological analysis that included both histological examination with hematoxylin and eosin staining for cellular infiltrates and Luxol fast blue staining for myelin damage. Within 12 days post inoculation, chickens infected with *C. jejuni* developed weakness and were not able to stand; some chickens were paralyzed. Both wing and head droop were also observed. The earliest onset of weakness was as early as day 5 post inoculation (94). At endpoint only the sciatic nerve was removed for analysis. Histopathological studies of the sciatic nerve showed Wallerian-like degeneration and varying degrees of lengthening of the nodes of Ranvier with rare occurrence of paranodal demyelination. The study notes the most severe Wallerian-like degeneration of the sciatic nerve was observed in a chicken that became weak 18 days post inoculation. In some instances cellular infiltration of macrophages could be detected around the axon of the sciatic nerve (94). The uninfected chickens showed no Wallerian-like degeneration in any of their sciatic nerves.

Chickens however are very different physiologically and anatomically from humans and therefore do not make good models of human GBS. For example, when screening the model for new treatments one would prefer that the animal's physiology closely mimics that of humans so that drug distribution and clearance would be analogous to those in the human. Therefore, we hypothesized that a mouse, which is physiologically similar to humans, could be a model of GBS secondary to *C. jejuni*

infection. This would offer an animal model that can be used to study the natural course to the development of GBS.

## RATIONALE

The role of *C. jejuni* in the pathogenesis of GBS is still not well understood. More comparative *in vivo* studies need to be performed to understand better the role of molecular mimicry in the development of GBS. However the current animal models used to study GBS are either not natural models of the course of development of the disease or are physiologically and anatomically different from humans (94, 158, 167). Therefore, a murine model that develops GBS secondary to *C. jejuni* infection is needed. Chapters 2 and 3 of this dissertation describe progress towards such a model.

Analysis of the role of LOS in molecular mimicry has revealed conflicting data that suggest that other genetic factors of *C. jejuni* may contribute to the development of GBS. Epidemiological studies have been performed to collect isolates from patients with defined clinical presentations to study the genetic relationship of enteric and neuropathic strains of *C. jejuni*. The flagella and major outer membrane protein (MOMP) have each been examined in these epidemiological studies because both molecules are located on the outer surface of the *C. jejuni* cell (27, 35). Studies have associated development of GBS with particular *C. jejuni* serotypes (120) or with strain clusters identified by amplified fragment length polymorphism sequence typing of the SVR of the *flaA* gene, or sequence typing of the *porA* gene encoding the MOMP (27, 144). These approaches have not yielded definitive molecular markers for strains likely to produce GBS (27, 35, 36, 144); therefore, additional work to improve molecular typing is needed. Chapters 4 and 5 of this dissertation describe molecular genetic typing methods targeting both conserved and variable loci of *C. jejuni* that were applied to strains

collected in two epidemiologic studies. Interestingly, both studies demonstrate that the LOS loci of many of the *C. jejuni* isolates demonstrated characteristics similar to those of *C. jejuni* strains associated with GBS. These GBS-like strains were found both in the general U.S. population with focus on the Michigan population (Chapter 4) and associated with diarrhea in calves on a Michigan dairy farm (Chapter 5).

Therefore, based on the stated hypotheses, I pursued the following specific aims in this dissertation:

**Specific Aim 1:** Assess the presence of autoimmune sequelae following infection of *C. jejuni* in Non-Obese Diabetic (NOD) mice based on neurological signs and presence of nerve lesions

**Specific Aim 2:** Correlate genetic differences between the LOS biosynthesis loci and other variable outer surface structures of *C. jejuni* strains with potential to elicit neuropathy

## CHAPTER 2

Non-Obese Diabetic (NOD) mice as working models of Guillain Barré Syndrome  
following *Campylobacter jejuni* infection

## ABSTRACT

*Campylobacter jejuni* is a leading cause of bacterial gastroenteritis linked to several serious autoimmune sequelae including Inflammatory Bowel Disease, Irritable Bowel Syndrome, Reiter's Arthritis, and Guillain Barré Syndrome (GBS). GBS is an acute peripheral neuropathy characterized by limb weakness and loss of tendon reflex. *C. jejuni* strains from GBS patients have lipo-oligosaccharides (LOS) structures that mimic gangliosides found on the peripheral nerves. The GM1 and GD1a gangliosides are most commonly associated with acute motor axonal neuropathy (AMAN), the form of GBS that follows *C. jejuni* infection. We hypothesized that GBS can result in NOD mice or their congenic IL-10 and B7-2 knockouts secondary to *C. jejuni* infection and that clinical signs and pathological changes can be detected. To address this hypothesis mice were gavaged orally with *C. jejuni* strains HB93-13 and 260.94 from patients with GBS. Mice were assessed for clinical neurological signs, anti-ganglioside antibodies, cellular infiltrates, and lesions in peripheral nervous tissue. Infected mice of the NOD WT and the NOD IL-10<sup>-/-</sup> genotypes produced anti-ganglioside antibodies that were of the IgG1 isotype directed against a mixture of gangliosides GM1 and GQ1b. Significant increases in anti-ganglioside antibodies against single gangliosides (GM1 and/or GD1a) occurred in infected mice of all genotypes. Phenotypic tests showed significant differences between treatment groups of all genotypes. Peripheral nerve lesions with macrophage infiltrates were significantly different between the sham-inoculated mice and *C. jejuni* infected mice of both the NOD WT and NOD IL-10<sup>-/-</sup>

genotypes. Based on these parameters, we conclude that NOD WT mice are the best candidate for a potential mouse model of natural onset GBS.

## INTRODUCTION

Guillain Barré Syndrome (GBS) is a post-infectious polyradiculoneuropathy considered to be an autoimmune disease (116). GBS is defined as a group of several disorders that are differentiated by particular forms of immune attack on the peripheral nervous system. Subtypes of GBS include acute inflammatory demyelinating polyneuropathy (AIDP), acute motor axonal neuropathy (AMAN), and Miller Fisher Syndrome (MFS). AIDP is the most common subtype; occurring in approximately 90% of GBS cases in North America and Europe (134, 163). AIDP presents as segmental demyelination affecting mainly the myelinated nerves of the limbs and lower cranial and sensory nerves. AMAN is a form seen in China, Japan, and Central and South America with a frequency of 38–65% (134). In patients, AMAN presents as damage to the motor neurons at the nodes of Ranvier. A related form—acute motor sensory axonal neuropathy (AMSAN) — has also been recognized where patients are affected in both motor and sensory peripheral nerve function (108). MFS is commonly seen in eastern Asia; at a rate of 20–25% (134, 163). MFS is an anatomically localized variant of GBS characterized by the triad of symptoms areflexia, ataxia, and ophthalmoplegia (17, 137). In contrast to GBS, MFS causes descending paralysis because different nerve groups are affected (139).

GBS is described as a monophasic disease in humans, with the most severe disease occurring 2–4 weeks after first onset of symptoms; however, 7% of GBS patients have reported reoccurrence (7, 163). Weakness is followed rapidly by symmetrical ascending paralysis and, if progressive, the muscles of respiration are

paralyzed. The mortality rate is 3–10%; 10–20% of patients do not recover completely and may suffer life-long disability (163). Current treatments of GBS include plasma exchange and intravenous immunoglobulin (7, 72). Males are more likely to develop GBS than females with a ratio of 1.25–1.5 males to 1.0 females; most autoimmune diseases present with a higher ratio of females than males (72, 116).

Two-thirds of GBS patients have a history of prior infection, most commonly respiratory or gastrointestinal infections (72, 116, 162, 163). Common bacterial and viral antecedent infections of GBS include *Campylobacter jejuni*, *Mycoplasma pneumoniae*, Epstein-Barr virus, and cytomegalovirus (7, 70, 116, 154, 157, 163). In 1993, Mishu and Blaser recognized that *C. jejuni* infection can result in development of GBS (67, 105). The Gram negative bacterium *C. jejuni* is the most frequent bacterial etiology for human gastroenteritis with 1–2.4 million cases annually in the U.S. and is the most common enteric infection associated with development of the AMAN form of GBS (19, 63, 162, 163, 165). The risk of developing GBS after *C. jejuni* infection is less than 1 GBS case per 1000 *C. jejuni* infections in the U.S. (4, 5, 7). Neurological symptoms of the AMAN subtype occur 1–3 weeks after the onset of *C. jejuni* induced enteric disease, although some GBS patients are colonized without enteritis (157, 163).

In GBS, molecular mimicry is thought to play a role in the production of anti-ganglioside antibodies, which bind to and trigger attack on host nerve tissue (7, 63, 76, 121, 128, 134, 157, 160, 162, 165). The structure of lipo-oligosaccharides (LOS) of *C. jejuni* can mimic nerve gangliosides in the host, eliciting an autoimmune response that cross-reacts with gangliosides in the peripheral nerves (7, 107). It has been shown both in humans and in animal models that the immune response to the bacterium results in

production of anti-ganglioside antibodies that leads to damage of nerves and Wallerian-like degeneration; such antibodies (“autoantibodies”) have been shown to bind to motor neurons, nodes of Ranvier, and neuromuscular junctions (5, 71, 107, 145, 159).

Autoantibodies directed against gangliosides GM1 and GD1a have been detected most commonly in patients with the AMAN variant of GBS, while autoantibodies against GQ1b are more often associated with MFS (13, 40, 150). The peak titers of anti-ganglioside antibodies following *C. jejuni* infection have been associated with onset of GBS symptoms in patients. An example of correlation between autoantibodies and disease manifestations occurred during an outbreak of *C. jejuni* in 2007 when 36 cases of GBS were identified in northern China in patients that produced high titers of anti-GM1 autoantibodies. Bacterial fecal culture was performed, and *C. jejuni* was identified as the antecedent infectious agent (169). Another study conducted in southeast England during 1983–1984 examined serum samples of 95 GBS patients and 88 control patients and demonstrated that 14/95 patients had high titers of antibodies reactive to GM1 based on ELISA testing (149).

Despite these advances little progress has been made in understanding the pathogenesis of GBS and even less in developing effective therapies, largely because of the lack of accurate, tractable animal models. Currently, rabbits and chickens serve as the induced animal models for GBS and other peripheral neuropathies. GBS is induced in the rabbit model by immunizing rabbits with *C. jejuni* LOS known to mimic particular gangliosides. Rabbits given a dose of 2.5 mg *C. jejuni* LOS subcutaneously at 3 week intervals developed flaccid limb weakness between 133 to 329 days after the initial inoculation, while rabbits treated similarly with 10 mg LOS developed tetraparesis

40 to 227 days after the initial inoculation (165). Anti-GM1 IgM and anti-GM1 IgG antibodies were detected 2–4 weeks and 4–6 weeks, respectively, after the first injections (135, 165). Although LOS exposure elicits anti-ganglioside reactivity, immunized rabbits are not a precise model for GBS induced following oral *C. jejuni* infection. Alternatively, chickens acquire a form of peripheral neuropathy secondary to oral inoculation with *C. jejuni* GBS patient strains. Thirty-three percent of chickens receiving *C. jejuni* HB93-13 became paralyzed within 12 days (94). In paralyzed chickens, early lesions included nodal lengthening and paranodal demyelination that were later followed by Wallerian-like degeneration and even paranodal re-myelination in some long-term survivors. Thus, chickens inoculated orally with GBS associated *C. jejuni* strains from patients can be considered a naturally occurring model for GBS. However, chickens are outbred and very different anatomically and physiologically from humans; these facts detract from their value as a model. Thus, a murine model is needed to study GBS pathogenesis, including the roles played by both host and pathogen genetics. Susceptible inbred mice would provide the ideal model where the interplay of host and pathogen genetics could be explored.

Non-Obese Diabetic (NOD) inbred mice have been documented to develop autoimmune diabetes mediated by auto-reactive T cells infiltrating the pancreas (66). They also develop autoimmune diseases of the salivary glands and thymus (13). Additionally, NOD mice deficient for the co-stimulatory molecule B7-2 (NOD-B7-2<sup>-/-</sup> mice) are largely protected from autoimmune diabetes but develop a spontaneous autoimmune peripheral polyneuropathy that resembles GBS called chronic inflammatory demyelinating polyradiculoneuropathy (CIDP) (13, 130). By 20 weeks of age, peripheral

nerves of neuropathic NOD-B7-2<sup>-/-</sup> mice have infiltrates of dendritic cells and CD4<sup>+</sup> and CD8<sup>+</sup> positive T cells. Based on knockout of genes in mice of the same genetic background, these investigators showed that neuropathy developed in the absence of perforin or fas proteins, suggesting that classic cytotoxicity pathways for nerve damage were not operating. Stronger evidence for the autoimmune basis of this neuropathy was provided by experiments which showed that the neuropathy was transferable to naïve NOD.SCID mice by CD4<sup>+</sup> T cells isolated from neuropathic animals (13, 130). Neither of these mouse models has been used to explore the effects of natural infection with *C. jejuni* in the initiation of clinical GBS or classical GBS lesions with Wallerian degeneration of the peripheral nerves.

We hypothesized that NOD mice or their congenic IL-10 and B7-2 knockouts develop spontaneous GBS secondary to *C. jejuni* infection and that neurological signs and pathological lesions can be detected by established methods such as neurological evaluation, enzyme-linked immunosorbent assays (ELISAs) for anti-ganglioside antibodies, and histological examination for Wallerian degeneration and inflammatory infiltrates. The strains of *C. jejuni* we used, *C. jejuni* HB93-13 and *C. jejuni* 260.94, were isolated from patients who presented with GBS. It has been shown that both strains mimic the GM1 ganglioside; *C. jejuni* HB93-13 also has been shown to mimic the GD1a ganglioside (2). Our rationale for using NOD mice and their congenic knockouts is based on the known propensity of mice of these genotypes to develop autoimmune diseases. These NOD mice exhibit autoimmune diseases due to defects in the activity of natural killer cells, cytokine production from macrophages, and regulation of adaptive

T cell populations (3). Furthermore, we previously established that NOD WT mice are colonized by *C. jejuni* and that NOD IL-10<sup>-/-</sup> mice are colonized and develop enteritis in a reproducible fashion after challenge with a pathogenic strain of *C. jejuni* (99). Also, minimal enteric disease was observed in NOD WT and NOD B7-2<sup>-/-</sup> genotypes for both *C. jejuni* strains tested compared to the NOD IL-10<sup>-/-</sup> mice. There were significant differences between the sham-inoculated mice and the *C. jejuni* infected mice in the presence of IgG1 antibody to the ganglioside mixture GM1/GQ1b in the NOD WT and NOD B7-2<sup>-/-</sup> mice. NOD WT, NOD IL-10<sup>-/-</sup>, and NOD B-7<sup>-/-</sup> mice had significant differences in plasma levels of anti-GD1a IgG3 antibody. Mice of all genotypes also had significant differences between the sham-inoculated mice and infected mice in one or more phenotypic tests. Based on our findings in long term time course studies with extensive neurological phenotype testing, we conclude that NOD WT mice have the greatest potential to be a natural murine model for GBS.

## MATERIALS AND METHODS

### Animals

NOD mice, along with their congenic IL-10 and B7-2 knockouts, were originally purchased from The Jackson Laboratory (Bar Harbor, ME, USA), and a breeding colony was established as described previously (98). For experimental work, mice were housed in individual filter top sterile cages at the Michigan State University Research Containment Facility (URCF). Cages were changed every 14 days, and mice were fed sterilized mouse diet 7913 (Harlan Teklad) and given autoclaved reverse osmosis water. Prior to inoculation, fecal samples were taken and tested for presence of colitogenic bacteria including *Campylobacter* spp., *Helicobacter* spp., *Citrobacter rodentium*, *Enterococcus faecalis*, and *E. faecium* by PCR. A modified PCR assay from Jackson Laboratories was used to confirm the genotypes of all experimental mice ([http://jaxmice.jax.org/pub-cgi/protocols/protocols.sh?objtype=protocol&protocol\\_id=346](http://jaxmice.jax.org/pub-cgi/protocols/protocols.sh?objtype=protocol&protocol_id=346)). DNA extraction from ear punches was performed using DNeasy Blood and Tissue Kit (Qiagen, Hilden, Germany) or from fecal pellets according to Murgatroyd *et al.*, with modifications (104). Mice were inoculated with *C. jejuni* strains between the ages of 7–10 weeks. This age range was used to enable the experiments to be performed before the age at which NOD B7-2<sup>-/-</sup> mice begin to develop spontaneous neuropathy. It is known that B7-2 knockout mice begin to develop mild clinical signs of spontaneous neuropathy no earlier than 20 weeks of age (Gadsden, unpublished data) (13, 130). After inoculation, mice were monitored daily for clinical signs of enteric disease and/or neurological disease. All animal experiments followed

NIH guidelines and were approved by the MSU All University Committee on Animal Use and Care under protocol numbers 04/07-030-00 and 06/09-092-00.

### ***Campylobacter jejuni***

*C. jejuni* strains, *C. jejuni* 260.94 (ATCC BAA-1234) and *C. jejuni* HB93-13 (ATCC 700297) used in these studies were purchased from the American Type Culture Collection (ATCC, Manassas, VA, USA) and were isolated from patients with GBS. The growth conditions of *C. jejuni* inocula, confirmation of the spiral morphology and motility, and mouse inoculation methods were previously described (98).

### **Experimental Design**

Three experiments were conducted to address our hypothesis that *C. jejuni* patient strains can elicit peripheral neuropathy in mice of the NOD genotype. In all three experiments, post inoculation testing was similar, but improvements were made with each experiment. Mice were subjected to a series of weekly phenotypic tests to detect any signs of neurological disorder as explained in further detail below. In Experiments 1 and 2 all mice were bled from the saphenous vein prior to inoculation to collect plasma to test for anti-ganglioside antibodies; mice were also bled 14 days after inoculation and at the endpoint. Mice were not bled prior to inoculation or at day 14 after inoculation in Experiment 3 based on the non-significance of the data of Experiments 1 and 2 at these time points.

*Experiment 1: Screening mice of various NOD genotypes for GBS following C. jejuni infection.*

The first experiment screened 3 groups of NOD mice of different genotypes—NOD wild type (WT), NOD IL-10<sup>-/-</sup>, and NOD B7-2<sup>-/-</sup>—with 30 mice in each group. Ten mice from each group were infected with the GBS-associated *C. jejuni* strain HB93-13, 10 were infected with the GBS-associated *C. jejuni* strain 260.94, and the remaining 10 were sham-inoculated with tryptose soya broth (TSB; negative controls). At day 12 post inoculation, fecal pellets were collected and cultured for the presence of *C. jejuni* to confirm colonization. Mice were euthanized and necropsied 56 days post inoculation. Samples of blood and sections of the GI tract were taken and examined for presence of anti-ganglioside antibodies and *C. jejuni* colonization respectively; detailed methods are given below.

*Experiment 2: Screening larger group sizes of NOD WT and NOD B7-2<sup>-/-</sup> mice for GBS.*

Sample size calculation based on experiment 1 results prompted screening of larger sample sizes for further optimization. Experiment 2 was performed using only NOD WT and NOD B7-2<sup>-/-</sup> mice and only *C. jejuni* 260.94. *C. jejuni* 260.94 was used because NOD WT, NOD IL-10<sup>-/-</sup>, and NOD B7-2<sup>-/-</sup> mice infected with this strain in Experiment 1 showed high colonization rates with little or no enteric disease. Each mouse genotype had a group size of 36 with 18 mice in each group orally inoculated with *C. jejuni* 260.94 and the remaining 18 mice in each group sham-inoculated with TSB. Group size for this experiment was determined based on numbers of mice in

Experiment 1 showing neurological signs. The sample size (15–18 mice per treatment group) was calculated based on a dichotomous study with two proportions (independent, prospective) and an uncorrected chi-square test design with  $\alpha=0.05$  and  $\text{power}=0.80$ . Mice were euthanized and necropsied at an endpoint of 80 days post inoculation. At necropsy, samples of the GI tract, sciatic nerve, and blood were taken to determine *C. jejuni* colonization, nerve lesions, and presence of anti-ganglioside antibodies respectively; detailed methods given below. A longer experimental endpoint was used to see if more mice developed clinical neurological signs.

*Experiment 3: Examination of NOD IL-10<sup>-/-</sup> mice using antibiotics to treat enteritis.*

Experiment 3 included 4 treatment groups, all NOD IL-10<sup>-/-</sup> mice. Thirty mice were given *C. jejuni* 260.94 alone, 20 mice were given *C. jejuni* 260.94 and then treated with the antibiotic chloramphenicol (2.5 mg/ml in drinking water for 26 days beginning at day 12 post infection), 20 mice were given TSB, and the remaining 20 mice were given TSB and then treated with chloramphenicol as above. Mice were euthanized and necropsied at 84 days post inoculation. Sections of the GI tract, blood, and the sciatic nerve from ankle to spinal nerve root were removed to determine *C. jejuni* colonization, presence of anti-ganglioside antibodies, and nerve lesions with presence of cellular infiltrates respectively; detailed methods are given below.

### **Neurological Phenotype Testing**

Neurological tests were performed on a weekly basis to detect any signs of neurological damage in mice infected with *C. jejuni* strains compared to sham

inoculated controls. Mice were introduced to the tests prior to bacterial inoculation to remove any effects of a learning curve (22). Tests used included the open field test (OFT), hang test, rotarod test, foot printing and tracking, and DigiGait™ analyses. Experiment 1 included the use of the OFT, hang test, and foot printing. Experiment 2 included those tests in experiment 1 with the addition of the rotarod. Experiment 3 only utilized the rotarod and DigiGait™.

#### *Open field testing*

The open field test, which allows a trained observer who is blinded to detect abnormal gait and ataxia, was performed using a large clear polycarbonate box with 4 quadrants marked on the bottom. Mice were placed at the center and observed for 30 seconds. Parameters recorded included the number of quadrants crossed, rearing, and unusual gait. This test was repeated three times and results were averaged (14, 24).

#### *Hang testing*

The hang test, which can detect loss of motor strength, consisted of placing a mouse on a wire grate surface suspended from a ring stand; the surface was then flipped over so that the mouse was upside down. The period of time the mouse could remain hanging upside down for up to 2 minutes was recorded (29). This test was repeated 3 times, with 15 minute rest periods between trials, and the longest time on the grate was recorded as the test value. The hang test was only used in Experiments 1 and 2 (22, 29).

### *Rotarod testing*

Rotarod (IITC Rotarod for Rats and Mice, IITC Inc. Life Science, Woodland Hills, CA) was used to detect loss of balance and motor function; this test was used in Experiments 2 and 3. Mice were placed on the rotarod for 60 seconds at a speed of 3 RPM with an acceleration of 0.10 RPM per second to reach 30 RPM for a maximum speed. The time that the mouse stayed on the rotating rod was recorded. The test was repeated 3 times, with 15 minute rest periods between trials, and the longest time the mouse achieved was used for analysis (14, 22).

### *Footprinting*

In Experiments 1 and 2, footprinting was used to detect foot drag, abnormal gait, or abnormal foot placement as previously described by Crawley and others (29). Briefly, the fore and hind paws of the mouse were painted with different colored non-toxic paint. Each mouse was placed at the end of a tube, with a slot cut out of the top to monitor mice. Mice were allowed to walk along the tube on a strip of filter paper to record the footprints. Footprints from three strides were then analyzed for stride length, hind base width, stride variability, toe width, and print length. This was done by identifying the midpoint of each paw and then measuring the distances between paws of the forelimbs and hind limbs for strides and stances. Length of the foot and width of the toe spread were measured and analyzed as well (14, 22, 29).

### *DigiGait™ testing*

In Experiment 3, a DigiGait™ apparatus (Mouse Specifics, Quincy, MA, USA), was used to measure stride variability, stance width, gait symmetry, and stride length. This machine is designed specifically to measure a rodent's gait using a clear motorized treadmill belt that can be set at various speeds. The mice are placed into the chamber on the belt and forced to run by the movement of the belt as a sensitive video camera records their movement from below. The video is then processed with specifically designed proprietary software to analyze the gait. Mice were trained on the DigiGait™ for 2 weeks prior to inoculation at speeds of 10 cm/sec, 15 cm/sec, and 20 cm/sec. For the experiment mice were run at both 15 cm/sec and 20 cm/sec for a minimum capture of 300 frames. Videos were then acquired and analyzed using DigiGait™ Imaging Software (Mouse Specifics, Quincy, MA, USA). Stride variability, stance width, gait symmetry, and stride length were all analyzed. Mice that were behaviorally uncooperative throughout the entire experiment, producing poor videos, were removed from the analysis.

We also used the weekly videos to provide clinical observations of the gait, stance, and toe positions of the mice. A clinical observation score sheet was developed that allowed for the quantification of clinical signs, including splayed hind legs, hind limb dragging, knuckling, foot drag, paddling, galloping, sidestepping, crossing over, and bunny hopping. Each of these clinical signs were given one point for presence and two points if it occurred at a high frequency; splayed hind legs and foot drags were given one point for present on one limb and two points if present on 2 limbs. Toes were also scored for being splayed, curled, or flaccid; points were assigned for each (1, 2 and 3

points respectively). The stance of the mouse was also examined for a shorter and/or wider stance; presence or absence was given one or no points, respectively (Table 2.1). Neurological scores for a mouse each week were then added to give a cumulative clinical phenotype score for each mouse. Three trained operators, one of whom was a veterinarian trained in neurological examination, watched the DigiGait™ videos simultaneously to assign the scores; they were blinded and unbiased. In the rare instances that the three disagreed, the videos were rescored to resolve the discrepancies.

### **Enzyme-Linked Immunosorbent Assays (ELISAs)**

Mice were bled from the saphenous vein prior to inoculation and at day 14 post inoculation, and from the heart post euthanasia at the time of necropsy. ELISA assays for anti-*C. jejuni* antibody detection were performed as previously described (98). For detection of autoantibodies against gangliosides GD1a, GM1, and GQ1b, ELISA assays were performed using antigens GD1a (Sigma Aldrich, St. Louis, MO, USA at 20 µg/ml), GM1 (US Biological, Swampscott, MA, USA at 2.0 µg/ml), and GQ1b (Calbiochem/EMD Millipore, Gibbstown, NJ, USA at 0.2 µg/ml). Positive control monoclonal antibodies used for GD1a and GM1 assays were purchased from Chemicon/EMD Millipore (Gibbstown, NJ, USA); anti-GQ1b was purchased from Associates of Cape Cod (East Falmouth, MA, USA). Detection of autoantibodies to a mixture of two gangliosides was also performed using gangliosides GM1 and GD1a with a mixture of 1:1. A 1:1 mixture of GM1 and GQ1b was also tested. Biotinylated goat antibodies included anti-mouse IgG1, IgG2a, IgG2b, and IgG3 (Jackson ImmunoResearch, West Grove, PA, USA) and

biotinylated goat anti-mouse IgM (Sigma Aldrich, St. Louis, MO, USA). Extravidin peroxidase (Sigma Aldrich, St. Louis, MO, USA) and TMB substrate (Rockland Immunochemicals Inc., Gilbertsville, PA, USA) were used for detection.

### **Assessment of Clinical Signs**

Mice were monitored once a day and then twice a day after the first onset of illness. Clinical signs for enteritis assessed included hunched posture, rough coat, diarrhea, inactivity, and dehydration. Any mice that exhibited clinical signs of enteric disease, based on a clinical score sheet (98), prior to end of experimental time points, were euthanized immediately to prevent any discomfort or distress. Neurological clinical signs were examined during the weekly phenotype tests.

### **Necropsy Methods and Assessment of Gross Pathology**

At the humane endpoint or at the end of each experiment, all mice were humanely euthanized using an overdose of CO<sub>2</sub> (1). After euthanasia, mice were weighed and a blood sample taken directly from the heart, followed by puncture of the diaphragm to ensure death. The entire GI tract was then removed from stomach to rectum, and upon examination any gross pathology features were noted, as previously described (98). Mice were then skinned from the back and the spinal cord was exposed. The sciatic nerve was also exposed on both hind limbs. The mouse and legs were placed in a specimen cup and fixed in 10% buffered formalin. The brain was then removed and placed in 10% buffered formalin.

### **Culture for Presence of *C. jejuni*, DNA Extraction and PCR Assays**

TSA-CVA agar plates (TSA supplemented with 5% sheep blood, 20  $\mu\text{g}/\text{mL}$  cefoperazone, 10  $\mu\text{g}/\text{mL}$  vancomycin, and 2  $\mu\text{g}/\text{mL}$  amphotericin B) on which GI tissues removed from mice were streaked were scored for presence of *C. jejuni* (98). Plates with *C. jejuni* growth were swabbed up and whole cell PCR was performed to verify that isolates were *C. jejuni* as previously described (98). DNA was extracted from cecal tissue of all control mice and PCR was performed to verify mice were *C. jejuni* negative (98).

### **Histopathological Scoring of the Gastrointestinal Tract**

At the time of necropsy, the ileocecolic junction was removed and fixed in 10% phosphate-buffered formalin; the junctions were paraffin embedded and stained with hematoxylin and eosin by the Investigative Histopathology Laboratory, Division of Human Pathology, Department of Physiology, Michigan State University. Sections were scored on a scale of 0 to 44 for lesions present in the lumen, epithelium, lamina propria, and the submucosa as previously described (98). Slides were evaluated by a single investigator (LSM) who was blinded to their identity.

### **Histopathological Scoring of the Sciatic Nerve**

For Experiment 2, at the time of necropsy, the sciatic nerves were removed as follows. The legs of each mouse were removed, skinned, and muscles were dissected to expose the nerves. The nerves were exposed from the pelvis to the tibial nerve.

One leg (left) was fixed in 10% buffered formalin for 6 hours and then placed in 60% ethanol for paraffin embedment for both longitudinal and cross sections at the Investigative Histopathology Laboratory, Division of Human Pathology, Department of Physiology, Michigan State University. One section was stained with hematoxylin and eosin and the other with Luxol fast blue. Both longitudinal and cross sections of nerves were then examined and photographed using a Nikon Eclipse E600 microscope with a SPOT camera with Windows TM version 4.09 software (RTSlider Diagnostic Instruments, Inc., Sterling Heights, MI). Nerves stained with hematoxylin and eosin were examined for cellular infiltrates and axonal degeneration. Nerves stained with Luxol fast blue were examined for myelin damage.

The other leg (right) with the exposed nerve was placed in 30% sucrose for up to one week and then placed in a plastic cassette, covered with OCT compound, and frozen at  $-80^{\circ}\text{C}$  to be saved for immunohistochemistry.

For Experiment 3, the dissection process was extended to remove the entire sciatic nerve up to and including the nerve root (L3–L5); the brain and the spinal cord were dissected and preserved separately. After removal of internal organs, the skin, and muscle along the sciatic nerve on both legs were removed to expose the sciatic nerve. The sciatic nerve was followed up to the spinal column and the vertebral bone removed to expose the nerve root. The dorsal portion of the vertebral column over the spinal cord was snipped off with Student Vannas Spring scissors (Fine Science Tools, Foster City, CA, USA) to expose the cord. The brain was removed by removing the dorsal surface of the skull and transecting the cranial nerves at the base. Then the mouse carcass with exposed nerves, spinal cord, and brain was placed in 10% buffered formalin for 24

hours and then transferred to 60% ethanol until further nerve preparation could be performed. After fixation, the dorsal root ganglia were exposed and removed, ensuring that the L4 nerve root was included. The sciatic nerve was then removed starting from the spinal cord all the way to anterior tibial nerve at the tarsus of the mouse. Finally the brachial plexus nerves at the foreleg were removed in their entirety as a group. All nerves were placed in a cassette and kept in 60% ethanol until paraffin embedment and analysis as described above for Experiment 2. During embedment, nerves were placed in longitudinal orientation to facilitate analysis. Sciatic nerves, dorsal root ganglia, and the brachial plexus sections were stained with either Luxol fast blue or hematoxylin and eosin. Sections were observed and imaged with a Nikon Eclipse E600 microscope with a SPOT camera (RTSlider Diagnostic Instruments, Inc., Sterling Heights, MI).

### **Nerve Histology Criteria**

The criterion for scoring nerve lesions were developed by 2 veterinary pathologists (BJG, JSP) and critiqued by a human pathologist (HTC). Specific features were evaluated on hematoxylin and eosin (H&E) stained sections and Luxol fast blue stained sections as follows. The H&E stained nerve root sections were evaluated for inflammatory infiltrate severity (0=normal, 1=mild infiltrate, 2=moderate infiltrate, and 3=marked infiltrate), distribution (scattered, clustered), and composition (lymphocytes, plasma cells, macrophages, neutrophils, eosinophils, and mast cells). The H&E stained sciatic nerve and brachial plexus nerve sections were evaluated in a similar manner except that the distribution of cells was scored as perivenular, endoneurial, perineurial, epineurial, and intramuscular. The H&E stained sciatic nerve sections were evaluated

for myelin sheath loss (0=not present, 1=mild in 0–30% of section, 2=moderate in 30–60% of the section and 3=severe in greater than 60% of the section). All histological sections were scored by a single board certified veterinary pathologist (BJG) who was blinded to the identities and experimental groups of the individual mice. Blinding of slides and data analyses were performed by a second investigator (JLS).

### **Immunohistochemical Staining (IHC)**

We examined the sciatic nerves for infiltration of T cells and macrophages using IHC. Nerves were removed, fixed, embedded, and sectioned as previously described above. Serial sections 3–5  $\mu\text{m}$  thick were cut, attached to silanized glass slides and stained for either CD3 (polyclonal, ab5690, abcam Cambridge, MA) or F4/80 (BM8, eBiosciences San Diego, CA). Sections were deparaffinized in 2 changes of xylene and rehydrated in a graded alcohol series. Sections were then incubated in 1% hydrogen peroxide in tris-buffered saline (TBS; pH 7.4) to block endogenous peroxidase. Subsequently the sections for CD3 were boiled for 15 minutes in citrate buffer (Vector Laboratories, Burlingame, CA); the F4/80 sections were incubated at 37°C for 15 minutes in Proteinase K antigen retrieval solution. The sections were blocked for 1–3 hours at room temperature with 1% bovine serum albumin (Sigma Aldrich, St. Louis, MO) +1.5% goat serum (Vector Laboratories, Burlingame, CA) in TBS 0.025% Triton X-100 (Sigma Aldrich, St. Louis, MO) and then incubated with the primary antibody at 4°C overnight. Sections were then washed twice and stained with the Vectastain ABC kit (Vector Laboratories, Burlingame, CA) for CD3 or rat on mouse HRP polymer kit (Biocare Medical, Concord, CA) for F4/80. The sections were developed with Impress

Nova Red kit (Vector Laboratories, Burlingame, CA), counterstained, differentiated, dehydrated and mounted with Permount™ (Sigma Aldrich, St. Louis, MO, USA).

Sections were observed and imaged using a Nikon Eclipse E600 microscope with a SPOT camera (RTSlider Diagnostic Instruments, Inc., Sterling Heights, MI).

## **Statistical Analyses**

Statistical analyses were performed using GraphPad Prism version 6.01 (GraphPad Software Inc., La Jolla, CA, USA). Analyses of results of the open field test, hang test, and rotarod phenotype tests in all experiments were done using two-way ANOVA with repeated measures followed by the Holm-Sidak multiple comparisons test if significance was obtained in the two-way ANOVA. If the assumption of normality was not met for the two-way ANOVA with repeated measures, data were transformed using the square root function, which resulted in the normality assumption being met. The assumption of equal variance was met as well. In Experiment 1, the footprint measurements stride length and hind base width were not analyzed with a two-way ANOVA with repeated measures because there were too many missing data points caused by individual mice refusing to perform the test at one or more time points during the experimental time span. These measurements were evaluated using a one-way ANOVA at each individual time point; if assumptions were not met, then a non-parametric Kruskal-Wallis ANOVA on ranks was used. In Experiment 2, few mice had missing data points during the experimental time span. To allow the repeated measures ANOVA to be performed, mice that did not have a complete set of measurements during the entire experiment were removed from the data set; the removal of mice

resulted in slightly smaller group sizes. This test was followed with the Holm-Sidak test if significance was obtained.

For evaluations that did not have time as a factor (histological scoring, ELISA, IHC), one-way ANOVA was used followed by the Holm-Sidak post hoc test. This approach was applied in Experiments 1 and 3. If normality and equal variance assumptions for one-way ANOVA were not met, then the non-parametric Kruskal-Wallis ANOVA on ranks was used followed by Dunn's post hoc multiple comparison test. Data for Experiment 2 were analyzed with the non-parametric Mann-Whitney *U* test, comparing uninfected mice to infected mice within each genotype. The Fisher Exact test was used to examine any cell types present in the nerve.

Stride length and hind base width measurements taken digitally by the DigiGait™ apparatus in Experiment 3 were not analyzed because there were too many missing data points. A clinical observation scoring system was developed for the raw DigiGait™ videos (Table 2.1), and results were analyzed using two-way ANOVA with repeated measures to examine only mice that were videotaped at every time point for the entire length of the experiment. Spearman's rank/ordinal correlation was used to examine the correlation of the clinical assessment of the DigiGait™ videos to the GI histological scores of the mice using the software, PAST version 1.89 (Øyvind Hammer, Oslo, Norway).

## RESULTS

### Selection of Mice for Analysis

NOD WT, NOD IL-10<sup>-/-</sup>, and NOD B7-2<sup>-/-</sup> mice were bred in a specific-pathogen free facility and tested by PCR to confirm genotype and to be free of the known colitogenic bacteria, *Campylobacter* spp., *Helicobacter* spp., *Citrobacter rodentium*, *Enterococcus faecalis*, and *E. faecium* as previously described (98). Preliminary and published results have shown that NOD B7-2<sup>-/-</sup> mice do not develop spontaneous neuropathy prior to 20 weeks of age (Gadsden, unpublished data) (13, 130); in all experiments, mice were used prior to 20 weeks of age. Mice that developed diabetes, prolapsed rectum, or died of respiratory failure after accidental inhalation of the inoculum during oral gavage in any experiment were removed from analysis. In the three experiments combined, there were 2/28 and 2/28 NOD WT mice that developed diabetes or respiratory disease respectively. Of the NOD IL-10<sup>-/-</sup> mice, 11/100 and 2/100 mice developed prolapsed rectums or respiratory failure respectively, both of which resulted in early euthanasia. Two mice (1/28 NOD WT and 1/28 NOD B7-2<sup>-/-</sup>) were removed from analysis due to failure to detect colonization by *C. jejuni* HB93-13 by either culture or PCR.

Body weight was also analyzed at the end of all experiments; we found no significant differences between treatment groups within each genotype using Kruskal-Wallis ANOVA on ranks test for Experiments 1 and 3 (data not shown) and Mann-

Whitney *U* for Experiment 2 (data not shown). Therefore we concluded body weight played no role in the examination of footprints.

### **Experiment 1: Screening mice of various NOD genotypes for GBS following *C. jejuni* infection**

#### *Experimental screen for GI disease with GBS-associated *C. jejuni* strains*

Colonization was determined by culture of GI tract tissue and/or *C. jejuni* specific PCR. As seen in Figure 2.1, panel A, all of the sham-inoculated control mice were negative by cecum culture and negative for *C. jejuni* specific PCR on DNA extracted from cecum tissue. Four of nine NOD WT, 7/10 NOD IL-10<sup>-/-</sup>, and 4/9 NOD B7-2<sup>-/-</sup> mice infected with *C. jejuni* HB93-13 were colonized. All NOD WT and NOD IL-10<sup>-/-</sup> mice infected with *C. jejuni* 260.94 were colonized as detected by culture and/or PCR. Nine of ten NOD B7-2<sup>-/-</sup> mice were colonized in the cecum by *C. jejuni* 260.94.

Three mice inoculated with *C. jejuni* HB93-13, one mouse of each genotype, had to be euthanized early due to high scores for clinical GI disease. Two NOD IL-10<sup>-/-</sup> mice, both in the *C. jejuni* 260.94 infection group, had to be euthanized early for high clinical scores of GI disease.

At necropsy, mice were examined for the following gross pathological changes: enlarged ileocecolic lymph nodes and thickened wall of gastrointestinal tract (Figure A-1, panel A). Four of nineteen *C. jejuni* infected NOD WT mice, 16/18 NOD IL-10<sup>-/-</sup> mice, and 4/19 NOD B7-2<sup>-/-</sup> mice exhibited gross pathological changes in the GI tract.

In addition, 4 sham-inoculated NOD IL-10<sup>-/-</sup> mice exhibited spontaneous colitis, as expected in IL-10 deficient mice. These 4 mice were not colonized with either strain of *C. jejuni* as confirmed by culture and PCR. No sham-inoculated NOD WT mice or NOD B7-2<sup>-/-</sup> mice exhibited gross pathological changes in the GI tract.

Most NOD IL-10<sup>-/-</sup> mice infected with both *C. jejuni* HB93-13 and *C. jejuni* 260.94 had pronounced gross pathological changes in the GI tract. More NOD B7-2<sup>-/-</sup> mice in the *C. jejuni* HB93-13 infection group had gross pathological changes than B7-2<sup>-/-</sup> mice in the *C. jejuni* 260.94 infection group. Mice in the NOD WT *C. jejuni* 260.94 and *C. jejuni* HB93-13 infection groups had similar levels of gross pathological changes in the GI tract (Figure A-1, panel A).

At necropsy the ileoceccocolic junction was removed, fixed, stained, and scored as previously described (98). Kruskal-Wallis ANOVA on ranks was used to analyze the histology scores; no significant differences were found between treatment groups within any of the three genotypes (Figure A-1, panel B). As with the gross pathological changes, the NOD IL-10<sup>-/-</sup> mice exhibited the highest GI histology scores, as did the *C. jejuni* HB93-13 infected NOD WT mouse that was euthanized early due to GI disease.

#### *Detection of anti-ganglioside antibodies*

ELISA assay results were statistically tested using one-way ANOVA followed by the Holm-Sidak post hoc test if a significant result was obtained in the ANOVA. When

normality and equal variance assumptions were not met for one-way ANOVA, the non-parametric Kruskal-Wallis ANOVA on ranks was used followed by Dunn's post hoc test.

Plasma samples obtained on days 0 and 14 were analyzed for the presence of anti-ganglioside GM1 and GD1a antibodies using ELISA assays. Only small amounts of blood can be taken from mice at these time points, so two ELISA assays were done. Mouse IgM was tested for anti-GM1 activity, and mouse IgG1 was tested for anti-GD1a activity. At days 0 and 14, no significant differences were found between the control and infected mice in levels of plasma IgM reactive to ganglioside GM1 and IgG1 reactive to ganglioside GD1a in the NOD WT, NOD IL-10<sup>-/-</sup>, and NOD B7-2<sup>-/-</sup> genotypes (Figure A-2, panels A and B). ELISA assays were performed at endpoint for the presence of anti-*C. jejuni* IgG2b antibody to verify the development of adaptive immune responses to *C. jejuni*. ELISA assays were also performed at endpoint for the presence of (1) anti-GD1a IgG1, IgG2a, and IgG3 antibodies, (2) anti-GM1 IgG1, IgG2a, IgG3, and IgM antibodies, and (3) anti-GQ1b IgG1, IgG2a, and IgG3 antibodies (Figure A-2, panels C and D; GQ1b data not shown). Further ELISA assays were performed at endpoint for the presence of IgG1 antibodies reactive with two mixtures of gangliosides: a GM1/GQ1b mixture and a GM1/GD1a mixture.

Significant differences between the treatment groups within all mouse genotypes at endpoint were found for IgG2b reactive with crude *C. jejuni* antigen (Kruskal-Wallis; NOD WT: p=0.0004, NOD IL-10<sup>-/-</sup>: p=0.0001 and NOD B7-2<sup>-/-</sup>: p<0.0001). Dunn's multiple comparison test demonstrated significant differences between the sham-inoculated and both the *C. jejuni* HB93-13 and *C. jejuni* 260.94 inoculated groups in all three genotypes as seen in Figure 2.1, panel B-1. No significant differences were found

for any of the gangliosides tested individually. A significant difference was found between IgG1 antibody levels in NOD WT uninfected mice and mice infected with *C. jejuni* 260.94 for the mixture of gangliosides GM1/GQ1b (one-way ANOVA;  $p=0.0100$ ). The Holm-Sidak post hoc test was used and a significant difference in plasma levels of IgG1 antibody to the ganglioside mixture GM1/GQ1b was found between the sham-inoculated and the *C. jejuni* 260.94 infected NOD WT mice ( $p \leq 0.01$ ) as noted in Figure 2.1, panel B-2. All other mouse genotypes had no significant differences in plasma levels of IgG1 antibody to the mixture of gangliosides GM1/GQ1b; NOD WT mice infected with *C. jejuni* HB93-13 also displayed no significant differences in levels of IgG1 antibody reactive with ganglioside mixture GM1/GQ1b. Levels of IgG1 antibody reactive with ganglioside mixture GM1/GD1a in sham-inoculated and *C. jejuni* infected mice were not significantly different in any of the three genotypes (Figure A-2 panel E).

#### *Neurological phenotype testing*

Statistical analyses for the open field test (examination of abnormal gait) and hang test (muscle strength) were performed with two-way ANOVA with repeated measures followed by the Holm-Sidak post hoc test for multiple comparisons. If the normality assumption was not met, data were transformed using the square root function. In the two-way ANOVA with repeated measures we tested for both (1) differences between treatment groups of the same genotype (discussed below) and (2) changes in the genotype over time (Table 2.2). The occurrence of significant differences within the treatment groups occurring over the course of the experimental time period was a general phenomenon in all phenotypic tests and will not be discussed further.

The stride length and hind base width footprint data sets (detection of gait abnormalities including foot dragging) for all mouse genotypes had many missing data points and therefore one-way ANOVA or Kruskal-Wallis ANOVA on ranks at each time point was performed.

***NOD WT mice.*** NOD WT infected mice had significant differences from the sham-inoculated control mice in the open field test, hang test, and hind base width.

Analysis of the open field test data (Figure 2.1, panel C) indicated significant differences between the treatment groups of the NOD WT mice (two-way ANOVA RM;  $p=0.0048$ ). Post hoc pairwise Holm-Sidak multiple comparison tests indicated significant differences between NOD WT sham-inoculated mice and *C. jejuni* HB93-13 infected mice at the 2-, 3-, and 6- week time points (wk2  $p\leq 0.01$ , wk3  $p\leq 0.05$ , wk6  $p\leq 0.01$ ). Holm-Sidak post hoc tests also indicated significant differences between sham-inoculated mice and *C. jejuni* 260.94 infected mice at weeks 2, 3, and 6 (wk2  $p\leq 0.05$ , wk3  $p\leq 0.05$ , wk6  $p\leq 0.01$ ).

Analysis of the hang test data (Figure 2.1, panel D) detected significantly different hang test times between the uninfected NOD WT mice and both the *C. jejuni* HB93-13 and *C. jejuni* 260.94 infected NOD WT mice (two-way ANOVA RM;  $p=0.0083$ ). Sham-inoculated mice had significant differences from those infected with *C. jejuni* 260.94 at weeks 1 and 3 of the experiment (Holm-Sidak post hoc pairwise multiple comparisons test; wk1  $p\leq 0.05$ , wk3  $p\leq 0.01$ ). Qualitative examination of the data shows that there was a decrease in hang time of most treatment groups at week 1; this observation could indicate that a longer training time was needed for this test. It was also observed that the NOD WT *C. jejuni* 260.94 infected mice followed a similar pattern

over time as the sham-inoculated mice and *C. jejuni* HB93-13 infected mice, but never had hang times as high as these treatment groups.

Footprint measurements of stride length and hind base width were analyzed with one-way ANOVA at each weekly time point; Holm-Sidak post hoc tests were used if significant results were indicated in the ANOVA (Figure A-3, panel B). No significant changes between the treatment groups were observed in the stride length data at any time point. Hind base width data showed significant changes between all the treatment groups at week 6 (one-way ANOVA;  $p=0.0494$ ). The post hoc test, Dunn's, indicated no significant changes between any 2 treatment groups.

***NOD IL-10<sup>-/-</sup> mice.*** Significant differences between the treatment groups were found in stride length measurements. No other test indicated any significant changes in treatment groups.

The open field test data (Figure A-3, panel A-1) showed no significant differences between the treatment groups. Analyzing the hang test time of the *NOD IL-10<sup>-/-</sup>* mice revealed no significant differences between the treatment groups. The sham-inoculated mice and *C. jejuni* HB93-13 infected mice both were qualitatively observed to have a decrease in hang time at week 1; this phenomenon did not occur in the *C. jejuni* 260.94 infected mice (Figure 2.1 panel D). This occurrence was also noted in the *NOD WT* above.

Footprint patterns (Figure A-3, panel C) were measured for stride length and hind base width and one-way ANOVA was performed at each time point. Significant differences in stride length were found between the treatment groups at weeks 4, 5, 6, and 8 (one-way ANOVA; wk4  $p=0.0363$ , wk5  $p=0.0298$ , wk6  $p=0.0054$ , wk8  $p=0.0042$ ).

Pairwise analysis indicated significant differences between the sham-inoculated mice and the *C. jejuni* 260.94 infected mice at weeks 5, 6, and 8 (Holm-Sidak; wk5  $p \leq 0.05$ , wk6  $p \leq 0.01$ , wk8  $p \leq 0.01$ ). Mice infected with *C. jejuni* HB93-13 and sham-inoculated mice had significant differences in stride length at weeks 6 and 8 (Holm-Sidak; wk6  $p \leq 0.05$  and wk8  $p \leq 0.01$ ). The hind base width data analysis showed no significant differences between the infected mice and the uninfected mice.

***NOD B7-2<sup>-/-</sup>* mice.** Significant differences between the treatment groups were observed in the hang test, stride length, and hind base width.

Two-way ANOVA with repeated measures analysis of the number of quadrants crossed in the open field test indicated no significant changes between the treatment groups of this genotype (Figure A-3, panel A-2). Qualitative examination of the data shows that mice infected with both *C. jejuni* HB93-13 and *C. jejuni* 260.94 exhibited an increase from a small number of quadrants crossed (weeks 2–3) to a higher number crossed (weeks 4–6) and back to a smaller number of quadrants crossed (weeks 7–8) during the course of the experiment.

Analysis of hang test data (Figure 2.1 panel D) with two-way ANOVA with repeated measures indicated significant differences between the treatment groups of the *NOD B7-2<sup>-/-</sup>* mice (two-way ANOVA RM;  $p = 0.0353$ ). Post hoc pairwise analysis indicated that significant differences between sham-inoculated mice and *C. jejuni* 260.94 infected mice occurred at week 1 of the experiment (Holm-Sidak;  $p \leq 0.05$ ). Qualitative examination of these data showed that there was a decrease in hang time occurring at week 1 in all treatment groups. This was noted previously in the other 2 genotypes and therefore suggests a longer training time was needed for this test.

Stride length and hind base width measurements were analyzed using one-way ANOVA at each time point (Figure A-3, panel D). Significant differences in stride length occurred between treatment groups at the 1- and 3- week time points (one-way ANOVA;  $p=0.0248$  and  $p=0.0085$  respectively). Pairwise analysis indicated significant differences between the sham-inoculated mice and the *C. jejuni* HB93-13 infected mice at week 3 (Holm-Sidak;  $p\leq 0.01$ ). Analysis of the hind base width measurements indicated significant changes in hind base width between the treatment groups at week 1 (one-way ANOVA;  $p=0.0157$ ). Holm-Sidak post hoc tests indicated significant differences between the sham-inoculated mice and the *C. jejuni* HB93-13 infected mice ( $p\leq 0.05$ ) and between the sham-inoculated mice and *C. jejuni* 260.94 infected mice ( $p\leq 0.05$ ).

## **Experiment 2: Screening larger group sizes of NOD WT and NOD B7-2<sup>-/-</sup> mice for GBS**

### *Experimental screen for GI disease with GBS-associated C. jejuni strains*

Colonization of mice with *C. jejuni* 260.94 was determined by culture of GI tract tissue fragments and/or PCR (Figure 2.2, panel A-1). All *C. jejuni* 260.94 infected mice of both NOD WT and NOD B7-2<sup>-/-</sup> genotypes were colonized. One *C. jejuni* 260.94 infected NOD B7-2<sup>-/-</sup> mouse was negative by culture, but positive by PCR. All sham-inoculated mice of both NOD WT and NOD B7-2<sup>-/-</sup> genotypes were negative for *C. jejuni* 260.94 by culture and/or PCR.

At necropsy, gross pathological changes in the GI tract were recorded Figure 2.2, panel A-2; these changes were thickened wall of the GI tract and enlarged lymph nodes. Gross pathological features in *C. jejuni* 260.94 infected mice were minimal; only 4/18 NOD WT mice and 1/18 NOD B7-2<sup>-/-</sup> mice exhibited a single gross pathology feature. All other mice had no gross pathological changes in the GI tract.

One mouse from the NOD WT *C. jejuni* 260.94 group had to be euthanized early due to a high clinical sign score for GI disease; this mouse still only presented a single gross pathological feature on necropsy.

At the end of the experiment (80 days), the ileoceocolic junction was examined histologically and scored by a single blinded investigator (LSM) (100). Non-parametric Kruskal-Wallis ANOVA on ranks indicated no significant difference between histological scores of infected and uninfected mice of either genotype (Figure B-1).

#### *Detection of anti-ganglioside antibodies*

ELISA data were analyzed using the non-parametric Mann-Whitney *U* test to compare uninfected mice to *C. jejuni* 260.94 infected mice within each genotype. ELISA assays were performed on plasma samples obtained at days 0 and 14 to test for the presence of IgM antibodies reactive with ganglioside GM1 and IgG1 antibodies reactive with ganglioside GD1a. On day 0, NOD WT mice that were going to be sham-inoculated had significantly lower levels of anti-GM1 IgM than NOD WT mice that were going to be inoculated with *C. jejuni* 260.94 ( $p=0.0229$ ). This significant difference observed at day 0 was the result of a few low values (3 of 17 mice). When these mice were removed from analysis the significant differences were no longer observed. All other ELISA tests

at both day 0 and day 14 showed no significant differences between groups (Figure B-2, panels A and B).

ELISA assays for anti-*C. jejuni*, -GM1, -GD1a, -GQ1b, and ganglioside mixtures GM1/GD1a and GM1/GD1a were performed at the endpoint of experiment (80 days) as in Experiment 1. Significant differences were found in levels of anti-*C. jejuni* IgG2b antibody in both NOD WT and NOD B7-2<sup>-/-</sup> mice when infected mice were compared to congenic uninfected mice (Figure B-2, panel C; Mann-Whitney *U*;  $p < 0.0001$  for both genotypes). Significantly different levels of IgG3 anti-ganglioside GD1a between infected and uninfected mice were found for both mouse genotypes (Figure 2.2, panel B-1; NOD WT:  $p = 0.0296$ ; NOD B7-2<sup>-/-</sup>:  $p = 0.0395$ ). Analyses of data from ELISA assay for antibodies reactive with the other individual gangliosides indicated no significant differences (Figure B-2, panels D-E; ganglioside GQ1b not shown). *C. jejuni* 260.94 infected NOD WT mice had significantly higher levels of IgG1 reactive with the mixture of gangliosides GM1 and GQ1b (Figure 2.2, panel B-2; Mann-Whitney *U*;  $p = 0.0351$ ); NOD B7-2<sup>-/-</sup> mice did not. No significant differences were detected in levels of IgG1 antibody reactive with the mixture of gangliosides GM1 and GD1a in either mouse genotype (Figure B-2, panel F).

### *Neurological phenotype testing*

Statistical analyses for the open field test, hang test, and rotarod were performed using two-way ANOVA with repeated measures; if significant differences between the uninfected mice and infected mice were observed, the ANOVA was followed with the

post hoc Holm-Sidak test. The footprint measurements of stride length and hind base width were analyzed with two-way ANOVA with repeated measures with the removal of any mice that did not have a measurement for a characteristic for every time point during the experiment. Only 4 mice were removed from the stride length measurement; none were removed for hind base width. Any significant changes within the treatment groups that occurred over the course of the experimental time are shown in Table 2.2 and will not be discussed any further as it was a general phenomenon.

***NOD WT mice.*** No significant changes between the uninfected mice and *C. jejuni* 260.94 infected mice were observed in any of the phenotypic tests below.

Data from the open field test, which is used to determine the presence of gait abnormalities and overall well-being of mice, had no significant differences in the number of quadrants crossed between treatment groups. As can be seen in Figure 2.2, panel C-1, there was high variability in the NOD WT *C. jejuni* 260.94 mice which resulted from a “circling” mouse in that group. NOD mice often exhibit an obsessively circling phenotype. The same mouse caused the high variability throughout the entire experiment. Removal of this mouse from the analysis did not affect the statistical non-significance of changes over time seen in the NOD WT mice.

The hang test (Figure B-3, panel A-1) was used to assess muscle strength and gripping ability of the mice. No significant differences were found in the NOD WT mice between the treatment groups. Nevertheless, most NOD WT mice infected with *C. jejuni* 260.94 had shorter hang times than uninfected NOD WT mice at week 4, slightly later than seen in Experiment 1.

Only one NOD WT sham-inoculated mouse had to be removed from the stride length measurements from lack of footprint patterns for the entire course of the experiment (Figure B-3, panel B). There were no significant changes in the stride length between treatment groups. There were also no significant changes in hind base width observed between treatment groups; no mice had to be removed for this analysis.

Use of a rotarod was introduced in this experiment; this apparatus is used to detect changes in balance and motor capability of mice. NOD WT sham-inoculated and *C. jejuni* 260.94 mice showed no significant change in the time spent on the rotarod between treatment groups (Figure 2.2, panel D-1). There was a statistically non-significant but qualitatively noticeable trend occurring within the *C. jejuni* 260.94 infected mice; most of these mice remained on the rotarod for shorter lengths of time than uninfected mice at 7 of 11 time points after inoculation.

***NOD B7-2<sup>-/-</sup> mice.*** Data analyses indicated significant differences between the uninfected mice and the *C. jejuni* 260.94 infected mice in the open field test and hind base width measurements.

NOD B7-2<sup>-/-</sup> mice had significant differences over time between the treatment groups of number of quadrants crossed (Figure 2.2, panel C-2; p=0.0299). However, no significant differences were noted at any particular time point using a pairwise test.

Analysis of the hang test data indicated no significant differences between the treatment groups of the NOD B7-2<sup>-/-</sup> mice. Data shown in Figure B-3, panel A-2.

To assess the stride length measurements of the NOD B7-2<sup>-/-</sup> mice, 1 sham-inoculated mouse and 2 *C. jejuni* 260.94 infected mice had to be removed from the data

set because they lacked complete footprint patterns for the course of the experiment. No significant changes in stride length occurred between the treatment groups (Figure B-3, panel C-1). Analysis of hind base width data indicated significant differences between the sham-inoculated mice and the mice infected with *C. jejuni* 260.94 (two-way ANOVA RM;  $p=0.0498$ ); pairwise tests indicated significant differences between the infected and uninfected mice occurring at week 11 of the experiment (Figure B-3, panel C-2; Holm-Sidak;  $p\leq 0.001$ ).

Analysis of rotarod data indicated no significant changes in the time spent on the cylinder between the treatment groups of NOD B7-2<sup>-/-</sup> mice. As seen in the NOD WT *C. jejuni* 260.94 mice, there was a qualitative trend toward shorter times spent on the rotarod at 10 of 11 time points after inoculation in the NOD B7-2<sup>-/-</sup> infected mice (Figure 2.2 panel D-2).

To determine whether this phenomenon of a decrease in time on the rotarod was limited to mice of the NOD genetic background, a control experiment with uninfected C57/BL6 WT and C57BL/6 IL-10<sup>-/-</sup> mice was performed for the same length of time. Both genotypes of C57/BL6 mice experienced a decrease in time spent on the rotarod over the course of 84 days (Figure D-1). This suggests that decrease of time spent on the rotarod over the experimental period is not limited to mice of the NOD genetic background. Most importantly, neurological disease can still be examined by comparison of the treatment groups.

*Presence of nerve lesions and detection of cellular infiltrates*

At endpoint the sciatic nerve was removed from the mouse to be fixed, stained and examined histologically. The nerves were stained with both H & E to examine for cellular infiltrates and Luxol fast blue (LFB) to examine for myelin damage. The nerves were scored blinded and unbiased by a board-certified pathologist (BJG). Cellular infiltrates, most commonly mast cells and lymphocytes, were observed in the nerve sections of some mice. However, no significant differences in the presence of mast cells or lymphocytes between the infected mice and the uninfected mice in either the NOD WT or the NOD B7-2<sup>-/-</sup> mice were detected by the Fisher Exact test. Histological scores (see Materials and Methods) were analyzed with non-parametric Mann-Whitney *U* test to identify any significant changes between treatment groups within each genotype. No significant results were observed between treatment groups in either the NOD WT mice or NOD B7-2<sup>-/-</sup> mice (Figure B-4). One *C. jejuni* 260.94 infected NOD B7-2<sup>-/-</sup> mouse did exhibit cellular infiltrates (mast cells, lymphocytes, neutrophils, and plasma cells) as well as myelin damage as seen in Figure 2.3.

Immunohistochemical staining was performed on sections of the sciatic nerve to examine them for the presence of T cells and macrophages. Since the nerve is so small and frail, only a subset of each treatment group could be analyzed depending on whether or not any nerve tissue remained in the paraffin block after sectioning for hematoxylin and eosin and Luxol fast blue staining. There were no significant differences in the presence of T cells between infected and uninfected mice of either genotype; however, the difference between infected and uninfected NOD B7-2<sup>-/-</sup> mice approached significance (Mann-Whitney *U*;  $p=0.0698$ ). Staining for macrophages

showed significant differences between infected and uninfected NOD WT mice (Mann-Whitney  $U$ ;  $p=0.0289$ ) but not between infected and uninfected NOD B7-2<sup>-/-</sup> mice as seen in Figure 2.4. Infiltration of macrophages in the NOD WT *C. jejuni* infected mice is shown in Figure 2.5.

### **Experiment 3: Examination of NOD IL-10<sup>-/-</sup> mice using antibiotics to treat enteritis**

#### *Experimental screen for GI disease with GBS-associated C. jejuni 260.94*

Colonization was determined at the end of the 84 day experiment by detection of *C. jejuni* in the GI tract of the mouse by culture and/or PCR (Figure C-1, panel A). Twenty six mice were colonized with *C. jejuni* 260.94 and two of twenty-eight mice infected with *C. jejuni* and not treated with chloramphenicol (CMP) were found to be negative for the bacteria. In the *C. jejuni* + CMP group, 13/17 mice were not colonized at the conclusion of the experiment. Fourteen of sixteen mice in the sham-inoculated group and 19/19 mice in the sham-inoculated and CMP-treated group were negative by culture and/or PCR. Two mice in the sham-inoculated group thought to be culture positive were determined to be negative for *C. jejuni* 260.94 based on PCR confirming that the colonies observed by culture were not campylobacters.

Two gross pathological features in the GI tract were noted: thickened GI wall and presence of enlarged ileocecal lymph nodes (Figure 2.6, panel A). Six of sixteen sham-inoculated mice, 22/28 *C. jejuni* 260.94 inoculated mice, 10/19 sham-inoculated and CMP-treated mice, and 14/17 *C. jejuni* 260.94 inoculated and CMP-treated mice presented with pathological features. A subset of mice that presented with gross

pathological features in all treatment groups presented with both thickened GI wall and enlarged lymph nodes (3/6 sham-inoculated, 19/22 *C. jejuni* 260.94 inoculated, 4/10 sham-inoculated and CMP-treated, and 9/14 *C. jejuni* 260.94 inoculated and CMP-treated mice). *C. jejuni* inoculated and CMP-treated mice had levels of gross pathological change similar to those mice that received *C. jejuni* only. Some sham-inoculated mice and sham-inoculated and CMP-treated mice presented with gross pathological features from spontaneous colitis that is common in IL-10 deficient mice (132).

Two of twenty-eight *C. jejuni* 260.94 infected mice were euthanized early for high clinical scores for enteric disease. No other mice were euthanized early due to high clinical scores for GI disease.

Analysis of histological scores of GI disease showed no significant differences between groups using Kruskal-Wallis ANOVA on ranks; mice in all treatment groups exhibited high histology scores (Figure C-1, panel B). Spontaneous colitis is expected in NOD IL-10<sup>-/-</sup> mice and accounts for the marked gross pathological changes and high GI histological scores seen in both sham-inoculated and the sham-inoculated and CMP-treated mice.

#### *Detection of anti-ganglioside antibodies*

Data from ELISA assays were analyzed using one-way ANOVA; if significant differences were obtained, the post hoc Holm-Sidak test was used. If assumptions of normality and equal variance were not met, Kruskal-Wallis ANOVA on ranks was used with post hoc Dunn's tests if significant differences were noted.

Levels of antibodies reactive with single and mixed gangliosides (GM1, GD1a and GQ1b; GM1/GQ1b and GM1/GD1a) were determined at the endpoint of the experiment (84 days). Anti-*C. jejuni* IgG2b levels were also tested and significant differences were obtained using Kruskal-Wallis ANOVA on ranks (Figure C-2, panel A;  $p < 0.0001$ ). Dunn's post hoc tests indicated significant differences in anti-*C. jejuni* IgG2b levels between the following groups: (1) the sham-inoculated mice and mice infected with *C. jejuni* 260.94 only ( $p \leq 0.0001$ ), (2) mice infected with *C. jejuni* 260.94 only and sham-inoculated mice treated with CMP ( $p \leq 0.0001$ ), and (3) sham-inoculated mice treated with CMP and mice inoculated with *C. jejuni* 260.94 and treated with CMP ( $p \leq 0.01$ ).

Levels of anti-GD1a IgG1 and IgG3 antibodies were observed to be significantly different (Figure C-2, panels C-1 and C-3; Kruskal Wallis,  $p = 0.0030$  and  $p = 0.0421$  respectively). Dunn's pairwise post hoc tests indicated significant differences in levels of both IgG1 and IgG3 antibody reactive with ganglioside GD1a between the sham-inoculated mice and mice infected with *C. jejuni* 260.94 not treated with CMP (IgG1:  $p \leq 0.01$  IgG3:  $p \leq 0.05$ ). Plasma levels of anti-GQ1b IgG2a antibodies were significantly different (Figure C-2, panel D; Kruskal-Wallis,  $p = 0.0007$ ). Dunn's pairwise post hoc tests indicated significant differences in the anti-GQ1b levels of the *C. jejuni* 260.94 infected mice treated with CMP and (1) mice that were sham-inoculated ( $p \leq 0.001$ ), (2) *C. jejuni* 260.94 infected mice (not treated with CMP) ( $p \leq 0.001$ ), and (3) sham-inoculated mice treated with CMP ( $p \leq 0.001$ ). Significant differences in plasma levels of anti-GM1 IgG3 antibody were observed (Figure C-2, panel B-4; Kruskal-Wallis;  $p = 0.0217$ ); Dunn's

pairwise post hoc tests found significant differences in antibody level between the sham-inoculated mice and the sham-inoculated mice treated with CMP ( $p \leq 0.05$ ).

Levels of IgG1 antibodies reactive with the mixture of gangliosides GM1 and GQ1b were significantly different between the treatment groups (Figure 2.6, panel C-1; Kruskal-Wallis;  $p = 0.0017$ ). Dunn's post hoc tests indicated significant differences in anti-GM1/GQ1b IgG1 antibody levels between the sham-inoculated mice and mice given both *C. jejuni* 260.94 and CMP ( $p \leq 0.001$ ). IgG1 antibodies reactive with the mixture of anti-GM1/GD1a were found to be significantly different between the treatment groups (Figure 2.6, panel C-2; Kruskal-Wallis;  $p = 0.0332$ ). All other ELISA assay data are shown in Figure C-2, panels B-C; GQ1b data are only shown for antibody IgG2a.

### *Neurological phenotype testing*

Two-way ANOVA with repeated measures was used to analyze any significant changes occurring in mouse performance on the rotarod. Stride length and hind base width measurements were computed using the DigiGait™ software, but could not be analyzed using two-way ANOVA with repeated measures because of missing measurements. One-way ANOVA was not performed as in Experiment 1 because missing measurements made group sizes too small. Visual clinical assessment of DigiGait™ videos was performed by blinded and unbiased scientists (LSM and JAB). Each clinical feature noted in videos was given a score as described above in Materials and Methods (Table 2.1); scores for the individual clinical features were then summed for each mouse at each week. Results for mice that had videos for every time point during the experimental time were analyzed using two-way ANOVA with repeated

measures. Cumulative clinical assessment scores for the entire length of the experiment were correlated with the GI tract histological scores using Spearman's rank/ordinal correlation test to assess the possible influence of enteritis on the assessment of neurological signs.

**Rotarod.** This test was used to examine balance and motor function in mice. No significant differences in time spent on the rotarod wheel were observed between treatment groups. Both antibiotic treated and untreated mice infected with *C. jejuni* 260.94 were observed to have shorter times in weeks 5 and 6. As seen in Experiment 2, there was also a decrease in time on the rotarod throughout the entire experiment in mice of all four treatment groups (Figure 2.6 panel B).

**DigiGait™.** This phenotypic test was introduced in this experiment to replace the footprint analysis used in the previous two experiments. Mice were videotaped from underneath while walking on a clear treadmill belt, and gait analysis was then performed using proprietary software supplied with the apparatus. We were able to apply a visual clinical evaluation of neurological changes by watching the videos of the mice and scoring them as shown in Table 2.1.

*Stride Length and Hind Base Width.* These measurements could not be obtained for mice that either: (1) were uncooperative and unable to be assessed in a given week or (2) whose videos were recorded but were unable to be analyzed by the software. The large number of missing measurements resulted in failure of all statistical tests and therefore these data were not analyzed (data not shown). Mice that were uncooperative never developed neurological disease based on visual observation and rotarod data.

*Clinical Analysis.* Comparison of both the cumulative clinical scores given to mice based on any neurological phenotype noted in the videos captured by the DigiGait™ apparatus and the GI histological assessment resulted in no statistical association between the enteritis and neurological phenotypes either when all mice were considered together (Spearman's rank/ordinal correlation;  $p=0.87$ ) or when treatment groups were analyzed separately ( $p=0.77$  for *C. jejuni*-infected mice,  $p=0.41$  for *C. jejuni*-infected and CMP-treated mice;  $p=0.20$  for sham-inoculated mice, and  $p=0.42$  for sham-inoculated and CMP-treated mice) (Figure 2.6 panel D). The scores of each week for mice that had a video for the entire length of the experiment were analyzed with a two-way ANOVA with repeated measures and no significant changes within treatment groups were observed.

The heat map in Figure 2.7 is based on weekly clinical neurological scores of individual mice based on DigiGait™ videos using a reduced scale; only mice for which videos were obtained in all weeks are included. To construct the heat map, the features examined in the videos were simplified to stance abnormality, gait abnormality, and other (toe abnormality and general weakness). The additional feature of balance (rotarod time < 40 secs) was also included in the heat map. A mouse could present in one of 5 features: (1) no features, (2) 1 feature, (3) 2 features, (4) 3 features, or (5) all features, which are demonstrated by intensity of color in the heat map. The heat map thus summarizes the clinical histories of the individual mice. While mice of all treatment groups displayed neurological signs, these signs tended to be more severe and to persist longer in the three groups of treated mice than in sham-inoculated mice. Also, included in the heat map is a summary of mice positive or negative for anti-ganglioside

antibodies. Mice positive or negative for anti-ganglioside antibodies were determined by using two standard deviations from the mean of the control mice. As seen in the map two thirds of the mice infected with *C. jejuni* 260.94 and no treatment were positive for presence of anti-ganglioside antibodies. All other treatment groups had less than two thirds of mice positive for anti-ganglioside antibodies.

#### *Presence of nerve lesions and detection of cellular infiltrates*

At necropsy (84 days), the entire sciatic nerve, including the nerve root(s), was removed, fixed, and stained with hematoxylin and eosin for histologic examination of cellular infiltrates. The brachial plexus was also removed, fixed, and examined. Blinded slides were read by a single pathologist (BJG). In some of the samples, hematoxylin and eosin staining revealed rare macrophages with small, round, clear intracytoplasmic vacuoles; these will be confirmed with IHC staining of F4/80 for macrophages. The Fisher Exact probability test indicated no significant differences in the presence of vacuoles between treatment groups. None of the vacuoles were stained with Luxol fast blue, indicating that they did not contain myelin. In addition, Luxol fast blue staining did not indicate myelin loss. No significant differences were found between groups in scores derived from hematoxylin and eosin staining of nerve roots, sciatic nerve and brachial plexus (data not shown).

#### *Detection of macrophages in nerves*

The hematoxylin and eosin staining of the sciatic nerves did not indicate the presence of cells with T cell morphology in nerves of mice any of the treatment groups

and therefore immunohistochemical staining for T cells was not performed.

Macrophages in nerves were examined in mice from the TSB with no treatment group and the *C. jejuni* with no treatment group. Only a subset of mice from each group was analyzed because the nerve sections were very small and not all mice had nerve remaining on the paraffin block after the histological stains were performed. No significant differences in the infiltration of macrophages were seen in the sciatic nerve or brachial plexus. As seen in Figure 2.8, the nerve root did have significant differences of infiltration of macrophages between the uninfected mice and the infected mice (Mann-Whitney *U*;  $p= 0.0436$ ). Also, based on our results we were able to conclude that the vacuoles observed with hematoxylin and eosin were fat vacuoles and not macrophages.

## DISCUSSION

Small animal models are needed to explore pathogenesis, treatment, and prevention of GBS. *C. jejuni*-associated GBS in humans is characterized by production of anti-ganglioside antibodies, clinically evident impairment of the peripheral nervous system, and histological evidence of damage to peripheral nerves (7, 38, 72). We addressed our hypothesis by screening three inbred strains of NOD mice for susceptibility to these three autoimmune manifestations following a single oral inoculation with GBS-associated strains of *C. jejuni*. These *C. jejuni* strains were isolates from patients who developed GBS, thereby increasing the likelihood of mice developing neuropathy. The outcomes were assessed using ELISA, clinical scoring and neurologic assessment tools developed previously (22), and histopathological examination of nerve tissue.

Based on our findings we have concluded that NOD mice, specifically NOD WT mice, have the greatest potential to be a murine model of GBS disease following *C. jejuni* infection. All NOD mice developed anti-ganglioside antibodies and exhibited clinical neurological signs; however, the anti-ganglioside antibodies and their isotypes varied between mouse genotypes. There was also variation between mouse genotypes in the neurological clinical signs exhibited and it was difficult to demonstrate nerve damage in histological analysis of sections of nerves in all mouse genotypes.

Macrophage infiltrates in the nerve root of infected NOD WT and IL-10<sup>-/-</sup> mice were notable, but cellular infiltrates other than macrophages were not found to be significant in any mice infected with *C. jejuni* GBS isolates. It is clear that because of their small

size it is difficult to demonstrate nerve lesions in peripheral nerves of mice without preliminary studies to allow specialized techniques to be employed on the relevant structures.

### **Comparison of NOD mouse genotypes**

In our studies we were able to conclude that NOD WT, NOD IL-10<sup>-/-</sup>, and NOD B7-2<sup>-/-</sup> mice can all be colonized with either *C. jejuni* HB93-13 or *C. jejuni* 260.94. Mice infected with *C. jejuni* HB93-13 displayed severe gross pathological changes in the GI tract in the first experiment. Such changes could mask any neurological signs that were present. Severe gross pathological changes in the GI tract were also associated with enteric disease which resulted in early euthanasia of affected mice. For these reasons *C. jejuni* HB93-13 was discontinued in Experiments 2 and 3.

NOD WT mice are all colonized by *C. jejuni* but experience minimal enteritis, produce anti-ganglioside antibodies, and have a significant infiltration of macrophages in nervous tissue after infection with *C. jejuni* when compared to sham-inoculated mice. *C. jejuni* infected mice developed a strong reaction to *C. jejuni* bulk antigen reactive with IgG2b. These mice also had significant differences of IgG3 and IgG1 antibody reactive to ganglioside GD1a and ganglioside mixture GM1/GQ1b respectively, when compared to their uninfected counterparts. Significant differences between the uninfected mice and *C. jejuni* infected mice were detected in stride length and hind base width. The *C. jejuni* 260.94 infected NOD WT mice had significant differences in infiltration of the nervous tissue by macrophages, but did not exhibit significant differences in myelin damage in these nerves at the light microscopic level. One disadvantage of the NOD

WT mice is that they begin to develop diabetes with age; diabetes could result in decreased sample sizes in long-term experiments.

NOD IL-10<sup>-/-</sup> mice developed a strong immune response to *C. jejuni* and developed anti-ganglioside antibodies to individual gangliosides GM1 and GD1a. They also developed antibodies to a mixture of gangliosides GM1 and GQ1b and a mixture of GM1 and GD1a. Stride length and hind base width measurements also varied significantly between the sham-inoculated mice and those infected with either *C. jejuni* HB93-13 or *C. jejuni* 260.94. The NOD IL-10<sup>-/-</sup> mice also had a significant difference between the uninfected mice and infected mice in the infiltration of macrophages in the nerve root.

*C. jejuni* infected NOD IL-10<sup>-/-</sup> mice developed enteric disease in Experiment 1 and Experiment 3. Therefore in Experiment 3, a group of *C. jejuni*-infected mice was treated with chloramphenicol (CMP) in an attempt to prevent enteric disease from occurring and interfering with neurological assessments. Mice that received *C. jejuni* with CMP still exhibited severe gross pathological changes and high histological scores, similar to those seen in the mice infected with *C. jejuni* only; suggesting that the CMP may have changed the microbiota of the gut and caused GI irritation. Another explanation is that these IL-10 deficient mice exhibited the high GI histological scores and gross pathological features observed in the experiments because they were unable to down-regulate the inflammation initiated by *C. jejuni* infection. The high histological scores at the ileocecolic junction and high levels of gross pathological changes noted in the NOD IL-10<sup>-/-</sup> mice also demonstrate that an increase in damage to the gut does

not necessarily result in an increase in neurological clinical signs. The NOD IL-10<sup>-/-</sup> mice did exhibit significant differences between uninfected and infected mice with the presence of anti-ganglioside antibodies. However, to continue work with NOD IL-10<sup>-/-</sup> mice as a GBS model it would be advisable to use GBS strains that are less likely to elicit spontaneous colitis in order to keep enteric disease to a minimum to maintain the sample sizes. Alternately, immunizing these mice with *C. jejuni* LOS that mimics gangliosides could be performed to develop neurological disease without enteritis.

NOD B7-2<sup>-/-</sup> mice had significant differences in anti-GD1a antibody responses to IgG3 between the sham-inoculated mice and the *C. jejuni* 260.94 infected mice. There were also significant differences between the sham-inoculated mice and the infected mice in both the hang test and open field test. A potential disadvantage to the use of NOD B7-2<sup>-/-</sup> mice is that they develop spontaneous autoimmune peripheral neuropathy that resembles human GBS past 20 weeks of age. An extensive study was performed in our laboratory to examine the onset of neurological disease in our NOD B7-2<sup>-/-</sup> mice because the phenotype was not well described. Results indicated that NOD B7-2<sup>-/-</sup> mice do not develop neuropathy prior to 20 weeks of age (Gadsden, unpublished). Therefore, all experiments with these mice were ended prior to 20 weeks of age to prevent any overlap of the spontaneous neuropathy and neuropathy triggered by *C. jejuni* infection. This strategy of using these mice at a younger age must be advocated for future work on inducible GBS.

## Difficulties encountered and their resolutions

Some difficulties encountered were identifying the right ELISA assays to use, determining the proper phenotypic tests to use to assess neurological clinical signs, and finding the correct location of nerve lesions in the peripheral nervous system. Two studies by Kaida *et al.* (2004 and 2007) showed that sera from GBS patients that are negative for presence of individual anti-ganglioside antibodies can be positive for antibodies reactive with ganglioside mixtures (85, 86). As seen in Table 2.3, we saw low levels of anti-ganglioside antibodies reactive with individual gangliosides, so we examined presence of antibody reactive to a mixture of gangliosides and detected significant differences between uninfected and infected mice in antibody levels reactive with the mixtures of gangliosides.

We concluded that the DigiGait™ was sensitive enough to detect the subtle neurological changes that occurred; however, the speed (20 cm/sec) that we used in Experiment 3 was not fast enough to allow for consistent running of all mice. This resulted in the DigiGait™ software not being able to statistically analyze all videos; in other experiments we increased the belt speed to 30 or 40 cm/sec and obtained better results; (Gadsden; unpublished data). Data from our clinical evaluations indicated significant differences in neurological signs in the uninfected mice and infected mice, suggesting nerve lesions may be present. Only a small section of the nerve was removed in Experiment 2 and no lesions were detected, so we improved our technique in Experiment 3 by removing the sciatic nerve from the tarsus to the spinal nerve root and removed the brachial plexus; however, no significant differences were detected

between the uninfected mice and those infected with *C. jejuni*; this will be discussed below.

### **Future work**

In future experiments we will examine the neuromuscular junction (NMJ); it is highly enriched with gangliosides (157). It also does not have the blood-nerve barrier present at other sites along the nerves; therefore, antibodies reactive to the gangliosides have ready access to the NMJ (157).

Another strategy would be staining for components of the complement system associated with the nerve to detect sites of damage as well as providing information on the mechanism of damage. Activation of the complement system has been implicated in damage to the axon of the nerve in GBS patients (53). Other evidence has been presented showing that IgG antibody and components of the complement system, such as C5a, are localized on the motor nerve axons, specifically the axolemma, of AMAN patients (59). Complement components were also shown to bind to Schwann cells of AIDP patients (60). These models (especially the NOD WT) could serve to confirm these mechanisms if the correct nerve locations are chosen and the correct fixation and level of examination (e.g. transmission electron microscopy) are conducted.

As described above, NOD WT mice have the greatest potential to be useful as a working murine model to study GBS following infection by *C. jejuni*. NOD WT mice have been shown to be colonized with GBS-associated *C. jejuni* with minimal enteric disease, produce anti-ganglioside antibodies, display clinical neurological signs, and have influx of activated macrophages present in the peripheral nerves. However, we use the term

“working model” because NOD WT mice need to be further assessed before they can be considered a true animal model of GBS. In particular, a time course experiment with these mice should be performed to measure peaks of antibody titers to describe the time of onset of disease in detail. ELISA assays require optimization to provide stronger evidence that anti-ganglioside antibodies are produced that react with the mixture of gangliosides. The neurological disease phenotypes of mice need to be analyzed using the DigiGait™, this apparatus has the potential to be the most sensitive means of detecting neurological clinical signs. Furthermore, these mice should be examined by other methods of identifying nerve lesions, immune cell or infiltrates, and complement binding to nervous tissue by staining for these immune system components. If the results of these tests show significant differences between mice infected with *C. jejuni* and uninfected mice, then validation of murine model to study the natural onset of GBS, would be complete and provide proof that molecular mimicry is the pathogenic mechanism behind GBS.

*Acknowledgements:* The authors thank Drs. Jon S. Patterson and Howard T. Chang for their contribution in the development of a histological criterion to score nerves.

**Table 2.1: Clinical Assessment for DigiGait™ videos.** Scoring method used for visual assessment of clinical neurological signs in the videos obtained weekly using the DigiGait™ apparatus. Each sign was assigned a score as shown; scores were added for each mouse at each week. Cumulative scores were used in statistical tests.

Score Methodology for Clinical Assessment of DigiGait™ videos

	<u>Absent</u>	<u>Present</u>	<u>Repeated</u>	
Sidestepping	0	1	2	
Crossing Over	0	1	2	
Bunny Hopping	0	1	2	
Paddling	0	1	2	
Galloping	0	1	2	
Rolling	0	1	2	
Shortened stance	0	1	NA	
Widen stance	0	1	NA	
Knuckled Over	0	1	NA	
Weakness	0	1	NA	
	<u>Absent</u>	<u>Present in 1 Leg</u>	<u>Present in both Legs</u>	
Splayed Hind Leg	0	1	2	
Foot Drag	0	1	2	
	<u>Absent</u>	<u>Toes Splayed Apart</u>	<u>Toes Curled</u>	<u>Toes Flaccid</u>
Toes	0	1	2	3

**Table 2.2: Statistical results for change within treatment groups over the course of the experimental time.** The table below shows results from two-way ANOVA with repeated measures analysis of change in time over the course of the experiment. No significant result obtained is designated . Abbreviations: NS, not significant; NA, not applicable.

	Experiment 1			Experiment 2		Experiment 3
	NOD WT	NOD IL-10 <sup>-/-</sup>	NOD B7-2 <sup>-/-</sup>	NOD WT	NOD B7-2 <sup>-/-</sup>	NOD IL-10 <sup>-/-</sup>
<b>OFT</b>	NS	p=0.0447	p<0.0001	p<0.0001	p<0.0001	NA
<b>Hang Test</b>	p<0.0001	p<0.0001	p<0.0001	NS	NS	NA
<b>Rotarod</b>	NA	NA	NA	p<0.0001	p<0.0001	p<0.0001
<b>Stride Length</b>	NA	NA	NA	p<0.0001	p<0.0001	NA
<b>Hind Base Width</b>	NA	NA	NA	p=0.0013	p=0.0004	NA

**Table 2.3: P values for ELISA assays for ELISA assays for all 3 experiments.** Abbreviations: 1W, one-way ANOVA; KW, Kruskal-Wallis ANOVA; MW, Mann-Whitney *U*.

	Experiment 1			Experiment 2		Experiment 3
	NOD WT	NOD IL-10-/-	NOD B7-2-/-	NOD WT	NOD B7-2-/-	NOD IL-10-/-
<b>ELISA</b>						
<b>GM1 (IgG1)</b>	1W; p=0.2933	1W; p=0.6478	KW; p=0.1909	MW; p=0.4275	MW; p=0.5148	KW; p=0.8321
<b>GM1 (IgG2a)</b>	KW; p=0.4515	KW; p=0.7704	1W; p=0.6926	MW; p=0.2634	MW; p=0.7087	KW; p=0.6412
<b>GM1 (IgG3)</b>	1W; p=0.8760	1W; p=0.2671	1W; p=0.4883	MW; p=0.9232	MW; p=0.7474	KW; p=0.0217
<b>GM1 (IgM)</b>	1W; p=0.8160	1W; p=0.2149	1W; p=0.9403	MW; p=0.6657	MW; p=0.8699	KW; p=0.9319
<b>GD1a (IgG1)</b>	KW; p=0.4051	KW; p=0.8051	1W; p=0.5113	MW; p=0.3232	MW; p=0.5148	KW; p=0.0030
<b>GD1a (IgG2a)</b>	1W; p=0.8416	1W; p=0.7702	1W; p=0.1925	MW; p=0.3248	MW; p=0.8392	KW; p=0.2208
<b>GD1a (IgG3)</b>	1W; p=0.8430	KW; p=0.5369	1W; p=0.2028	MW; p=0.0296	MW; p=0.0395	KW; p=0.0421
<b>GQ1b (IgG2a)</b>	1W; p=0.6931	1W; p=0.5181	1W; p=0.6903	MW; p=0.2686	MW; p=0.3751	KW; p=0.0029
<b>GM1/GD1a (IgG1)</b>	1W; p=0.3624	KW; p=0.1086	1W; p=0.7989	MW; p=0.3795	MW; p=0.7132	KW; p=0.0332
<b>GM1/GQ1b (IgG1)</b>	1W; p=0.0100	1W; p=0.9237	1W; p=0.8887	MW; p=0.0351	MW; p=0.5361	KW; p=0.0017
<b>Cj (IgG2b)</b>	KW; p=0.0004	KW; p=0.0001	KW; p<0.0001	MW; p<0.0001	MW; p<0.0002	KW; p<0.0001
<b>Day 0 GD1a (IgG1)</b>	KW; p=0.9020	1W; p=0.2053	1W; p=0.9429	MW; p=0.7498	MW; p=0.9382	NA
<b>Day 14 GD1a (IgG1)</b>	1W; p=0.5481	1W; p=0.1695	1W; p=0.9854	MW; p=0.2292	MW; p=0.4709	NA
<b>Day 0 GM1 (IgM)</b>	1W; p=0.7371	1W; p=0.5059	1W; p=0.9255	MW; p=0.0229	MW; p=0.9545	NA
<b>Day 14 GM1 (IgM)</b>	1W; p=0.7070	1W; p=0.6219	KW; p=0.3752	MW; p=0.2683	MW; p=0.2230	NA

**Figure 2.1: Experiment 1 Data Summary.** Panel A shows the number of NOD WT, NOD IL-10<sup>-/-</sup>, and NOD B7-2<sup>-/-</sup> mice colonized in the cecum with *C. jejuni* HB93-13 and *C. jejuni* 260.94. Panel B shows the levels of plasma IgG2b antibody reactive with *C. jejuni* in all mice (B-1) and the plasma levels of IgG1 antibody reactive with the ganglioside mixture GM1/GD1a (B-2). Panel C shows the number of quadrants crossed in the open field test for only the NOD WT mice. Panel D shows the hang time for mice of all genetic backgrounds during the course of the experiment with the hang test. The Holm-Sidak pairwise test found significant differences in hang times between sham-inoculated NOD WT mice and *C. jejuni* 260.94 infected NOD WT mice at week 1 ( $p \leq 0.05$ ) and week 3 ( $p \leq 0.01$ ). Unless stated otherwise, significance levels in all graphs are denoted by \* ( $p \leq 0.05$ ); \*\* ( $p \leq 0.01$ ); \*\*\* ( $p \leq 0.001$ ); and \*\*\*\* ( $p \leq 0.0001$ ).

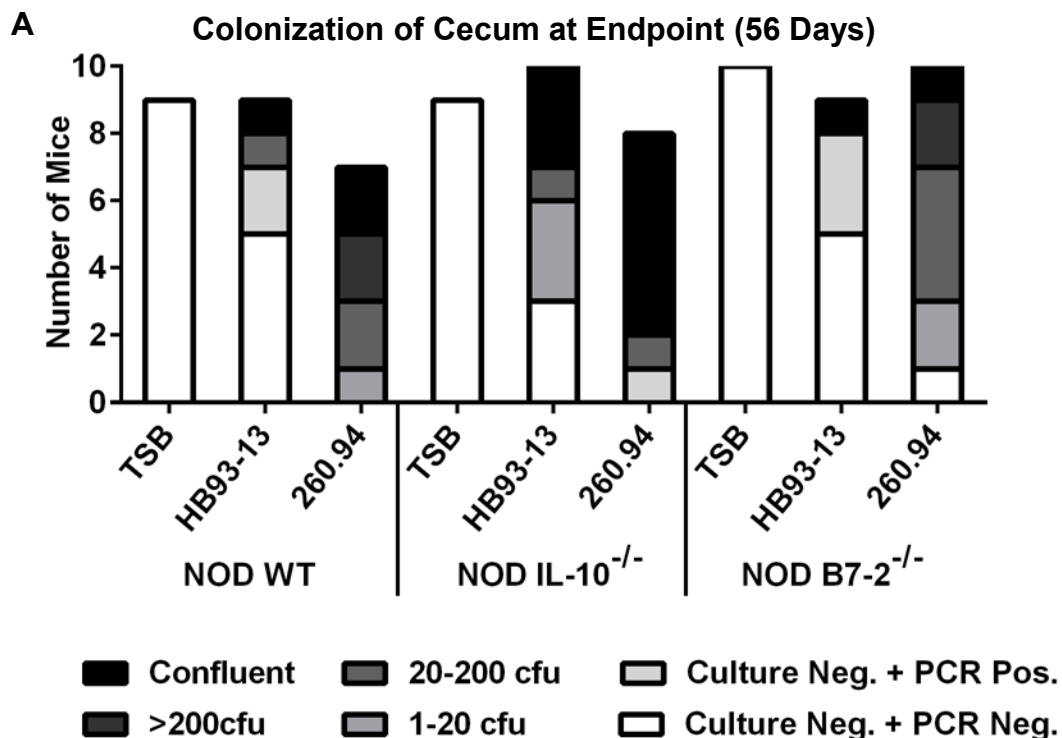


Figure 2.1 (cont'd)

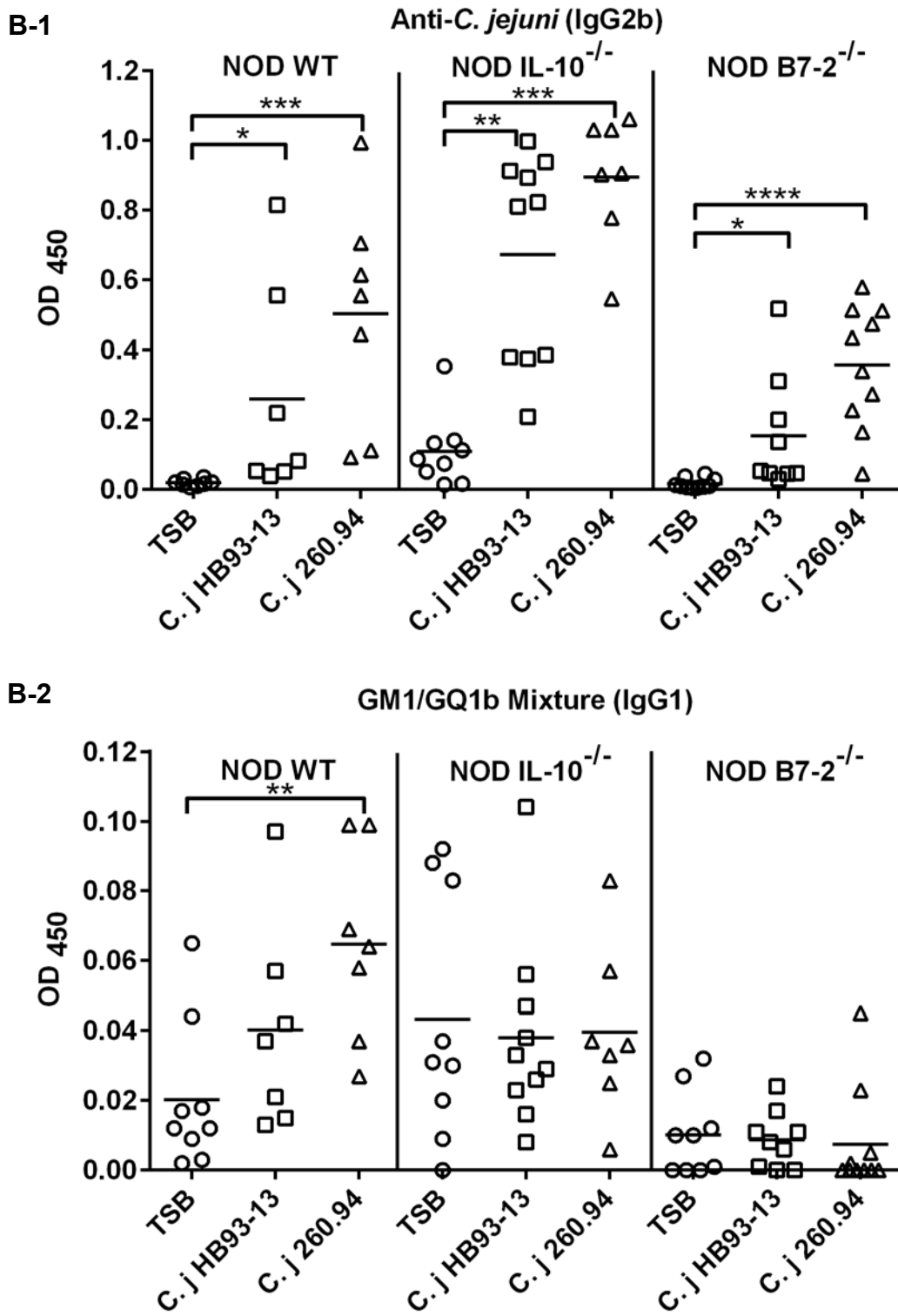
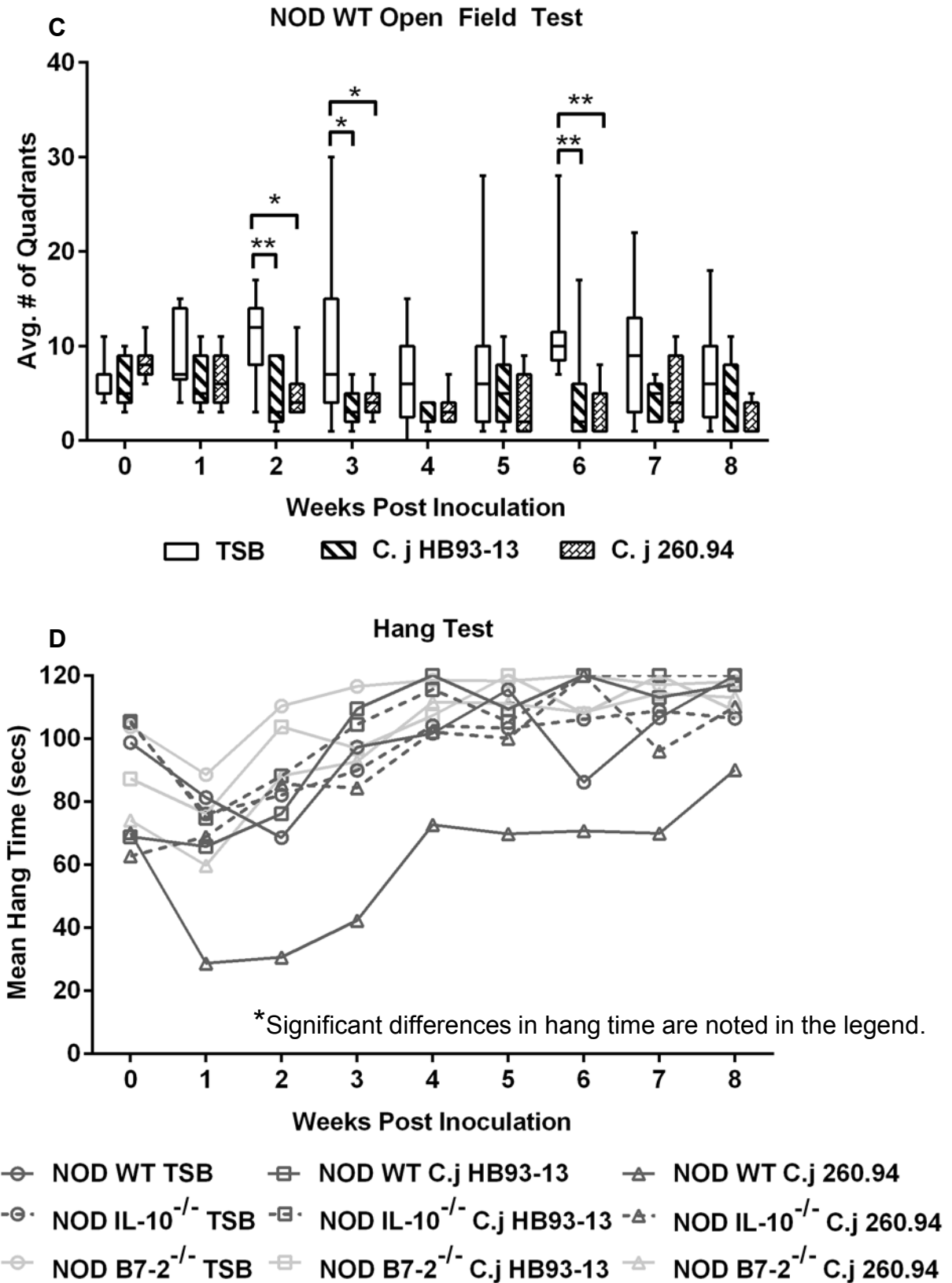


Figure 2.1 (cont'd)



**Figure 2.2: Experiment 2 Data Overview.** Panel A -1 shows the colonization levels of *C. jejuni* 260.94 in the ceca of the mice at endpoint of experiment (80 days). Panel A-2 indicates the gross pathological features present in mice at time of necropsy. Gross pathological features examined were enlarged lymph nodes and thickened wall of the GI tract. Panel B shows ELISA results. Panel B-1 shows plasma levels of antibody IgG3 reactive with the ganglioside GD1a and panel B-2 demonstrates the plasma levels of IgG1 antibody reactive with ganglioside mixture GM1/GQ1b. Note that only NOD WT mice had significant differences in plasma levels of IgG1 to ganglioside mixture GM1/GD1a. Panel C shows the number of times a quadrant was crossed over the course of the experiment; panel C-1 displays the NOD WT mice and panel C-2 shows the NOD B7-2<sup>-/-</sup> mice. Panel D shows the time spent on the rotarod by NOD WT mice (panel D-1) and NOD B7-2<sup>-/-</sup> mice (panel D-2). Unless stated otherwise, significance levels in all graphs are by \* (p≤0.05), \*\* (p≤0.01), \*\*\* (p≤0.001) and \*\*\*\* (p≤0.0001).

Figure 2.2 (cont'd)

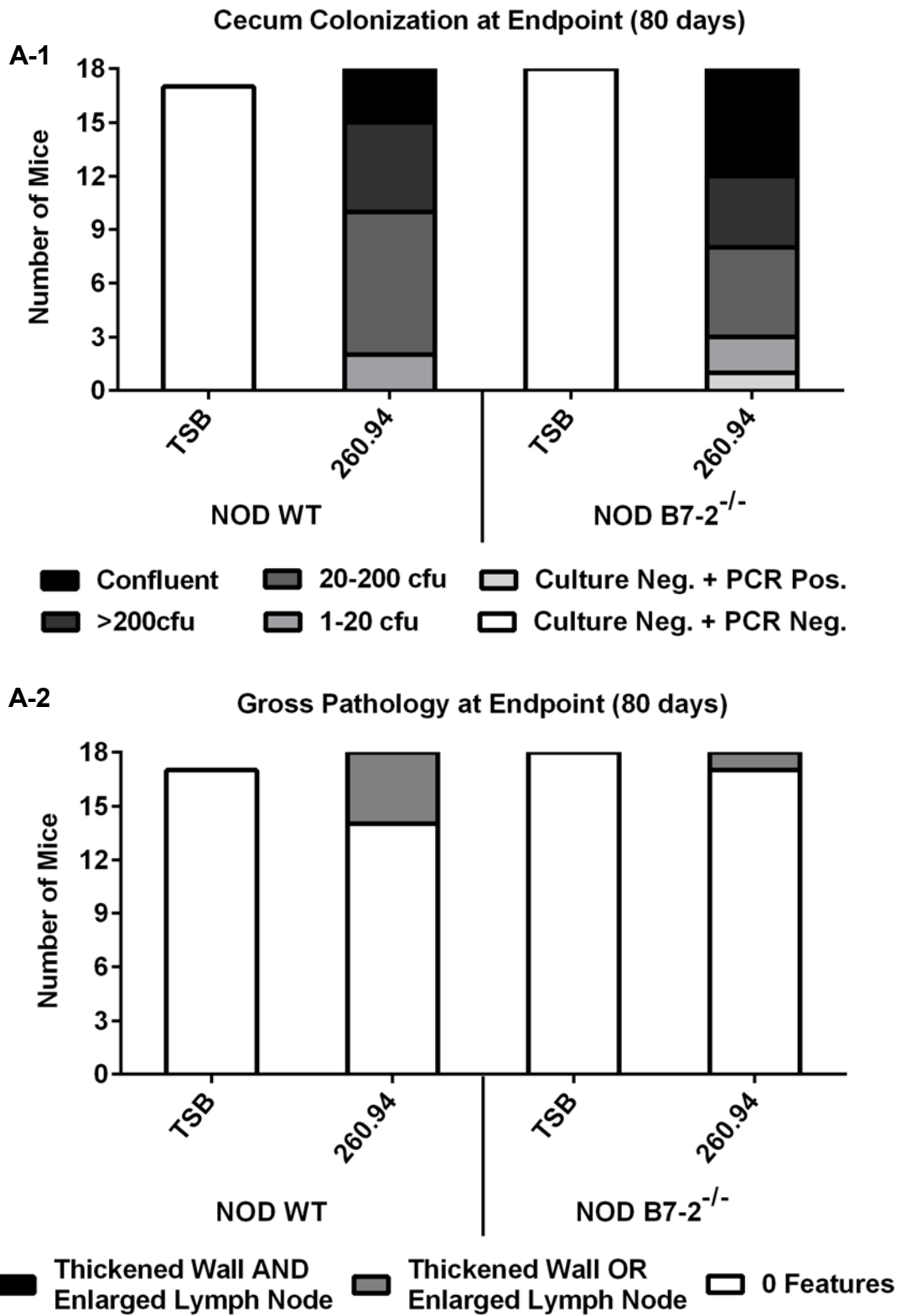


Figure 2.2 (cont'd)

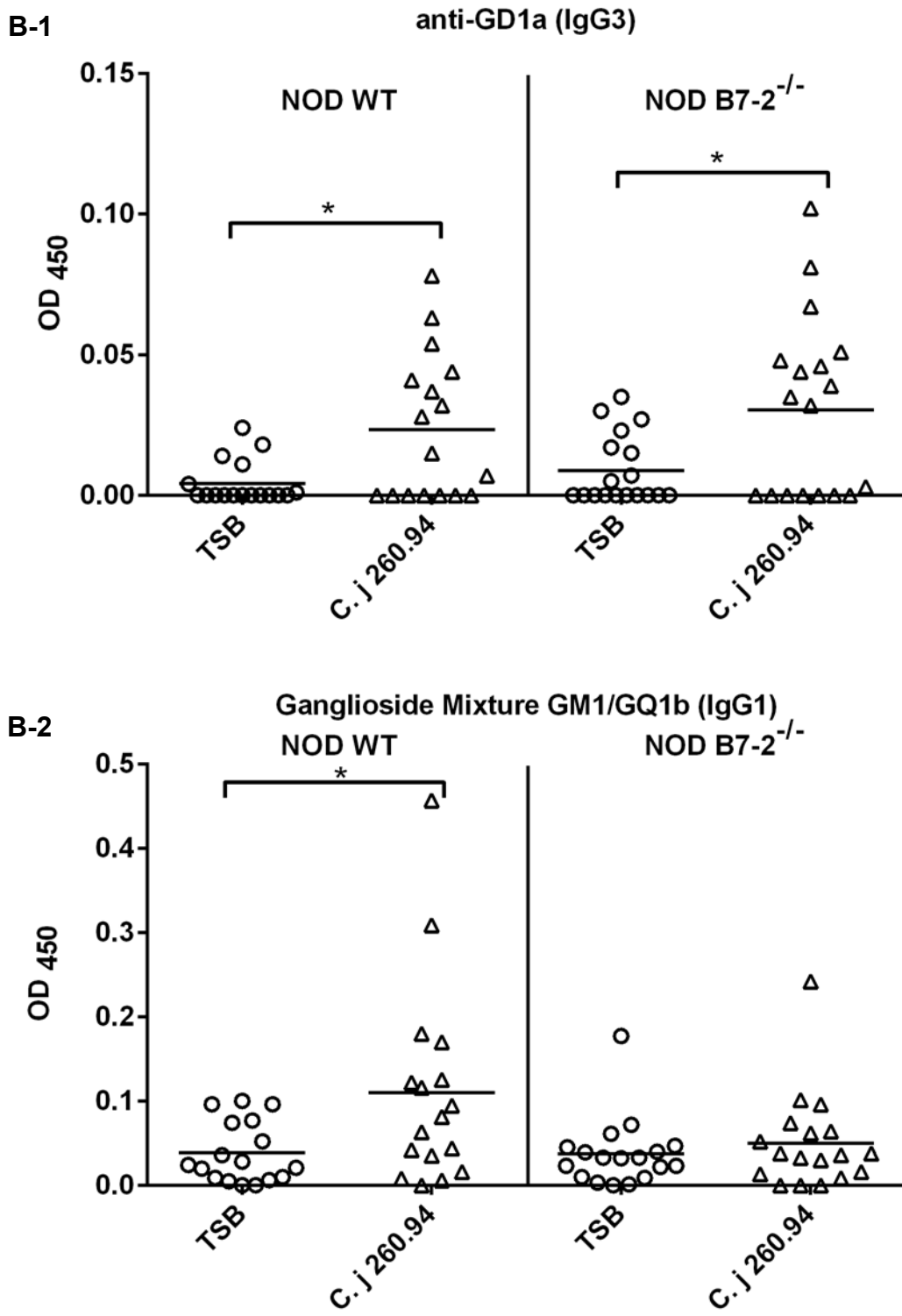


Figure 2.2 (cont'd)

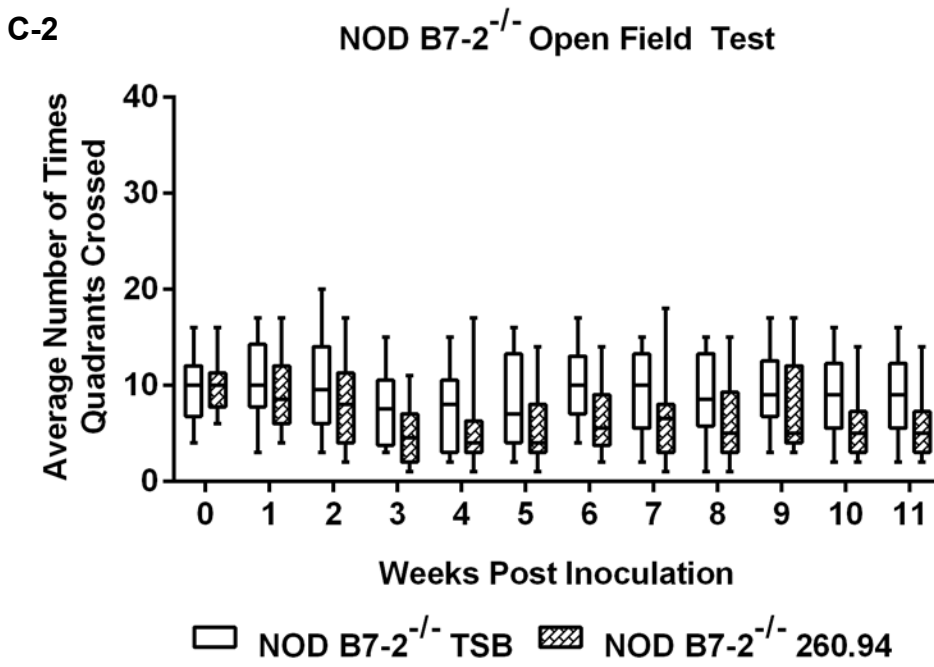
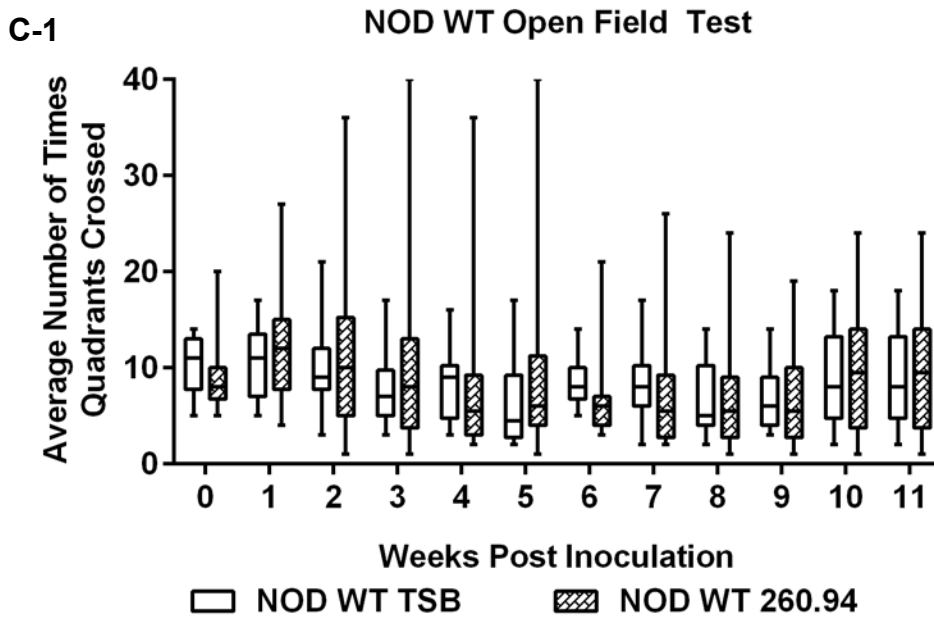
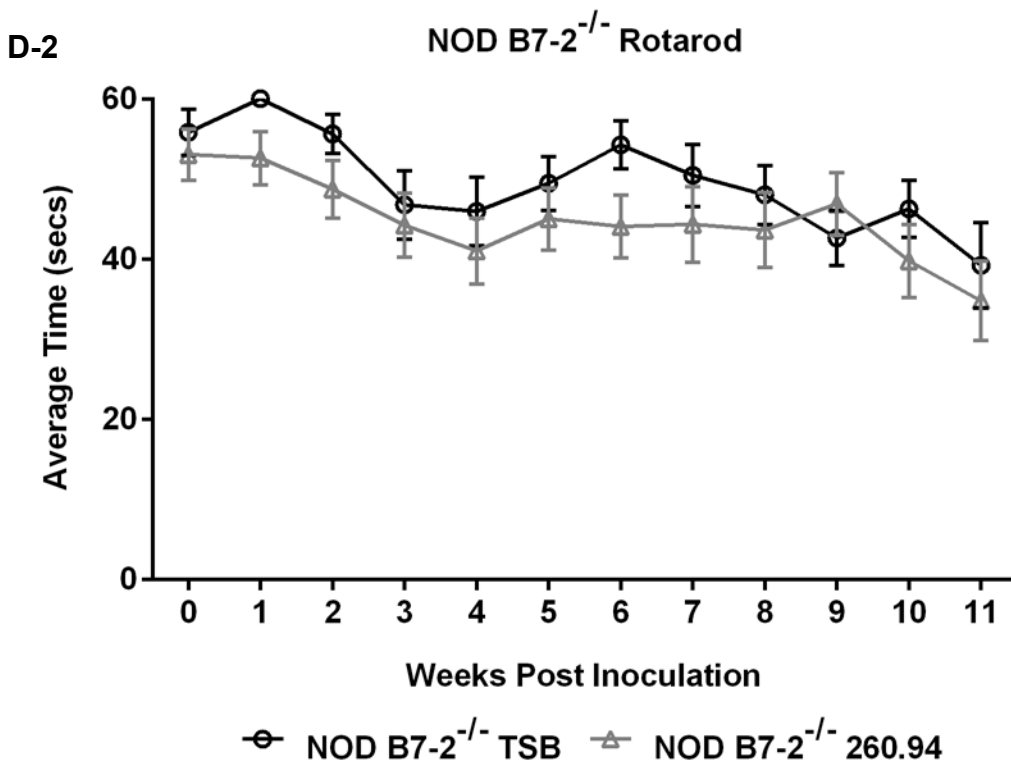
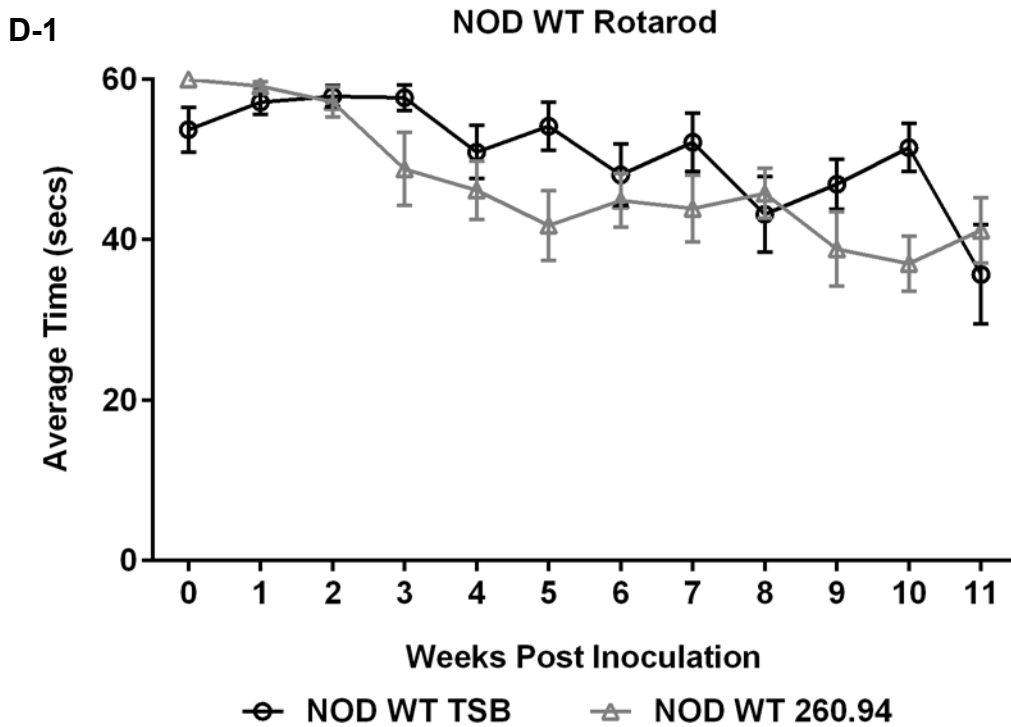
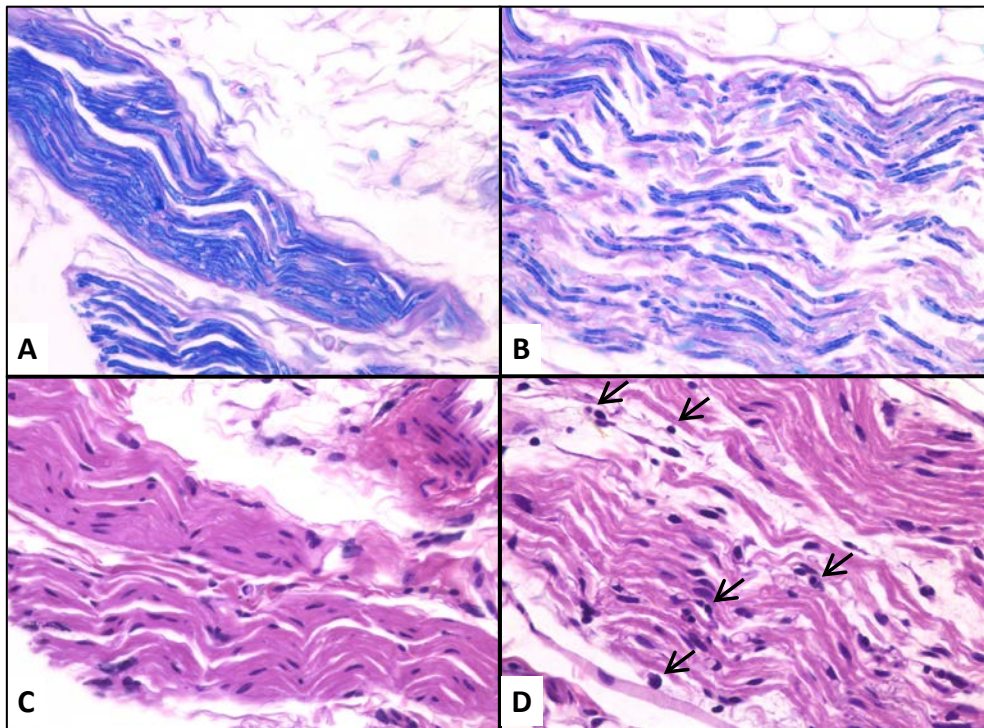


Figure 2.2 (cont'd)



**Figure 2.3: Examination of Peripheral Nerves.** Panel A shows a Luxol fast blue stain of a sciatic nerve section from a sham-inoculated NOD B7-2<sup>-/-</sup> mouse; panel B shows a Luxol fast blue stain of sciatic nerve section from a *C. jejuni* 260.94 infected NOD B7-2<sup>-/-</sup> mouse. There is myelin loss visible in panel B, but as seen in panel A, the nerve from the uninfected mouse has intact myelin. Panels C and D show H & E stained sections of sciatic nerve section from a NOD B7-2<sup>-/-</sup> sham-inoculated mouse and a *C. jejuni* 260.94 infected mouse, respectively. The arrows in panel D indicate cellular infiltration within the nerve. All panels are shown at the same magnification (40X). For interpretation of the references to color in this and all other figures, the reader is referred to the electronic version of this dissertation.



**Figure 2.4: Immunohistochemical Data for Experiment 2.** Panel A shows the number of cells that stained positive for CD3 (T cells). Panel B shows the number of cells that stained positive for F4/80 (activated macrophages). Significance is noted with \* ( $p \leq 0.05$ ).

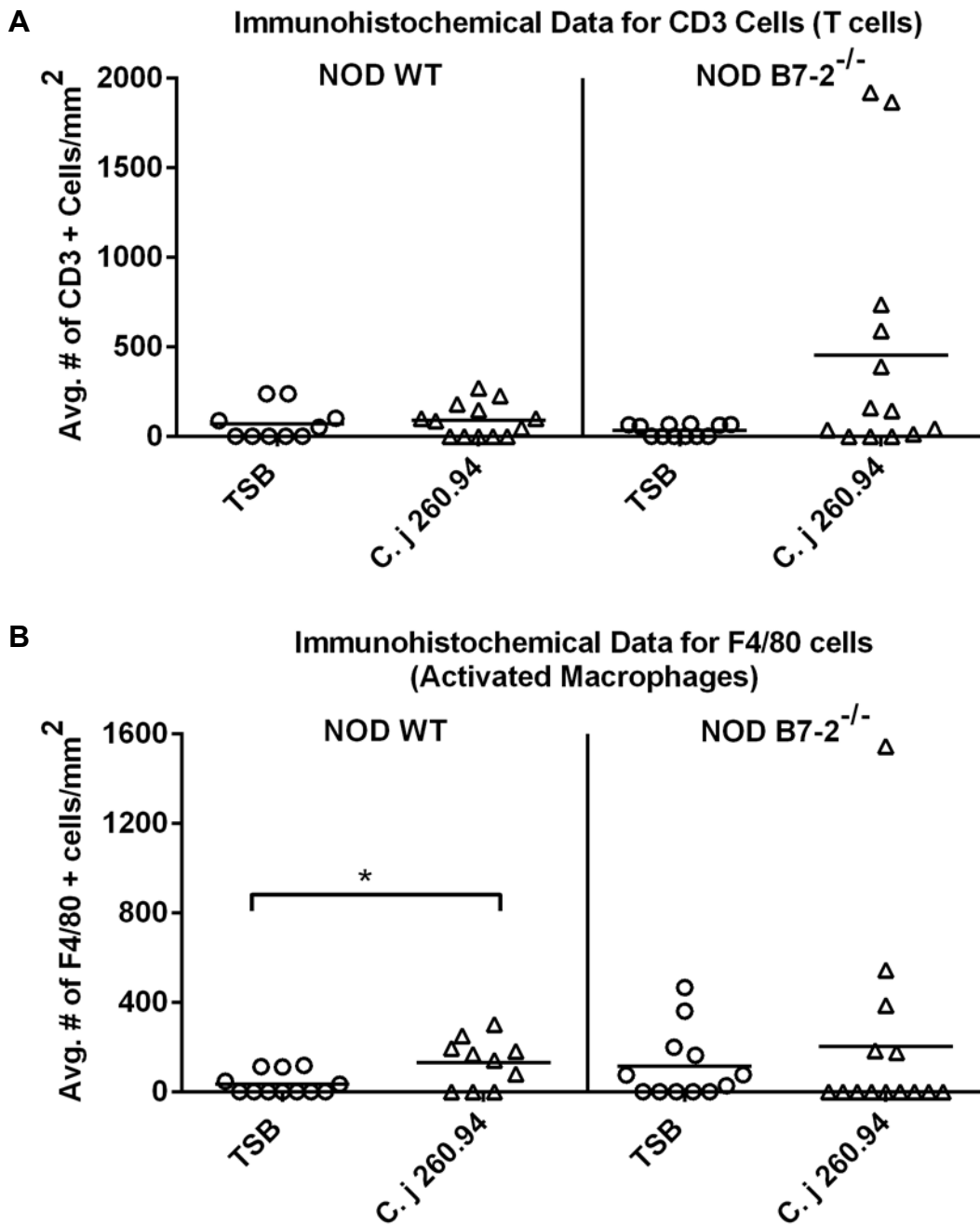


**Figure 2.5: Macrophage infiltration of NOD WT mice.** Panels A and C show sciatic nerve sections from sham-inoculated NOD WT mice stained with F4/80; panels B and D show a F4/80 stain of sciatic nerve sections from *C. jejuni* 260.94 infected NOD WT mice. There is visible infiltration of macrophages in panels B and D, but none is seen in panels A and C. The black arrows indicate stained macrophages. Panels A–D are shown at the same magnification (20X). Panels F–I show the same sciatic nerve sections at 40X magnification; panels F and H are sham-inoculated NOD WT mice and panels G and I are *C. jejuni* 260.94 infected NOD WT mice.

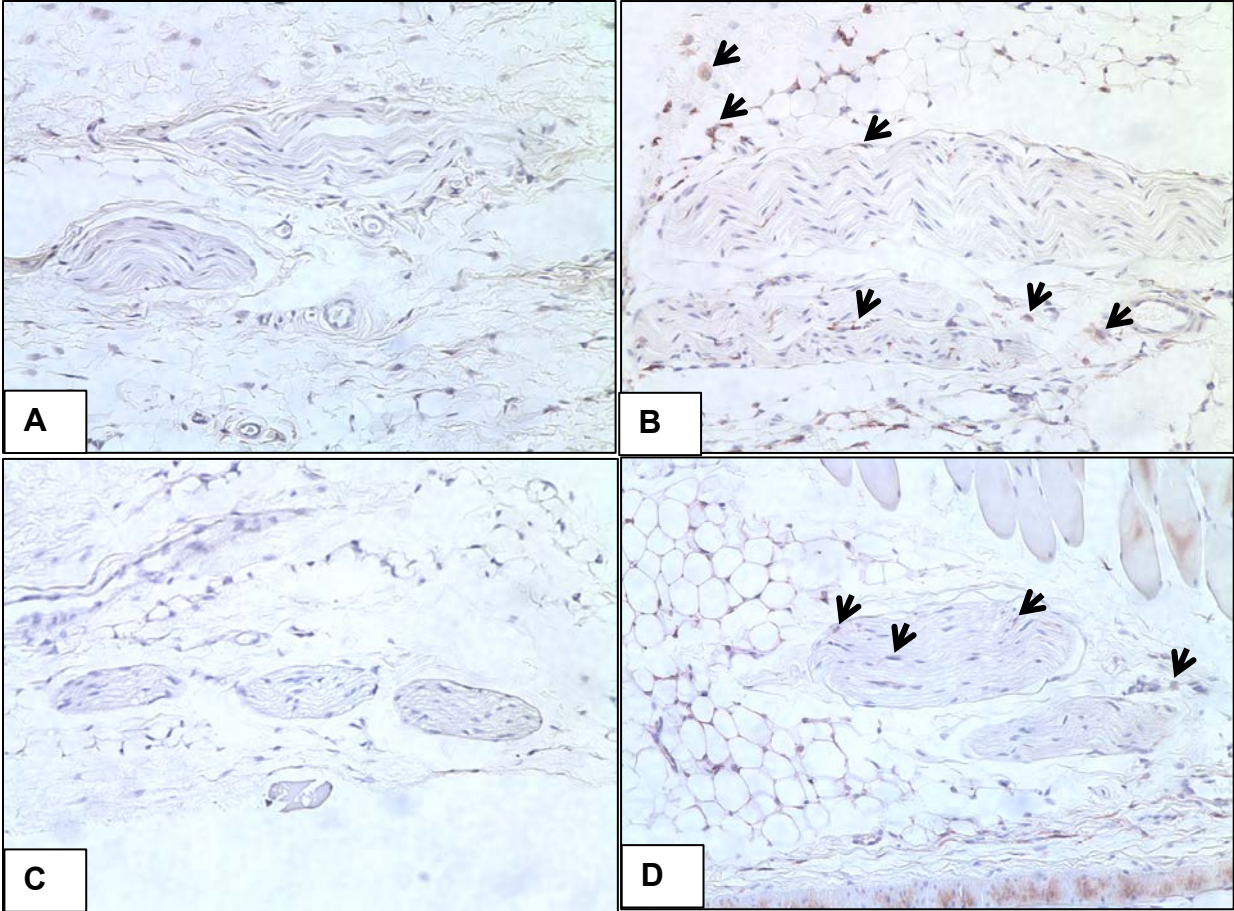
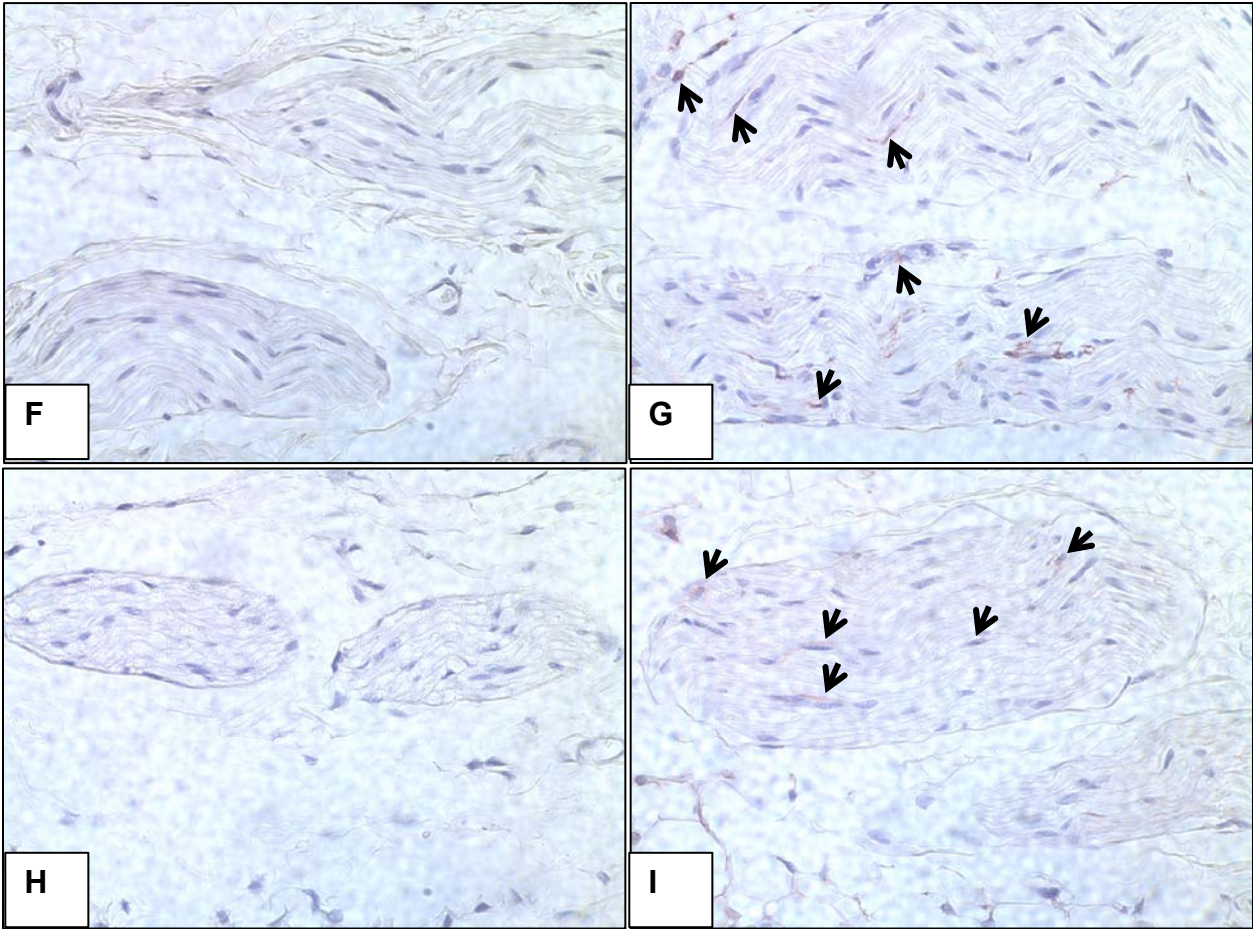


Figure 2.5 (cont'd)



**Figure 2.6: Experiment 3 Data Summary.** Panel A shows colonization levels of *C. jejuni* 260.94 in the cecum at the end of the experiment (84 days). Panel B shows the time spent on the rotarod over the course of the experiment. Panel C shows the ELISA assay data for plasma levels of IgG1 reactive with ganglioside mixture GM1/GQ1b in panel C-1; ganglioside mixture GM1/GQ1b is in panel C-2. There were significant differences between the sham-inoculated mice and *C. jejuni* infected mice treated with CMP in both assays. Panel D displays the cumulative scores of the clinical assessment of neurological signs using the videos obtained from the DigiGait™; only mice that had videos for the entire length of the experiment are shown. The black line indicates the median of scores for each time point. No significant differences were observed between treatment groups with a two-way ANOVA with repeated measures. Unless stated otherwise, significance levels in all graphs are by \* ( $p \leq 0.05$ ), \*\* ( $p \leq 0.01$ ), \*\*\* ( $p \leq 0.001$ ) and \*\*\*\* ( $p \leq 0.0001$ ).

Figure 2.6 (cont'd)

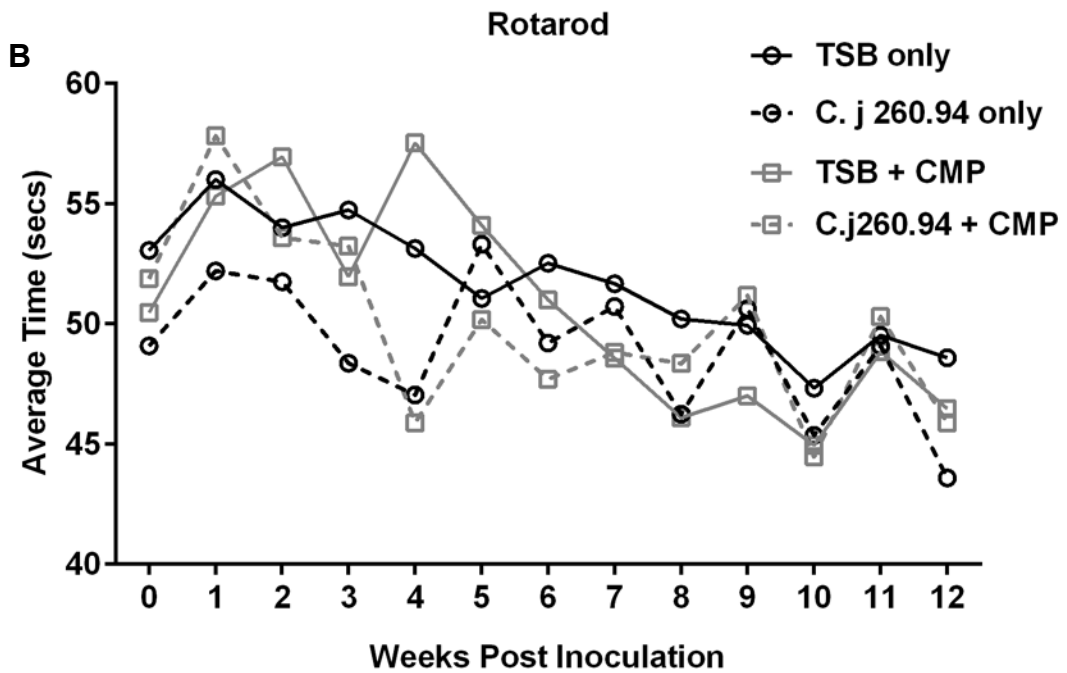
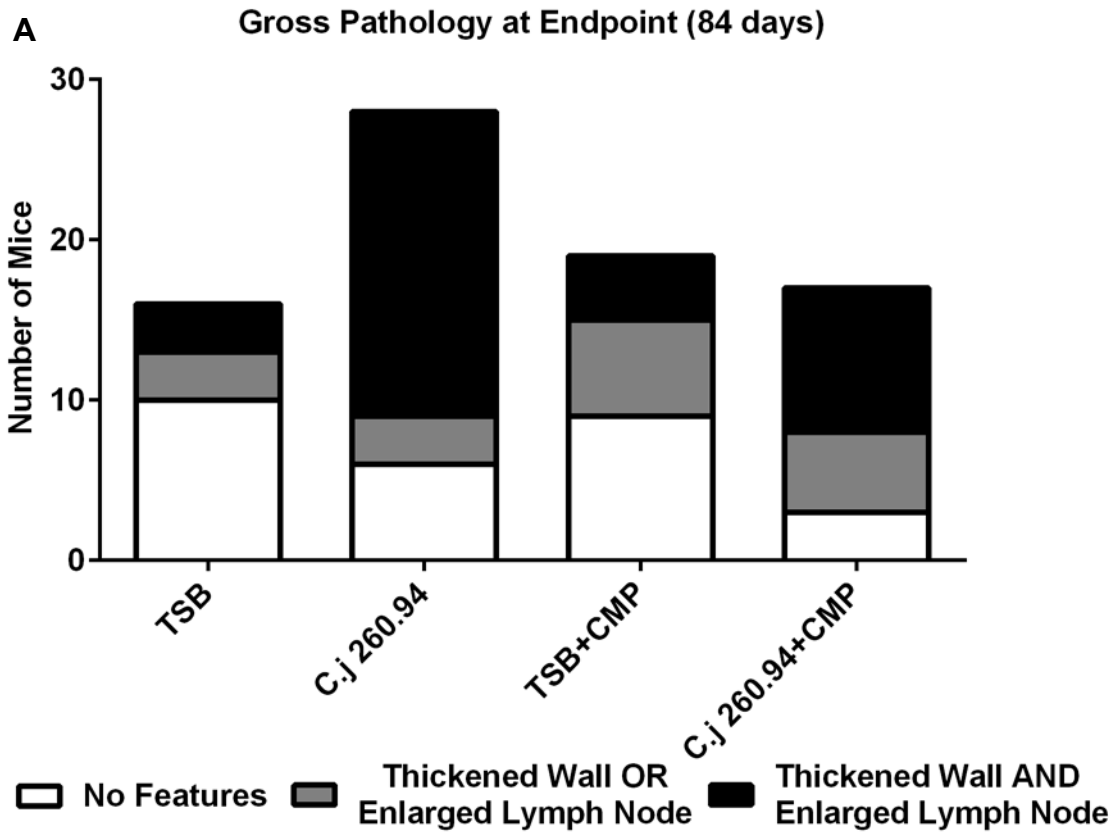
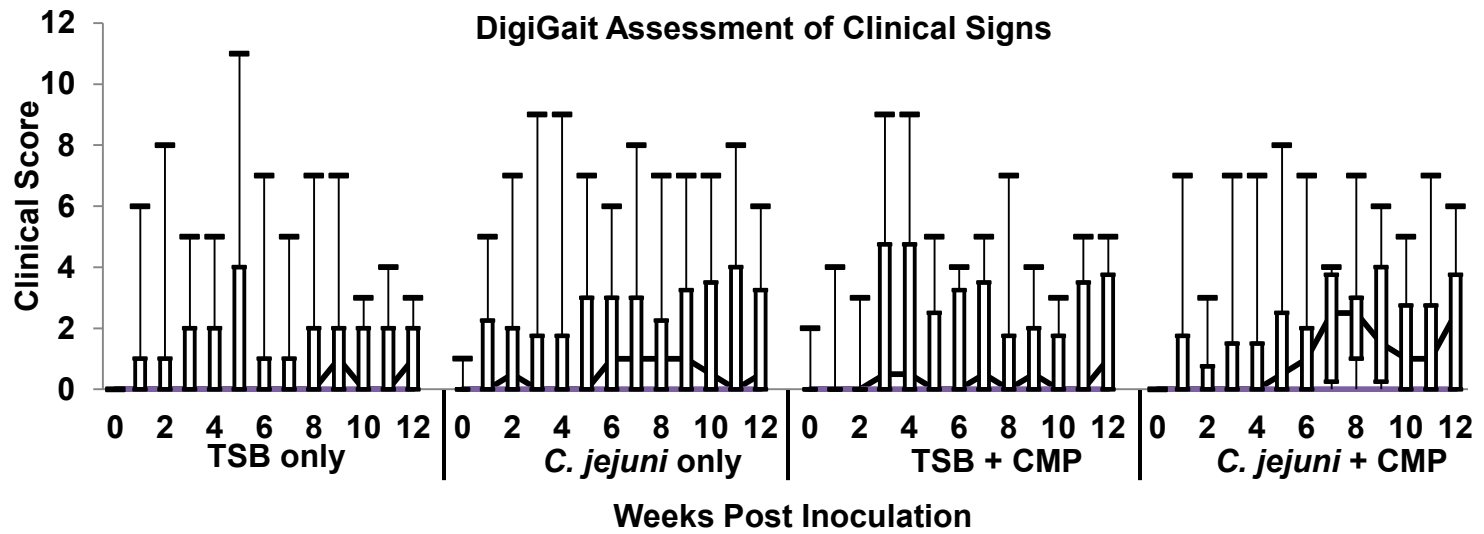


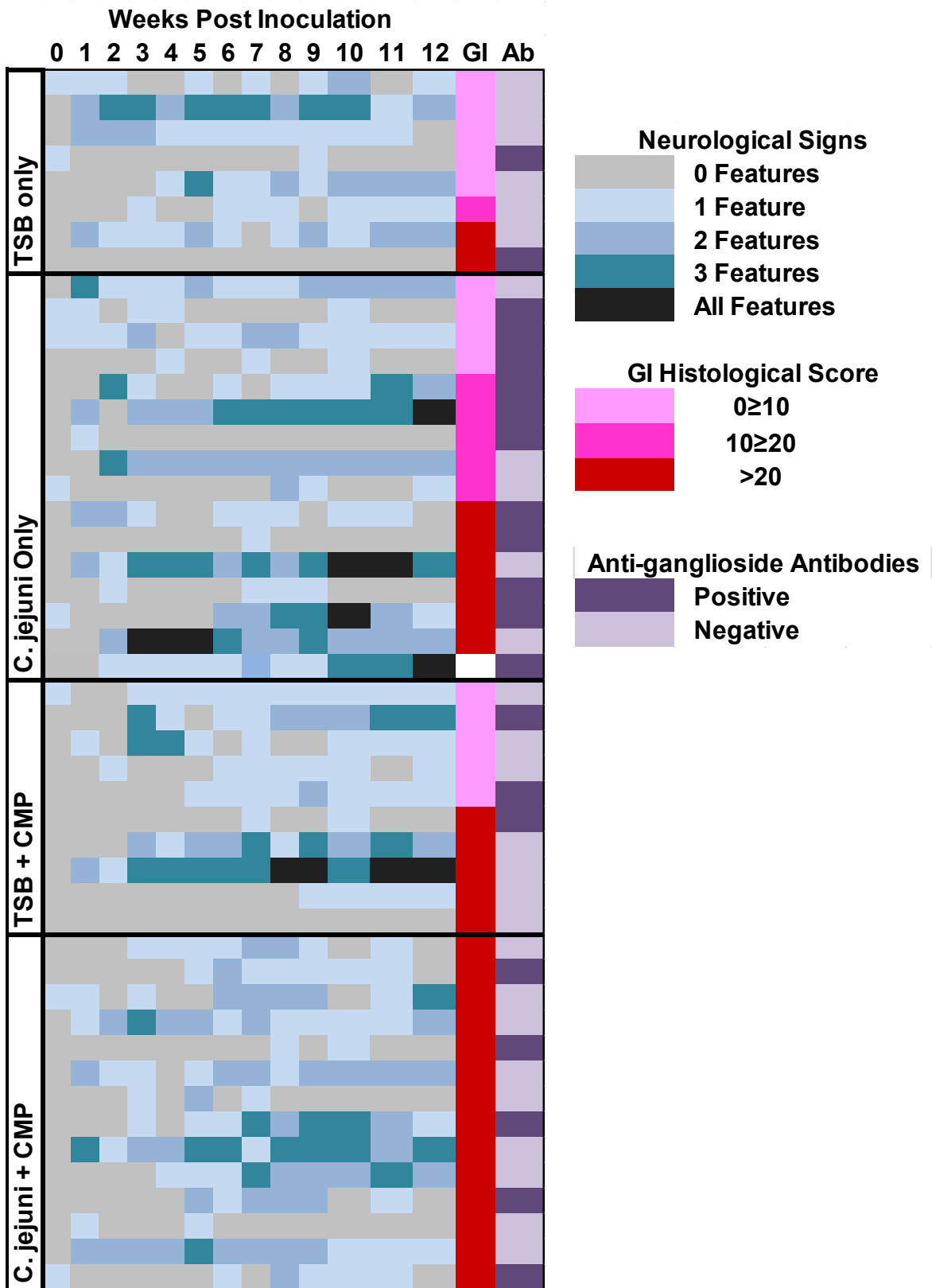


Figure 2.6 (cont'd)

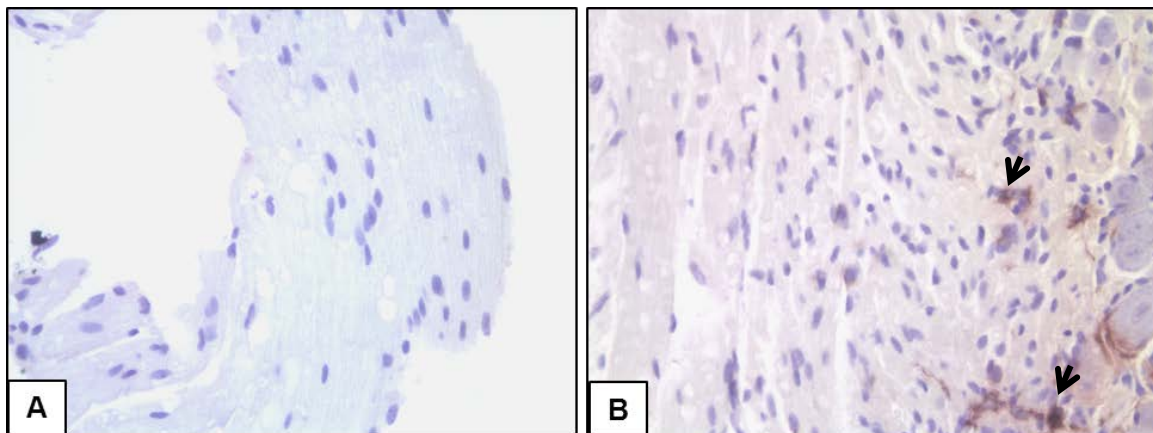


**Figure 2.7: Heat Map of Clinical Neurological Assessment.** This heat map demonstrates the assessment of clinical neurological signs obtained from DigiGait™ videos and from rotarod testing for each mouse that provided videos for entire experiment (84 days). To construct this graph, features observed in the primary assessment of clinical signs with the initial scoring of the video were categorized into 3 main features: 1) gait abnormalities, 2) stance abnormalities, and 3) other (toe abnormalities and general weakness). Balance was also assessed; a mouse was classified as having an abnormality in balance if spent <40 secs on the rotarod. Thus, a mouse could be assigned to one of 5 groups: 1) no features, 2) 1 feature, 3) 2 features, 4) 3 features, or 5) all features. These features are expressed based on color intensity of the weekly rectangles on the heat map. To the far right of the heat map the histological scores of the ileocecolic junction are shown. As seen on the graph, a high histological score did not interfere with assessment of clinical neurological signs. Presence of anti-ganglioside antibodies is also shown on the far right of the heat map. Over two-thirds of mice that had anti-ganglioside antibodies were *C. jejuni* infected mice not treated with CMP.

Figure 2.7 (cont'd)



**Figure 2.8: Infiltration of macrophages in the nerve root.** Panels A and B are nerve root sections stained with F4/80 (activated macrophages). Panel A is a sham-inoculated mouse and panel B is a *C. jejuni* infected mouse. The black arrows indicated macrophages. Panel C shows graphically the presence of activated macrophages in the nerve root sections of *C. jejuni* mice not treated with CMP and sham-inoculated mice not treated with CMP. Significance levels are noted by \* ( $p \leq 0.05$ ).





## CHAPTER 3

Examination of Miller Fisher Syndrome in NOD WT and C57BL/6 WT mice subsequent  
to *Campylobacter jejuni* CF93-6 infection

## ABSTRACT

Acute neuropathies Guillain Barré Syndrome (GBS) and Miller Fisher Syndrome (MFS) can follow *Campylobacter jejuni* infection. GBS is an ascending symmetrical paralysis affecting the peripheral nervous system. MFS is a descending neuropathy affecting the central nervous system before affecting peripheral nerves. Lipooligosaccharides (LOS) of *C. jejuni* mimic nerve gangliosides in the peripheral nervous tissue of the host, resulting in autoimmune attack on host gangliosides. Antibodies to gangliosides GM1 and GD1a are associated with GBS and antibodies to GQ1b with MFS. We hypothesized that NOD WT and C57BL/6 WT mice infected with MFS-associated *C. jejuni* CF93-6 would exhibit neurological signs, autoantibodies, and lesions consistent with MFS; whereas NOD WT mice infected with GBS-associated *C. jejuni* 260.94 would exhibit features of GBS disease. Orally infected mice of both the NOD and C57BL/6 genetic backgrounds were tested weekly for neurological phenotypes; GI tract, nerves, and blood were taken to determine *C. jejuni* colonization, nerve lesions, and presence of anti-ganglioside antibodies at endpoint. ELISA assays showed significant differences in the presence of IgG1 antibody reactive to ganglioside mixture GM1 and GQ1b between sham-inoculated NOD WT mice and *C. jejuni* 260.94 infected NOD WT mice. No other significant differences in levels of IgG1 or any other IgG isotype tested were observed in either the NOD WT *C. jejuni* CF93-6 infected mice or between the uninfected mice and infected mice of the C57BL/6 WT mice. For all phenotypic tests that were performed (open field test, hang test, rotarod, and footprints), there were no significant differences between the uninfected and *C. jejuni* infected mice

in either the NOD WT or C57BL/6 WT mice. Therefore no clinical manifestation of neurological disease was observed. Examination of sections of the sciatic nerve for cellular infiltrates and nerve lesions revealed no significant changes between the treatment groups of either background. These results suggest that there is no manifestation of MFS caused by *C. jejuni* CF93-6 in either C57BL/6 or NOD mice that is distinguishable from that of the subclinical manifestation of GBS (anti-ganglioside antibody production) caused by *C. jejuni* 260.94 in NOD mice in this experiment. They also suggest that infection with *C. jejuni* CF93-6 does not result in a neurological phenotype in NOD WT or C57BL/6 WT mice.

## INTRODUCTION

Guillain-Barre Syndrome (GBS) is a post-infectious autoimmune-mediated neuropathy of the peripheral nerves (7, 63, 76). GBS is described as an ascending symmetrical paralysis with limb weakness, acute flaccid paralysis, and in some instances sensory loss; muscle weakness frequently affects the respiratory and facial muscles (7, 147, 161). GBS is defined as many clinical subtypes: 1) acute inflammatory demyelinating polyneuropathy (AIDP), 2) acute motor axonal neuropathy (AMAN), and 3) Miller Fisher Syndrome (MFS). Studies of pathological changes in AIDP show macrophages invading the myelin sheath, resulting in myelin damage and demyelination (134, 147, 154, 160). AIDP is the most common form in the Western world, affecting approximately 69–90% of GBS patients (134, 147). The clinical subtype AMAN is more common in China and Central and South America, affecting 38–65% of GBS patients; only 5–10% of GBS patients in the Western world present with AMAN (134, 147, 160). Acute motor sensory axonal neuropathy (AMSAN) has also been recognized as a subtype that affects both the motor and sensory nerves. The targets of the macrophages are different in AMAN than in AIDP; in AMAN the macrophages target the nodes of Ranvier and the axolemma of the nerve (147, 161). Worldwide, the mean annual incidence rate of GBS is 0.6–4 cases per 100,000 with males more often affected than females (79, 154).

Unlike GBS, MFS is characterized by a descending neuropathy that affects the central nervous system, especially the brainstem, before affecting the periphery (97). The classic triad of MFS symptoms includes: ataxia, areflexia, and ophthalmoplegia;

though not all symptoms are always present (93, 137, 138, 159). MFS is more commonly found in patients in eastern Asia; 20% of Taiwanese and 25% of Japanese GBS patients present with MFS (134, 163). Symptoms of MFS peak at 1 week, and patients tend to begin recovery 1–3 months later, with most patients making a complete recovery by 6 months (97, 163). The mean annual occurrence of MFS is 0.09 cases per population (97). MFS is less common than GBS, yet can still produce lifelong debilitating symptoms.

The onset of GBS is usually preceded by respiratory or gastrointestinal infections with 2/3 of patients reporting antecedent illness (72). *Campylobacter jejuni*, a gram negative bacterium, is the most common preceding infection leading to the onset of GBS and MFS (67, 76, 105, 147, 162). The role of *C. jejuni* in the onset of GBS is thought to be molecular mimicry (7). The lipo-oligosaccharide (LOS) on the surface of *C. jejuni* can mimic gangliosides found on host nerves therefore resulting in an autoimmune response (7). Gangliosides are membrane glycolipids highly enriched in the nervous tissue (63, 162). Antibodies to gangliosides GD1a and GM1 are more commonly associated with people displaying the AMAN subtype of GBS (150, 161). Approximately 75% of AMAN GBS patients and 10–15% AIDP patients have antibodies reactive with these gangliosides (157). It has been demonstrated that IgG antibodies reactive to the ganglioside GQ1b are commonly found in patients displaying MFS phenotype (80, 90, 134, 150). Approximately 83–100% of MFS patients have antibody reactive to GQ1b gangliosides; only approximately 26% of GBS patients present with GQ1b antibody (93, 97, 137).

Studies have demonstrated that ganglioside GQ1b is highly enriched in the ocular nerves (147). In MFS, the 3<sup>rd</sup>, 4<sup>th</sup>, and 6<sup>th</sup> cranial nerves are commonly affected (153, 154). It also has been demonstrated that ganglioside GQ1b is localized in the nerve fibers innervating extrinsic muscles of the eye. When the immune system attacks GQ1b on nerves the result is ophthalmoplegia (7). Studies have shown that anti-GQ1b antibodies bind to and affect the function of the neuromuscular junction (NMJ). One such study demonstrated that antibodies reactive to GQ1b could fix complement resulting in disruption to the NMJ (54). Plomp *et al.* (1999) showed that anti-GQ1b IgM antibody bound to mouse NMJ, which resulted in a release of large amounts of acetylcholine from the nerve terminals. This phenomenon eventually led to blocked transmission at the NMJ (117).

We hypothesized that orally infected mice would present with clinical signs and anti-ganglioside antibodies similar to those seen in humans following infection with a MFS associated *C. jejuni* strain. We used non-obese diabetic (NOD) WT and C57BL/6 WT mice inoculated with *C. jejuni* strain CF93-6 isolated from a patient with MFS. Also, we inoculated NOD WT mice with *C. jejuni* 260.94 from a patient with GBS to serve as a positive control. Mice were analyzed weekly starting before infection for clinical neurological signs using phenotypic tests; plasma was collected to detect presence of anti-ganglioside antibodies, and the sciatic nerve was removed to examine cellular infiltrates and loss of myelin. Our results showed that mice of both genetic backgrounds can be colonized by the MFS-associated *C. jejuni* strain CF93-6 with minimal gross pathological features in the gastrointestinal tract. The NOD WT mice infected with *C. jejuni* 260.94 had significant differences in plasma levels of IgG1 antibody reactive to

ganglioside mixture GM1/GQ1b. However, there were no significant differences in anti-ganglioside antibodies or clinical neurological phenotypes between the sham-inoculated and *C. jejuni* CF93-6 infected mice of both genetic backgrounds (NOD WT and C57BL/6 WT). No other significant differences were observed between infected and uninfected mice of either genetic background. Based on our findings we were not able to distinguish an MFS clinical phenotype; neither the NOD WT nor the C57BL/6 WT mice displayed any phenotype. More work needs to be done to define a mouse model of GBS before distinguishing an MFS-like clinical presentation from a GBS-like presentation will be possible.

## MATERIALS AND METHODS

### Animals

Non-Obese Diabetic wild type mice (stock # 001976) and C57BL/6 wild type mice (stock # 00064) were purchased from The Jackson Laboratory (Bar Harbor, ME, USA) at 6 weeks of age and sent directly to the Michigan State University Research Containment Facility. Mice were housed individually in sterile filter top cages and allowed to acclimate for 14 days. All mice were given autoclaved reverse osmosis water; NOD WT mice were fed sterilized mouse diet 7913 (Harlan Teklad) and C57BL/6 mice were fed sterilized diet 7904 (Harlan Teklad). Fecal pellets were taken and DNA was extracted using a DNeasy Blood and Tissue Kit (Qiagen, Hilden, Germany) with modifications to a published protocol (104) to assess the genotype of all mice. Genotype was confirmed using a modified PCR assay from The Jackson Laboratory ([http://jaxmice.jax.org/pub-cgi/protocols/protocols.sh?objtype=protocol&protocol\\_id=346](http://jaxmice.jax.org/pub-cgi/protocols/protocols.sh?objtype=protocol&protocol_id=346)). Fecal samples were also taken from mice to test for presence of colitogenic bacteria by PCR prior to inoculation; colitogenic bacteria tested included *Campylobacter* spp., *Enterococcus faecalis*, *E. faecium*, *Helicobacter* spp., and *Citrobacter rodentium*. At 8 weeks of age, mice were inoculated orally with *C. jejuni* strains or sham-inoculated with tryptose soya broth (TSB). During the course of the experiment mice were monitored daily for clinical signs of enteric disease and weekly for neurological signs. This animal experiment followed all of the guidelines set by NIH and was approved by the MSU All University Committee on Animal Use and Care under protocol number 06/09-092-00.

### ***Campylobacter jejuni***

*C. jejuni* strains were both purchased from the American Type Culture Collection (ATCC, Manassas, VA, USA). *C. jejuni* 260.94 (ATCC BAA-1234) and *C. jejuni* CF93-6 (ATCC BAA-1456) were isolated from patients that presented with GBS and MFS respectively. To prepare the inoculum, *C. jejuni* strains were incubated for 48 hours at 37°C on tryptose soya agar (TSA) plates with 5% sheep's blood (Cleveland Scientific, Bath, OH, USA) in anaerobic jars containing CampyGen packs (Oxoid, Basingstoke, UK) (98). Bacterial growth was collected after two rounds of growth and mixed into a single master tube of TSB to a final concentration of  $\sim 5 \times 10^{10}$  CFU/ml (1:10 dilution approximately 1.0 at OD<sub>600</sub>). Motility of bacterial cultures was confirmed in a wet mount and a Gram stain was used to confirm gram negative rods (98).

### **Experimental Design**

The experiment consisted of 5 groups: 1) 15 mice of C57BL/6 WT background sham-inoculated with TSB, 2) 15 C57BL6/WT mice infected with MFS-associated *C. jejuni* CF93-6, 3) 14 sham-inoculated NOD WT mice, 4) 16 MFS-associated *C. jejuni* CF93-6 infected NOD WT mice, and 5) 15 NOD WT mice infected with GBS-associated *C. jejuni* 260.94. During the course of the experiment mice were tested weekly for neurological signs with three phenotypic tests and monitored daily for enteric disease. Mice were euthanized and necropsied at day 53. At necropsy sections of the GI tract, sciatic nerve, and blood were taken for examination of the presence of *C. jejuni*

colonization and histological evidence of enteritis, lesions and cellular infiltrates in nerve tissue, and presence of anti-ganglioside antibodies, respectively. Detailed methods are given below.

## **Neurological Testing**

*C. jejuni* infected mice and sham-inoculated mice were analyzed for clinical signs of neurological disease through a series of phenotypic tests given on a weekly basis. Prior to inoculation with *C. jejuni*, mice were trained on each test to remove any influence of a learning curve (22). The tests used in this experiment included footprint measurements, open field test, and rotarod.

### *Open field testing*

The open field test was used to examine mice for abnormal gait. Mice were set in the center of a polycarbonate box with four quadrants marked on the bottom and watched for 30 seconds. Mice were assessed for the number of quadrants crossed, rearing, and abnormal walking. Mice performed this test 3 times with 15 minute breaks in between each test interval (14, 24).

During the first interval, mice were recorded using a video camera and the resulting videos were analyzed with JWatcher<sup>TM</sup> 1.0 software (Daniel Blumstein Laboratory, University of California Los Angeles, and The Animal Behaviour Lab, Macquarie University, Sydney, Australia), by an individual blinded to the group identity of the mice. JWatcher<sup>TM</sup> is a computer software program designed to assess and score the movements of an animal (12). With this software, the videos recorded during the

open field test were analyzed by using a keystroke for each movement/clinical sign detected during the duration of the recorded time. The software then computed the number of times a keystroke was made and the length of time that keystroke was maintained (*i.e.*, assessing the length of time a clinical sign was observed) (12).

During the second and third test intervals the number of quadrants crossed was the only parameter recorded. These results were included in the final analysis with the number of quadrants recorded with the JWatcher™ program during the first interval. The number of times each mouse reared was analyzed using JWatcher™ during the first interval only. Abnormal gait was also recorded if it occurred.

#### *Rotarod testing*

A rotarod (IITC Rotarod for Rats and Mice, IITC Inc. Life Science, Woodland Hills, CA) was used to assess the balance of all mice. Mice were placed on the rotating wheel for 60 seconds. The speed was set at 3 RPM and was accelerated 0.10 RPM per second to a final speed of 30 RPM. Thereafter the length of time the mouse remained on the wheel was recorded. This test was repeated three times with a 15 minute rest between each test: the longest time spent on the wheel was used for analysis (14, 22).

#### *Footprinting and tracking*

Footprint measurements were taken to detect abnormal gait, foot drag, and splayed limbs (29). To assess walking, we prepared a runway for the mice by cutting a longitudinal slot out of a cardboard tube to monitor the movement of each mouse. A filter paper strip was cut to fit the length of the tube and cover the bottom surface. The

fore and hind paws of each mouse were painted with different colored non-toxic paint and the mouse was placed at one end of the tube and allowed to walk to the other end. The filter paper provided a record of the footprints and distinguished fore and hind feet. Measurements were then taken by identifying the midpoint of each paw print and measuring the distances between fore paws and hind paws for strides and stances. The spread of the toes and length of the paw print were also measured. Stride length and hind base width were then analyzed and compared between groups (14, 22, 29).

### **Enzyme-Linked Immunosorbent Assays (ELISA)**

Prior to inoculation and 14 days post inoculation, mice were bled from the saphenous vein. At necropsy mice were bled from the heart post euthanasia. Blood samples were then centrifuged at 3000 RPM for 5 minutes to collect the plasma. ELISA assays were performed to detect *C. jejuni* IgG2b antibody as previously described (98). ELISA assays were performed to detect the presence of antibodies directed against gangliosides GQ1b, GM1, and GD1a (Calbiochem/EMD Millipore, Gibbstown, NJ, USA at 0.2 µg /ml, US Biological, Swampscott, MA, USA at 2.0 µg/ml, and Sigma Aldrich, St. Louis, MO, USA at 20 µg /ml respectively). Anti-GQ1b was purchased from Associates of Cape Cod (East Falmouth, MA, USA); anti -GD1a and -GM1 were purchased from Chemicon/EMD Millipore (Gibbstown, NJ, USA) and were used as positive controls. ELISA assays were also performed to detect IgG1 antibodies reactive with a 1:1 mixture of two gangliosides; a mixture of GM1/GQ1b or a mixture of GM1/GD1a. Secondary antibodies used included anti-mouse IgM (Sigma Aldrich, St. Louis, MO, USA) and anti-mouse IgG1, IgG2a, IgG2b, IgG2c, and IgG3 (Jackson ImmunoResearch, West Grove,

PA, USA). Detection of antibodies was done using extravidin peroxidase (Sigma Aldrich, St. Louis, MO, USA) and TMB substrate (Rockland Immunochemicals Inc., Gilbertsville, PA, USA). All ELISA assays were performed in triplicate.

### **Assessment of Clinical Signs**

During the course of the experiment mice were monitored once a day until first onset of illness; thereafter mice were monitored twice daily. Enteric disease was assessed using clinical signs that included rough hair coat, diarrhea, hunched posture, and lack of movement as described previously (98). Clinical score sheets were maintained for any mouse exhibiting clinical signs and severe enteric disease. If a mouse exhibited a high clinical score, it was euthanized with an overdose of CO<sub>2</sub> to prevent any discomfort or distress. Neurological disease was assessed weekly using the phenotypic tests described above.

### **Necropsy Procedure and Assessment of Gross Pathological Features**

Mice were humanely euthanized with an overdose of CO<sub>2</sub> either at humane endpoints or at end of experiment (53 days) based on approved methods (1). Immediately following euthanasia, mice were weighed, blood was taken via the heart, and a puncture to the diaphragm followed to ensure death of the mouse. The entire GI tract was excised from stomach to rectum and any gross pathological features were noted. The GI tract was cut into 4 fragments: 1) stomach-duodenum, 2) jejunum, 3) ileum-cecum-proximal colon, and 4) distal colon-rectum and placed in 10% phosphate buffered saline to rinse away any contents in the lumen. These fragments were further

sectioned into subfragments of the stomach, jejunum, cecum, and colon which were further cut into three fragments. One fragment was streaked onto TSA + 5% sheep blood plates supplemented with antibiotics (TSA-CVA: 20 µg/mL cefoperazone, 10 µg/mL vancomycin and 2 µg/mL amphotericin B); these plates were placed in an anaerobic jar with CampyGen packs (Oxoid, Basingstoke, UK) and incubated for 48 hours at 37°C. The other two fragments were flash frozen for DNA and RNA extraction. Portions of the cecum, distal ileum, and proximal colon (ileocecocolic junction) were all placed on a sponge in a histological cassette and placed in 10% phosphate buffered formalin for fixation. The remaining portions of the GI tract, kidneys, liver, lungs, reproductive organs, heart, and brain were all placed in 10% phosphate buffered formalin for 24 hours for fixation and then transferred to 60% ethanol for storage. The mouse was skinned and the spinal cord was exposed for fixation in 10% phosphate buffered formalin. Both hind limbs were removed, skinned, the sciatic nerve was exposed, and the limb placed in 10% phosphate buffered formalin. Upon return to the laboratory, the sciatic nerve was then removed carefully under a microscope with some intact muscle and placed in a histological cassette stored in 60% ethanol. Paraffin embedding, sectioning, and staining were performed at the Michigan State University Investigative Histopathology Laboratory.

### **Assessment of Enteric Disease**

The TSA-CVA plates that were streaked with fragments of the four sections of the GI tract were assessed and scored for the presence of *C. jejuni* growth. Scoring was done on a scale of 0–4 based on the amount of bacterial growth; 0 for no growth up to 4

for confluent growth as previously described (98). Any plates that had bacterial growth were swabbed, the bacterial growth suspended in TSB containing 15% glycerol, and the tubes frozen at -80°C. These cultures were then sampled with a toothpick and whole cell PCR was used to confirm that the culture was *C. jejuni*, as previously described (98). Any mouse that was negative for *C. jejuni* growth on all GI tissue plates and all control mice had DNA extracted (Qiagen DNeasy tissue kit, Qiagen, Valencia, CA, USA) from the frozen cecal tissue, and PCR was performed to verify presence/absence of *C. jejuni*.

## **Histopathological Scoring for the GI Tract and Sciatic Nerve**

### *Gastrointestinal tract*

At the time of necropsy the ileoceocolic junction was removed, placed in a histological cassette and fixed in 10% phosphate buffered formalin and placed in 60% ethanol. These specimens were sent to the Michigan State University Investigative Histopathology Laboratory to be paraffin embedded and stained with hematoxylin and eosin. Sections were blinded and scored for the presence of lesions in the lumen, lamina propria, epithelium, and submucosa as previously described (98). A score from 0 to 44 was given; slides were read by a single veterinary expert in enteric disease/lesions (LSM).

### *Sciatic nerve*

The sciatic nerve was exposed at time of necropsy, placed in 10% phosphate buffered formalin for 6 hours, and then placed in 60% ethanol. Nerves were removed

from the entire length of the leg and placed on a sponge in a histological cassette for paraffin embedment at the Michigan State University Investigative Histopathology Laboratory. After embedment; two 5  $\mu\text{m}$  sections were cut with a Reichert Jung 2030 rotary microtome. One section was stained with hematoxylin and eosin and the second section with Luxol fast blue. Nerve sections were then examined and scored as previously described in Chapter 2 for lesions, myelin degradation, and cellular infiltration by one veterinary pathologist who was blinded and unbiased (BJG).

### **Statistical Methods**

GraphPad Prism version 6.01 (GraphPad Software Inc., La Jolla, CA, USA) was used for all statistical analyses. For all statistical tests both the NOD WT and C57BL/6 WT were assessed separately from one another. ELISA assays and histological scoring were analyzed with either the non-parametric Kruskal-Wallis ANOVA on ranks (NOD WT) followed by Dunn's if significant differences were noted or Mann-Whitney *U* test (C57BL/6 WT). All phenotypic tests were analyzed with a two-way ANOVA with repeated measures and if significant results were obtained, the Holm-Sidak post hoc test was used.

## RESULTS

### Screening for Enteric Disease with GBS-associated and MFS-associated *C. jejuni* Strains

Examination of the cultures from GI tract tissue and/or *C. jejuni* specific PCR was used to determine colonization by the *C. jejuni* strains. All cultures derived from *C. jejuni* infected mice were confirmed by *C. jejuni* specific PCR. All 29 sham-inoculated mice (14 NOD WT and 15 C57BL/6 WT) were both culture negative and PCR negative for detection of *C. jejuni*. As seen in Figure 3.1, panel A, 11/16 NOD WT mice and 13/15 C57BL/6 WT mice infected with *C. jejuni* CF93-6 were colonized at end point; 3 mice (1 NOD WT and 2 C57BL/6 WT) were negative by culture but positive when tested by *C. jejuni* specific PCR from DNA taken from cecal tissue. All NOD WT infected with *C. jejuni* 260.94 were colonized as detected by culture and/or PCR. One NOD WT mouse infected with *C. jejuni* CF93-6 had to be euthanized early because of a high clinical score for GI disease; no neurological disease was observed.

Gross pathological features were assessed at necropsy and noted. Features that were noted included presence of enlarged ileocecolic lymph nodes and thickened wall of the gastrointestinal (GI) tract (Figure 3.1, panel B). No gross pathological features were observed in the C57BL/6 WT sham-inoculated mice. Seven of fifteen *C. jejuni* CF93-6 infected C57BL/6 WT mice exhibited gross pathological changes. Only 1/14 NOD WT negative control mice presented with one feature. Twelve of thirty-one infected NOD WT mice presented with one of the features; 6/16 *C. jejuni* CF93-6

infected mice and 6/15 *C. jejuni* 260.94 infected mice. No mouse of any of the treatment groups presented with both gross pathological changes.

At necropsy, the ileoceccocolic junction was removed, fixed, stained, and scored as described above. Kruskal-Wallis ANOVA on ranks was used to compare the scores of the NOD WT mice; no significant differences were observed between the treatment groups. The Mann-Whitney *U* test was used to examine the C57BL/6 WT mice; no significant differences were noted between the uninfected and infected mice. The histological scores for all three infected groups of mice were minimal; no mouse ever scored above 10 (data not shown).

### **Detection of Anti-Ganglioside Antibodies with ELISA Assays**

Mice were bled at days 0 and 14 post inoculation from the saphenous vein as described above. The amount of blood taken at these time points was small and therefore only one ELISA assay was performed. Antibody IgM levels reactive to ganglioside GQ1b was measured at these time points. No significant differences were found between any treatment groups in the either NOD WT or the C57BL/6 WT mice at day 0 and day 14 post inoculation (Table 3.1).

At necropsy mice were bled from the heart, and plasma was used to detect *C. jejuni*-specific and auto-antibodies. ELISA assays were performed to detect the presence of IgG2b antibody levels reactive to *C. jejuni* antigen to verify an adaptive immune response to infection with the *C. jejuni* strains (Figure 3.2, panel A). Significant differences in the plasma levels of IgG2b reactive to *C. jejuni* were observed in the NOD WT mice using Kruskal-Wallis ANOVA on ranks ( $p < 0.0001$ ). Pairwise post hoc Dunn's

tests indicated significant differences between the sham-inoculated mice and both the *C. jejuni* CF93-6 infected mice ( $p \leq 0.001$ ) and the *C. jejuni* 260.94 infected mice ( $p \leq 0.01$ ). Significant differences in IgG2b antibody levels were also noted between infected and uninfected C57BL/6 WT mice (Mann-Whitney *U*;  $p < 0.0001$ ). ELISA assays were also performed for the presence of antibodies IgG1, IgG2a/2c, IgG3, and IgM reactive with gangliosides GD1a, GM1, and GQ1b. NOD WT mice were measured for levels of IgG2a antibody and C57BL/6 WT mice were measured for levels of the isotype IgG2c antibody. Presence of IgG1 antibody reactive to a mixture of gangliosides GM1 and GD1a and to a mixture of gangliosides GM1 and GQ1b were also performed with ELISA assays. Antibody levels of IgG1 reactive to ganglioside mixture GM1/GQ1b were observed to be significantly different between treatment groups (Kruskal-Wallis;  $p = 0.0031$ ). Dunn's post hoc test indicated significant differences in plasma levels of IgG1 reactive to ganglioside mixture GM1/GQ1b between the sham-inoculated mice and the *C. jejuni* 260.94 infected mice (Figure 3.2, panel B;  $p \leq 0.01$ ). No significant differences between the two treatment groups of the C57BL/6 WT mice or among the three treatment groups of the NOD WT mice were observed in levels of IgG1 antibody reactive to ganglioside mixture GM1/GD1a (Table 3.1). No significant changes in antibody levels to any of the three individual gangliosides were observed between treatment groups in either the NOD WT or the C57BL/6 WT mice (Figure 3.2, panel C; Table 3.1).

## Neurological Testing

Mice were assessed on a weekly basis for a neurological phenotype using neurological tests. These tests included rotarod, open field test, and footprinting. A two-way ANOVA with repeated measures was used to analyze the NOD WT mice and C57BL/6 WT mice in all phenotype tests. If significant results were obtained then the Holm-Sidak pairwise post hoc test was performed. Analysis of the footprint measurements, stride length and hind base width required the removal from the data set of mice that lacked a complete set of footprint measurements for the entire length of the experiment due to lack of cooperation.

#### *Rotarod*

Mice were placed on the rotating wheel of the rotarod to detect changes in balance and motor abilities. There were no significant differences in time spent on the rotarod between treatment groups in both the NOD WT and C57BL/6 WT mice. A change in the time spent on the rotating wheel over the course of the experimental time period was observed in all treatment groups of the NOD WT mice ( $p < 0.0001$ ). All observers noted that qualitatively that the C57BL/6 WT mice generally spent less time on the rotarod than the NOD WT mice over the course of the experiment (Figure 3.3, panel A).

#### *Open Field Test*

The open field test was used to detect abnormal gait and observe the general neurological health of the mouse. Mice were videotaped and assessed with the JWatcher™ program. Analysis of the number of quadrants a mouse crossed during the

test showed no significant differences in quadrants crossed between treatment groups of either the NOD WT mice or the C57BL/6 WT mice. Mice of both genetic backgrounds did have a significant change in quadrants crossed observed in all treatment groups over the course of the experimental time (NOD WT:  $p < 0.0001$  and C57BL/6 WT:  $p = 0.0001$ ). Observers noted qualitatively that the C57BL/6 WT mice generally were less mobile and curious in the open field test during the entire course of the experiment; all treatment groups of the NOD WT mice moved around much more (Figure 3.3, panels C and D).

A rear occurs when a mouse stands on its hind legs; this behavior was recorded during the videotaped interval with the JWatcher™ program. The program recorded the length of time the mice were rearing; data are shown in Figure 3.3, panel B. No significant difference in time spent rearing was found between treatment groups of either the NOD WT mice or the C57BL/6 WT mice. Qualitatively it was observed that the NOD WT sham-inoculated and both *C. jejuni* CF93-6 NOD WT infected mice and *C. jejuni* 260.94 NOD WT infected mice all spent more time rearing over the course of the experiment than both uninfected and infected C57BL/6 WT mice.

### *Footprint Measurements*

This test was used to detect abnormal gait and foot drag in experimental mice. Measurements for stride length, hind base width, print length, stride variability, and toe spread were all recorded. Only stride length and hind base width (Figure 3.3, panels E–F) will be discussed here. Some mice were uncooperative during this test (no clean footprints recorded after 2 trials), and therefore a footprint measurement was not always

taken at every week. These mice had to be removed from analysis to enable a two-way ANOVA with repeated measures to be performed. Two sham-inoculated, three *C. jejuni* CF93-6 infected, and two *C. jejuni* 260.94 infected NOD WT mice had to be removed from the analysis. Only two sham-inoculated C57BL/6 WT mice had to be removed from the analysis. Body weight was measured at end of the experiment and no significant differences in weight were found between treatment groups of either the NOD WT or C57BL/6 WT mice. Therefore we concluded that body weight of mice did not play a role in footprint measurements (data not shown).

No significant differences in stride length were found between the sham-inoculated mice and either the *C. jejuni*- 260.94 infected or *C. jejuni*- CF93-6 infected NOD WT mice. The C57BL/6 WT mice also showed no significant difference in stride length between uninfected and infected mice. Measurements of the hind base width revealed no significant changes between treatment groups of either the NOD WT mice or the C57BL/6 WT mice. Hind base width changed over the course of the experimental time in all treatment groups of both mouse strains (NOD WT:  $p=0.0048$ ; C57BL/6 WT:  $p<0.0001$ ), but there were no significant differences between treatment groups within mice of either genetic background.

### **Presence of Nerve Lesions**

At necropsy, sections of the sciatic nerve were removed, fixed, and stained with hemotoxylin and eosin and scored as described above. No significant differences in histopathological scores were observed between treatment groups of NOD WT mice using a Kruskal-Wallis ANOVA on ranks. The C57BL/6 WT mice did not have a

significant difference between the uninfected mice and infected mice as shown by a Mann-Whitney *U* test. The presence of cellular infiltrates including mast cells, plasma cells, neutrophils, lymphocytes, and macrophages was assessed. Fisher's Exact test detected no correlation in the presence of cellular infiltrates between treatment groups of both mouse genetic backgrounds. It was observed that one C57BL/6 WT mouse infected with *C. jejuni* CF93-6 had infiltration of mast cells, neutrophils, and macrophages. One NOD WT *C. jejuni* CF93-6 infected mouse presented with infiltration of lymphocytes, neutrophils, and mast cells. It was noted that the lymphocytes and neutrophils were directly associated with the nerve in this mouse.

Sections of the nerve were also stained with Luxol fast blue to detect any degradation of the myelin sheath surrounding the axon. Some C57BL/6 mice did exhibit myelin loss, but Fisher's Exact test indicated no significant difference between sham-inoculated mice and *C. jejuni* CF93-6 infected mice of the C57BL/6 WT background. No significant differences were observed between the treatment groups of the NOD WT mice using Fisher's Exact test.

## DISCUSSION

Miller Fisher Syndrome is a clinical subtype of GBS that is distinguished by a descending paralysis that affects both the central and peripheral nervous systems. In previous work in our laboratory we have identified a potential murine model to study GBS using NOD WT mice infected with two different *C. jejuni* strains, one from an AMAN patient and one from an AIDP patient (St. Charles, unpublished). We also observed significant differences in presence of anti-ganglioside antibodies in C57BL/6 IL-10<sup>-/-</sup> mice infected with GBS-associated *C. jejuni* compared to sham-inoculated mice (Malik, unpublished). To further our understanding of the autoimmune neuropathies that follow *C. jejuni* infection, we sought to develop a mouse model of MFS. To accomplish this, we infected both NOD WT mice and C57BL/6 WT mice with strains of *C. jejuni* associated with MFS and GBS.

Our results showed no significant differences between the sham-inoculated mice and the *C. jejuni* CF93-6 infected mice in clinical neurological signs, presence of anti-GQ1b antibodies, and cellular infiltration of the sciatic nerve in either mouse genetic background. NOD WT mice infected with *C. jejuni* 260.94 had significantly higher levels of IgG1 antibody reactive to ganglioside mixture GM1/GQ1b; however they showed no significant differences in any of the phenotypic tests, suggesting a subclinical phenotype. Furthermore, examination of the sciatic nerve showed no significant differences between treatment groups of either the NOD WT mice or the C57BL/6 WT mice for cellular infiltrations and nerve lesions. We were unable to observe significant differences in anti-ganglioside antibody levels, nerve lesions, and or neurological

phenotype in MFS-associated *C. jejuni* CF93-6 infected animals for either C57BL/6 WT mice or NOD WT mice. Only the GBS-associated *C. jejuni* 260.94 NOD WT infected mice produced anti-ganglioside antibodies. These results were obtained despite the high level of gastrointestinal colonization of both *C. jejuni* strains and the strong *C. jejuni* specific antibody responses developed against each *C. jejuni* strain in colonized mice. Thus, the *C. jejuni* strains were present in the majority of mice throughout the experiment, but only the NOD WT mice infected with *C. jejuni* 260.94 developed manifestations of autoimmunity in the form of autoantibodies.

Previous experiments performed in this laboratory with NOD WT and the GBS-associated *C. jejuni* 260.94 strain have shown a neurological phenotype and presence of macrophages in peripheral nerve sections. Similar results were not seen in this experiment. The mice used in this experiment were purchased directly from The Jackson Laboratory; previous experiments used NOD WT mice from our established specific pathogen free mouse colony. Therefore, differences seen between previous experiments and this experiment could be a result of different microbiota of purchased versus breeding colony mice. Our breeding colony mice may also have experienced some genetic drift during several years of breeding in our colony, resulting in the differences observed between experiments.

Studies have shown that approximately 80–100% of MFS cases present with antibodies reactive to ganglioside GQ1b; however, some patients can still develop MFS without any antibody production to GQ1b (93, 97, 137). Lee *et al.* (2012), discuss a case study of a 13 year old boy who presented with the classical clinical profile of MFS but tested negative for any antibody to ganglioside GQ1b (93). A similar phenomenon

could have occurred in our experiment; we performed ELISA assays to detect the presence of antibodies IgG1, IgG2a/2c, and IgG3 reactive to ganglioside GQ1b, but found no significant differences between the sham-inoculated mice and those infected with *C. jejuni* CF93-6. We could also test for antibodies reactive to gangliosides GT1a and GD3 which have been shown to cross react with antibodies reactive to GQ1b (117). Additionally, the primary antibody response may have already waned by the time of necropsy.

Analysis of the nerve sections examined histologically showed no significant differences between uninfected mice and infected mice in nerve lesions and cellular infiltrates. GQ1b is highly enriched in the ocular motor nerves and therefore in future experiments we should remove and examine these nerves histologically. We should also identify the NMJ in the mice and determine if there is binding of anti-GQ1b antibody resulting in disruption of the NMJ.

**Table 3.1: P values for ELISA assays.** Abbreviations: KW, Kruskal-Wallis ANOVA;

MW, Mann-Whitney *U*.

	Genotype	
	NOD WT	C5BL/6 WT
<b>ELISA</b>		
<b>GM1 (IgG1)</b>	KW; p=0.0678	MW; p=0.6491
<b>GM1 (IgG2a)</b>	KW; p=0.1666	MW; p=0.6762
<b>GM1 (IgG3)</b>	KW; p=0.9595	MW; p=0.2243
<b>GM1 (IgM)</b>	KW; p=0.6377	MW; p=0.7042
<b>GD1a (IgG1)</b>	KW; p=0.7730	MW; p=0.4418
<b>GD1a (IgG2a)</b>	KW; p=0.1153	MW; p=0.3194
<b>GD1a (IgG3)</b>	KW; p=0.2913	MW; p=0.3253
<b>GD1a (IgM)</b>	KW; p=0.1446	MW; p=0.6948
<b>GQ1b (IgG1)</b>	KW; p=0.4553	MW; p=0.2000
<b>GQ1b (IgG2a)</b>	KW; p=0.4867	MW; p=0.9334
<b>GQ1b (IgG3)</b>	KW; p=0.4552	MW; p=0.8276
<b>GQ1b (IgM)</b>	KW; p=0.4999	MW; p=0.1329
<b>GM1/GD1a (IgG1)</b>	KW; p=0.3293	MW; p=0.4234
<b>GM1/GQ1b (IgG1)</b>	KW; p=0.0031	MW; p=0.7828
<b>Cj (IgG2b)</b>	KW; p<0.0001	MW; p<0.0001
<b>Day 0 GQ1b (IgM)</b>	KW; p=0.4751	MW; p=0.1019
<b>Day 14 GQ1b (IgM)</b>	KW; p=0.0524	MW; p=0.3611

**Figure 3.1: Examination of GI disease.** Panel A shows colonization of mice based on culture and/or PCR of the cecum at endpoint. No sham-inoculated mouse was colonized. Panel B shows the gross pathological features present in mice at time of necropsy. Features examined were thickened wall of the GI and enlarged lymph nodes.

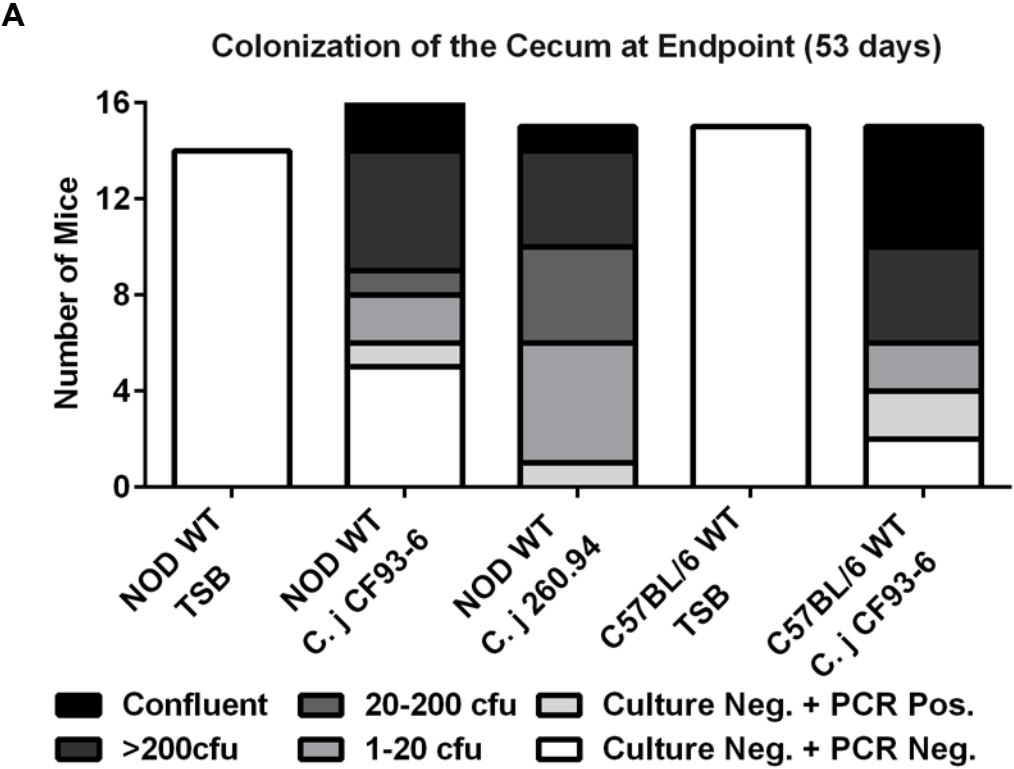
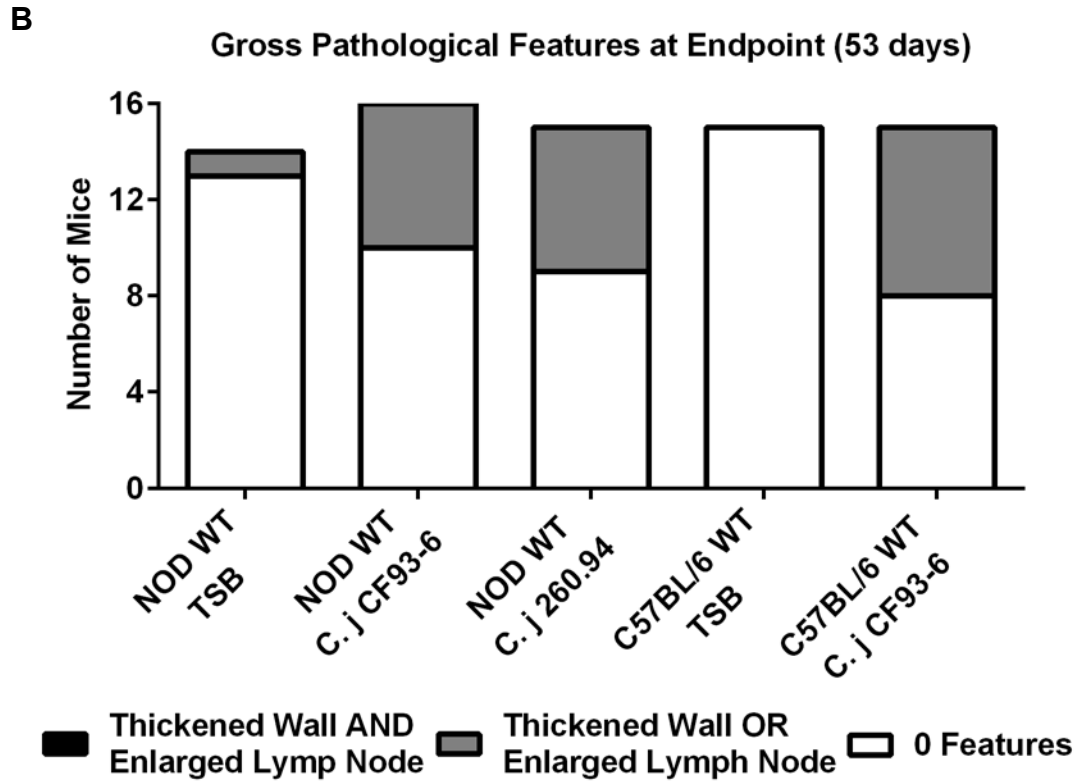


Figure 3.1 (cont'd)



**Figure 3.2: ELISA data.** Panel A shows the levels of antibody IgG2b reactive with *C. jejuni* antigen. Panel B shows plasma levels of IgG1 reactive with ganglioside mixture GM1/GQ1b. Panels C-1, C-2, and C-3 show the antibody plasma levels for IgG1, IgG2a/IgG2c, and IgG3, respectively. NOD WT mice have the IgG2a receptor and were tested for IgG2a antibody levels; C57/BL6 WT mice have the IgG2c receptor and were tested for levels of IgG2c antibody. Unless stated otherwise, significance levels in all graphs are by \* ( $p \leq 0.05$ ), \*\* ( $p \leq 0.01$ ), \*\*\* ( $p \leq 0.001$ ) and \*\*\*\* ( $p \leq 0.0001$ ).

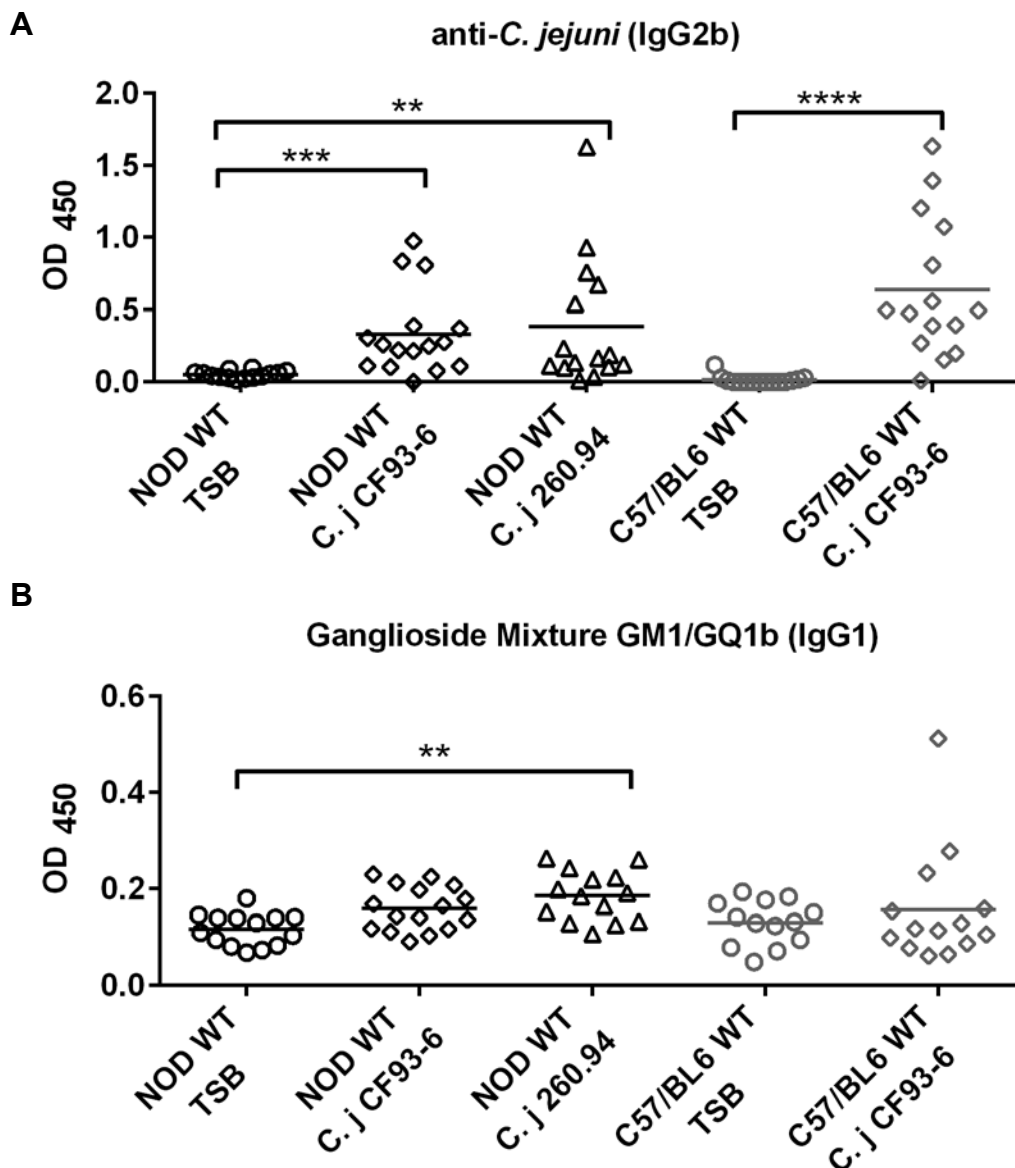
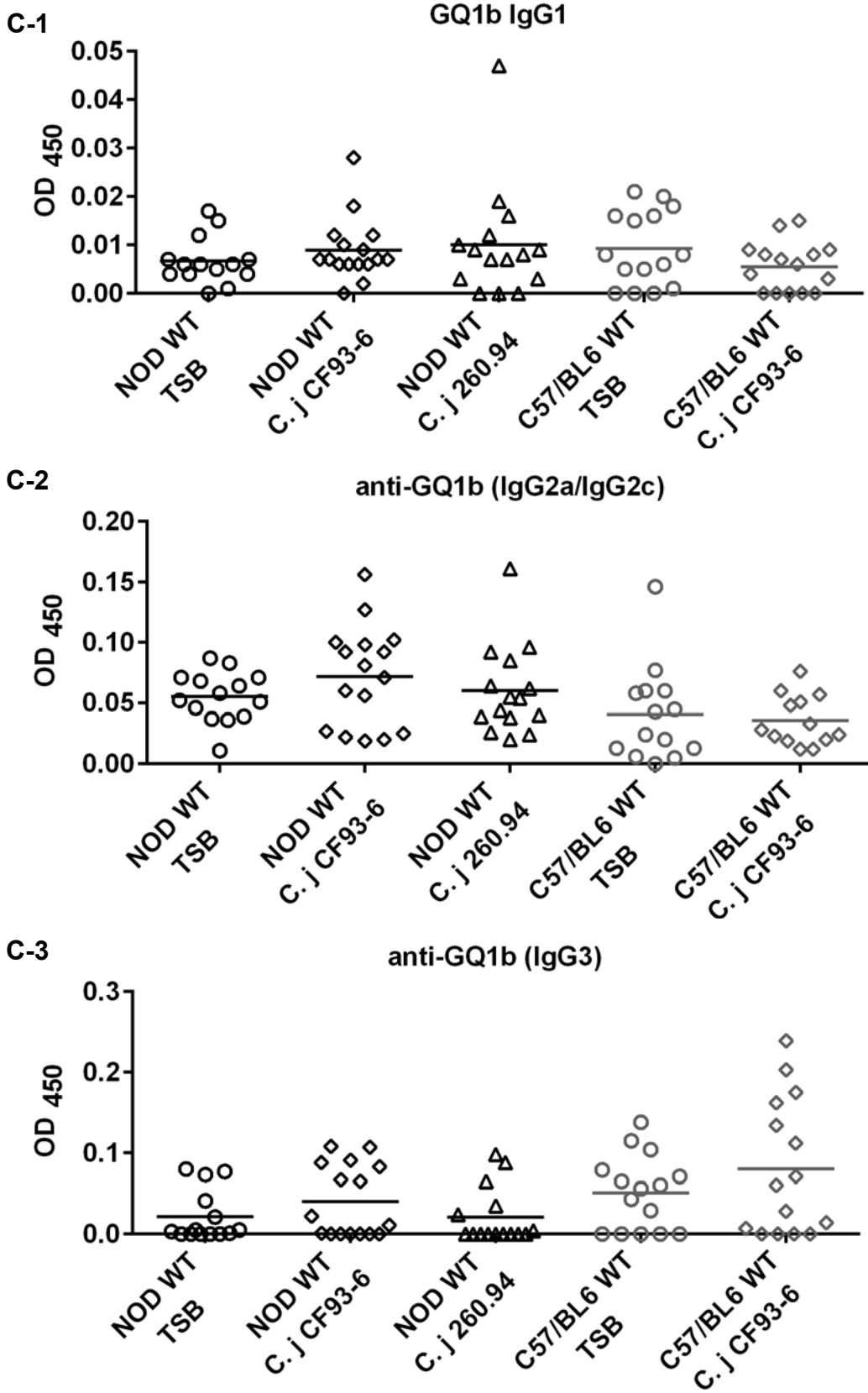


Figure 3.2 (cont'd)



**Figure 3.3: Assessment of Clinical Neurological Signs with Phenotype Tests.**

Panel A shows time spent on the rotarod; no significant differences between treatment groups in either the NOD WT mice or the C57BL/6 WT mice were observed. The C57BL/6 WT mice generally spent less time on the rotarod over the entire course of the experiment. Panel B shows the time spent rearing in the first interval of the open field test as calculated with JWatcher™. NOD WT mice spent more time rearing than C57BL/6 WT mice. Panels C and D show the number of quadrants crossed during the three intervals of the open field test for NOD WT and C57BL/6 WT mice, respectively. Stride length and hind base width measurements are shown in panels E and F for NOD WT mice and C57BL/6 WT mice respectively. No significant differences in either measurement were observed between the three treatment groups of NOD WT mice or between uninfected and infected C57BL/6 WT mice.

Figure 3.3 (cont'd)

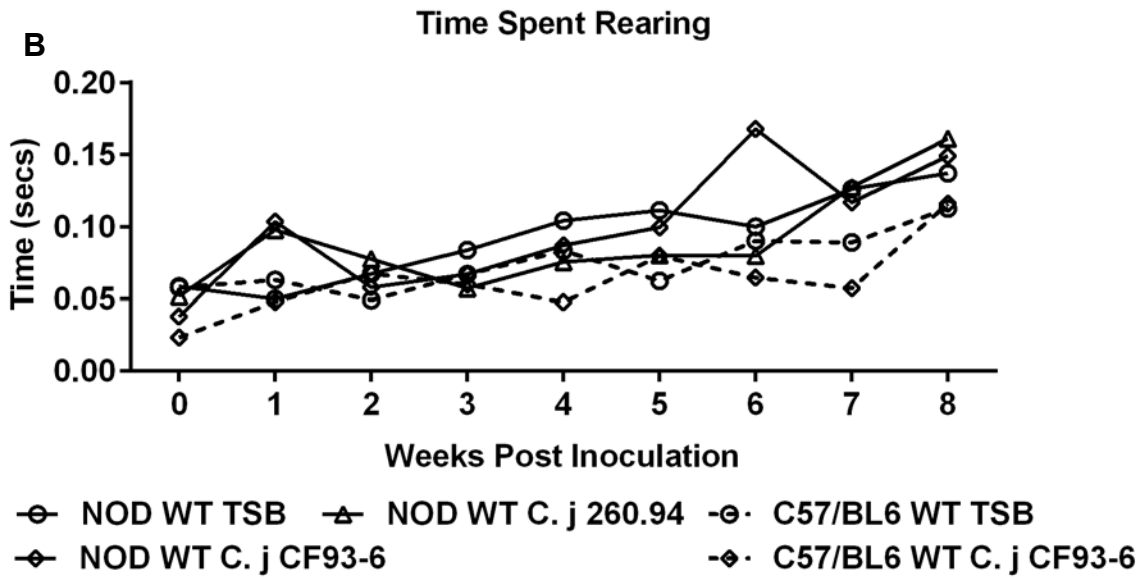
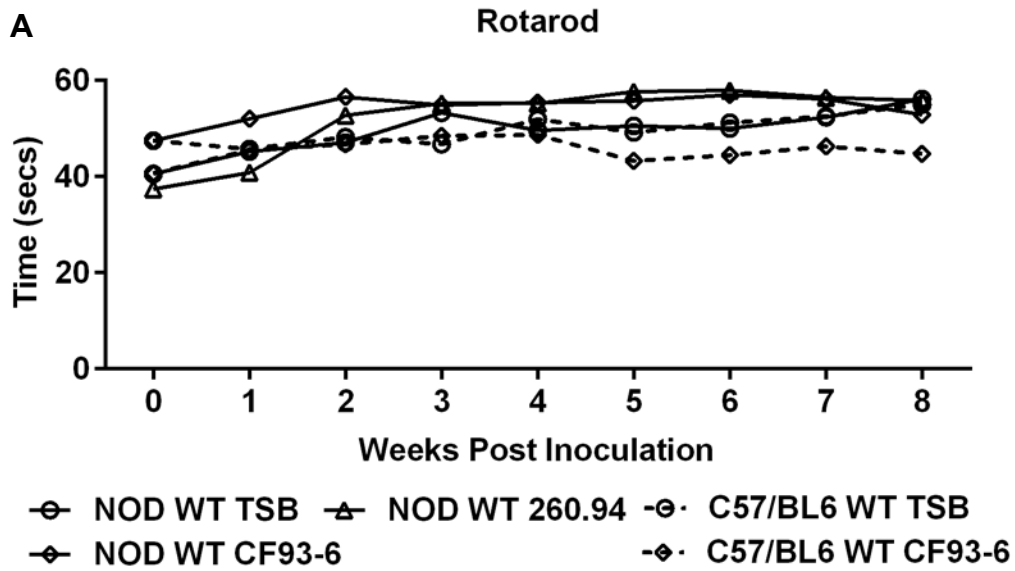


Figure 3.3 (cont'd)

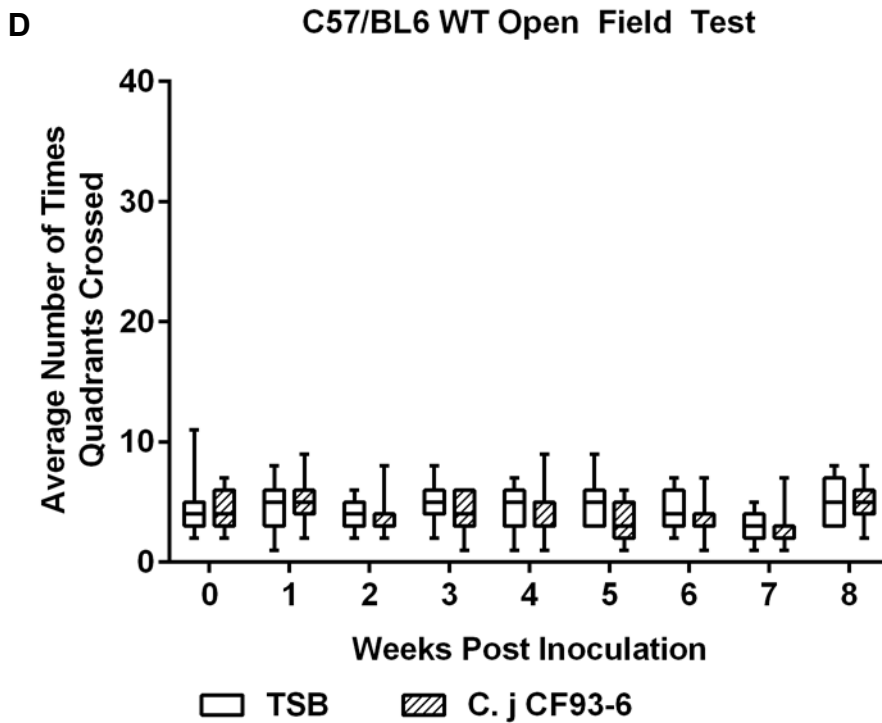
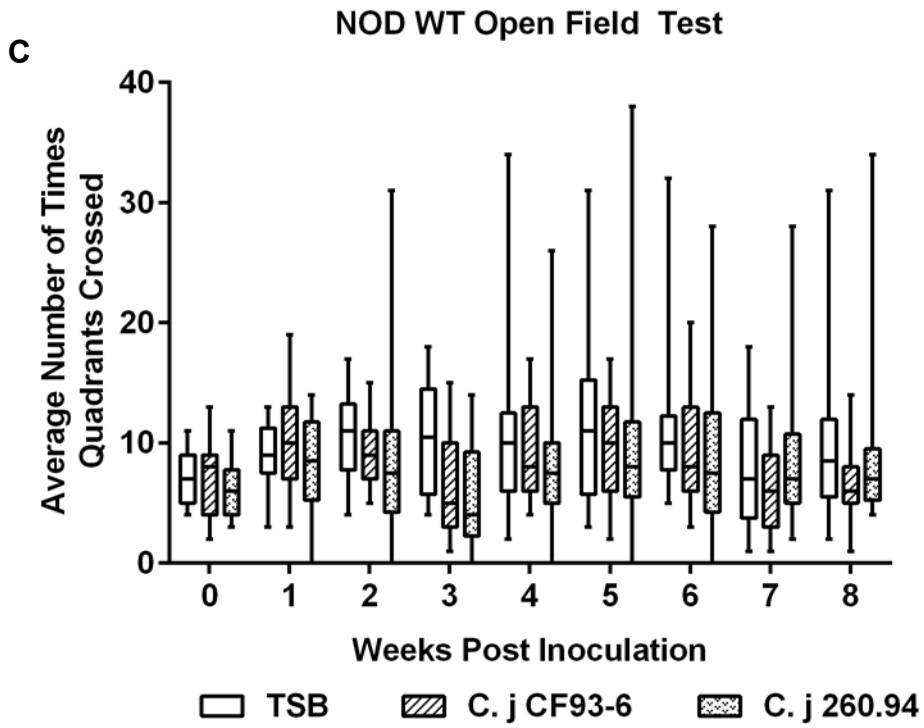


Figure 3.3 (cont'd)

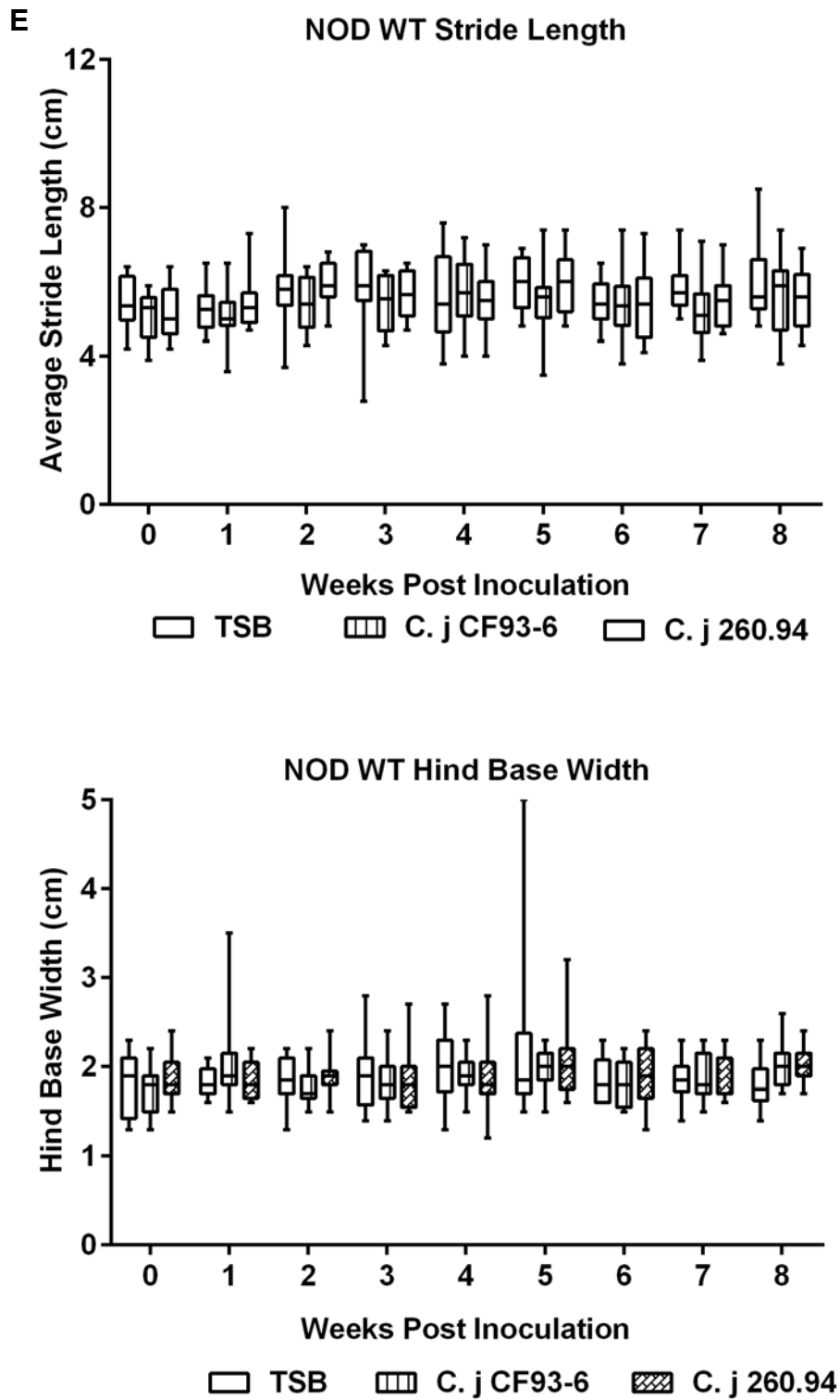
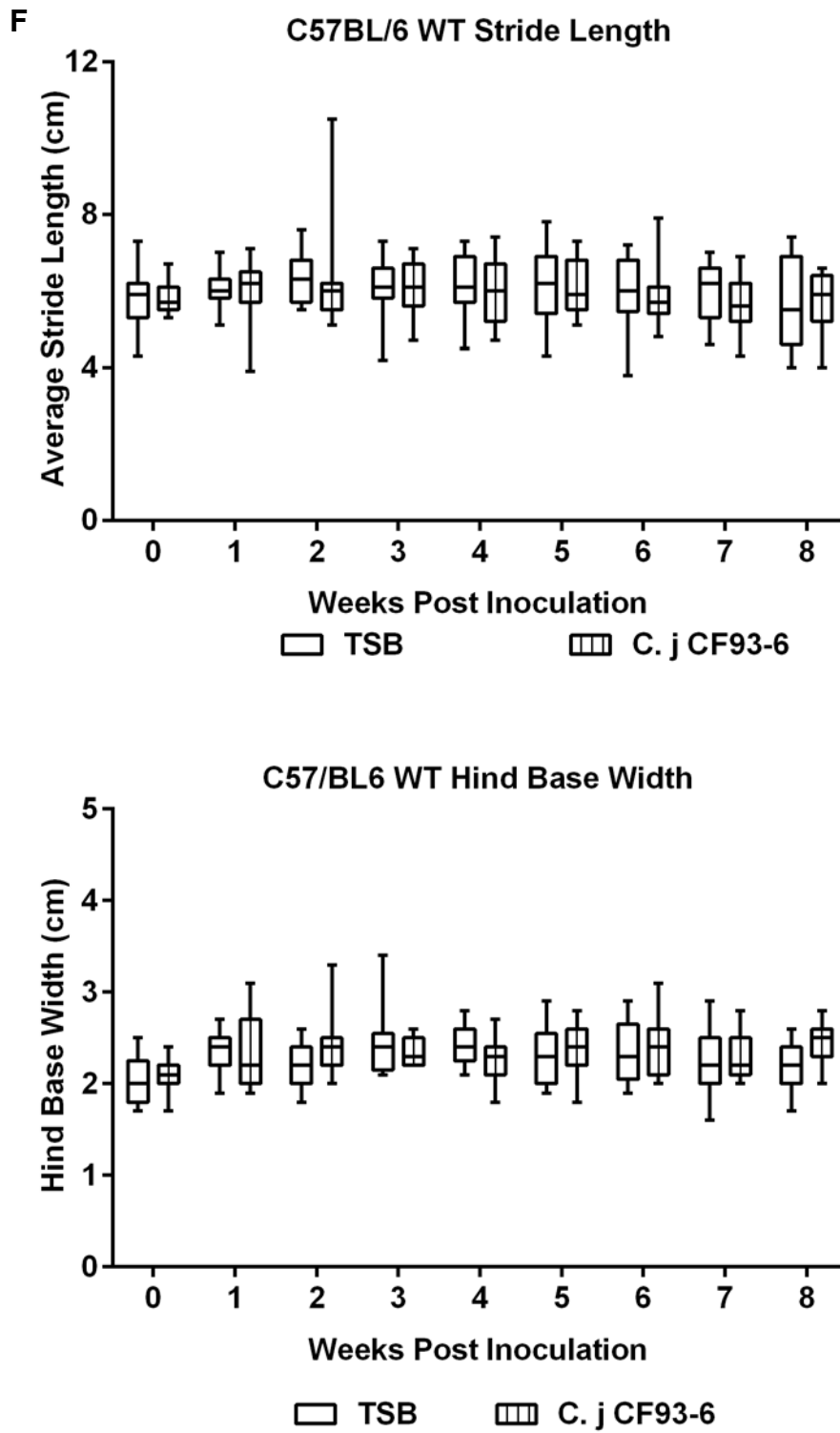


Figure 3.3 (cont'd)



## CHAPTER 4

Multiple molecular typing schemes applied to define genetic relationships among *C.*

*jejuni* isolates that share the same LOS classification

## ABSTRACT

The Gram negative bacterium *Campylobacter jejuni* is the leading cause of bacterial gastroenteritis in the Western world. Symptoms of *C. jejuni* infection include fever, abdominal cramping, and watery or bloody diarrhea. Sequelae that can occur after infection include Guillain Barré Syndrome (GBS), Miller Fisher Syndrome (MFS), Reiter's Arthritis, and both Irritable Bowel Syndrome and Inflammatory Bowel Disease. *C. jejuni* is the most common antecedent infection associated with development of GBS. The suggested mechanism of GBS is molecular mimicry of the *C. jejuni* lipooligosaccharide (LOS) and neurogangliosides resulting in development of anti-ganglioside antibodies. Gangliosides are sialylated glycolipid structures highly enriched in nervous tissue, and it has been demonstrated that *C. jejuni* sialylated LOS can mimic gangliosides. Serotyping and several molecular typing methods (LOS classification, multi-locus sequence typing (MLST), *flaA* SVR sequence typing, and *porA* allele typing) have been applied to define possible genetic relationships among *C. jejuni* isolates from GBS, MFS, and enteritis patients, but outcomes have been inconsistent. We hypothesized that there would be associations between MLST, *flaA*, or *porA* sequence types and *C. jejuni* strains belonging to LOS classes associated with GBS and MFS in a temporally and geographically limited set of strains. We applied these molecular typing schemes to 68 *C. jejuni* isolates from patients that presented with enteritis; a small set of unrelated strains, including strains from three patients known to have developed neuropathy were included in the analysis. We expected to see a genetic relationship between LOS classes and the *porA* allele types or *flaA* SVR sequence types. We did

expect to find strains of some clonal complexes defined by MLST to contain one predominant LOS class.

In our study we were able to classify 56/68 *C. jejuni* isolates into LOS classes A–F; however no isolate was determined to be in LOS class D. Our MLST studies indicated that the strain collection included 36 different sequence types that were clustered into 19 different clonal complexes. DNA sequencing of a portion of the *porA* gene and *flaA* SVR gene resulted in the assignment of 43 different *porA* alleles and 39 different sequence types respectively. Analysis of the LOS classification, MLST, *porA* gene, and *flaA* SVR gene resulted in 49/68 isolates that were singletons; the remaining isolates were grouped into 8 different groups of 2 or more isolates based on allele assignments. These data demonstrate that *C. jejuni* populations associated with enteritis are highly diverse based on several genotyping systems. The only clonal complexes with three or more strains were CC 21 (16), CC 353 (7), CC 45 (5), and CC 206 (3). Furthermore, several clonal complexes had associations with particular LOS classes.

## INTRODUCTION

*Campylobacter jejuni*, a gram negative bacterium, is the most frequent cause of human bacterial gastroenteritis (19). Common sources of *C. jejuni* infection include consumption of contaminated chicken meat, water, or unpasteurized milk (111). Serious disease sequelae can be triggered by *C. jejuni* infection, including the acute neuropathies Guillain Barré Syndrome (GBS) and Miller Fisher Syndrome (MFS) (105). Incidence of GBS secondary to *C. jejuni* infection is estimated to be 0.25–0.65 cases per 1000 cases of *C. jejuni* infection (163). Neurological symptoms appear 1–3 weeks after recovery from the initial *C. jejuni* gastrointestinal infection. Symptoms may start with weakness of extremities and progress within hours to weeks to paralysis of the limbs, trunk, or extraocular and facial muscles (7, 80, 116). About 3–10% of GBS patients die, and up to 10–20% of GBS patients have long term disability (7, 72, 163).

The mechanism thought to play a role in the induction of GBS is a molecular mimicry between the LOS of *C. jejuni* and host gangliosides found on peripheral nerves (7, 145). The LOS structure consists of a lipid A tail that is inserted into the outer membrane of *C. jejuni* and a highly variable oligosaccharide moiety that extends into the extracellular space (112). Gangliosides are glycolipids that are enriched on the cell surface of neural tissues. They consist of variable oligosaccharide moieties containing one or more sialic acid residues that protrude into the extracellular space and a ceramide tail that is inserted into the lipid bilayer of the membrane (7, 80, 156). Gangliosides play a role in maintenance of cell membrane structure and are important

in cell-cell recognition; they have been shown to be present in the nerve myelin sheaths and axons of peripheral nerves (7).

In 2000, completion of the genome sequence of the *C. jejuni* strain 11168 defined the genes involved in LOS biosynthesis and their arrangement in the LOS biosynthesis locus (112). Since then the genes of LOS biosynthesis loci have been identified in both sequenced and unsequenced strains of *C. jejuni*; the results have shown that the gene content of the LOS loci is highly variable (47, 112), as are the LOS structures produced by the pathway (45, 48, 50, 113). The LOS biosynthesis locus extends from Cj1131c to Cj1151c in the genome of *C. jejuni* 11168. Genes that have been identified in the locus include glycosyltransferases and genes involved in sialic acid biosynthesis. To date, 23 different classes (A–W) of *C. jejuni* strains have been defined based on both gene content as detected by PCR and organization of the genes within the LOS biosynthesis loci (111, 112, 125). Previous work by Gilbert *et al.* (2002) identified a variable region of the LOS that contains the *cgtA* (orf5abl) and *cgtB* (orf6ab) genes that results in 2 alternative allele types: 1) orf5abl1/orf6ab1 (allele 1) or 2) orf5abl2/orf6ab2 (allele 2). Both LOS class A and LOS class B can be further defined by the presence of these alleles; either class can contain either allele type 1 or allele type 2 based on the presence of the *cgtA* and *cgtB* genes (47, 112). A study by Godschalk *et al.* (2004) demonstrated an association between GBS and *C. jejuni* LOS classes that contain the genes necessary to synthesize a sialylated LOS that mimics gangliosides (49). The genes needed to synthesize sialic acid and transfer it to the LOS sugar backbone are *neuBCA* (biosynthesis of sialic acid) and *cstII and III* (sialic acid transferases) (47, 49, 111, 112, 125); *cstIII* and one of the two alleles of *cstII* have

different transferase activities and produce different ganglioside mimics. *C. jejuni* strains in LOS classes A, B, C, M, R, and V possess these genes.

Other outer membrane surface molecules have been examined to define possible epidemiological genetic relationships between these molecules and *C. jejuni* strains associated with GBS and MFS. One such molecule that has been studied is the *flaA* gene of the polar flagellum of *C. jejuni*. Meinersmann *et al.* (1997) showed that sequencing of a short variable region (SVR) in the *flaA* gene produced results similar to those found with sequences of the entire *flaA* gene (101). Thus a quicker method of typing *C. jejuni* isolates using *flaA* SVR was proposed (101). Many studies have been performed to determine possible associations between *flaA* SVR sequence typing and GBS-associated strains of *C. jejuni*. Tsang *et al.* (2001) reported that they had identified a *flaA* SVR sequence type that was associated with *C. jejuni* strains from GBS patients (144), while Dingle *et al.* (2001) found no correlation between the *flaA* SVR sequence type identified by Tsang *et al.* and GBS or MFS in a study of 25 *C. jejuni* isolates (35).

Another outer membrane surface molecule that has been studied is the *porA* gene encoding the major outer membrane protein. Clark *et al.* (2007) characterized the *porA* sequence of 105 *C. jejuni* isolates and defined 3 sequence types (27). They found no association in their study of any particular sequence type with GBS-associated or MFS-associated *C. jejuni* isolates; all 3 sequence types were associated with GBS-associated and MFS-associated *C. jejuni* strains (27).

Another typing scheme used to identify genetic relationships among *C. jejuni* isolates is multi-locus sequence typing (MLST). MLST was first described for *C. jejuni* in 2001 by Dingle *et al.* using 194 *C. jejuni* isolates (34). MLST is based on use of

sequence variation in 7 conserved housekeeping genes to compare genetic relationships among different bacterial isolates. The partial gene sequences used vary in length and are assigned allele numbers based on sequence variation. In the study by Dingle *et al.* (2001), the authors were able to assign 155 sequence types (STs) to 62 different clonal complexes (34). Multiple studies using MLST have been performed to compare the genetic relationships among *C. jejuni* strains isolated from GBS and MFS patients. Revez *et al.* (2012) combined the molecular typing schemes of LOS classification and MLST to compare the genetic relationships among 403 *C. jejuni* isolates revealed by the two methods and were able to show an association between LOS classes and sequence types of MLST (124).

The PCR-based classification scheme for the LOS locus and MLST have been very useful tools in comparing and contrasting relatedness and LOS genetic content of enteric and neuropathic strains of *C. jejuni*; however there are conflicting data for the molecular typing of *C. jejuni* with *flaA* and *porA*. Therefore, we conducted our own analysis of 68 *C. jejuni* isolates. In our study, 5/68 isolates were previously sequenced; these strains included *C. jejuni* 11168; 2 strains isolated from GBS patients and 1 from an MFS patient; and *C. jejuni* CG8421, which has been demonstrated to have an LOS that does not mimic gangliosides (143). We determined the LOS classification of the 68 *C. jejuni* isolates; 86% of the isolates typed as LOS classes A–C. To determine genetic relationships between the LOS classification and other variable outer membrane structures (*porA* and *flaA*) of the bacterium, we performed molecular typing of the *porA* and *flaA* SVR; we also included MLST to examine the association of highly conserved genes. We hypothesized that known isolates that were associated with GBS and MFS

would be of similar sequence types as those isolates that only caused enteritis; there would be a genetic relationship between other outer membrane surface molecules and LOS class. We analyzed each molecular typing method individually and then combined them for a comparative study of the techniques. Based on our results, the 68 isolates of *C. jejuni* were highly diverse. Analysis of combined data from the three sequence-based typing schemes resulted in 49 singletons with 8 different groups of isolates of 2 or more isolates; LOS classes A–C were distributed among all groups.

## MATERIALS AND METHODS

### ***Campylobacter jejuni* Strains and Growth Conditions**

Sixty-eight isolates of *Campylobacter jejuni* were collected and maintained for molecular typing (Table 4.1); of the 68 isolates 5 have previously been sequenced. Of the previously sequenced strains, two are from GBS cases (*C. jejuni* 260.94 and *C. jejuni* HB93-13), one is from an MFS patient (*C. jejuni* CF93-6), one is the genome strain *C. jejuni* 11168, and one is *C. jejuni* CG8421, which has been demonstrated not to mimic gangliosides (143). *C. jejuni* 260.94 was isolated from a patient in the Red Cross Children's Hospital in Cape Town, South Africa who presented with the acute inflammatory demyelinating polyneuropathy (AIDP) subtype of GBS (2). *C. jejuni* HB93-13 was isolated from an 8 year boy who presented with the acute motor axonal neuropathy (AMAN) subtype of GBS (2). The MFS-associated *C. jejuni* strain CF93-6 was isolated from an MFS patient in Japan (2). These strains were streaked for growth on Bolton agar plates (Bolton Broth, Thermo Fisher Scientific, Pittsburgh, PA, containing 15% Bacteriological Agar, Neogen, Lansing, MI) for DNA extraction (10).

Forty-nine of sixty-eight isolates were recovered from patients by the Michigan Department of Community Health. These isolates were de-identified and graciously supplied by Dr. Shannon Manning (Michigan State University Microbial Evolution Laboratory, East Lansing, MI). Upon arrival in the laboratory, samples were streaked for isolation onto Bolton agar plates and grown for 48 hours at 37°C in anaerobic jars with CampyGen packs (Oxoid, Basingstoke, UK). Isolated colonies were collected and streaked for growth under the same conditions. After 48 hours, bacterial growth was

harvested and suspended in tryptose soya broth (TSB) containing 15% glycerol to produce a stock culture and stored at  $-80^{\circ}\text{C}$ .

Four of sixty-eight isolates were obtained from soil samples of calf pens from dairy farms in Pennsylvania and Virginia. These isolates were graciously supplied by Dr. Terence Marsh, Michigan State University Department of Microbiology and Molecular Genetics; his laboratory isolated the *C. jejuni* strains and supplied us with stock cultures. We streaked the stock cultures on Bolton agar plates (Bolton Broth, Thermo Fisher Scientific, Pittsburgh, PA, containing 15% Bacteriological Agar, Neogen, Lansing, MI) to check viability as described above. Bacterial growth was harvested and stored at  $-80^{\circ}\text{C}$  in TSB + 15% glycerol.

The 10/68 remaining isolates were supplied by the Centers for Disease Control (CDC; Atlanta, Georgia) from different *C. jejuni* infections in both the U.S. and Canada (10, 11). One isolate included in this group, *C. jejuni* D8942, was obtained from a GBS patient in New Mexico. All other isolates have no association with GBS to the best of our knowledge. All strains were previously acquired by our laboratory; stock cultures were maintained in TSB + 15% glycerol at  $-80^{\circ}\text{C}$  (10, 11).

### **Preparation of Genomic DNA**

Frozen cultures were streaked on Bolton agar plates (Bolton Broth, Thermo Fisher Scientific, Pittsburgh, PA, containing 15% Bacteriological Agar, Neogen, Lansing, MI) for growth at  $37^{\circ}\text{C}$  for 48 hours in anaerobic jars containing CampyGen packs (Oxoid, Basingstoke, UK). Growth was collected and DNA was isolated using Wizard<sup>®</sup>

Genomic DNA Purification Kits (Promega, Madison, Wisconsin) according to the manufacturer's instructions. All genomic DNA was diluted to a final concentration of 25 ng/ $\mu$ L.

### **Determination of *Campylobacter* spp.**

Verification of isolates as *C. jejuni* or *C. coli* was performed using a previously described multiplex PCR (96). Hot Start Syzygy Mean Green (Integrated Scientific Solutions, San Diego, CA) was used as the DNA polymerase with addition of buffer, primers, and water. Enzyme activation was for 15 minutes at 95°C followed by 25 cycles of denaturation at 95°C for 30 seconds, annealing for 1.5 minutes at 58°C, and extension for 1 minute at 72°C, with a final extension of 7 minutes at 72°C.

### **Classification of LOS Classes by PCR**

Determination of LOS classes was performed as previously described (112). To date, 23 classes (A–W) have been described; in this study we only classified isolates into 6 classes (A–F) using the 12 primers previously described by Parker *et al.* (2005) (112). Some isolates were unable to be typed into one of the 6 classes, however more primer sets could be used to further classify these isolates (111). As described above, we also further distinguished LOS class A and class B by the presence of allele type 1 or type 2. LOS class A and class B were assigned alleles based on the presence/absence of orf5abl1/orf6ab1 and orf5abl2/orf6ab2.

## DNA Sequencing and Allele Assignment

### *Multi-locus sequence typing (MLST)*

MLST was performed on the CDC and environmental isolates as previously described only using the inner primers (<http://pubmlst.org/campylobacter/>) as described by Bell *et al.* (2009) (10, 11, 83). A protocol using KAPA2G Fast HotStart DNA (KAPABiosystems, Woburn, MA) polymerase was optimized for MLST of the 49 isolates from Michigan. KAPA2G Fast HotStart DNA polymerase (KAPABiosystems, Woburn, MA) was used with 10  $\mu$ M of both the forward and reverse primer and water. The reaction consisted of 35 cycles of denaturation at 95°C for 15 sec, annealing for 15 sec at 60°C, followed by extension for 5 seconds at 72°C.

### *flaA SVR*

*flaA* SVR sequences were obtained with PCR. The reaction consisted of 35 cycles with a denaturation step at 94°C for 1 minute, annealing at 45°C for 1 minute, and extension for 3 minutes at 72°C. Primers used were previously described (101). Platinum® Taq DNA Polymerase High Fidelity (Life Technologies, Grand Island, NY) was used in reactions with 25 ng/ $\mu$ l of template DNA and 40 pmol of primer.

### *porA*

Three different primers were used to sequence the entire length of the *porA* gene; these primers may be found on the PubMLST website

([http://pubmlst.org/campylobacter/info/porA\\_method.shtml](http://pubmlst.org/campylobacter/info/porA_method.shtml)) (83). We encountered problems with these primers: they did not amplify the entire portion of the *porA* gene we wished to sequence. Therefore we developed four additional primers to amplify the entire *porA* gene: 1) *porA* A (5'-TTTCCTAARRAAGCACCTTC-3'), 2) *porA* B (5'-GATGCWASYCTTGGTGGTTT-3'), 3) *porA* C (5'-GGWCAATTMAACCCACAA-3'), and 4) *porA* D (5'-ACAWAWCRAAGATATTACC-3'). Primers were added at the concentration of 40 pmol; enzyme used was Platinum<sup>®</sup> Taq DNA Polymerase High Fidelity (Life Technologies, Grand Island, NY) with 25 ng/μl of template DNA. The PCR reactions were 40 cycles beginning with a denaturation step at 94 °C for 30 seconds followed by annealing for 30 seconds at 45 °C and ending with extension for 90 seconds at 72 °C.

### **Sequence Analysis**

All PCR products were submitted to the Michigan State University Genomics Technology Support Facility for sequencing. PCR products were fluorescently labeled and then separated on an ABI 3730 Genetic Analyzer (Life Technologies, Grand Island, NY) by capillary electrophoresis. Purified PCR product was sequenced in both the forward and reverse directions. DNA sequences were compiled and analyzed with SeqMan 5.06 (DNASTAR, Madison, WI); alleles of each gene, sequence type, and clonal complex were assigned using the PubMLST <http://pubmlst.org/campylobacter/> website (83).

*C. jejuni* strains 260.94 (GenBank® #AANK01000001.1), HB93-13 (GenBank® #AANQ01000001.1), CF93-6 (GenBank® #AANJ01000005.1), CG8421 (GenBank® #AANT02000001.1), and 11168 (GenBank® #NC 018521.1) have all previously been sequenced; therefore, DNA sequences for the portions of the *flaA* SVR gene and the *porA* gene of those strains were derived from the NCBI database using Basic Local Alignment Search Tool (BLAST) ([http://www.ncbi.nlm.nih.gov/sutils/genom\\_table.cgi](http://www.ncbi.nlm.nih.gov/sutils/genom_table.cgi)).

### Statistical Analysis

DNA sequences for MLST, *porA*, and *flaA* SVR were aligned; phylogenetic trees and tree files were created using [phylogeny.fr](http://phylogeny.fr) using a maximum likelihood calculation (23, 33, 39).

The allelic profiles of MLST, *porA*, and *flaA* SVR were analyzed with PAST version 1.89 (Øyvind Hammer, Oslo, Norway); cluster analysis of allelic profiles was performed using the Hamming similarity coefficient and unweighted pair group with arithmetic averaging (UPGMA). All bootstrapping was performed at 1000 repetitions. Dendrograms of the MLST, *porA*, and *flaA* SVR DNA sequences were compared using Compare2Trees: pairwise comparison of phylogenies (<http://www.mas.ncl.ac.uk/~ntmwn/compare2trees/index.html>). This test results in an overall topological score that describes the percent similarity between the two trees being analyzed (106). eBurst was used to assess the similarity of the results obtained using the different molecular typing methods based on allele assignments (<http://eburst.mlst.net/default.asp>).

## RESULTS

### LOS Classification

Of the 68 (63 unknown and 5 previously sequenced) *C. jejuni* isolates analyzed we were able to classify 56 (82%) into LOS classes A–F (Table 4.1). Forty-eight of fifty-six (86%) isolates were classified into LOS classes A–C, the three classes shown to have the ability to sialylate the LOS structure to mimic gangliosides (47). Seven of the fifty-six (13%) isolates were determined to belong to LOS class A1 and 1/56 (2%) belonged to class A2. Four of fifty-six (7%) were classified as class B1 and 11/56 (20%) were class B2. The remainder of the 56 classified isolates were categorized as LOS class C (25/56; 45%), class E (5/56; 9%), and class F (3/56; 5%). Twelve of sixty-three unknown isolates could not be assigned to a single LOS class (A–F) because the gene content of their LOS loci as determined by PCR was a composite of two classes; LOS class E was one of the two classes in all 12 isolates.

The two GBS-associated strains, *C. jejuni* 260.94 and *C. jejuni* HB93-13, and the MFS-associated strain, *C. jejuni* CF93-6, all belong to LOS class A1. The genome strain, *C. jejuni* 11168, belongs to LOS class C. *C. jejuni* CG8421, a strain shown to not mimic gangliosides (143), was classified as LOS class E.

Cluster analysis of the gene content of the LOS loci used in classification (0 for absent; 1 for present) of the 68 isolates is shown in Figure 4.1. The cophenetic coefficient for this tree was 0.97, indicating that the tree reflects the data accurately. Bootstrapping analysis indicated three well supported groups (bootstrap values  $\geq 50\%$ ).

## MLST Analysis

The 68 *C. jejuni* isolates included 37 different sequence types (ST) in 19 clonal complexes (CC). Three of sixty-eight (4%) isolates did not match any sequence type in the PubMLST database and were classified in this study as “unknown.” Four of sixty-eight (6%) isolates could not be assigned to described clonal complexes. Clonal complexes CC 21 and CC 45 have been demonstrated to be the most common among *C. jejuni* (124); CC 21 was the most common complex in this study. Twenty-one of sixty-eight (31%) *C. jejuni* isolates belonged to CC 21 and 8/68 (12%) belonged to CC 45. *C. jejuni* 11168 and *C. jejuni* CF93-6 both belonged to CC 21. *C. jejuni* HB93-13, *C. jejuni* CG8421, and *C. jejuni* 260.94 belonged to CC 22, CC 52, and CC 362 respectively.

Comparison of the MLST results with LOS classification showed that some clonal complexes contained isolates of only one LOS class. Four of four CC48 isolates belonged to LOS class B2; two of two CC 508 isolates belonged to LOS class A1, and two of two CC 607 isolates belonged to LOS class B1. The remaining clonal complexes with more than one isolate had a mixture of LOS classes (Figure 4.2). The majority of *C. jejuni* CC 21 isolates belonged to LOS class C (18/20; 90%); one CC 21 isolate belonged to LOS class A1 (1/20; 5%); and 2/20 (10%) isolates could not be classified. Strains of LOS class A1 were found in 5 clonal complexes: CC 21(1/20; 5%), CC 22 (2/4; 50%), CC 206 (1/3; 33%), CC 362 (1/1; 100%), and CC 508 (2/2; 100%). The LOS class A2 was only present in one isolate that did not belong to a known clonal complex. Two of two CC 607 isolates belonged to LOS class B1 (2/2:100%); LOS class B1 was also present in clonal complexes CC 42 (1/1; 100%) and CC 353 (1/9; 11%). Four of four CC 48 isolates belonged to LOS class B2, but LOS class B2 was also found in CC

257 (1/1; 100%), CC 353 (3/9; 33%), and CC 403 (1/1; 100%). Two other isolates that were classified as LOS class B2 could not be assigned to known clonal complexes. LOS class C was represented in four clonal complexes: CC 21 (18/20; 90%), CC 206 (2/3; 67%), CC 353 (4/9; 44%), and CC 658 (1/1; 100%). The 5 isolates that belonged to LOS class E were distributed among 4 clonal complexes: CC 45 (2/9; 22%), CC 52 (1/2; 50%), CC 61 (1/1; 100%), and one isolate could not be assigned to a known clonal complex. LOS class F was present in 3 clonal complexes: CC 49 (1/1; 100%), CC 52 (1/2; 50%), and CC 446 (1/1; 100%).

### ***porA* Typing**

Analysis of the *porA* gene sequences in the 68 different *C. jejuni* isolates revealed 43 different alleles. Figure 4.3 represents a phylogenetic tree of the *C. jejuni* isolates based on *porA* sequences; two groups were well supported (bootstrap values  $\geq 50\%$ ). Allele 119 was the most common among the 68 isolates with seven (10%) isolates. The 5 previously sequenced strains had different *porA* allele types. *C. jejuni* 11168 and *C. jejuni* CG8421 had alleles 27 and 606 respectively. The GBS-associated strains *C. jejuni* 260.94 and *C. jejuni* HB93-13 had alleles 866 and 70 respectively. The MFS-associated strain *C. jejuni* CF93-6 had allele 131.

Comparison of the *porA* allele types with the LOS classification showed that strains of five allele types contained isolates of the same LOS class. Allele 14 (2/2; 100%) and allele 808 (2/2; 100%) were associated only with LOS class B2. LOS class C was associated with isolates that had 3 different *porA* alleles; allele 27 (2/2; 100%), allele 119 (7/7; 100%) and allele 738 (3/3; 100%). Three of three isolates having allele

44 could not be classified in LOS typing; all 3 isolates had the same gene content based on the LOS PCR. All other allele types were associated with more than one LOS class.

### ***flaA* SVR Sequence Types**

The short variable region (SVR) of the *flaA* gene was sequenced and analyzed (data not shown) for the 68 *C. jejuni* isolates; 39 different sequence types were present in the strain collection. ST-47 was the most common sequence type (9/68; 13%). Each of the 5 sequenced strains was assigned to a different *flaA* SVR sequence type. Based on the DNA sequences of the *flaA* SVR two clusters were identified (bootstrap values  $\geq 50\%$ ).

Comparison of the *flaA* SVR sequence types with the LOS classes showed that two sequence types were only associated with LOS class C isolates, ST-103 (3/3; 100%) and ST-784 (2/2; 100%). Sequence types ST-22 and ST-106 were both (2/2; 100%) associated only with isolates that could not be classified using the LOS classification scheme used in this paper; however, the LOS gene content of each pair of isolates having each ST was identical based on PCR. All other sequence types of *flaA* SVR were associated with a mixture of LOS classes.

### **Comparison of Isolates with All Molecular Typing Methods**

Analysis of the alleles assigned to each DNA sequence in MLST, *porA*, and *flaA* SVR was performed with eBurstV3. This analysis identified 6 different groups of 2 or more isolates and 41 (59%) singletons. Addition of the LOS classification to the MLST, *flaA* SVR sequence type, and *porA* allele type resulted in 49/68 (72%) isolates that were

singletons. Eight different groups containing more than one isolate were identified in the combined allelic profile and LOS class data; 3/8 groups had 3 isolates per group and 5/8 groups were pairs of isolates that contained identical alleles and sequence types.

Pairwise analyses of the dendrograms generated from the MLST, *porA*, and *flaA* SVR DNA sequences were performed; all pairs of dendrograms were found to have low similarity. The overall topological score for the pairwise comparison of the MLST data and the *porA* data was 37.9%. The overall topological scores for the comparison of the MLST data and the *flaA* data was 33.8%; analysis of the *flaA* SVR and *porA* data resulted in an overall topological score of 33.6%.

## DISCUSSION

Multiple studies have been performed to determine the gene content of the LOS loci of *C. jejuni* isolates from both enteric and GBS/MFS patients. The results have indicated that LOS classes strongly associated with GBS (A and B) are also present in patients that clinically presented with enteritis only and that some *C. jejuni* isolates from GBS patients had LOS classes that lacked genes needed to synthesize a sialylated LOS (112).

We analyzed 68 *C. jejuni* isolates, 5 of which had published genome sequences. Of the 68 isolates 56 were categorized into LOS classes A–F; with a plurality classifying as LOS class C (45%). LOS class A represented 14% of the isolates; class B, 27% of the isolates; class E, 9% of the isolates, and class F, 5% of the isolates. No isolate was classified as LOS class D. Eighty-six percent of the isolates analyzed were found to belong to LOS classes A–C. Previous studies have been done with human *C. jejuni* isolates to associate the prevalence of LOS classes A–C among the population, but because these studies varied in location, duration of the study period, and duration of the study period, direct comparisons are difficult. One study in Finland found 32% of human *C. jejuni* isolates were assigned to LOS classes A, B, and C (124). Two other studies performed in Belgium and Bangladesh found 53% and 61% respectively, of LOS classes A–C in the collections of human isolates they sampled (57, 78). In South Africa, 50% of human isolates positive for *C. jejuni* were of the LOS classes A–C (123). Furthermore, another study done in New Zealand identified 77% of *C. jejuni* human isolates as belonging to LOS classes A–C (69). Additionally, in this study 34/49 (69%)

*C. jejuni* strains associated with enteritis cases in Michigan had LOS class assignments consistent with strains documented from GBS patients, suggesting that the risk of acquiring a strain capable of eliciting neurological disease is relatively high in Michigan. However, these isolates from Michigan were collected during a short period of time and a limited geographical location; therefore a more extensive study including a bigger geographical area and more *C. jejuni* isolates would need to be conducted to conclude that Michigan does have a high prevalence of GBS-associated *C. jejuni* strains.

Twelve isolates were not categorized into LOS classes A–F because based on gene content of their LOS loci as determined by PCR, these isolates could be classified into two or more LOS classes. Additional primers would be needed to further classify these isolates beyond LOS class A–F (111). All twelve of these isolates were a mixture of LOS class E with either LOS class A, class B, or class C; 7/12 have the necessary *csfII* or *csfIII* gene needed to transfer sialic acid to the LOS. This result suggests that further typing of these isolates would place them in LOS class M, class R, or class V. The remaining 5/12 isolates do not contain either *csfII* or *csfIII* and therefore are hypothesized to belong to LOS classes not associated with sialylation of the LOS.

We were able to determine that CC 21 was the most common clonal complex assigned in this study with 29% of our isolates belonging to it; this result coincides with previous reports of CC 21 and CC 45 as the two most prevalent clonal complexes among the *C. jejuni* human population (124). By comparison of results from the variable LOS locus classification to those from the more conserved loci of MLST, we determined that 90% of the isolates in CC 21 in our own study belonged to LOS class C. Other studies that have compared MLST data to LOS classification have also identified LOS

class C to as the most common class associated with CC 21 (57, 69, 78, 123, 124). Previous studies have also commonly found *C. jejuni* LOS classes that lack the ability to sialylate an LOS to be prevalent in CC 45 (69, 124). These studies have associated LOS classes E and H specifically with CC 45. In our study we found that 22% of our isolates assigned to LOS class E to belong to CC 45; we did not classify beyond LOS class F and therefore have no data about LOS class H. The majority of the LOS classes belonging to CC 45 in our study were unknown LOS class types. Further studies to determine these LOS classes may reveal that they belong to LOS class H, which would correspond to previous studies.

Analysis of the LOS biosynthesis loci resulted in 86% of the isolates categorized into LOS classes A–C; therefore we wanted to explore the genetic relationship of other outer membrane surface molecules. MLST and *porA* allele typing, and *flaA* SVR sequence typing did not reveal strong relationships of LOS classes A–C with any sequence type by any method used. MLST analysis resulted in 37 different sequence types that could be grouped into 18 different clonal complexes. The *flaA* SVR sequence typing resulted in 39 different sequence types and the *porA* assigned 43 different alleles, therefore *porA* molecular typing method produced the greatest diversity among the *C. jejuni* isolates.

Pairwise comparisons of the separate dendrograms and cluster analyses of the four molecular typing methods indicated that the 68 isolates examined in this paper were genetically diverse. eBurst analysis of combined MLST allele profiles, *porA* alleles, and *flaA* SVR sequences indicated 41 unique strains (60%) and 6 groups of 2 or more isolates that were identical to one another within each group. Addition of the LOS

classification to this analysis resulted in 49 unique strains (72%) with 8 groups of 2 or more isolates that were genetically identical based on allele types; 3/8 were groups of 3 isolates and 5/8 were groups of 2 isolates that contained identical alleles and sequence types. Addition of the LOS classification thus revealed even more diversity among the isolates. Combination of these typing schemes should be useful in the analysis of the genetic relationships among *C. jejuni* isolates in a population. We are able to conclude from the individual analyses of these molecular typing schemes that there is no relationship between these schemes and the LOS classes of the isolates except for the association of some LOS classes with some MLST clonal complexes. However, there were also instances of members of a clonal complex having LOS loci of multiple classes. We also were able to conclude that the Michigan strains form a genetically diverse group of isolates with both the individual analyses and the combined results of the four molecular schemes.

Recently, Clark *et al.* (2012) presented a new molecular method for typing *C. jejuni* isolates: comparative genomic fingerprinting (CGF); this method employs a multiplex PCR to detect highly variable genes in *Campylobacter spp.* (28). These authors were able to demonstrate that molecular typing of *C. jejuni* isolates with CGF was potentially useful in detecting genetic clusters of *Campylobacter* isolates in population surveys of *Campylobacter spp.* (28). There are 4 LOS biosynthesis locus genes that are in common with the LOS classification and the CGF molecular typing: Cj1134, Cj1136, Cj1141 (needed for sialic acid biosynthesis) and Cj1151. These genes alone with both methods would not be sufficient to identify genetic relationship to an LOS class. With the addition of this new typing tool and the molecular typing methods

employed above, genetic relationships among *C. jejuni* populations could be well defined.

**Table 4.1: Summary of *C. jejuni* Isolates and their assigned allele types.** The table below corresponds the isolate name with the ID's given throughout the chapter in the first two columns. The ID's were given based on source of the isolate: CDC# for strains received from the Center for Disease Control, ENV# for the *C. jejuni* isolates taken from cow pen soil samples, MI# for the isolates collected in Michigan, and REF# are the previously sequenced *C. jejuni* strains. The allele types for the MLST genes (*aspA*, *glnA*, *gltA*, *glyA*, *pgm*, *tkt*, and *uncA*) are given along with the assigned sequence type (ST) and clonal complex (CC). The next column is the sequence type of the *flaA* SVR sequence. The *porA* column indicates the allele assigned based on the DNA sequences. The final column is the LOS classification based on PCR for presence/absence of gene content. Some isolates were unable to be classified and/or sequenced; therefore are given "unk" for unknown.

Table 4.1 (cont'd)

Isolate	I.D.	aspA	glnA	gltA	glyA	pgm	tkf	uncA	ST	CC	<i>flaA</i>	<i>porA</i>	LOS
D2586	CDC1	2	1	5	3	4	1	5	43	21	335	27	C
D0835	CDC2	7	4	5	2	11	1	5	429	48	970	1728	B2
D0121	CDC3	4	7	10	4	1	7	1	45	45	270	44	unk
D6844	CDC4	1	3	6	4	3	3	3	22	22	1434	48	A1
D6845	CDC5	7	17	5	2	10	3	6	353	353	663	2	B2
D6846	CDC6	9	2	2	2	11	5	6	824	257	270	98	B2
D6847	CDC7	7	17	5	2	10	3	6	353	353	147	55	unk
D6848	CDC8	2	1	12	3	2	1	5	50	21	174	92	C
D6849	CDC9	2	4	1	2	7	1	5	48	48	147	14	B2
D8942	CDC10	1	6	22	24	12	28	1	132	508	289	790	A1
LM28	ENV11	4	7	10	4	1	7	1	45	45	270	44	unk
LM31	ENV12	4	7	10	4	1	7	1	45	45	270	44	unk
LM36	ENV13	2	1	1	3	1	1	3	186	21	37	8	C
LM41	ENV14	10	1	59	19	10	1	7	933	403	122	1539	B2

Table 4.1 (cont'd)

Isolate	I.D.	<i>aspA</i>	<i>glnA</i>	<i>gltA</i>	<i>glyA</i>	<i>pgm</i>	<i>tkt</i>	<i>uncA</i>	ST	CC	<i>flaA</i>	<i>porA</i>	LOS
TW16361 1	MI15	1	3	6	4	3	3	3	22	22	106	48	unk
TW16362 1	MI16	1	3	6	4	3	3	3	22	22	106	48	unk
TW16370 1	MI17	2	1	2	3	2	1	5	982	21	49	1696	unk
TW16373 2	MI18	7	17	5	2	13	3	6	3510	353	142	808	B2
TW16374 2	MI19	2	4	1	2	7	1	5	48	48	147	14	B2
TW16397 3	MI20	2	21	5	2	59	1	5	222	206	103	131	C
TW16398 1	MI21	2	1	2	3	2	1	5	982	21	46	752	C
TW16399 1	MI22	7	17	5	2	10	3	6	353	353	147	119	C
TW16400 2	MI23	2	21	5	2	59	1	5	222	206	103	131	C
TW16401 1	MI24	10	2	50	62	91	1	45	unk	unk	632	766	E
TW16402 3	MI25	4	7	10	4	1	7	1	45	45	249	49	E
TW16409 2 1	MI26	6	4	5	2	2	1	5	122	206	49	7	A1
TW16420 1	MI27	2	1	12	3	2	1	5	50	21	147	6	C
TW16422 1 1	MI28	47	55	5	10	11	3	8	862	446	222	116	F
TW16429 1	MI29	7	4	5	2	11	3	165	1838	353	121	1479	B1
TW16430 1 1	MI30	8	2	5	53	11	3	1	607	607	1011	116	B1
TW16431 1	MI31	2	1	12	3	2	1	23	3574	21	78	529	C
TW16435 1	MI32	4	7	10	4	1	7	1	45	45	249	49	unk
TW16438 1	MI33	7	84	5	10	119	178	26	1911	unk	350	1101	B2
TW16441 1	MI34	4	7	10	4	42	7	1	137	45	239	53	E
TW16442 1	MI35	4	7	40	4	42	51	1	267	283	239	73	unk
TW16443 1	MI36	7	17	5	2	10	3	6	353	353	604	164	B2

Table 4.1 (cont'd)

TW16444 1	MI37	2	1	1	3	2	1	6	8	21	122	1231	C
TW16445 1	MI38	7	17	5	2	10	3	6	353	353	965	119	C
TW16446 1	MI39	1	2	3	3	5	9	3	459	42	274	199	B1
TW16451 1	MI40	2	1	12	3	2	1	5	50	21	147	119	C
TW16452 1	MI41	2	1	1	3	2	1	6	8	21	122	745	unk
TW16453 1	MI42	3	1	5	84	11	11	6	467	49	247	55	F
TW16455 1	MI43	166	2	5	72	151	3	1	2310	607	825	1087	B1
TW16463 2	MI44	4	7	10	4	1	7	1	45	45	22	53	unk
TW16464 1	MI45	4	7	10	4	1	7	1	45	45	22	53	unk
TW16467 1	MI46	1	6	60	24	12	28	1	508	508	289	17	A1
TW16469 1	MI47	8	1	6	3	2	1	1	44	21	142	839	C
TW164711	MI48	2	1	12	3	2	1	5	50	21	147	119	C
TW16475 2	MI49	2	1	2	83	2	3	6	3007	658	211	1653	C
TW16478 2	MI50	1	1	2	2	225	3	17	1244	61	249	37	E
TW16491 1	MI51	1	1	2	83	2	3	6	922	unk	14	744	A2
TW16493 1	MI52	2	1	2	3	2	1	5	982	21	46	738	C
TW16494 1	MI53	2	1	2	3	2	1	5	982	21	46	738	C
TW16495 1	MI54	2	1	12	3	2	1	5	50	21	147	119	C
TW16498 1	MI55	2	1	2	3	2	1	5	982	21	46	738	C
TW16499 2	MI56	2	17	1	2	7	1	5	453	48	147	808	B2
TW16506 3	MI57	9	1	2	10	22	3	6	4506	52	337	1	F
TW16510 3	MI58	2	1	1	3	2	1	6	8	21	1623	745	C
TW16511 2	MI59	7	17	2	2	22	3	6	unk	unk	142	745	B2

Table 4.1 (cont'd)

TW16512 1	MI60	2	1	1	3	140	3	5	806	21	1069	843	C
TW16513 1	MI61	2	1	1	3	140	3	5	806	21	1600	48	C
TW16514 1	MI62	7	17	5	2	10	3	6	353	353	784	119	C
TW16515 3	MI63	7	17	5	2	10	3	6	353	353	784	119	C
11168	Ref64	2	1	5	3	4	1	5	43	21	103	27	C
CF93-6	Ref65	2	17	2	3	2	1	5	883	21	285	131	A1
HB93-13	Ref66	1	3	6	4	1	3	3	unk	22	1256	70	A1
260.94	Ref67	1	2	49	4	11	66	51	362	362	1058	866	A1
CG8421	Ref68	9	2	2	10	10	3	5	1919	52	46	606	E

**Figure 4.1: Dendrogram of the LOS biosynthetic loci.** Cluster analysis of the gene content at the LOS biosynthesis loci based on our PCR classification.

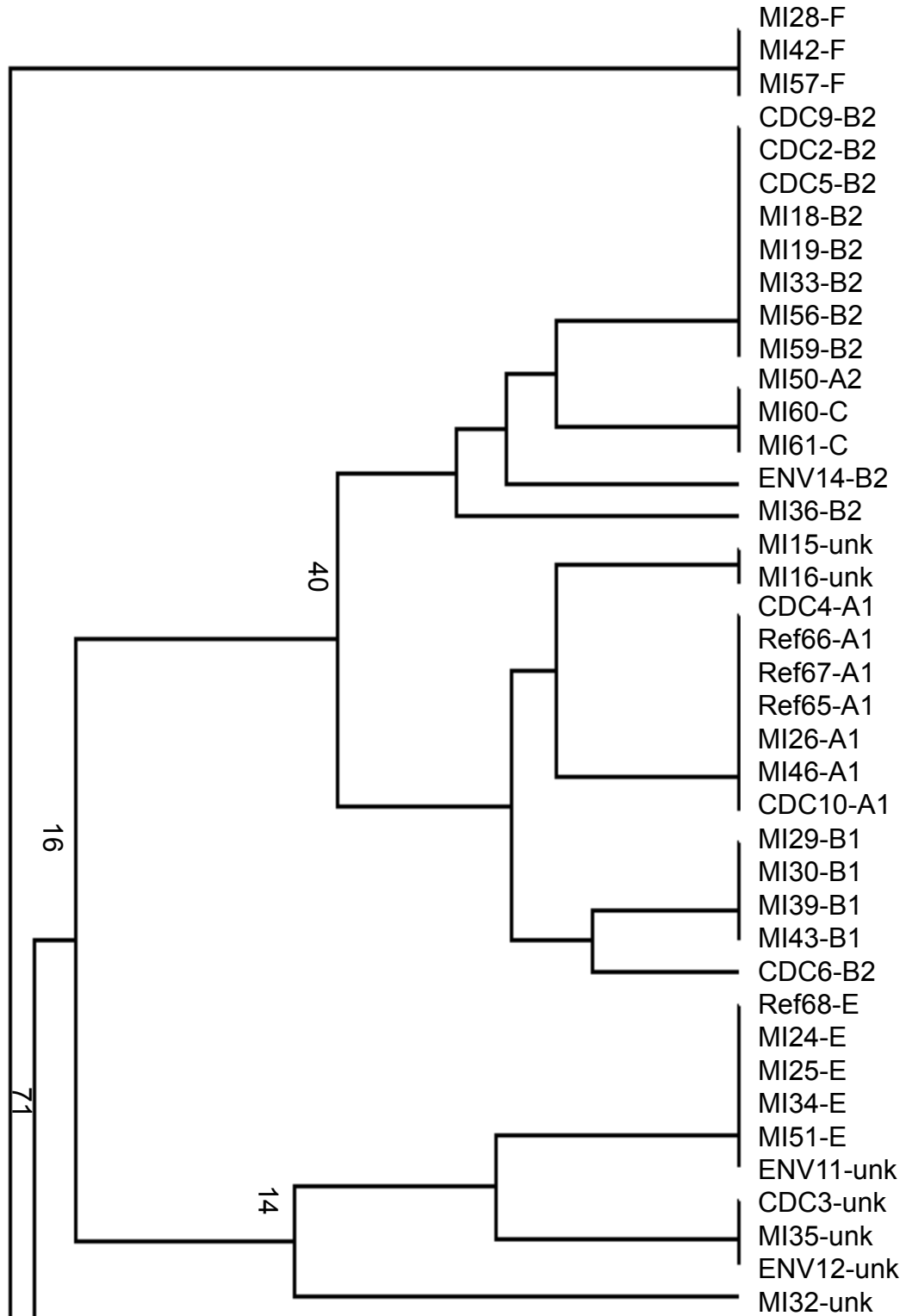
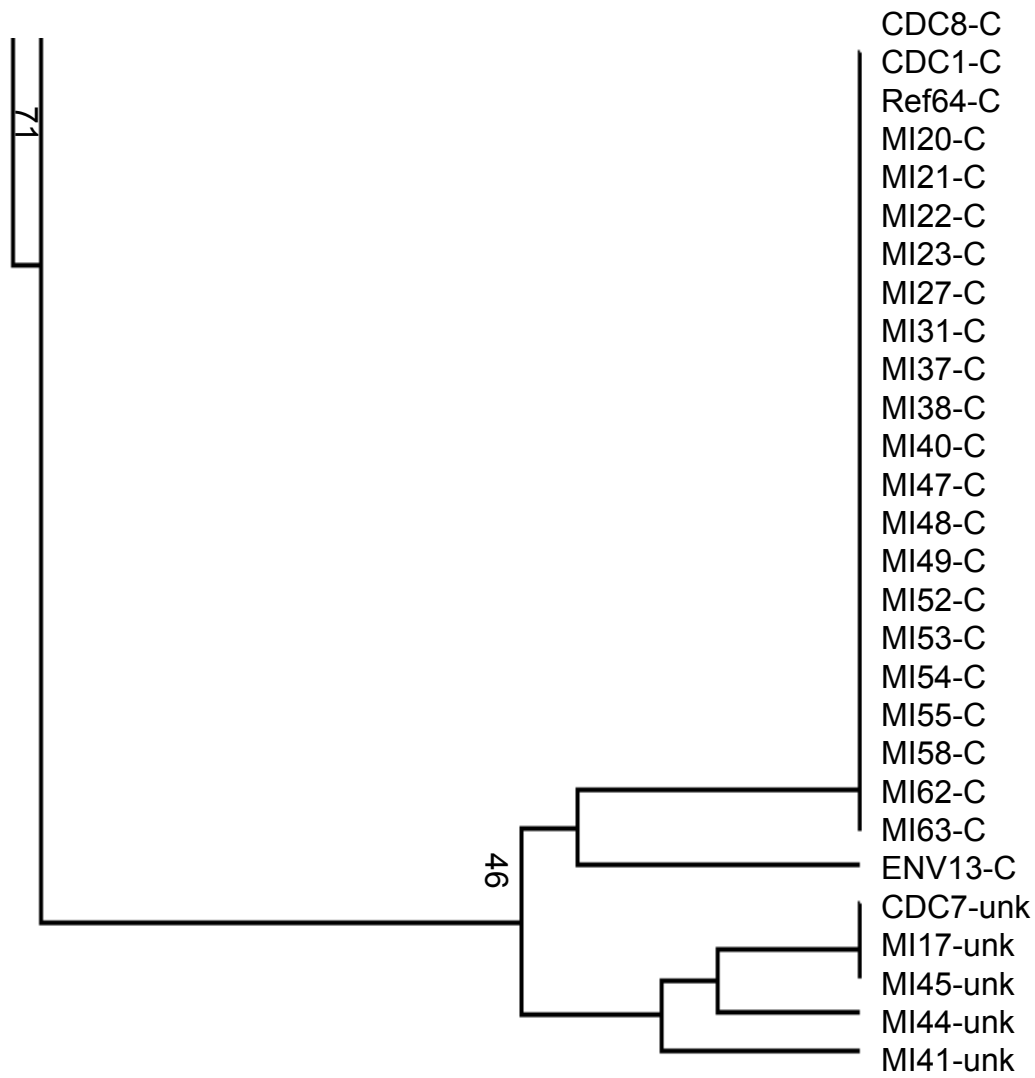
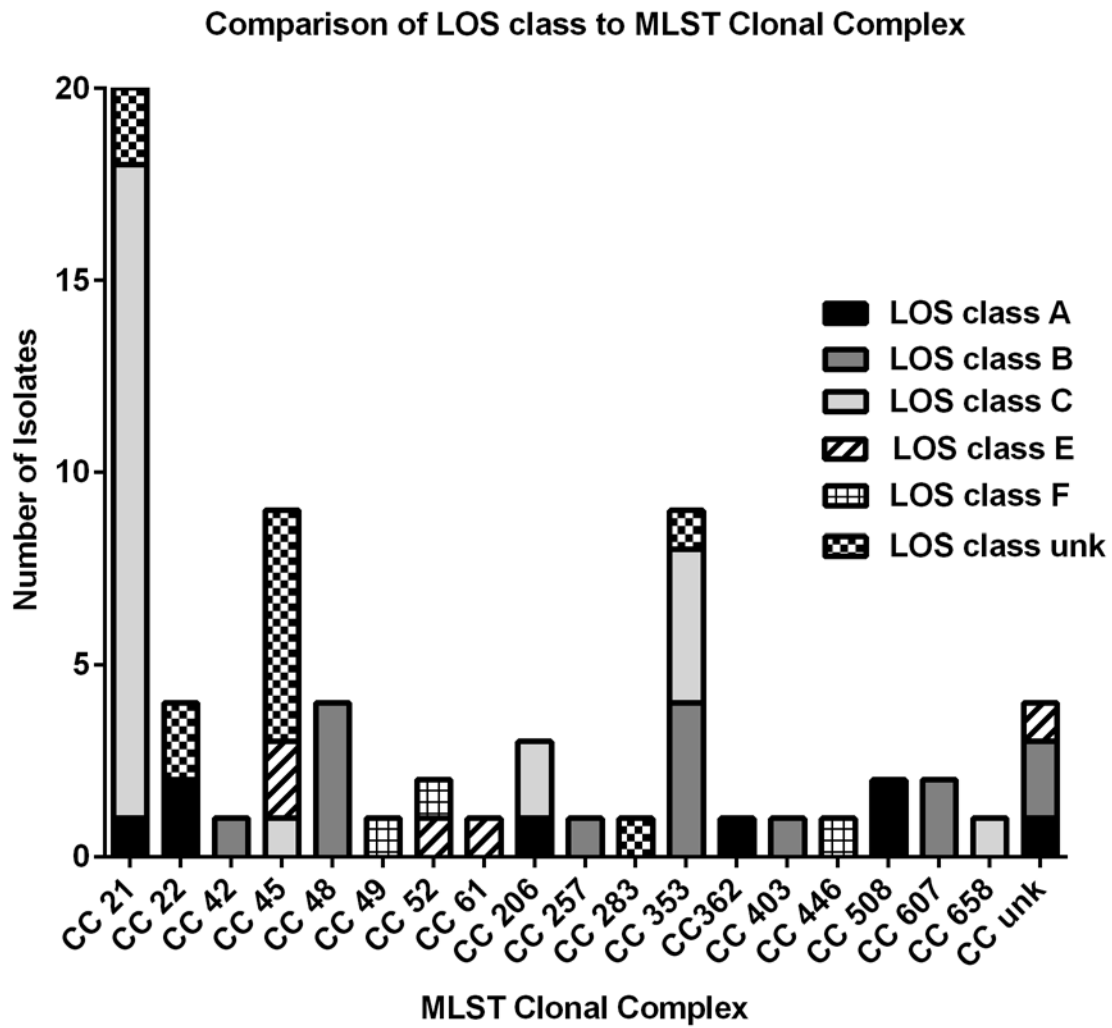


Figure 4.1 (cont'd)



**Figure 4.2: Comparison of LOS class to MLST Clonal Complexes.** The figure below shows the distribution of the 68 isolates based on their LOS class into the 19 MLST clonal complexes.



**Figure 4.3: Phylogenetic tree of the *porA* based on DNA sequences.** Data indicates 2 well supported clusters (bootstrap values  $\geq 50\%$ ). The LOS class assigned to each isolate follows the isolate ID.

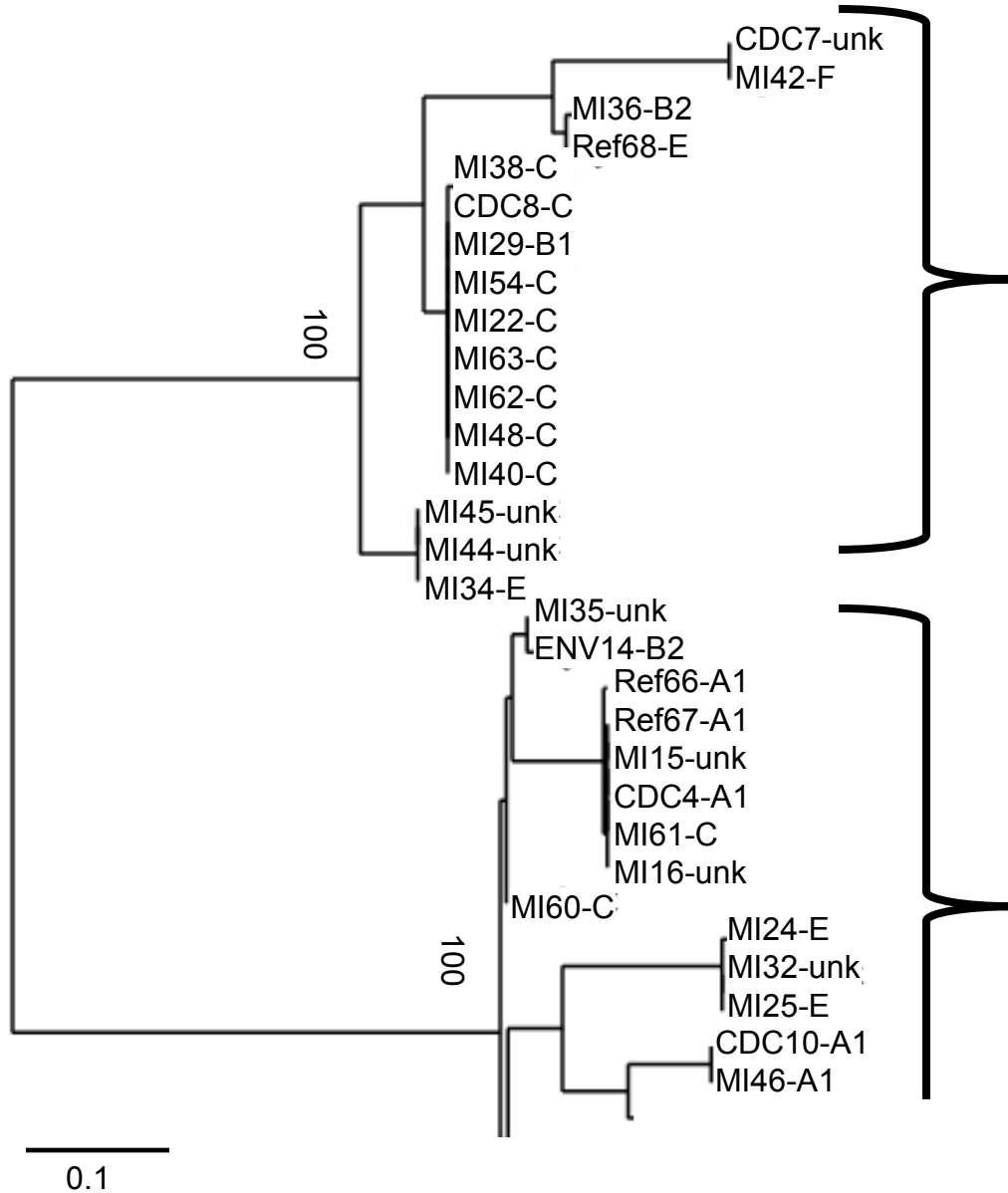
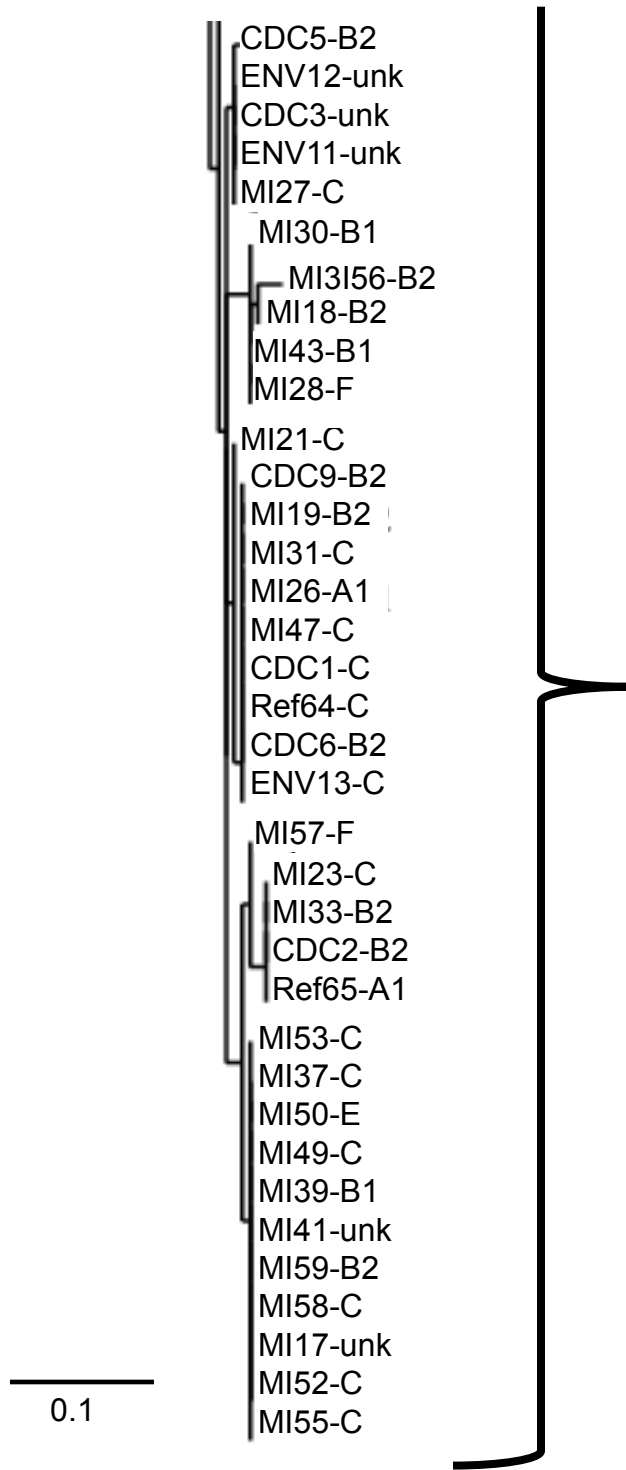


Figure 4.3 (cont'd)



## CHAPTER 5

*Campylobacter jejuni* isolates from calves have A, B, and C lipo-oligosaccharide (LOS) biosynthetic locus classes similar to human Guillain Barré Syndrome associated strains

## ABSTRACT

*Campylobacter jejuni*, a Gram negative zoonotic bacterium, is a frequent cause of human gastroenteritis. The acute neuropathy Guillain Barré Syndrome (GBS) is a post-infectious polyradiculoneuropathy triggered by *C. jejuni* through molecular mimicry. The lipo-oligosaccharide (LOS) of *C. jejuni* is variable; some forms can mimic gangliosides enriched on peripheral nerves leading to autoimmunity. Classification of the LOS can be determined by PCR based on gene content of the complex LOS biosynthesis locus; 23 classes have been identified. Infection with *C. jejuni* strains of LOS classes A–C has been strongly associated with GBS. Members of a family managing a large southwest Michigan dairy operation reported a history of *C. jejuni* infections that lasted several days and recurred over the course of two years. Because up to 37.7% of dairy cattle have been found to shed *C. jejuni*, we sought to determine whether calves were the source of the family infections. Fecal samples were obtained from 25 randomly selected calves, 1 dog, and all family members and cultured for *C. jejuni*. Human and calf isolates were characterized by LOS biosynthesis locus class typing, multi-locus sequence typing (MLST), *porA* allele typing, and *flaA* SVR sequence typing. *C. jejuni* was cultured from 15 (60%) of calves and one asymptomatic family member; the dog was negative. *Campylobacter coli* was cultured from 2 (1%) of calves. Some calves had diarrhea, but most were clinically normal. Typing of LOS biosynthetic loci showed that 10 of 15 calf *C. jejuni* isolates fell into LOS classifications A, B, and C. The human isolate belonged to LOS class E, which is associated with enteric disease. Two calves had *C. jejuni* with LOS class E. Thus, the typing results suggest that some

calf and human *C. jejuni* isolates have similar characteristics. Molecular typing with MLST, *porA* allele typing, and *flaA* SVR typing indicated that one calf strain and the human isolate of the same LOS class share the same phylogenetic lineage, thereby providing direct support for zoonotic transmission. Furthermore, finding multiple MLST sequence types, *flaA* SVR sequence types, *porA* alleles, and LOS classes in isolates from these calves demonstrates that there are diverse *C. jejuni* populations present on this farm.

## INTRODUCTION

*C. jejuni* is the leading cause of human bacterial gastrointestinal infection in the Western world (25, 127, 146). It is estimated that 2.1–2.5 million cases of campylobacteriosis occur annually in the U.S. (41). *C. jejuni* infection symptoms include fever, abdominal cramping, and watery or bloody diarrhea (6, 127). The majority of *C. jejuni* infections are the result of ingestion of undercooked chicken, but it has been shown that contact with household pets and the ingestion of raw milk, contaminated water, or undercooked beef or pork can lead to infection (6, 127). Farm animals and milk are natural reservoirs for *C. jejuni*. *C. jejuni* has been isolated from the intestines of chickens and found in the feces of domesticated household pets, beef cattle, and dairy cattle (41, 146). Dairy products are highly associated with *C. jejuni* outbreaks, while poultry products are mostly associated with sporadic infections (81). A Swiss study by Busato *et al.* (1999) examined 395 calves from cow-calf farms for enteropathogenic bacteria and showed that *C. jejuni* was present in 32% of the calves (18). Results of a molecular typing study of *C. jejuni* isolates from farm animals by Fitzgerald *et al.* (2001) demonstrated a link between *Campylobacter* isolates from farm animals with isolates from human cases within the community (41). Other studies have shown a correlation between *C. jejuni* infections and people exposed to farm animals (44, 88).

Guillain Barré Syndrome (GBS) is an acute neuromuscular autoimmune disease of the peripheral nervous system and is the most common cause of acute flaccid paralysis since the near eradication of polio (25, 119). GBS commonly develops following gastrointestinal infections with *C. jejuni*; recently a systematic review of

published studies between 1998 and 2010 was performed to estimate the number of GBS cases as a result of *C. jejuni* infection. It was determined that *C. jejuni* infection preceded 13–72% of GBS cases (119). Molecular mimicry of the LOS structures found on the outer membrane of *C. jejuni* that resemble gangliosides enriched in nervous tissue is thought to be the mechanism behind the pathogenesis of GBS (7). Symptoms may start with limb weakness and loss of tendon reflexes, but may develop into paralysis of the limbs, trunk, and facial muscles; 25% of patients may require mechanical ventilation (73, 80, 148). Ten to twenty percent of patients do not completely recover and have life-long disabilities; 3–10% die (7, 148). It has been estimated that the annual incidence of GBS is 1–2 individuals per 100,000 people in North America and Europe (136).

In 2007, Price *et al.* showed that there is an increase in development of peripheral neuropathy in people who work with poultry (122). Additionally, results of one study in Iowa and North Carolina by Vegosen *et al.* (2012) demonstrated that neurological symptoms associated with exposure to *C. jejuni* are more commonly reported among people who handle beef cattle (146).

In this study, residents of a family-owned southwest Michigan dairy farm complained of recurring *C. jejuni* infections over a course of two years. To explore this problem, stool samples were taken from 25 calves and 1 dog on the dairy farm and tested for presence of *C. jejuni*. Fifteen of twenty-five calves tested positive for *C. jejuni*. We hypothesized that transmission of *C. jejuni* was occurring between the family members and the calves. To test this hypothesis, we used multiple molecular typing schemes to determine the genetic relationships among the *C. jejuni* isolates. Isolates

were examined using MLST, LOS locus class determination, *flaA* SVR typing, and *porA* typing. Based on our results, the majority of the calf isolates (67%) belonged to LOS classes that are associated with the development of GBS; this result is consistent with previous studies of increased rates of neurological symptoms in farm workers. One calf isolate and the isolate from the only family member colonized by *C. jejuni* had identical alleles for the seven MLST loci, *flaA* SVR, and *porA*; both isolates belonged to LOS class E. These data strongly suggest that zoonotic transmission occurred between the dairy calves and the family members.

## MATERIALS AND METHODS

### Case Study

Residents of a family-owned dairy farm in the southwest Michigan reported *C. jejuni* infection among the family that lasted several days in summer, 2012. The family had experienced previous recurring *C. jejuni* infections for the previous two years. A veterinarian obtained 2 stool samples from dairy calves to eliminate them as possible carriers of *C. jejuni* and sent the samples to the Diagnostic Center for Population and Animal Health (DCPAH) at Michigan State University (East Lansing, MI). Using bacteriological tests, DCPAH staff confirmed that the stool samples were positive for *C. jejuni*. DCPAH staff then contacted our laboratory, the Comparative Enteric Disease Laboratory at Michigan State University (East Lansing, MI). We contacted the veterinarian, who obtained 25 randomly chosen calf samples along with one stool sample from the farm dog and submitted them for further testing. The family members enrolled in concurrent study conducted by Dr. Shannon Manning and the Microbial Evolution Laboratory (Michigan State University, East Lansing, MI). The single positive family sample was recovered by the Michigan Department of Community Health and de-identified. It was graciously given to us by Dr. Shannon Manning. Our laboratory had no interaction with the family members or farm workers.

### ***Campylobacter jejuni* Isolation**

Stool samples from the calves and dog were streaked on tryptose soya agar plates with 5% sheep's blood (Cleveland Scientific, Bath, OH, USA) and supplemented

with antibiotics (TSA-CVA: 20 µg/mL cefoperazone, 10 µg/mL vancomycin and 2 µg/mL amphotericin B) upon arrival. The plates were then placed in anaerobic jars containing CampyGen packs (Oxoid, Basingstoke, UK) and incubated for 48 hours at 37°C.

Isolates were selected and streaked again for growth and purification; bacterial growth was collected and stored at -80°C in TSB + 15% glycerol.

The isolate from the family member who tested positive for *C. jejuni* was streaked onto Bolton agar plates (Bolton Broth, Thermo Fisher Scientific, Pittsburgh, PA, containing 15% Bacteriological Agar, Neogen, Lansing, MI) upon arrival in the laboratory. The plates were incubated at 37°C for 48 hours in anaerobic jars containing CampyGen packs (Oxoid, Basingstoke, UK). Bacterial growth was harvested and stored as described above.

### **Preparation of Genomic DNA and Confirmation of *Campylobacter* spp.**

Frozen cultures were streaked for growth onto Bolton agar plates (Bolton Broth, Thermo Fisher Scientific, Pittsburgh, PA, containing Bacteriological Agar, Neogen, Lansing, MI) and incubated for 48 hours at 37°C in anaerobic jars with CampyGen packs (Oxoid, Basingstoke, UK). Bacterial growth was collected and DNA was extracted using Wizard® Genomic DNA Purification Kits (Promega, Madison, Wisconsin) according to the manufacturer's instructions. All genomic DNA was diluted to a final concentration of 25 ng/µL for PCR.

Identification of *Campylobacter* isolates as *C. jejuni* or *C. coli* was performed with a multiplex PCR that has previously been described (96). Hot Start Syzygy Mean Green

DNA polymerase was used (Integrated Scientific Solutions, San Diego, CA). The reaction had an enzyme activation step of 15 minutes at 95°C followed by 25 cycles of denaturation for 30 seconds at 95°C, annealing for 1.5 minutes at 58°C, and extension for 1 minute at 72°C, with a final extension of 7 minutes at 72°C. In addition, *C. jejuni* isolates were verified with a previously described *C. jejuni gyrA*-specific PCR used in our lab (96).

### **Classification of LOS Biosynthesis Loci**

LOS classification was performed as previously described by Parker *et al.* (2005) (112). Parker *et al.* (2005 and 2008) described 19 classes (A–S) of LOS based on gene content. This was supplemented by the procedures of Stanhope *et al.* (2013) who described an additional 4 LOS classes (T–W) (111, 112, 125).

### **Multi-locus Sequence Typing (MLST)**

MLST based on 7 conserved housekeeping genes was performed on DNA from the calf isolates as previously described (10, 11); only the inner primers were used to amplify the partial gene sequences. Platinum® Taq DNA Polymerase High Fidelity (Life Technologies, Grand Island, NY) was used; primer concentrations used were 37.5 pmol. The PCR reaction contained 35 cycles of denaturation of 2 minutes at 95°C, annealing for 1 minute at 50°C, followed by an extension for 1 minute at 72°C. The family member isolate was included in a concurrent study with the MSU Microbial

Evolution Laboratory; and the protocol for MLST differed. MLST PCR reactions were performed on DNA from the family member isolate using KAPA2G HotStart DNA polymerase (KAPABiosystems, Woburn, MA). Briefly, 10  $\mu$ M of both the forward and reverse primer, 25 ng/ $\mu$ l of genomic DNA template, water, and the DNA polymerase were used for the reaction. The reactions began with an enzyme activation step of 3 minutes at 95 $^{\circ}$ C and consisted of 35 cycles of denaturation for 15 seconds at 95 $^{\circ}$ C, annealing for 15 seconds at 60 $^{\circ}$ C, and an extension for 5 seconds at 72 $^{\circ}$ C.

### ***porA* Allele Typing and *flaA* SVR Sequence Typing**

*porA* allele typing was done using 7 different primers previously defined in Chapter 4 of this dissertation or on the PubMLST website ([http://pubmlst.org/campylobacter/info/porA\\_method.shtml](http://pubmlst.org/campylobacter/info/porA_method.shtml)) (83). The PCR reaction consisted of 40 cycles of denaturation for 30 seconds at 94 $^{\circ}$ C followed by an annealing step for 30 seconds at 45 $^{\circ}$ C and extension for 90 seconds at 72 $^{\circ}$ C. Platinum<sup>®</sup> Taq DNA Polymerase High Fidelity (Life Technologies, Grand Island, NY) was used with 40 pmol of primer.

The *flaA* SVR sequence typing was done with Platinum<sup>®</sup> Taq DNA Polymerase High Fidelity (Life Technologies, Grand Island, NY) and 40 pmol of primer. The PCR reaction consisted of a denaturation step at 94 $^{\circ}$ C for 1 minute, annealing at 45 $^{\circ}$ C for 1 minute, and extension for 3 minutes at 72 $^{\circ}$ C for 35 cycles. The primers used were previously described (101).

## Sequence Analysis

PCR products were purified with QIAquick PCR Purification Kit (Qiagen, Germantown, MD) according to the manufacturer's instructions and submitted for sequencing to the Michigan State University Genomics Technology Support Facility (East Lansing, MI) on an ABI 3730 Genetic Analyzer (Life Technologies, Grand Island, NY). Each PCR product was sequenced in both the forward and reverse directions. SeqMan 5.06 (DNASTAR, Madison, WI) software was used to align the sequences; the PubMLST website was used to determine allele, sequence type, and clonal complex assignments (<http://pubmlst.org/campylobacter/>) (83).

## Statistical Analysis

Alignments, cluster analysis, and dendrograms for *porA* and *flaA* SVR DNA sequences were performed using [phylogeny.fr](http://www.phylogeny.fr), which uses a maximum likelihood clustering method (23, 33, 39).

The allelic profiles of MLST, *porA*, and *flaA* SVR were analyzed with LIAN 3.5 available at the PubMLST website (<http://pubmlst.org/campylobacter/>) (65, 83). The standardized Index of Association ( $sI_A$ ) was calculated and a Monte-Carlo test of the hypothesis that the population was in linkage equilibrium (that is, that alleles at the different loci were randomly distributed among the isolates) was run with 1000 bootstrap repetitions.

Cluster analysis was performed using the Hamming similarity coefficient and unweighted pair group with arithmetic averaging (UPGMA). All bootstrapping was

performed at 1000 repetitions. Tree files of the *porA* and *flaA* SVR DNA sequences were compared using Compare2Trees: pairwise comparison of phylogenies (106). This algorithm produces an overall topological score that describes the percent of similarity between the trees (106).

## RESULTS

### Verification of *C. jejuni*

Based on culture, 15/25 calf stool samples were positive for *C. jejuni* and 2/25 calf stool samples were positive for *C. coli*. The dog sample was negative. One family member tested positive for *C. jejuni* without reporting any symptoms; therefore, this family member was considered an asymptomatic carrier (Table 5.1).

### LOS Classification

Based on the PCR results of 12 different genes in LOS biosynthesis loci, 10/15 (67%) of the calf isolates were classified into one of the LOS classes A–C. One of fifteen calf isolates belonged in class A2, 5/15 were in class B2, and 4/15 belonged to LOS class C. Two of fifteen calf isolates were determined to belong to LOS class E; the family member isolate also belonged to class E. Three of fifteen isolates were in the LOS class F. No isolates were determined to belong in the LOS class D.

### MLST Analysis

MLST allelic profiles are shown in Table 5.1. Six sequence types (ST; 806, 922, 928, 982, 1712, and 6227) were observed based on the DNA sequences compiled for 15 calf isolates and the single family member. Five of these sequence types could be further classified into 2 clonal complexes (CC; 21 and 257); ST-922 is currently not assigned to a defined clonal complex according to the *C. jejuni/C. coli* PubMLST website (<http://pubmlst.org/campylobacter/>) (83). The family member isolate also

belonged to ST-922; the clonal complex of the four ST-922 isolates is designated “unknown” in Table 5.1. One of the 15 calf isolates (C2) and the single family member isolate (FM1) had identical alleles at all loci. Calf isolate C7 was found to have the same LOS class (E), MLST sequence type (ST-922), and clonal complex (unknown) as FM1, and had identical allele sequences for 6 of the 7 MLST loci, but varied in the allele of the *pgm* gene, which encodes a phosphoglucosyltransferase.

Linkage analysis of the MLST alleles using LIAN 3.5 indicated that the population is in linkage disequilibrium (Monte Carlo  $p < 0.0001$ ), that is, particular alleles at different loci are more commonly associated with each other than expected by chance. The Index of Association  $s_I$  was 0.47, consistent with a population in linkage disequilibrium with low levels of recombination between strains. Figure 5.1 shows a split decomposition analysis of the MLST allelic profiles; the presence of the network suggests that recombination may be occurring among the population of *C. jejuni*, although at low levels.

One of 9 isolates of CC 21 belonged to LOS class A2 (1/1); 5 of 9 isolates, to LOS class B2 (5/5); and 3/9 isolates, to LOS class C. The 3 CC 257 isolates included one isolate of LOS class C and two isolates of LOS class F. The 4 ST-922 strains that could not be assigned to a clonal complex included 3 LOS class E and 1 LOS class F isolates.

### ***porA* Allele Typing and *flaA* SVR Sequence Typing**

DNA sequences for the *porA* gene were analyzed and assigned allele types; 4 different alleles were detected. Two alleles, 749 and 1696, were each present in 5/15 of

the calf isolates. Allele 744 was found in 4/15 of the calf isolates and the family member isolate. Allele 351 was found in a single calf isolate. Cluster analysis of the *porA* DNA sequences revealed 2 clusters of strains that were well supported by bootstrap values  $\geq 50\%$  (Figure 5.2, panel A).

*porA* allele 749 was present in all five isolates of LOS class B2. Allele type 744 was present in both LOS class E calf isolates, the family member isolate, the single LOS class A2 calf isolate, and 1 of the 3 calf isolates in LOS class F. The other LOS class F calf isolates had *porA* allele 1696. LOS class C isolates contained 2 *porA* alleles 351 and allele 1696.

Cluster analysis of *flaA* SVR sequences produced 3 strongly supported clusters of strains (Figure 5.2, panel B). DNA sequence analysis resulted in the detection of 6 different *flaA* SVR sequence types among the isolates. Four of 15 calf isolates had *flaA* SVR sequence type 16. Two of fifteen calf isolates had SVR sequence type 14; 2/15 calf isolates had *flaA* SVR sequence type 227; and 5/15 calf isolates had *flaA* SVR sequence type 41. The remaining sequence types, 327 and 111, were each found in a single calf isolate. The family member isolate carried *flaA* SVR sequence type 14.

Comparison of the *flaA* SVR sequence types with the LOS classification showed that all of the LOS class E isolates carried *flaA* SVR sequence type, ST-14; as did the family member isolate. The single isolate that classified as LOS class A2 carried *flaA* SVR sequence type 41; LOS class B2 isolates carried *flaA* SVR sequence types 41 (4/5) and 222 (1/5). The four calf isolates with LOS class C carried *flaA* SVR sequence types 16 (2/4), 227 (1/4) and 111 (1/4). The three calf isolates with LOS class F were isolates carried *flaA* SVR sequence types 16 (2/3) and 327 (1/3). Comparison of the

*porA* and *flaA* SVR DNA sequence dendrograms resulted in an overall topological score of 67%; reinforcing the similarity of the results from the two molecular typing schemes.

### **Composite Profiles**

The allele profiles derived from MLST, *flaA* SVR sequence typing, and *porA* allele typing were assessed together; results are shown in Figure 5.3. LIAN 3.5 was used to calculate linkage equilibrium parameters; the results indicated that the population is in linkage disequilibrium (Monte Carlo  $p < 0.0001$ ) with an index of association  $sI_A$  of 0.43. The average genetic diversity,  $H$ , for the composite allele profiles from MLST (7 loci), *flaA* SVR, and *porA* was calculated using LIAN 3.5;  $H$  was  $0.67 \pm 0.05$ . It was also observed that within the 16 different isolates (15 calf and 1 family member) analyzed in this study, there were 13 distinct composite profiles based on MLST, *porA* alleles, and *flaA* SVR sequence type; this demonstrated a very diverse population of isolates.

## DISCUSSION

*Campylobacter jejuni* is the leading cause of bacterial gastrointestinal infection and is commonly found in the intestines of farm animals, including chickens and cattle (146). *C. jejuni* is the most common antecedent infection to the development of the autoimmune muscular neuropathy, Guillain Barré Syndrome (GBS). Studies have been performed that show an increase in neurological symptoms in people who work with or handle farm animals compared to people who do not (122, 146). Previous studies have demonstrated that *C. jejuni* is prevalent in 0–51.2% of dairy farms in the U.S. (64, 131). Therefore when a small outbreak of *C. jejuni* occurred in humans living on a on a dairy farm in southwest Michigan, we not only analyzed the isolates to determine whether zoonotic transmission had occurred between family members on the farm and the dairy cattle, but also to determine the genetic relationships among the isolates and to evaluate whether dairy calves could be a significant reservoir of *C. jejuni* strains having LOS locus types associated with GBS.

### **Zoonotic Transmission Between the Calves and Family Members**

Analysis of the LOS classification of the 15 *C. jejuni* calf isolates and 1 family member isolate showed that 2 calf isolates (C2 and C7) shared the same LOS class as the family member isolate (FM1); all carried LOS locus class E, which lacks the genes needed to synthesize sialic acid and transfer it to the LOS outer core sugar residues. Calf isolate C2 and family member isolate FM1 were identical in LOS classification (class E), MSLT sequence type (ST-922; unknown clonal complex), *flaA* sequence

(sequence type 14), and *porA* sequence (allele 744). Calf isolate C7 differed from isolates C2 and FM1 only in the sequence of the *pgm* gene in the MLST analysis, but still shared the same sequence type (ST-922). It has been demonstrated that a great deal of recombination occurs in the *pgm* and *uncA* loci of *C. jejuni* (43). We suspect that the C7 calf isolate experienced a mutation at the *pgm* locus resulting in a different *pgm* allele assignment than that of isolates C2 and FM1; BLAST analysis of the two sequences resulted in a difference of 2 nucleotides. Based on these data, we concluded that *C. jejuni* isolate C2 could have been transmitted from the calf to the family member. However, it is impossible to exclude the possibility that the family member infected the calf.

### **Examination of Genetic Relationships Among Calf Isolates with LOS Locus Classes A–C**

We determined that 67% of the calf isolates belonged to LOS classes A–C, which are commonly associated with GBS; these locus classes contain the genes necessary to synthesize a sialylated LOS structure on the outer membrane of *C. jejuni*. To dissect further the population structure of these isolates, we typed them by a standard MLST protocol and by sequencing portions of the variable *porA* gene and *flaA* SVR, both of which are outer membrane structures of *C. jejuni*.

Our results are similar to those obtained in other studies of *C. jejuni* in dairy cattle. A study done by Sanad *et al.* (2013) on a dairy farm in Ohio showed that 36.6% of the cattle were positive for *C. jejuni* (131). In this study they examined the genetic relationships of the *C. jejuni* isolates found in both dairy cattle and starling birds with

MLST and found the most common clonal complexes in the cattle to be CC 21, CC 42, CC 45, and CC 62 (131). Clonal complex 21 was also the most common complex identified in our study. In a Finnish study, that authors performed MLST on 102 bovine *C. jejuni* isolates and found that 51% of the isolates belonged to CC 21 (32). Also, Dingle *et al.* (2001) determined that clonal complexes CC 21 and CC 45 were the most common clonal complexes among human *C. jejuni* infections (34).

Jay-Russell *et al.* (2013) utilized *porA* sequencing and MLST sequences of human *C. jejuni* isolates to isolates taken from dairy cattle to study a milk-borne outbreak of campylobacteriosis (81). These authors concluded that the level of strain discrimination provided by *porA* typing was very useful in identifying an association of dairy farm *C. jejuni* isolates with the milk-borne outbreak strain. In addition, MLST CC 21 was the most prevalent clonal complex among the cow isolates analyzed in that study (81). Our results from *porA* sequencing also provided important support for our hypothesis of zoonotic transmission. We identified 4 *porA* alleles in our sample and determined that the family member isolate and the calf isolate, C2, both shared the same *porA* allele.

The *C. jejuni* strains in our study were isolated from a small set of calves from a single breeder and probably reflect a larger *C. jejuni* population in the breeding herd. The high incidence (67%) of strains carrying LOS locus classes associated with GBS even in this small sample justify larger studies in US dairy herds, especially given the growing popularity of raw milk consumption. Based on our study and studies by others there is compelling evidence to look for a link between *C. jejuni* from cattle and development of GBS.

**Table 5.1: Summary of Molecular Typing.** The first column shows the strain ID's for the 15 calf *C. jejuni* isolates (C1-C15) and the single family member *C. jejuni* isolate (FM1). The next 7 columns are the allele assignments for the genes analyzed in MLST followed by the sequence type (ST) and clonal complexes (CC). The column labeled *flaA* shows the alleles assigned to the *flaA* SVR DNA sequences. The *porA* column shows the alleles assigned to the *porA* sequences. The last column is the LOS biosynthesis locus classification as determined by PCR. Three calf isolates and the single family member isolate were not assigned to a clonal complex and therefore labeled “unk” for unknown.

ID	<i>aspA</i>	<i>glnA</i>	<i>gltA</i>	<i>glyA</i>	<i>pgm</i>	<i>tkl</i>	<i>uncA</i>	ST	cc	<i>flaA</i>	<i>porA</i>	LOS
<b>C1</b>	9	2	4	62	4	5	1	1712	257	16	1696	C
<b>C2</b>	1	1	2	83	2	3	6	922	unk	14	744	E
<b>C3</b>	2	1	1	362	2	1	6	6227	21	227	351	C
<b>C4</b>	2	1	1	3	140	3	5	806	21	41	749	B2
<b>C5</b>	2	1	1	3	140	3	5	806	21	227	749	B2
<b>C6</b>	2	1	1	3	140	3	5	806	21	41	744	A2
<b>C7</b>	1	1	2	83	447	3	6	922	unk	14	744	E
<b>C8</b>	2	1	1	3	140	3	5	806	21	41	749	B2
<b>C9</b>	2	1	1	362	2	1	6	6227	21	16	1696	C
<b>C10</b>	9	2	4	62	4	5	38	928	257	16	1696	F
<b>C11</b>	1	1	16	83	1	3	6	922	unk	327	744	F
<b>C12</b>	9	2	4	62	4	5	38	928	257	16	1696	F
<b>C13</b>	2	1	2	3	2	1	5	982	21	111	1696	C
<b>C14</b>	2	1	1	2	140	3	5	806	21	41	749	B2
<b>C15</b>	2	1	1	3	140	3	5	806	21	41	749	B2
<b>FM1</b>	1	1	2	83	2	3	6	922	unk	14	744	E

**Figure 5.1: SplitsTree diagram based on MLST alleles.** As seen in the tree below, C2 and FM1, which are 1 calf isolate and the single family member positive for *C. jejuni*, are identical in allele types based on MLST. The presence of the network suggests the occurrence of low levels of recombination.

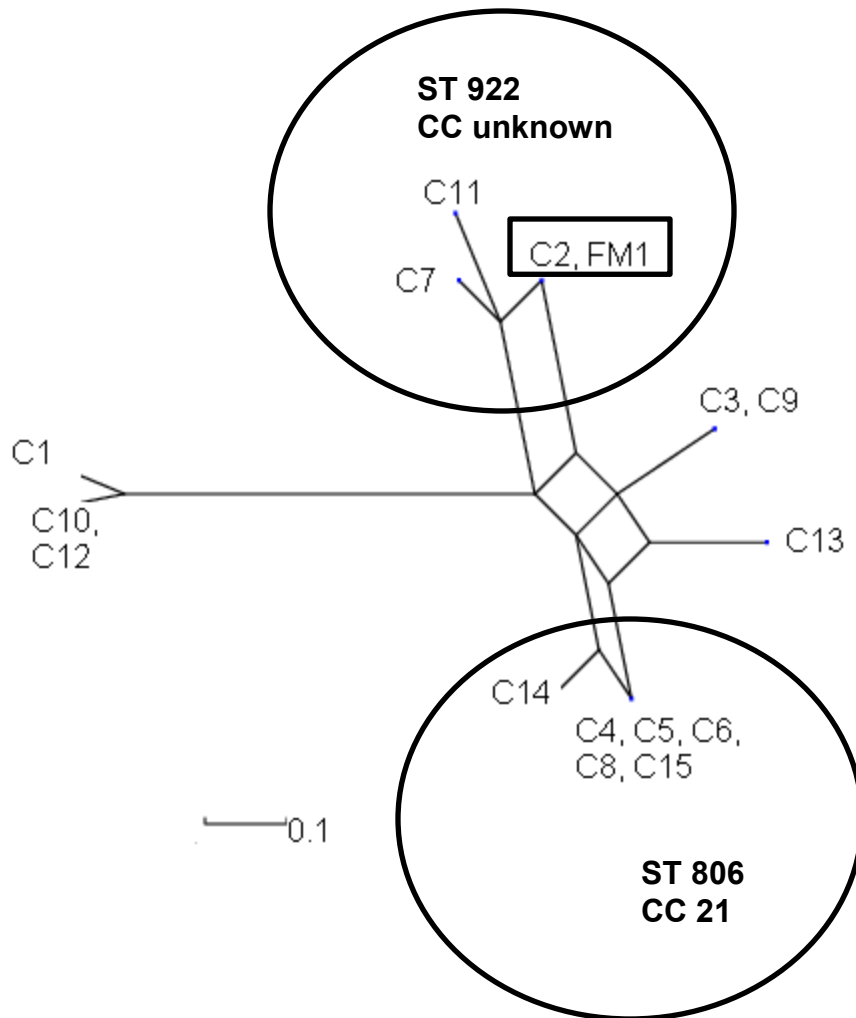


**Figure 5.2: Dendograms of *porA* and *flaA* SVR DNA sequences.** Panel A is a dendrogram of the *porA* sequences; two well supported clusters were observed. Panel B is a dendrogram of the *flaA* SVR DNA sequences; 3 well supported clusters were observed. These clusters are defined based on bootstrap values  $\geq 50\%$  and indicated with brackets. Isolates C2 and FM1 both shared the same *porA* allele type and *flaA* SVR sequence type; they are indicated by a ★.

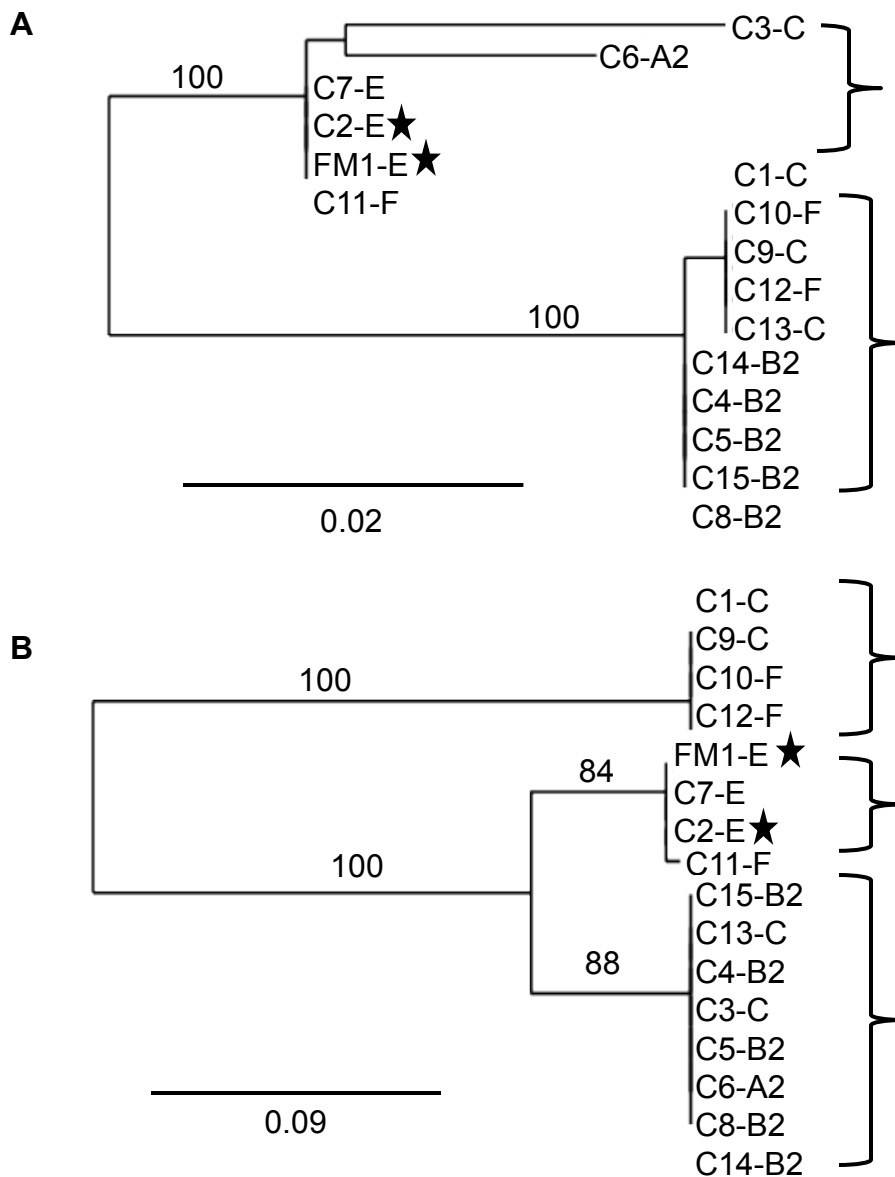
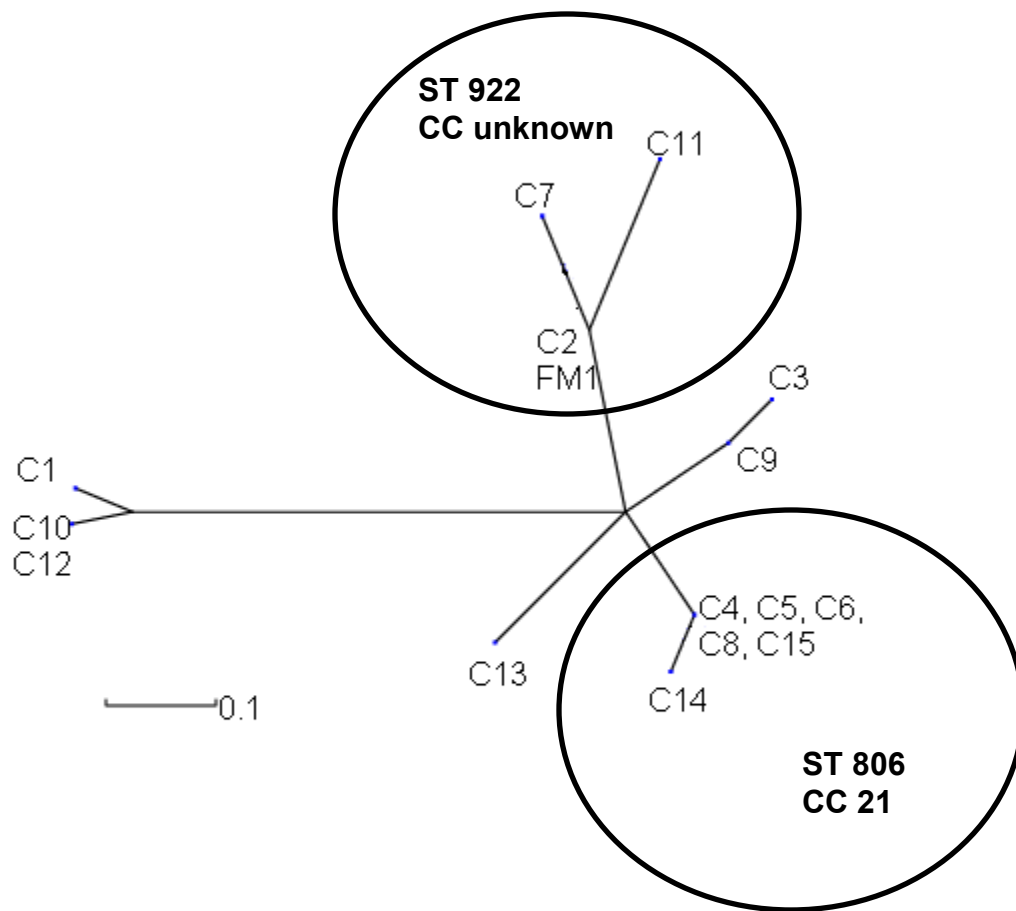


**Figure 5.3: SplitsTree analysis of combined allelic profiles of 7 MLST loci, *porA* alleles, and *flaA* SVR sequence types.**



## CHAPTER 6

### Conclusions

## SUMMARY

All disease results from one or more of the following factors: pathogens (and their genetics), host genetics/immune responses, the microbiota, and the environment. These factors interact in many diseases such as the role of the hygiene hypothesis in the development of allergies and the role of parasites (155). Some autoimmune diseases are associated with prior infection; Guillain Barré Syndrome (GBS) are prominent examples (7). GBS is an autoimmune disease of the peripheral nerves in which both the myelin sheath and axons may be involved; it is the most frequent cause of acute flaccid paralysis (116, 160). GBS frequently follows gastrointestinal infections caused by *Campylobacter jejuni* (105). *C. jejuni* may also result in the development of other autoimmune diseases such as Reiter's Syndrome, Inflammatory Bowel Disease, and Irritable Bowel Syndrome (44, 68, 75, 87, 125). The overall aim of my work was on GBS induced by *C. jejuni* with focus on two aspects of the disease—host genetics/immune responses and pathogen genetics. Pathogen genetics is thought to provide the primary mechanism of pathogenesis of the disease. The pathogenesis of GBS following *C. jejuni* infection is believed to involve immune responses to ganglioside-like structures displayed by the lipo-oligosaccharides (LOS) on the outer surface of *C. jejuni* cells that mimic neurogangliosides (7).

The LOS loci of *C. jejuni* can be assigned to classes A–W based on the presence or absence and organization of the LOS biosynthesis genes (47, 111, 112, 125). LOS classes A, B, C, M, R, and V all have the necessary genes to synthesize a sialylated LOS to mimic gangliosides enriched in the nervous tissues. *C. jejuni* strains with LOS

classes A and B have been isolated from GBS patients and therefore are highly associated with development of GBS. However, it has been documented that *C. jejuni* strains that express an LOS with class A or B have also been isolated from patients who only developed enteritis (47, 111). This result suggests that the host's genetics and immune response is important to development of disease, but the basis for this interaction is currently unknown. *C. jejuni* isolates from GBS patients have also been shown to have LOS loci (F, H, K and P) that do not have the necessary genes to synthesize an LOS structure capable of mimicking a ganglioside. These data suggest that there may be alternative mechanisms in *C. jejuni* that result in the sialylation of the LOS and subsequent production of anti-ganglioside antibodies; there could also be involvement of specific pathogen or host genes that have not been identified. There may also be alternative targets on nerves that are shared on *C. jejuni* strains. A better understanding of the genetic relationships among LOS classes A–C is needed.

Molecular typing schemes have been applied to assess the genetic relationship of LOS classes A–C with variation in other genes within the genomes of *C. jejuni* strains. These schemes include multi-locus sequence typing (MLST), *porA* allele typing, and *flaA* SVR sequence typing (27, 28, 34, 101). MLST is a widely used typing tool based on the partial sequences of 7 highly conserved housekeeping genes in *C. jejuni*. Sequence typing of the major outer membrane protein, *porA*, and the short variable region (SVR) of the *flaA* gene of the flagellum, both of which are outer surface molecules of *C. jejuni*, has provided conflicting data about the genetic relationships among *C. jejuni* isolates in LOS classes A–C versus those that have LOS classes not associated with ganglioside mimicry. These two outer surface molecules are highly

variable, and therefore it has been suggested that combined molecular typing using all of these techniques (MLST, *porA*, *flaA* SVR, and LOS) might provide less conflicting data than when these typing schemes are used separately.

GBS is characterized as a group of disorders affecting the peripheral nerves that include acute inflammatory demyelinating polyneuropathy (AIDP), acute motor axonal neuropathy (AMAN), and Miller Fisher Syndrome (MFS). AIDP is the most common subtype of GBS found in humans, is characterized by myelin damage, and affects most myelinated motor nerves of the limbs as well as lower cranial motor and sensory nerves (145). AMAN is the most common subtype identified in Asia and is characterized by damage to motor neurons, specifically the nodes of Ranvier. Tissue damage in AMAN occurs mainly in the nerve roots or distal nerve terminals (145). MFS is an anatomically localized variant of GBS characterized by acute onset of ophthalmoplegia, ataxia, and areflexia. In some instances, patients with MFS progress to GBS (109, 138, 159). Anti-ganglioside antibodies have been detected in approximately 60% of GBS patients (84).

The current animal models used to study the pathogenesis of GBS include an AMAN model in rabbits, an AIDP model in mice, and an AMAN model in chickens. The rabbit model is based on immunization of rabbits with purified *C. jejuni* LOS that is known to mimic gangliosides. The rabbits develop neuropathy and anti-ganglioside antibodies, but this is not a model of GBS secondary to *C. jejuni* infection (natural model) to study development of GBS (164, 165). In the mouse model of AIDP, mice are immunized with bovine myelin and develop nerve lesions; demyelination occurs that is similar to that in GBS patients that present with AIDP (8, 126). Like the rabbit model, this mouse model does not develop GBS secondary to *C. jejuni* infection and therefore

is not a natural model of GBS. The chicken model of AMAN is the only natural animal model used to study GBS. Chickens inoculated with *C. jejuni* isolated from a GBS patient developed paralysis and nerve lesions similar to those seen in AMAN patients (94). However, chickens are anatomically and physiologically different from humans: therefore a mouse model is needed to study the natural development of GBS secondary to *C. jejuni* infection.

## **Chapter 2 Summary: Non-Obese Diabetic (NOD) mice as working models of Guillain Barré Syndrome following *Campylobacter jejuni* infection**

We attempted to develop a mouse model of GBS using wild type Non-Obese Diabetic (NOD) mice and their congenic knockouts NOD IL-10<sup>-/-</sup> and NOD B7-2<sup>-/-</sup> mice infected with *C. jejuni* isolates from GBS patients. These GBS-associated strains were *C. jejuni* HB93-13, which was isolated from a AMAN patient in China, and *C. jejuni* 260.94, which was isolated from an AIDP patient in South Africa (2). Our experiments included confirmation of *C. jejuni* colonization, detection of anti-ganglioside antibodies, assessment of clinical neurological phenotypes, and detection of nerve lesions (myelin damage and cellular infiltrates).

Based on our results, we determined that NOD WT mice have the greatest potential as a suitable model. When inoculated with the two *C. jejuni* isolates taken from GBS patients, these mice were colonized with *C. jejuni* but had minimal enteric disease as assessed by evaluation of both gross and histopathological changes in the GI tract. Thus enteric disease should not have influenced clinical evaluation of neurological signs. During infection with *C. jejuni*, NOD WT mice developed anti-ganglioside

antibodies to both individual gangliosides and ganglioside mixtures and displayed a neurological phenotype. The infected NOD WT mice also had significantly greater infiltration of macrophages into the sciatic nerve. However, nerve lesions were not detected in the sciatic nerve. This likely resulted because we only removed a small portion of the sciatic nerve when following standard technique for removing nerves from the mouse. The lesions could also occur in locations other than the sciatic nerve, such as the dorsal root ganglia. Therefore other sections of the peripheral nervous system should be removed in the future for analysis. Another reason for not detecting lesions could be a problem with selecting the appropriate time to sacrifice the animals. We may not have waited long enough for lesions to form since infiltration of macrophages could be an early step in lesion development. More work is needed to confirm that the NOD WT mice are a true murine model of GBS secondary to *C. jejuni* infection and to select the optimal time for sampling after lesion development.

NOD IL-10<sup>-/-</sup> mice developed enteritis from the *C. jejuni* infection in Experiment 1 and therefore were given chloramphenicol (CMP) in Experiment 3 to attempt to prevent enteritis from occurring and potentially interfering with the assessment of clinical neurological phenotypes. The NOD IL-10<sup>-/-</sup> mice were colonized with *C. jejuni*, developed gross pathological changes (enlarged lymph nodes and thickened wall of the gastrointestinal tract), displayed high scores for histological assessment of the GI tract lesions, developed anti-ganglioside antibodies, and displayed clinical neurological phenotypes as determined by the DigiGait™. In Experiment 3 we also improved our techniques for removal of the sciatic nerve: we removed the entire length of the nerve,

the nerve roots (L3–L5), and also removed the brachial plexus for analysis of nerve lesions and cellular infiltrates. Here, we identified a significant increase in the number of macrophages in the nerve roots of infected mice compared to uninfected mice. We also identified structures we termed “fat vacuoles” in the sciatic nerves of all treatment groups of the NOD IL-10<sup>-/-</sup> mice. These fat vacuoles could actually be macrophages that were ingesting damaged myelin. Myelin has lipid components, and therefore these fat vacuoles could indicate myelin damage. To confirm this hypothesis, we could use a stain for lipids or myelin proteins in order to assess the significance of this finding.

In Experiment 3, treatment with CMP alone resulted in development of enteritis. This was a somewhat surprising finding because *C. jejuni* are susceptible to CMP. However, these mice were IL-10 deficient and therefore would not have been able to down-regulate an inflammatory response, whether it was a result of *C. jejuni* infection or a disruption in the intestinal microbiota. To continue studying these mice as a potential GBS model, a ganglioside mimicking *C. jejuni* strain that colonizes but doesn't cause enteric disease should be identified.

In both the NOD WT and the NOD IL-10<sup>-/-</sup> mice, we saw an increase in infiltration of macrophages in the sciatic nerve sections and nerve roots, respectively. In both locations there are resident macrophages and neutrophils present; however we found a significant increase in the number of macrophages in both locations in mice infected with *C. jejuni* 260.94 when compared to their sham-inoculated counterparts. This elevation in macrophage numbers suggests that we were observing additional macrophages in the mice due to the infection with *C. jejuni*.

NOD B7-2<sup>-/-</sup> mice were colonized by the *C. jejuni* strains we used for our infection studies with minimal enteric disease. These mice developed anti-ganglioside antibodies after infection and displayed clinical neurological phenotypes. However, no lesions or cellular infiltrates of the nerves were identified in these mice. Perhaps, for the same reasons no lesions were detected in NOD WT mice, we missed the right location and time for taking nerve samples. Nevertheless, we did not pursue these animals as a model because these mice develop spontaneous neuropathy and nerve lesions at or after 20 weeks of age, which would be a disadvantage in long term studies.

As stated above, GBS is characterized as a group of disorders that all result in damage to the motor nerves. Each of the NOD background mice examined in our experiments displayed neurological phenotypes; however not all mice developed such a phenotype. During the course of the experiments we used or developed neurological tests for detection of motor function failure in the peripheral nervous system. The tests we used included the open field test (OFT), hang test, rotarod, and footprint and DigiGait™ analysis that allowed detection of ataxia, loss of motor strength, loss of balance, and abnormal gait, respectively. Each of these tests focused only on the loss of motor function. However, the first onset of symptoms in humans usually includes tingling sensations, suggesting that sensory nerves are involved. Sensory nerves have no Schwann cells, are poorly myelinated, and have a slow conduction velocity while motor nerves are highly myelinated, have Schwann cells, and have a fast conduction velocity. Given these differences between the two types of nerves, it would be beneficial to develop sensory tests that could be applied to mice since our current neurological tests focus solely on the motor nerves. Therefore, we suggest that future work with the

NOD WT murine model include sensory tests to determine if there is loss of sensory function.

Sensory tests that could be performed include tail flick and hotplate tests. The tail flick test consists of applying a thermal stimulus to a mouse's tail that results in a simple spinal reflex of the tail flicking (30). The hotplate test consists of placing a mouse on the surface of a hotplate that is maintained at 50–55°C. The length of time required for the mouse to raise and lick its forepaw or jump up is then recorded. If no response is observed after 30 seconds then the mouse is removed from the plate (30). Mice infected with *C. jejuni* strains associated with MFS could also be tested for the palpebral reflex by touching the eyes noting whether the eyelid closes (42). These tests could all be added to future experiments. As described above, many of the subtypes of GBS are mainly associated with motor nerves, and therefore our previously defined tests would continue to be used.

### **Chapter 3 Summary: Examination of Miller Fisher Syndrome in NOD WT and C57BL/6 WT mice subsequent to *Campylobacter jejuni* CF93-6 infection**

This experiment assessed the development of MFS and GBS in mice infected with a MFS-associated *C. jejuni* strain compared to mice infected with a GBS-associated *C. jejuni* strain. There were two groups of infected NOD WT mice: one group received the GBS-associated *C. jejuni* strain and the other received the MFS-associated *C. jejuni* strain. The C57BL/6 WT mice only received the MFS-associated *C. jejuni* strain. Results from this experiment were all insignificant except for presence of anti-ganglioside antibodies in the NOD WT mice infected with the GBS-associated *C. jejuni*

strain compared to sham-inoculated NOD WT mice. All other treatment groups of both the NOD WT and C57BL/6 WT mice were not significantly different from sham-inoculated mice in any of the parameters examined. The origin of the mice could provide an explanation for the lack of significant results in the NOD WT mice in this experiment. The NOD WT mice used in Experiment 1 were all bred in our laboratory's specific pathogen free breeding colony; the NOD WT mice used in this experiment were purchased directly from The Jackson Laboratory and sent straight to the MSU containment facility for inoculation. These mice may have a different GI tract microbiota from the mice from our breeding colony, which could result in the different results seen between experiments. Furthermore, the NOD WT mice in the breeding colony could have diverged genetically from mice at The Jackson Laboratory since the breeding colony was established five years prior to Experiment 1 from only three pairs of breeding mice. Regardless, the results suggest that further work to develop a mouse model of MFS should include reconsideration of other inbred mouse strains and other strains of *C. jejuni* from patients with MFS.

#### **Chapter 4 Summary: Multiple molecular typing schemes applied to define genetic relationships among *C. jejuni* isolates that share the same LOS classification**

The LOS biosynthesis loci have been analyzed in numerous sequenced and unsequenced strains of *C. jejuni* and a classification scheme has been developed based on the gene content of the loci. In this study we characterized the LOS loci of *C. jejuni* isolates collected in our laboratory (68 total: 63 unsequenced and 5 previously sequenced); the majority were collected in Michigan (49/68), but a subset came from

other locations in the US. One strain was from Canada. To date there have been 23 LOS classes (A–W) identified, but in our analysis we only classified the LOS into seven groups: classes A–F or unknown (unclassified). We identified 12/68 isolates that could be classified as members of more than 1 of the previously described LOS classes and therefore were termed “unknown.” Of the remaining 56 isolates, 86% belonged to LOS classes A–C and the remaining 14% were classified as LOS class E or class F; no isolate was classified as LOS class D. An examination of only the 49 Michigan isolates showed that 69% of them belong to LOS classes A–C; this percentage is near the upper end of the range shown by previous studies (32–77%) (57, 69, 78, 123, 124), suggesting that there is a higher than average likelihood of becoming infected with a *C. jejuni* strain associated with GBS in Michigan.

In these studies, the identification of the LOS classes showed that a high proportion of *C. jejuni* isolates typed with LOS classes A–C. Therefore we wanted to examine possible genetic relationships of other outer membrane surface molecules with the LOS classes in these isolates using previously described molecular typing schemes—*porA* allele type and *flaA* SVR sequence type—both of which are highly variable. We also included MLST analysis since it assesses the gene content of conserved housekeeping genes and provides a phylogenetic framework for the strain collection.

Analysis of MLST data showed that the collection contained 37 different sequence types (ST) that were further grouped into 19 clonal complexes. Comparison of the MLST data with the LOS classification showed that only 3 clonal complexes of the 19 contained only one kind of LOS class. The alleles assigned to the *porA* sequences

resulted in 43 different allele types with only 2 *porA* alleles associated with a single LOS class. *flaA* SVR sequence typing resulted in 39 different sequence types; only 2 of which were associated with a single LOS class. Overall analysis of these molecular typing schemes indicated the possibility that some recombination occurred; the group of isolates was genetically diverse.

To further understand the role of the LOS biosynthesis locus genes, the *flaA* SVR, and the *porA* gene of the *C. jejuni* isolates we examined, future experiments could be performed to determine whether these genes are being expressed during infection. We believe that determining whether a gene is present or absent or the sequence of that gene does not provide enough information to discern the characteristics of GBS-associated *C. jejuni* strains. We need to determine whether that gene is being expressed in the host during infection.

### **Chapter 5 Summary: *Campylobacter jejuni* isolates from calves have A, B, and C lipo-oligosaccharide (LOS) biosynthetic locus classes similar to human Guillain Barré Syndrome associated strains**

Chapter 5 focused on a small epidemiological study of a *C. jejuni* outbreak on a Southwest Michigan dairy farm. Family members on the farm had complained of reoccurrence of *C. jejuni* infections in previous years, so 25 stool samples were obtained from calves on the farm, along with 1 stool sample from a pet dog. All family members were tested for *C. jejuni* as well. Our results indicated that 15/25 (60%) of the calves were positive for *C. jejuni* and 2/25 (8%) were positive for *C. coli*; no calf was positive for both *C. jejuni* and *C. coli*. The dog and all family members but one tested

negative. The 15 calf and 1 human *C. jejuni* isolates were analyzed with PCR-based LOS classification and MLST to determine whether zoonotic transmission occurred between the family member and the calves. The LOS classification of the calf strains showed that 10 of the calf isolates typed as LOS class A, B, or C. Two calf isolates fell into LOS class E and 3 calf isolates class F. The family isolate was classified as LOS class E. MLST results showed that there were 5 different sequence types among the strains; the sequence types were further grouped into 2 defined clonal complexes and 1 unknown clonal complex. All isolates typed as LOS class A2 or class B2 fell into the same clonal complex. The family member isolate grouped in the same sequence type (ST-922; unknown clonal complex) as the LOS class E isolates from the calves. DNA sequence analysis of the *porA* gene grouped the calf isolates into 4 different allele types; the family member isolate carried the same allele of the other LOS class E isolates. *flaA* SVR sequence typing defined 6 different sequence types; the LOS class E isolates had the same *flaA* SVR sequence type as the LOS class E isolate from the family member. Analysis of the combined allele profiles from the three typing schemes with LIAN 3.5 indicated that minimal recombination occurred.

Based on MLST data, one calf isolate (C2) and the family member isolate had identical MLST allele types and were both LOS class E. The family member isolate also shared the same *porA* allele type and *flaA* SVR sequence type as calf isolate C2. These results therefore suggest zoonotic transmission between the calf and the family member. Since all but one calf isolate had different allele and sequence types, it suggests that the family member contracted the *C. jejuni* from the single calf that carried a *C. jejuni* strain that shared sequence type, LOS class and *porA* allele and *flaA* SVR

sequence type with the human isolate. Alternatively, the calf may have been infected from the family member. The direction of transfer cannot be discerned from this analysis.

One other *C. jejuni* calf isolate, C7, belonged to the LOS class E and shared the same MLST sequence type and clonal complex, *porA* allele type, and *flaA* SVR sequence types as calf isolate C2 and the family member isolate. The C7 calf isolate differed from the calf isolate C2 and family isolate in the allele assignment to the MLST housekeeping gene, *pgm*, which has been shown to be subject to high rates of recombination. These data suggest recombination occurred in the C7 calf isolate.

## FUTURE DIRECTIONS

### Defining the NOD WT mouse as a natural model of GBS

As stated previously, more work needs to be done to determine if NOD WT mice are suitable models of GBS disease that occurs secondary to *C. jejuni* infection. First, a time course experiment should be performed. An important goal in this experiment would be to determine the time at which anti-ganglioside antibodies peak. We propose to employ the DigiGait™ apparatus to detect clinical neurological phenotypes since it has been shown to be sensitive enough to detect the subtle changes seen in GBS. The DigiGait™ was not available during experiments performed with NOD WT mice; therefore, assessment of NOD WT mice using this apparatus could result in a more detailed assessment of the clinical neurological phenotype than in our previous experiments. In future experiments an assessment of sensory nervous system function will also be included as described above.

Examination of the nerve root for infiltration of macrophages should also be done with NOD WT mice exhibiting GBS. In our previous experiments with NOD WT mice, we only examined a small section of the sciatic nerve; future experiments should include the entire length of the sciatic nerve, including the nerve roots because we have shown this to be effective in finding peripheral nerve lesions wherever they occur. Previous experiments also suggest that light microscopy does not provide enough detail to detect the exact location of cellular infiltrates along the nerve. We propose to identify the presence of these cell types (*i.e.* macrophages, neutrophils, lymphocytes) with light microscopy, and to then employ transmission electron microscopy to localize these cell

types to various locations on the nerve—*i.e.* nodes of Ranvier, the paranodal region, mid-axon, or Schwann cells—where damage is occurring. In addition, the presence of anti-ganglioside antibodies at the neuromuscular junction (NMJ) should be assessed using IHC, since it has been demonstrated that anti-GM1 and anti-GQ1b antibodies both bind at the NMJ in a complement deficient murine model (62, 160). Gangliosides are highly concentrated at the NMJ, and this site lacks the nerve-blood barrier (157), therefore allowing easy access for antibodies reactive to the gangliosides. To determine which side of the NMJ the anti-gangliosides are binding to, we could stain with alpha bungarotoxin to identify the post-synaptic side. Furthermore, to assess the binding of anti-ganglioside antibodies to the pre-synaptic side of the NMJ, we could stain for the soluble NSF attachment protein receptor (SNARE) proteins associated with this side of the NMJ. By performing these stains, we can isolate which part of the NMJ is involved in GBS in the mice. We could also perform additional stains for Schwann cell integrity, components of the complement cascade, and for antibody binding directly to the nerve.

In addition to these approaches, we could switch to plastic embedding of the nervous tissue in place of paraffin embedment. In our previous experiments with paraffin embedment we were only able to get 2–3 slides per section of nerve. With plastic embedding, thinner sections (1–2  $\mu\text{m}$ ) can be made, resulting in more slides per animal. This would allow us to do the additional histology and immunohistochemistry analyses described above. In addition to providing thinner sections, plastic embedding also allows more accurate orientation of the nerve sections.

### **Potential for the NOD IL-10<sup>-/-</sup> mouse as a natural model of GBS**

The NOD IL-10<sup>-/-</sup> mice developed enteritis and spontaneous colitis that complicated the assessment of clinical neurological phenotypes. If work with this strain of mouse is to continue, then a *C. jejuni* strain associated with GBS that colonizes without causing enteritis in these mice would have to be identified or developed in the laboratory. We could also try to identify an antibiotic that would kill the *C. jejuni* selectively but not disrupt the gut microbiota as the CMP did in Experiment 3. Another approach to understand what occurs in these IL10-deficient mice would be to move away from the natural model of GBS and immunize them with purified LOS from a *C. jejuni* isolate of a GBS patient. This immunization model would allow us to understand the immune system products and effects resulting from the LOS in the absence of other outer membrane components. However, this immunization would remove the interaction of the bacteria with the gut microbiota and immune system that results in the development of enteritis, and, as stated earlier, this would be then no longer a natural model of GBS.

If a natural model is one that develops GBS secondary to infection with *C. jejuni*, another option would be to investigate C57BL/6 IL-10<sup>-/-</sup> mice as a model for GBS. Previous studies in our lab have shown that these mice are colonized by the GBS-associated *C. jejuni* strain 260.94 without developing enteric disease (99). Anti-ganglioside antibodies have been detected in plasma of C57BL/6 IL-10<sup>-/-</sup> mice infected with GBS-associated *C. jejuni* (Malik and Mansfield, unpublished). However, these mice have never been assessed for a clinical neurological phenotype or nerve lesions.

Preliminary experiments with C57BL/6 IL-10<sup>-/-</sup> mice would have to be performed to determine the potential of these mice as a mouse model of GBS.

### **Examination of other factors contributing to the pathogenesis of GBS**

The LOS biosynthesis locus of *C. jejuni* has been highly scrutinized with respect to its role in molecular mimicry leading to the development of GBS. Strains classified as having LOS classes A and B have been found in both GBS patients and enteric patients; furthermore, strains having LOS loci that do not contain the necessary genes to synthesize an LOS capable of mimicking gangliosides have been identified in GBS patients (111). These findings suggest there are other factors contributing to the development of GBS that need to be explored.

One such mechanism that should be explored more thoroughly to determine its possible role in the development of GBS is the protein C-Dps. C-Dps is a DNA binding protein produced by *C. jejuni* in response to nutritional or oxidative stress; it is thought to protect the bacterial DNA from damage. Sulfatide, a glycosphingolipid, is needed for paranodal junction formation and maintenance of ion channels along axons; C-Dps has been shown to bind to sulfatide (114, 115). In one study by Piao *et al.* (2010), the authors injected C-Dps directly into sciatic nerves of rats and found that it localized to the outermost parts of the myelin sheath and nodes of Ranvier, resulting in myelin detachment and axonal degeneration. These findings were confirmed by a reduction in action potentials in nerve conduction studies of dissected tissue (115). In the same study, the authors infused C-Dps intrathecally into rats and showed that it bound to the nodal regions and myelin sheath (115). In another study, Piao *et al.* (2011) examined

the binding properties of C-Dps immunohistochemically and found that not only does the protein bind to the nodes of Ranvier, the outer part of the myelin sheath, and the basement membrane of the peripheral nerves, but it also binds to the anterior horn cells in the spinal cord grey matter and to myelin in the white matter (114). These findings suggest that C-Dps could play a role in the pathogenesis of GBS.

Kawamura *et al.* (2011) examined sera from GBS patients for the C-Dps protein and antibodies to the protein and found that 5/27 patients had C-Dps protein in their sera and that 15/24 patients had antibodies to the C-Dps protein in their sera (89). This study offers further evidence that this protein, C-Dps, may play a role in pathogenesis of GBS. Therefore, our future work with the mouse model could include detection of anti-C-Dps antibodies and the protein itself in the plasma of GBS-associated *C. jejuni* infected mice. To do this, we could perform ELISA on stored frozen plasma from mice in our previous experiments as well as plasma obtained in future experiments.

Development of a C-Dps knockout strain of *C. jejuni* could be used to assess the role of C-Dps *in vitro* and *in vivo*. If the C-Dps gene is found to play a role in the pathogenesis of GBS, further experiments could be performed to determine if both C-Dps and sialylated LOS are needed in the pathogenesis of GBS. This could be done by taking a GBS-associated strain of *C. jejuni* that causes GBS in mice and making 3 knockouts: 1) knock out only the C-Dps gene to assess its role in pathogenesis of GBS, 2) knock out only the sialic acid related genes in the LOS (*cst* and *neuBCA*) to examine their role in the pathogenesis of GBS, and 3) knock out both the C-Dps gene and sialic acid related genes to determine if GBS still develops.

Host factors should also be assessed; they may play an important role in the development of GBS as well, since *C. jejuni* with LOS classes A or B can be isolated from patients who developed enteritis but not neurological disease. Some host factors that have been studied include temperature, CD1 antigen presenting molecules, and *KM* immunoglobulin genes. One study showed that *C. jejuni* grown at 37°C is more likely to produce an LOS capable of mimicking gangliosides than *C. jejuni* grown at 42°C (133); the internal body temperature of a mice and humans is approximately 37°C. In another study, polymorphisms of the CD1 antigen-presenting molecules in 65 GBS patients were examined; CD1 has recently been shown to present self-glycolipids to antigen specific T cells (21, 118). Caporale *et al.* (2006) examined 3 genes of the CD1 molecule (CD1A, CD1D, and CD1E) at exon 2 where known polymorphisms exist. They differentiated the alleles by PCR and found that subjects with a certain CD1E allele are 2.5 times more likely to develop GBS (21). In another study of genetic markers in the constant region of immunoglobulin kappa chains, Pandey *et al.* (2003) genotyped 83 GBS patients for the *KM1* and *KM3* alleles using PCR-RFLP. They found that *KM3* homozygosity was significantly associated with GBS while *KM1/KM3* heterozygosity was significantly associated with control patients; they did not examine any patients with *KM1* homozygosity (110). These data suggest that host genotype for specific *KM* and CD1 alleles could play a role in the development of GBS.

## **APPENDICES**

## **APPENDIX A**

### Chapter 2 Experiment 1

**Figure A-1: Examination of enteric disease from *C. jejuni* infection in Experiment**

1. Panel A shows the gross pathological features present at the endpoint of the experiment. Features examined were thickened wall of the GI tract and enlarged lymph nodes. Panel B shows the histopathological scores at the ileocecolic junction.

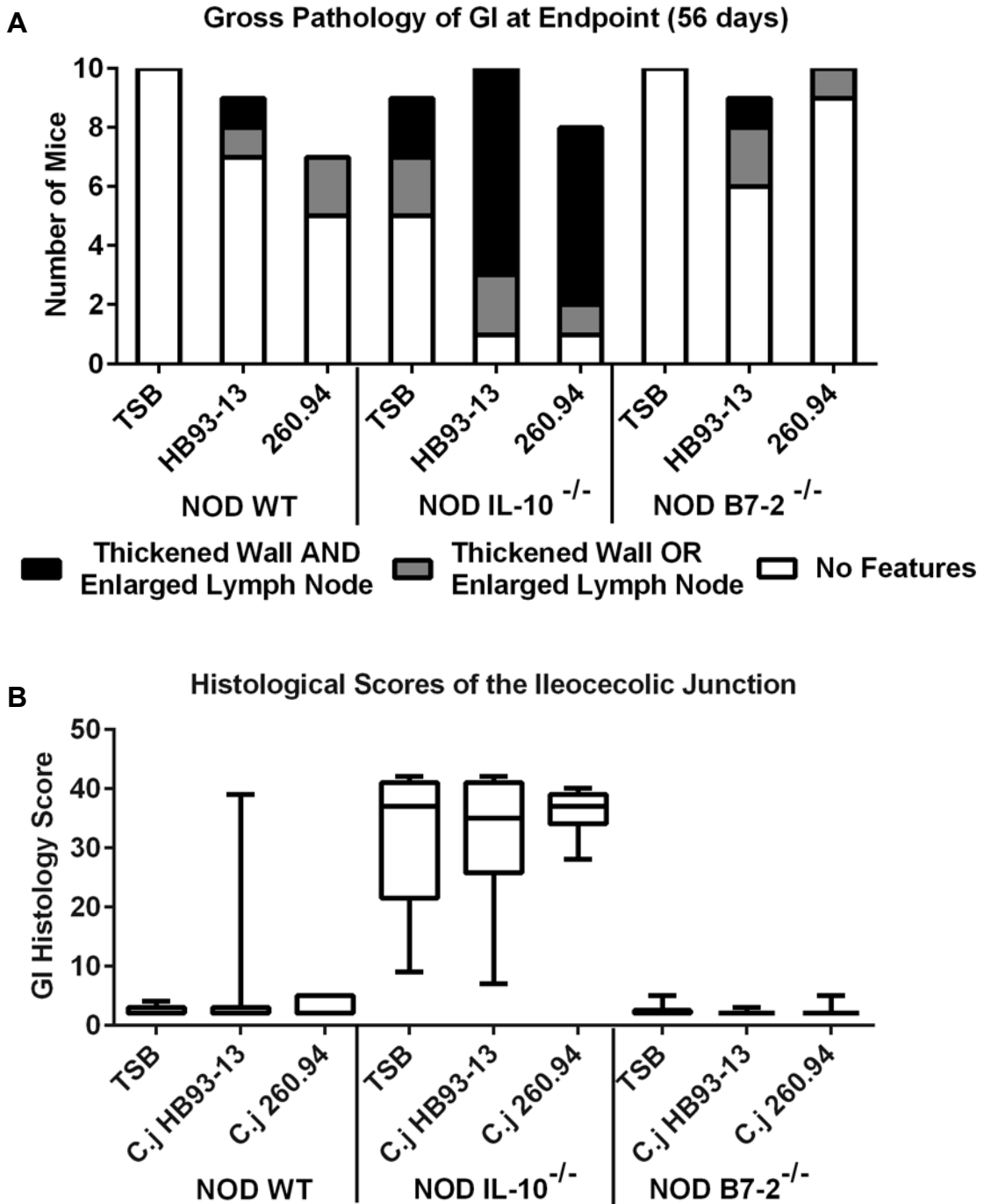


**Figure A-2: Experiment 1 ELISA assay data.** Panel A shows plasma levels of IgG1 reactive to ganglioside GD1a on day 0 (A-1) and day 14 P.I. (A-2). Panel B shows the plasma levels for IgM reactive to ganglioside GM1 on day 0 (B-1) and day 14 P.I. (B-2). Panel C shows ELISA data for plasma levels of antibody reactive with ganglioside GM1 in samples taken at the end of the experiment (56 days); antibody isotypes IgG1, IgG2a, and IgG3 are shown in panels C-1, C-2, and C-3, respectively. Panel D shows endpoint ELISA assay data for ganglioside GD1a with plasma levels of antibodies IgG1, IgG2a, and IgG3 shown in panels D-1, D-2, and D-3, respectively. In panel E, plasma levels of antibody isotype IgG1 reactive with the ganglioside mixture GM1/GD1a at the endpoint of the experiment are shown. No significant differences in levels of antibody were detected in treatment groups of any of the genotypes in any of these assays.

Figure A-2 (cont'd)

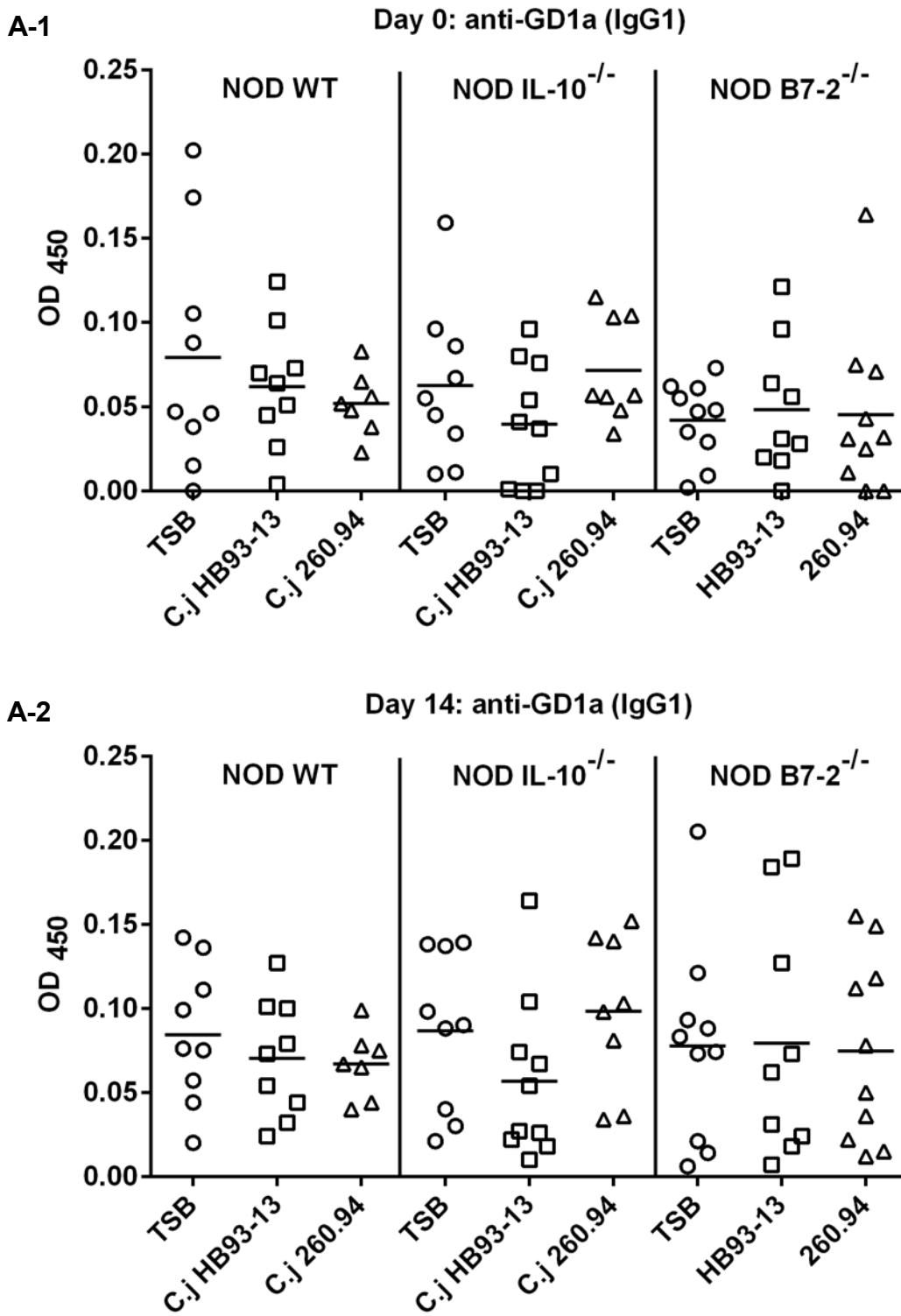


Figure A-2 (cont'd)

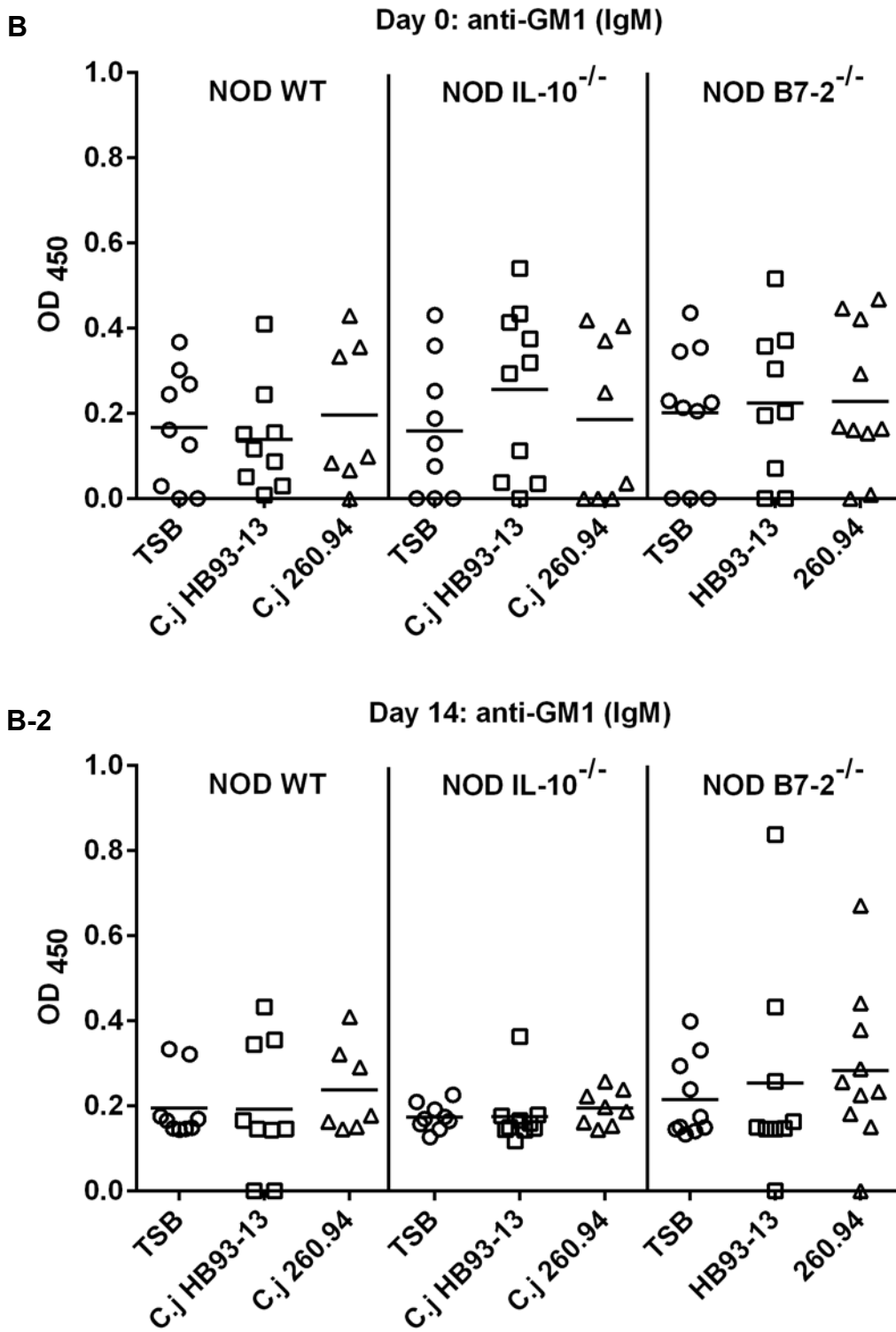


Figure A-2 (cont'd)

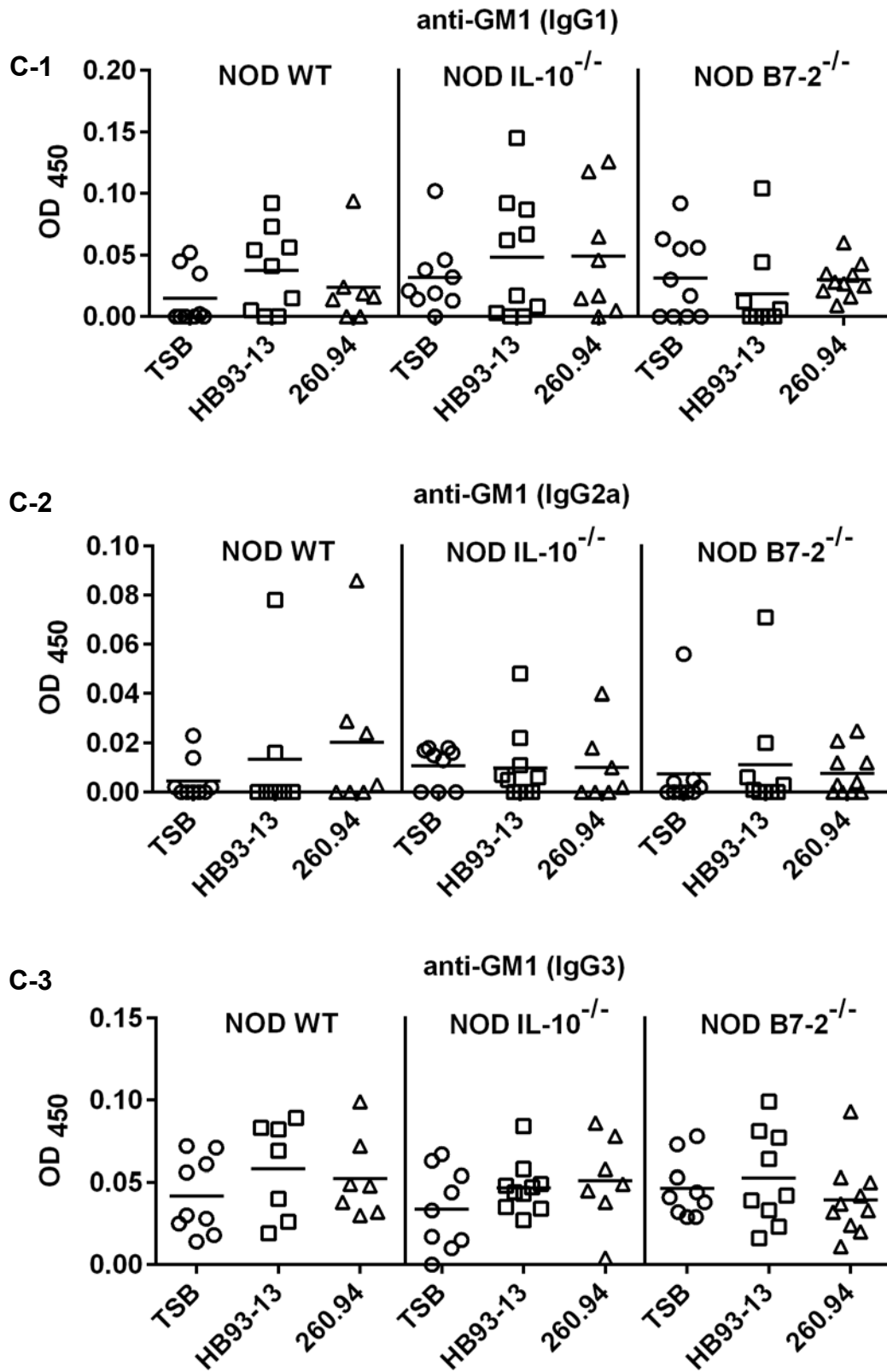


Figure A-2 (cont'd)

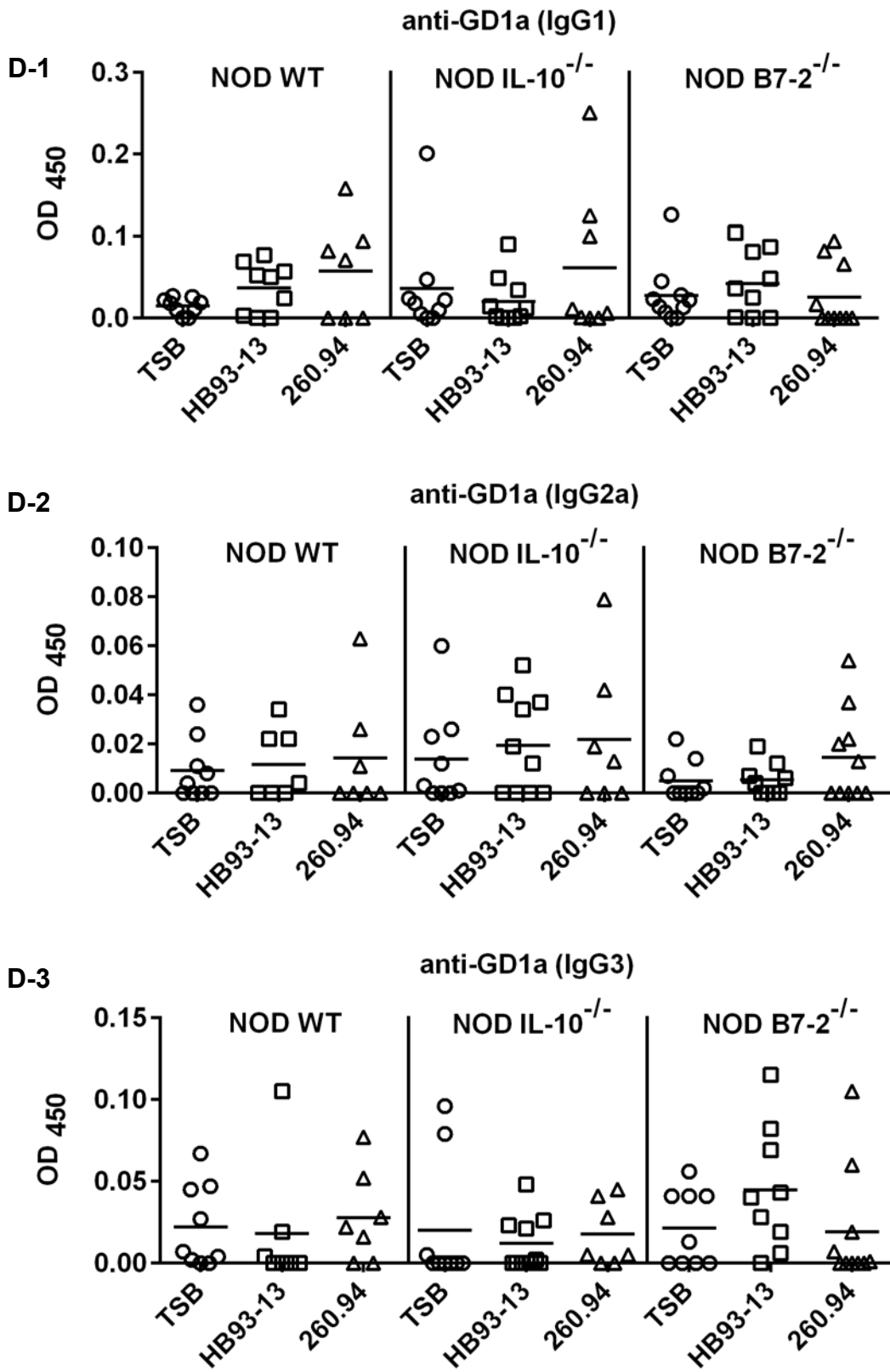
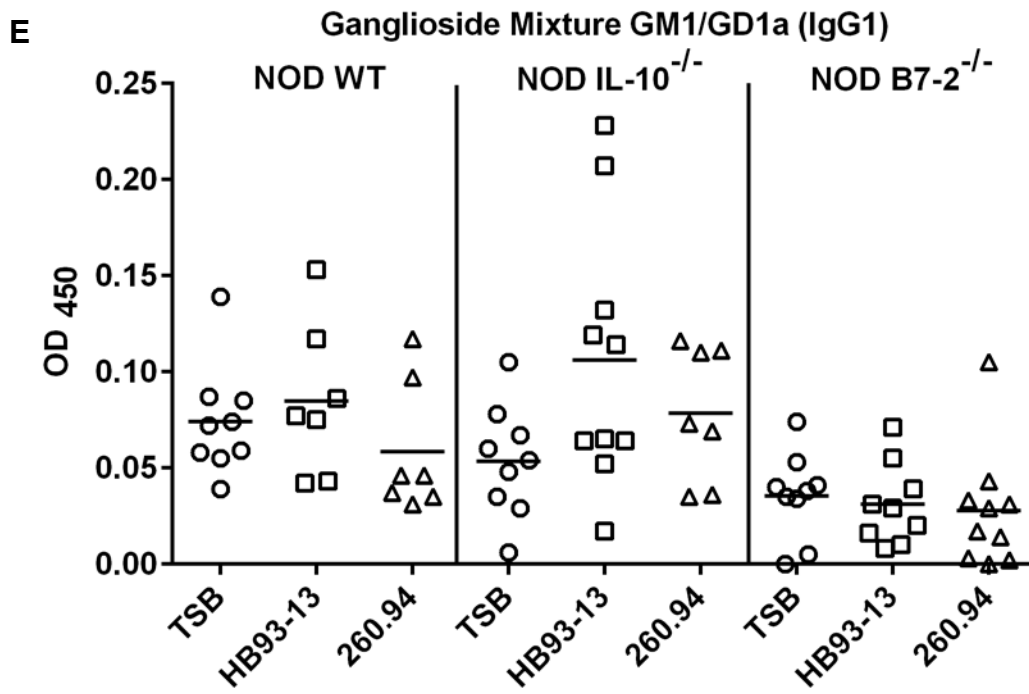


Figure A-2 (cont'd)



**Figure A-3: Phenotypic data for Experiment 1.** Panel A shows the number of quadrants crossed during the open field test for NOD IL-10<sup>-/-</sup> mice (A-1) and NOD B7-2<sup>-/-</sup> mice (A-2). Panels B-D show stride length and hind base width measurements. NOD WT are in panels B-1 (stride length) and B-2 (hind base width), NOD IL-10<sup>-/-</sup> mice are in panels C-1 (stride length) and C-2 (hind base width), and panel D are the NOD B7-2<sup>-/-</sup> mice (panel D-1, stride length; panel D-2, hind base width). Unless stated otherwise, significance levels in all graphs are by \* (p≤0.05), \*\* (p≤0.01), \*\*\* (p≤0.001) and \*\*\*\* (p≤0.0001).

Figure A-3 (cont'd)

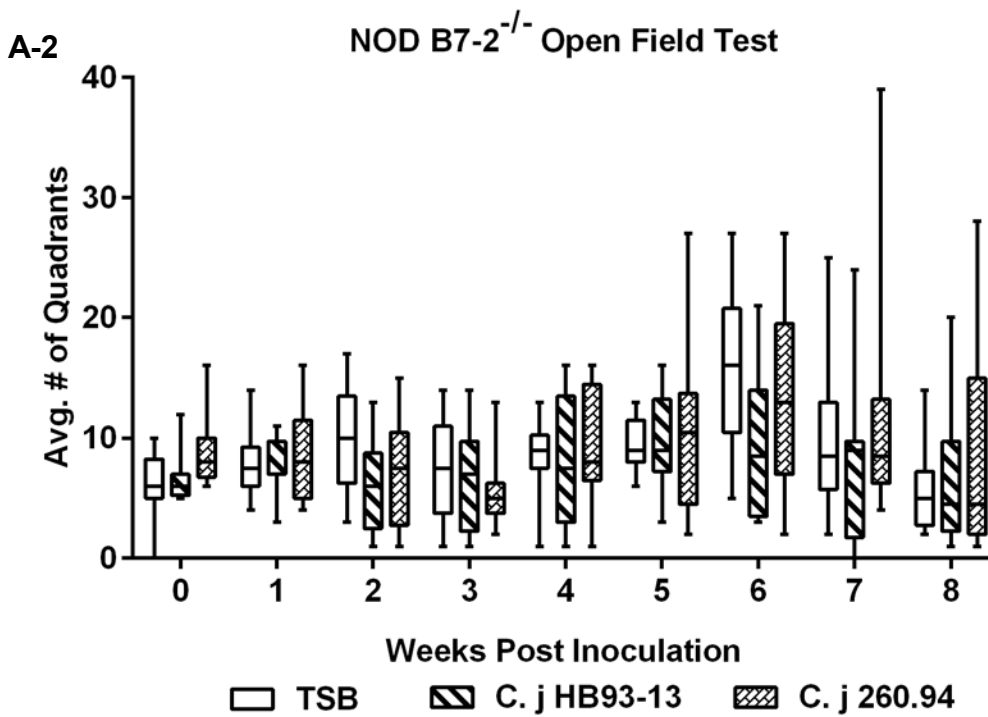
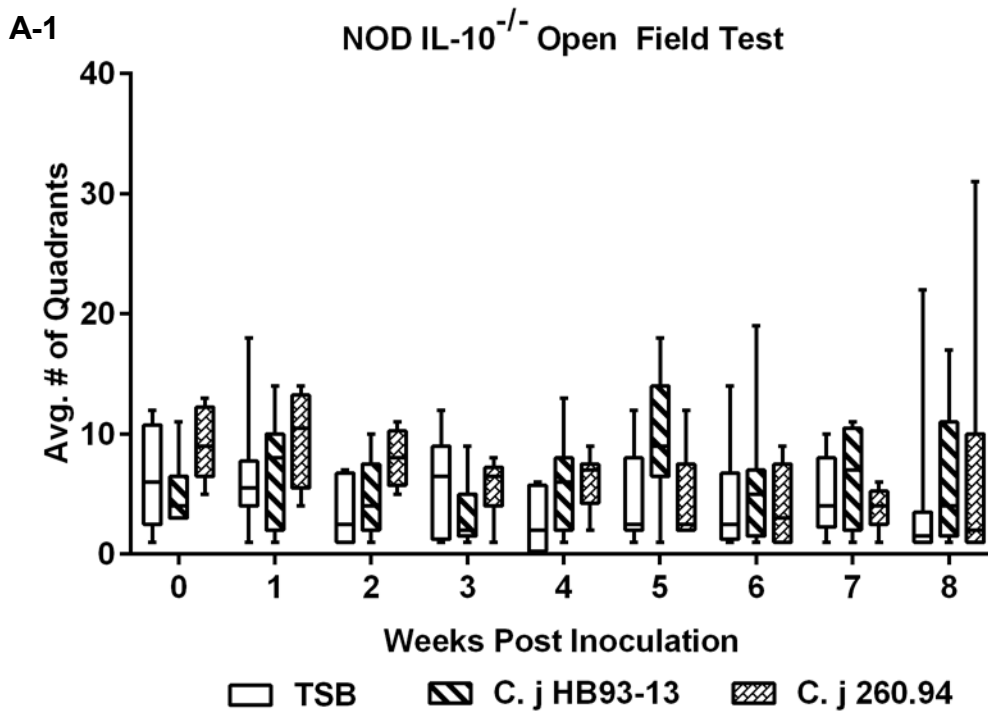


Figure A-3 (cont'd)

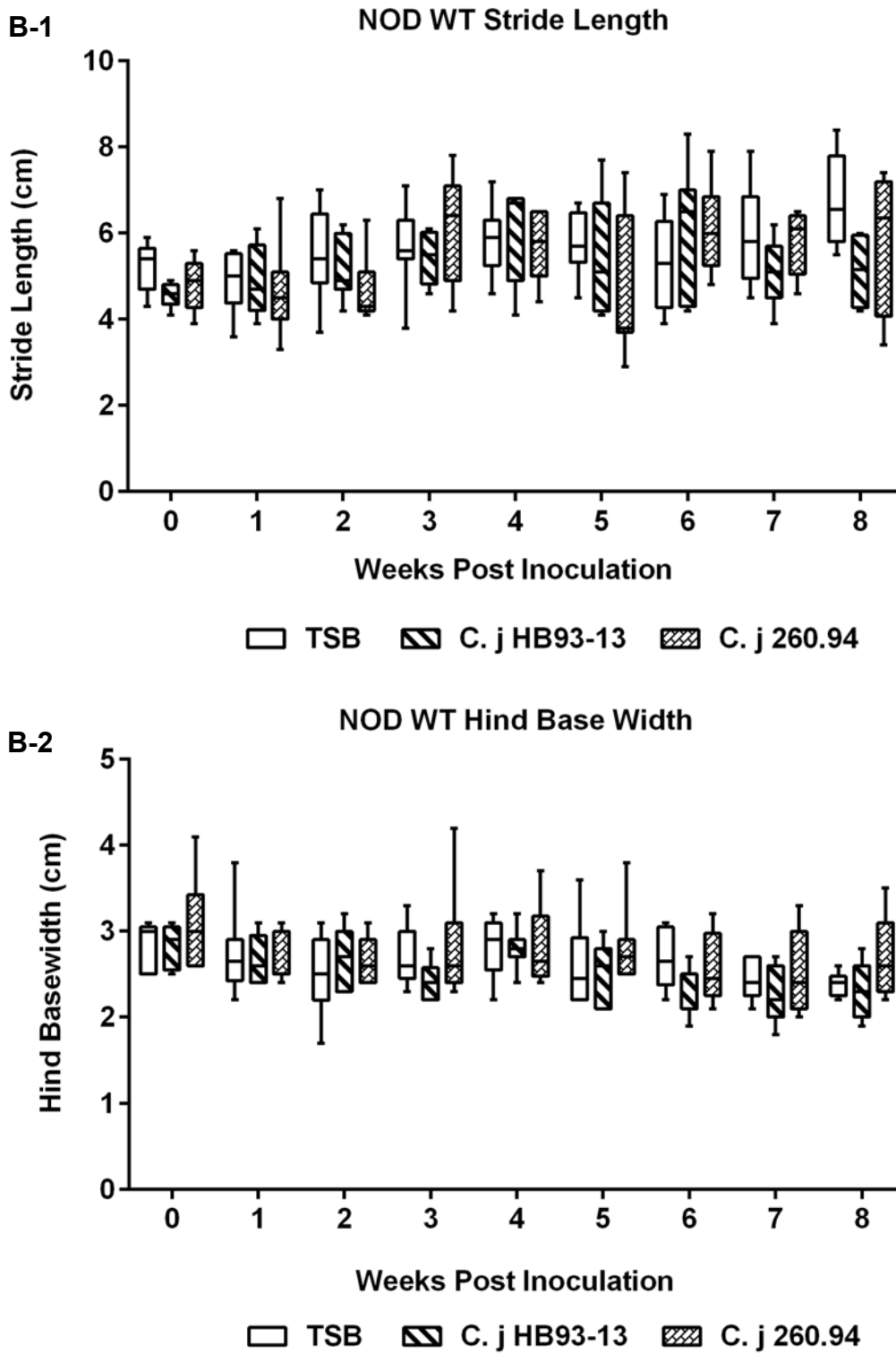


Figure A-3 (cont'd)

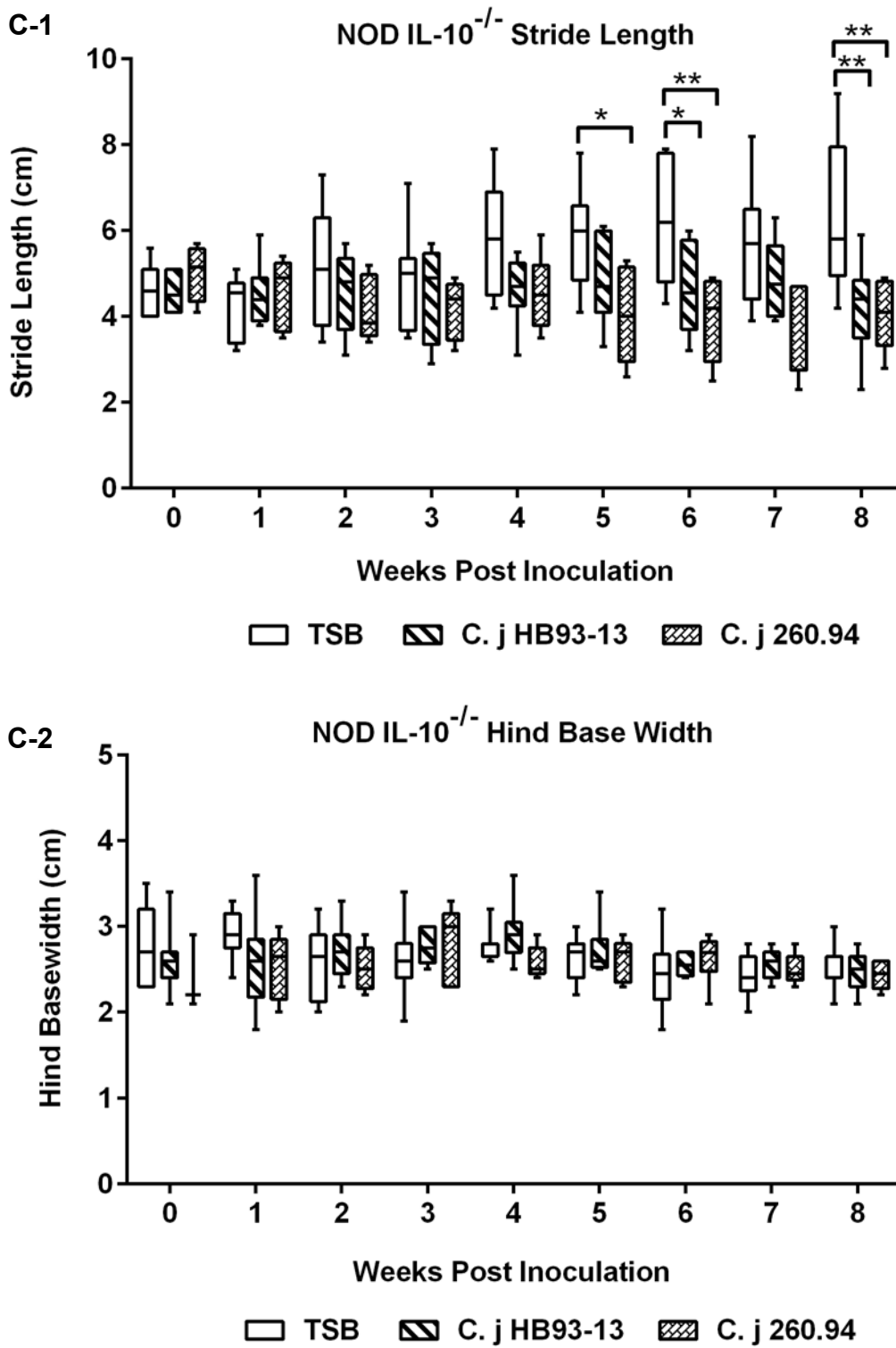
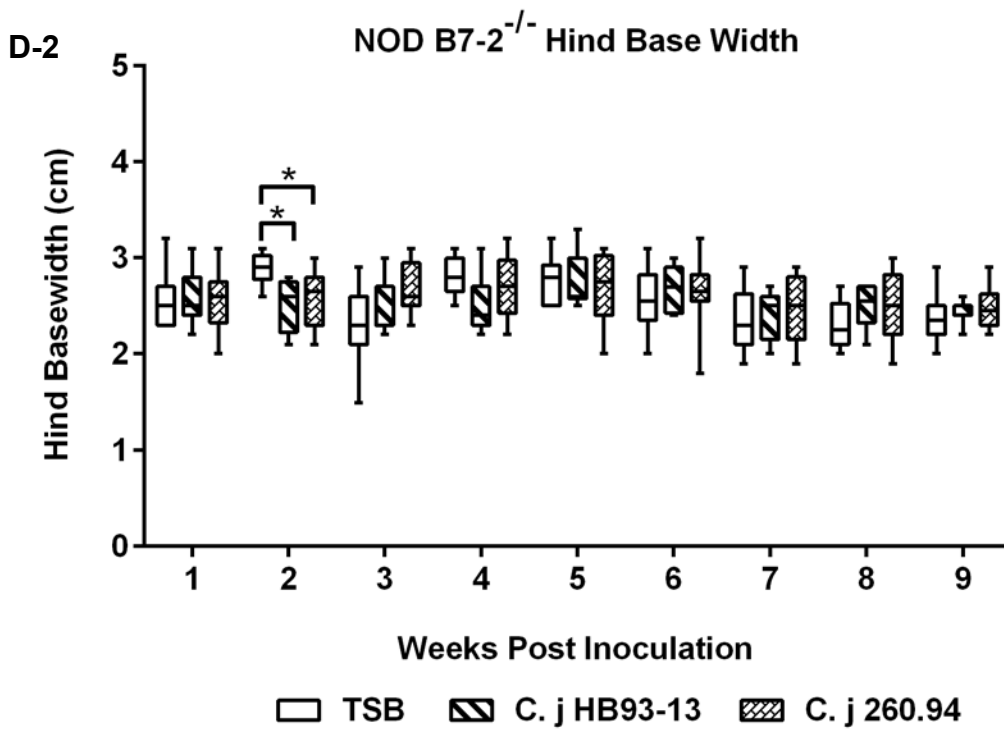
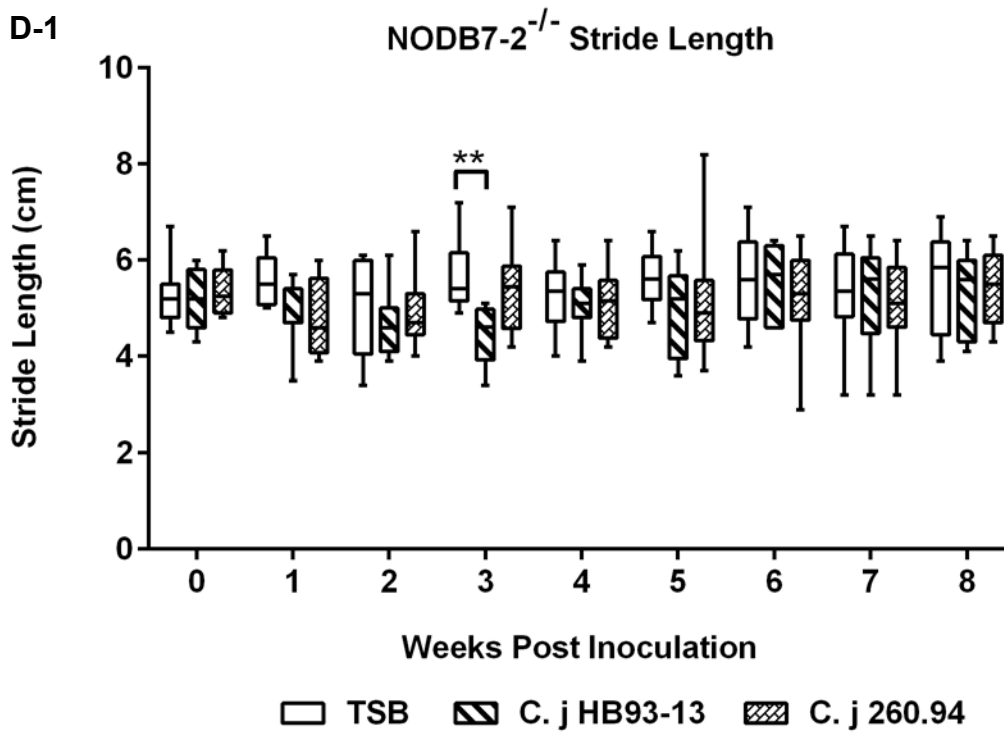


Figure A-3 (cont'd)



## **APPENDIX B**

### Chapter 2 Experiment 2

**Figure B-1: Examination of enteric disease caused by *C. jejuni* infection in Experiment 2.** Histopathological scores of the ileocecolic junction taken from mice at necropsy (80 days). No significant differences were found between uninfected mice and infected mice in either genotype (Mann-Whitney *U*).

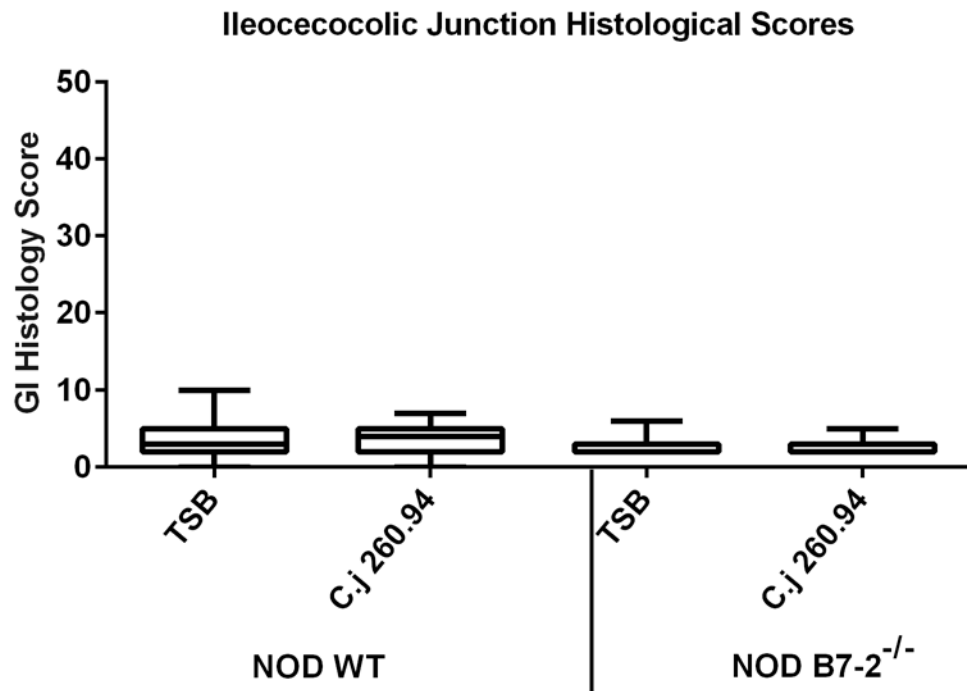


**Figure B-2: ELISA assay data for days 0 and 14 P.I.** Panel A shows data for plasma levels of IgM antibody reactive to ganglioside GM1 at day 0 (A-1) and day 14 P.I. (A-2). Panel B indicates the IgG1 antibody plasma levels reactive to ganglioside GD1a at day 0 (B-1) and day 14 P.I. (B-2). Levels of IgG2b reactive with *C. jejuni* crude antigen are shown in panel C. Panel D shows levels of antibody isotypes IgM, IgG1, IgG2a, and IgG3 to ganglioside GM1 (D-1, D-2, D-3, and D-4 respectively). Panel E shows the plasma levels of antibody isotypes IgG1 and IgG2a reactive with ganglioside GD1a (E-1 and E-2). Panel F shows the plasma levels of IgG1 antibody to ganglioside mixture GM1/GD1a. Unless stated otherwise, significance levels in all graphs are by \* ( $p \leq 0.05$ ), \*\* ( $p \leq 0.01$ ), \*\*\* ( $p \leq 0.001$ ) and \*\*\*\* ( $p \leq 0.0001$ ).

Figure B-2 (cont'd)

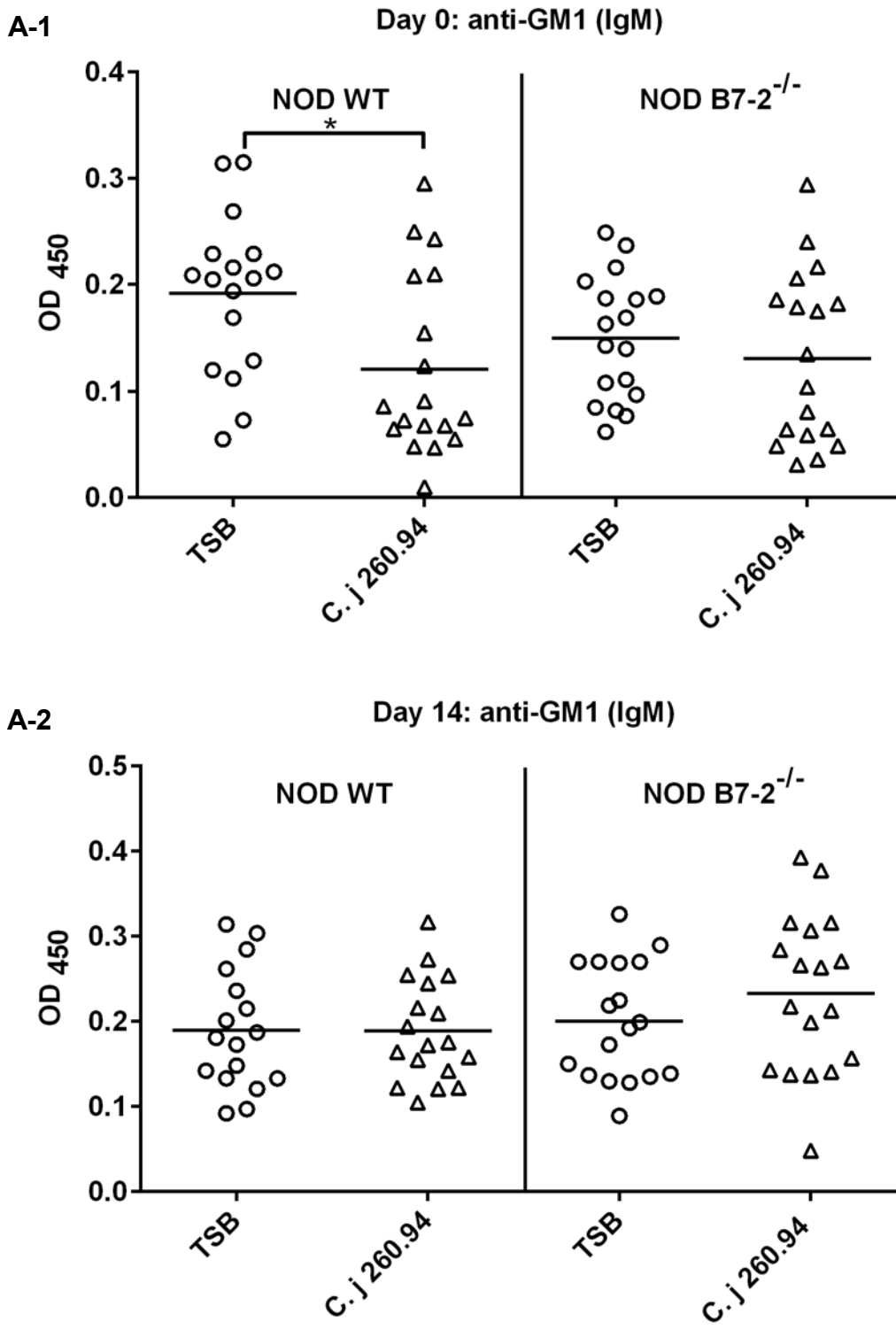


Figure B-2 (cont'd)

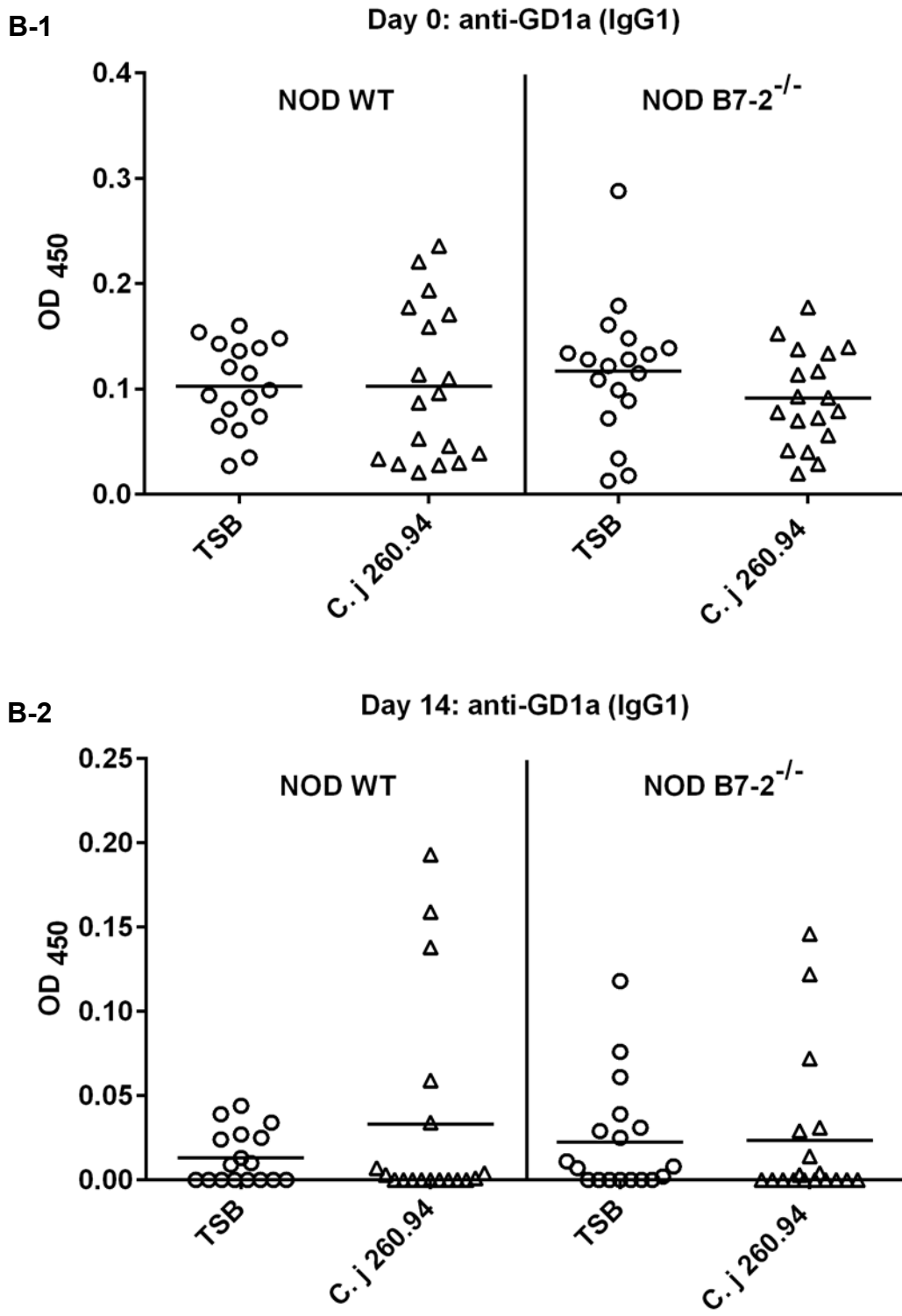


Figure B-2 (cont'd)

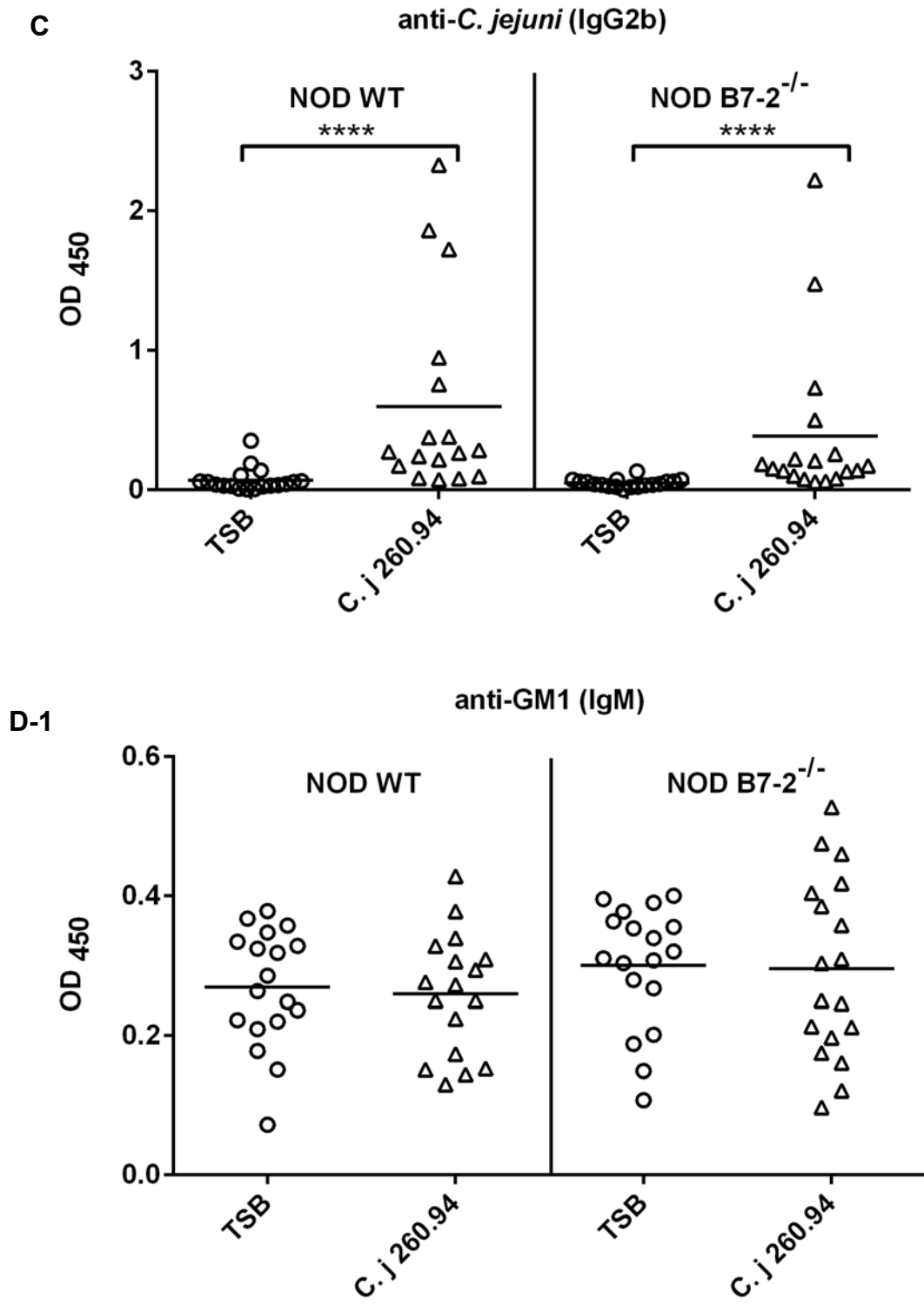
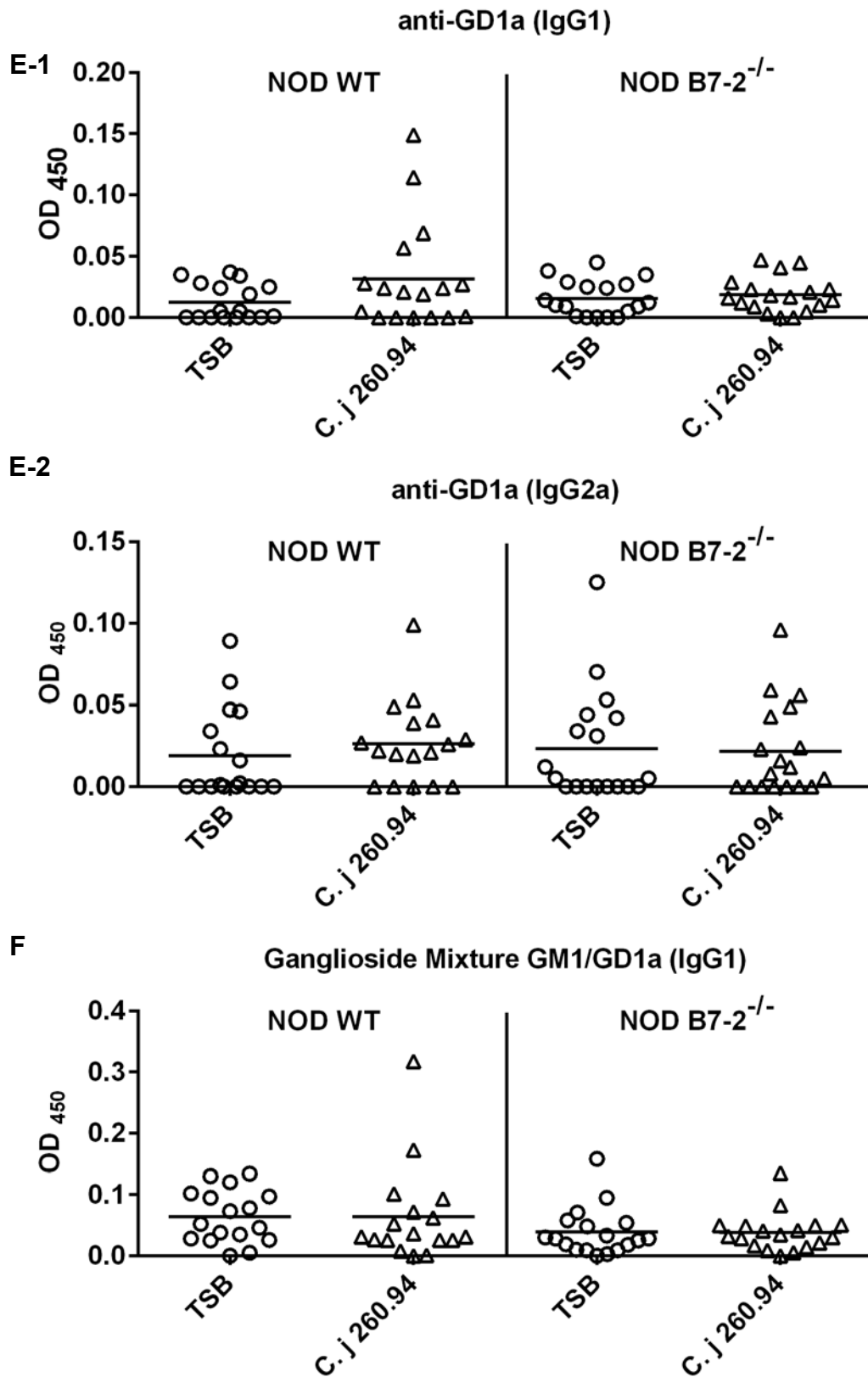




Figure B-2 (cont'd)



**Figure B-3: Experiment 2 Phenotype Data.** Panel A shows the length of time mice spent on the hang test; NOD WT (A-1) and NOD B7-2<sup>-/-</sup> (A-2). No significant differences were found between treatment groups in either mouse genotype. Panels B and C show footprint measurements taken for stride length and hind base width; panels B-1 and B-2 show stride length and hind base width measurements, respectively, for NOD WT mice. Panels C-1 and C-2 show stride length and hind base width measurements, respectively, for NOD B7-2<sup>-/-</sup> mice.

Figure B-3 (cont'd)

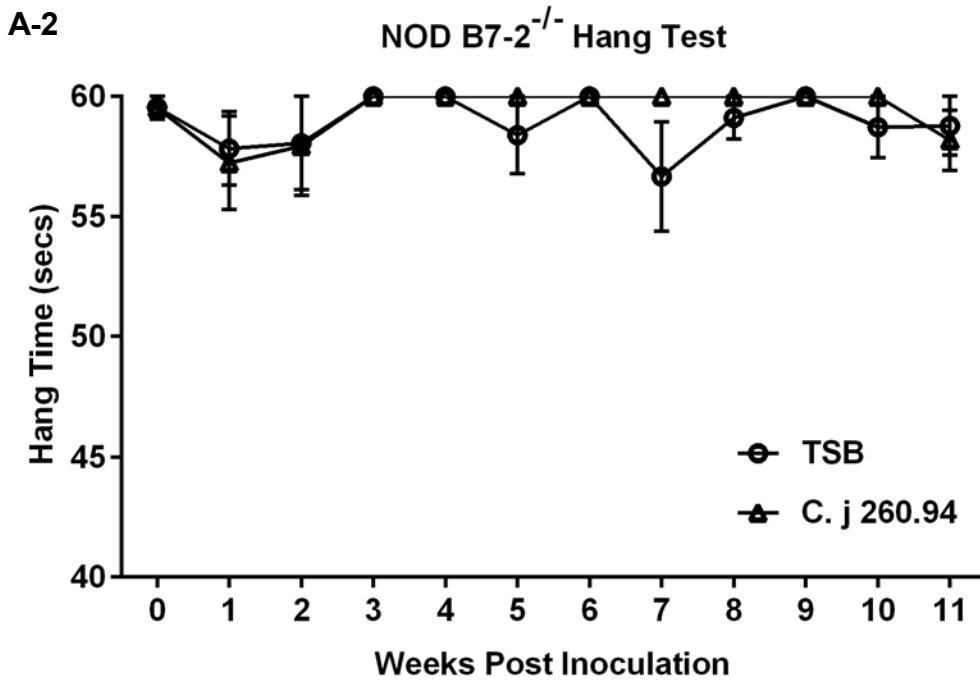
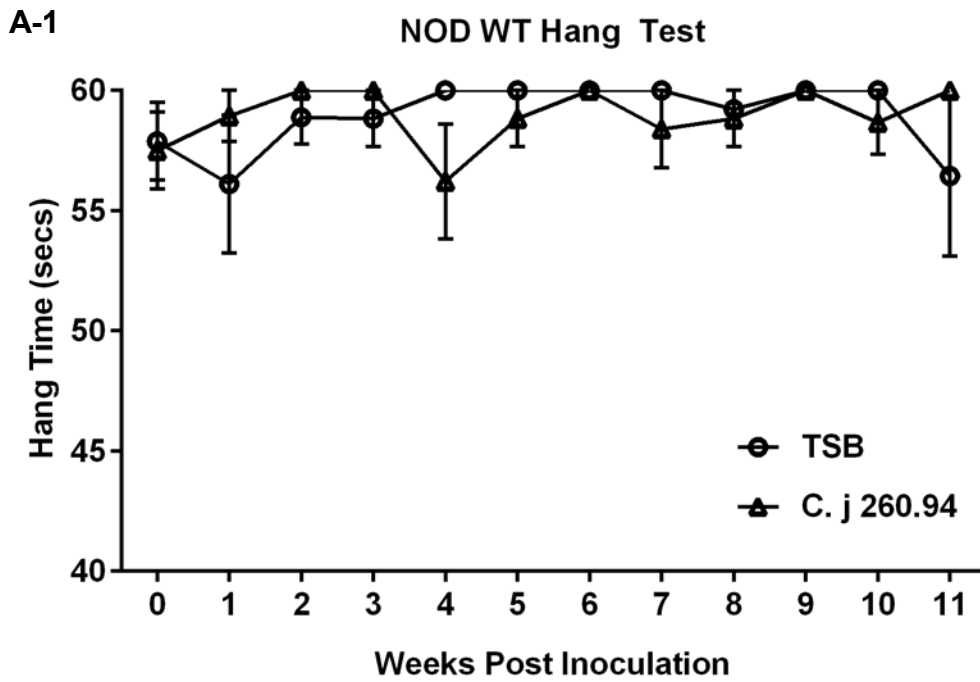


Figure B-3 (cont'd)

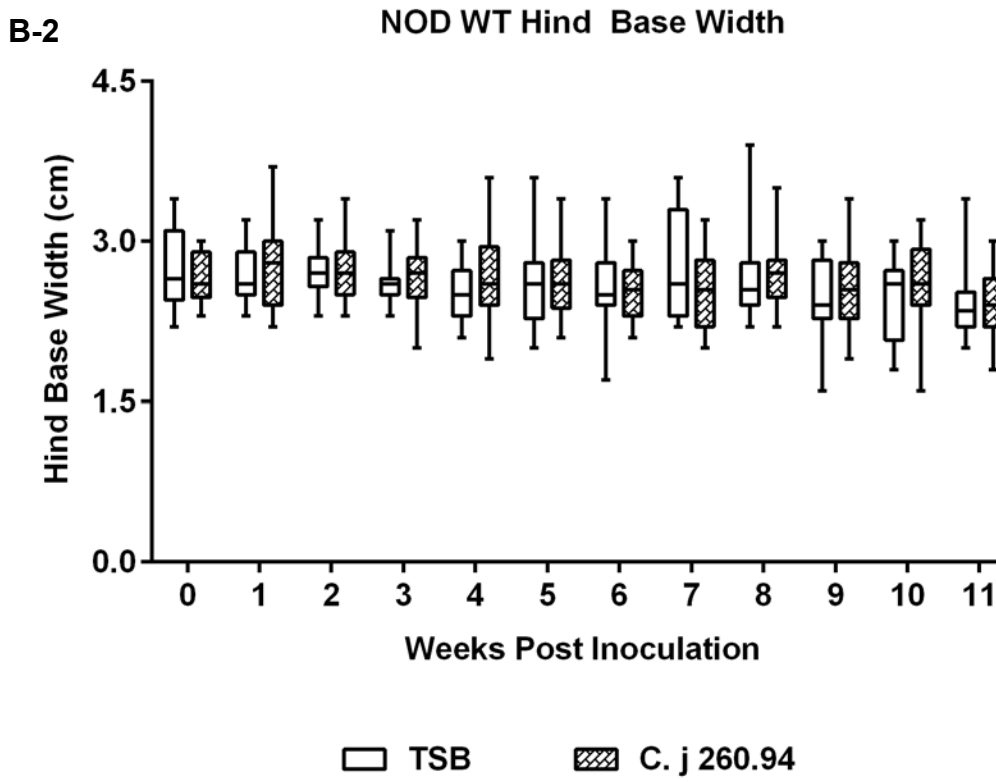
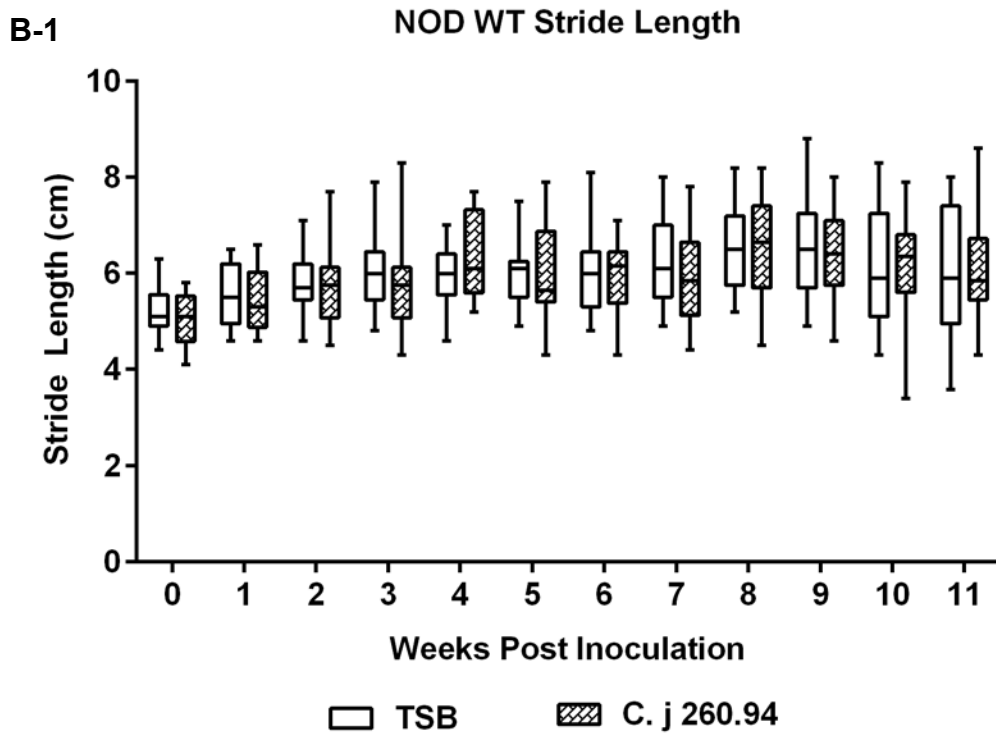
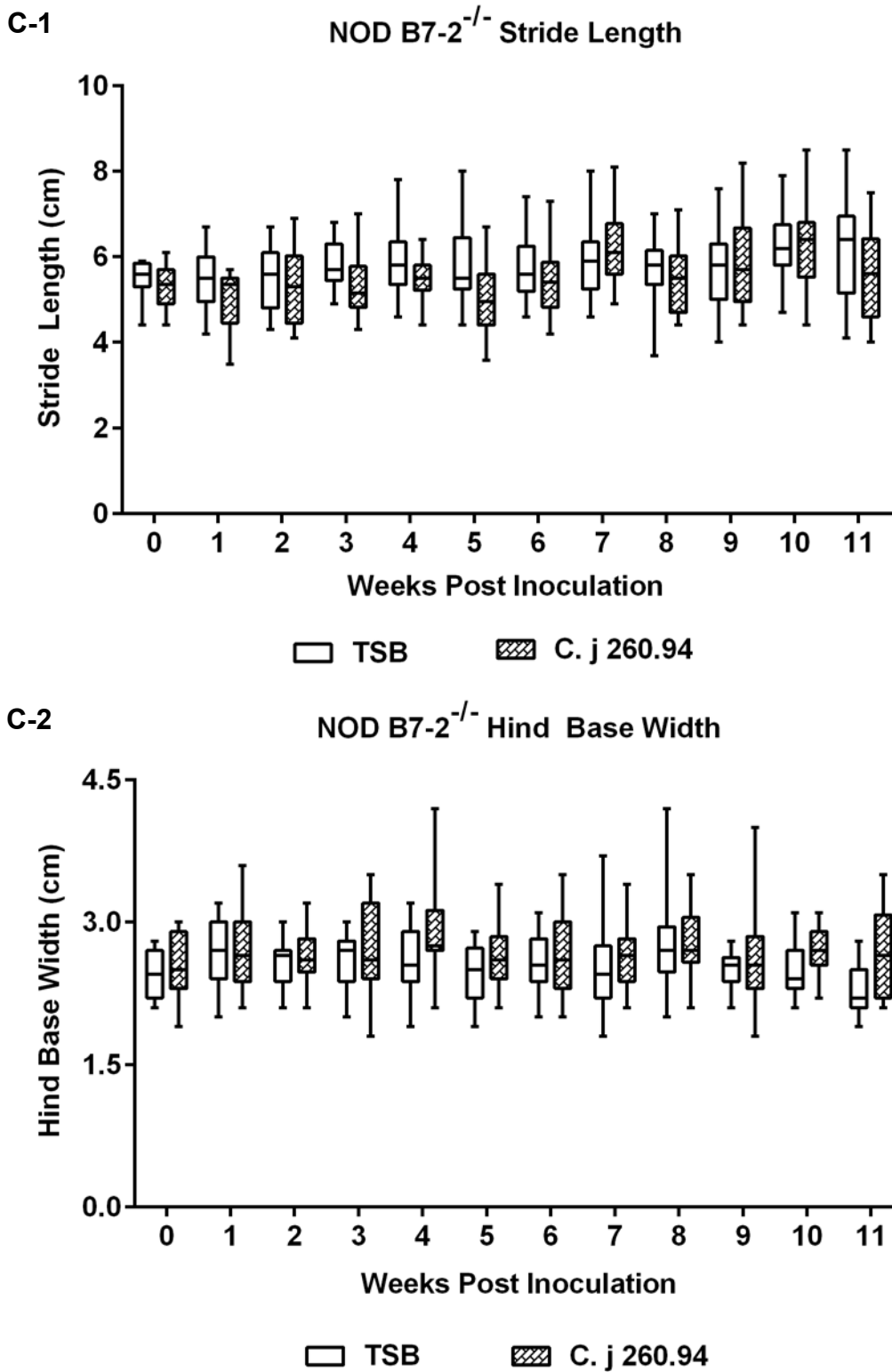
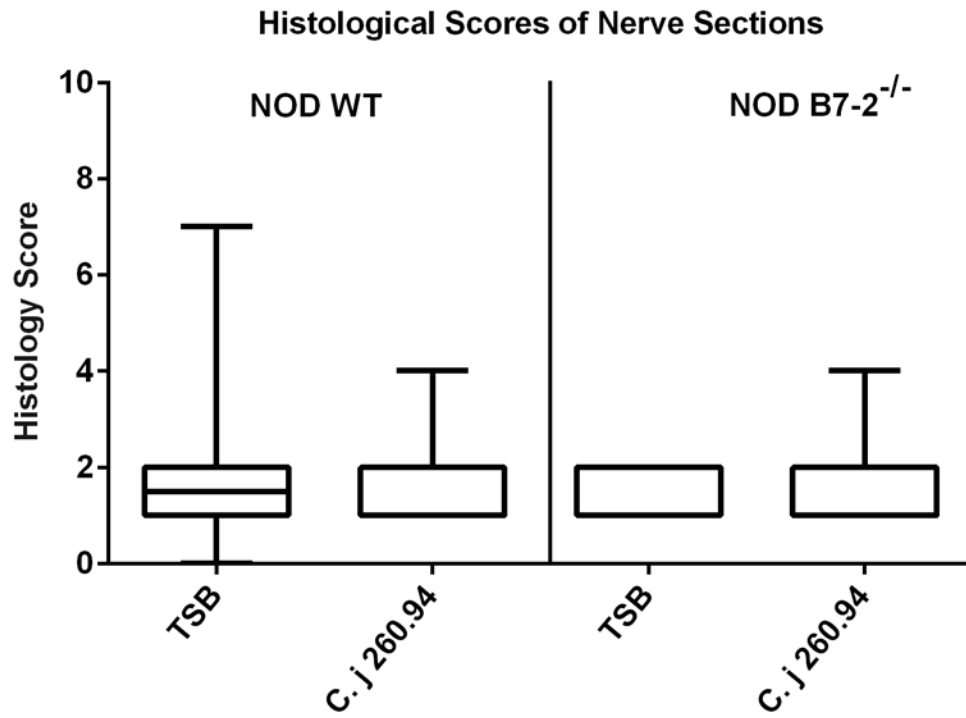


Figure B-3 (cont'd)



**Figure B-4: Presence of Nerve Lesions in Experiment 2.** Histological scores of sciatic nerve sections examined with H & E staining. No significant differences were observed between treatment groups in either of the genotypes.



## **APPENDIX C**

### Chapter 2 Experiment 3

**Figure C-1: Evidence of enteric disease in Experiment 3.** Panel A shows the colonization of *C. jejuni* 260.94 in the cecum at end point. Note that one sham-inoculated mouse was PCR positive for *C. jejuni* 260.94, but produced no other evidence of colonization with *C. jejuni* based on ELISA assay data, gross pathological features, and presence of clinical neurological or enteric signs. Panel B shows the histological scores for the ileoceccocolic junction at endpoint. No significant differences were found.

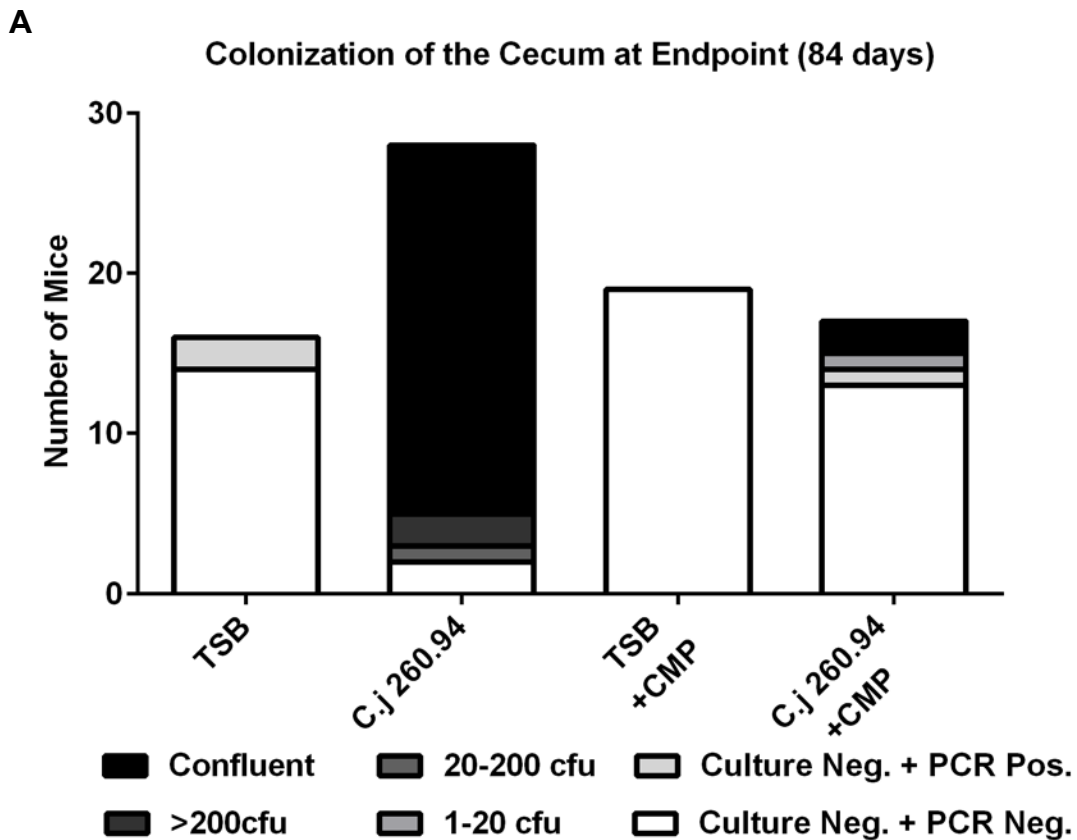
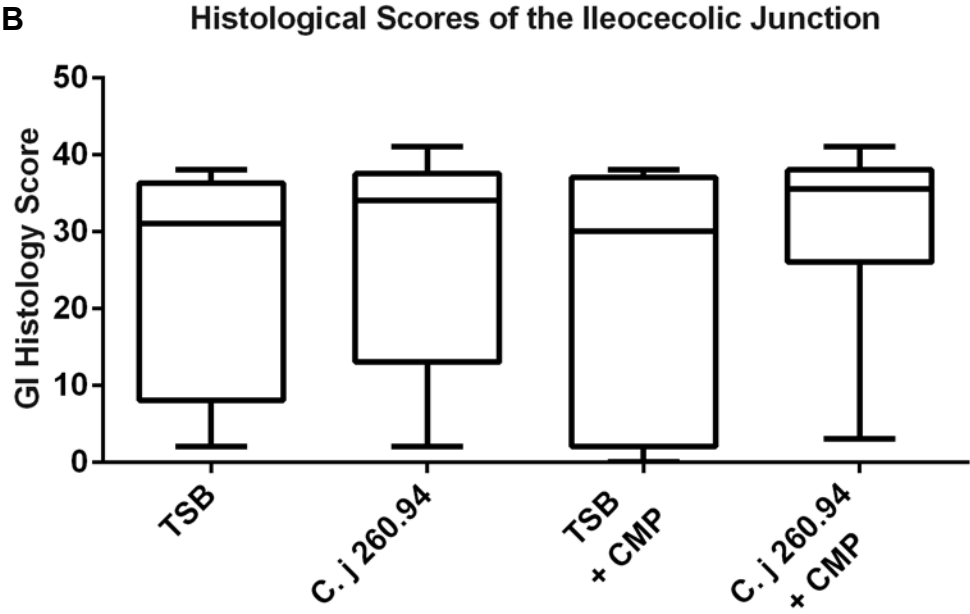


Figure C-1 (cont'd)



**Figure C-2: ELISA assay data for Experiment 3.** Panel A displays the plasma levels of IgG2 antibody reactive with *C. jejuni*. Panels B1–B4 show the antibody levels of IgM, IgG1, IgG2a, and IgG3, respectively, to gangliosides GM1. Panels C-1–C-3 show the plasma levels of reactive antibody IgG1, IgG2a, and IgG3, respectively, to ganglioside GD1a. Panel D shows the IgG2a antibody levels reactive to ganglioside GQ1b. Unless stated otherwise, significance levels in all graphs are by \* ( $p \leq 0.05$ ), \*\* ( $p \leq 0.01$ ), \*\*\* ( $p \leq 0.001$ ) and \*\*\*\* ( $p \leq 0.0001$ ).

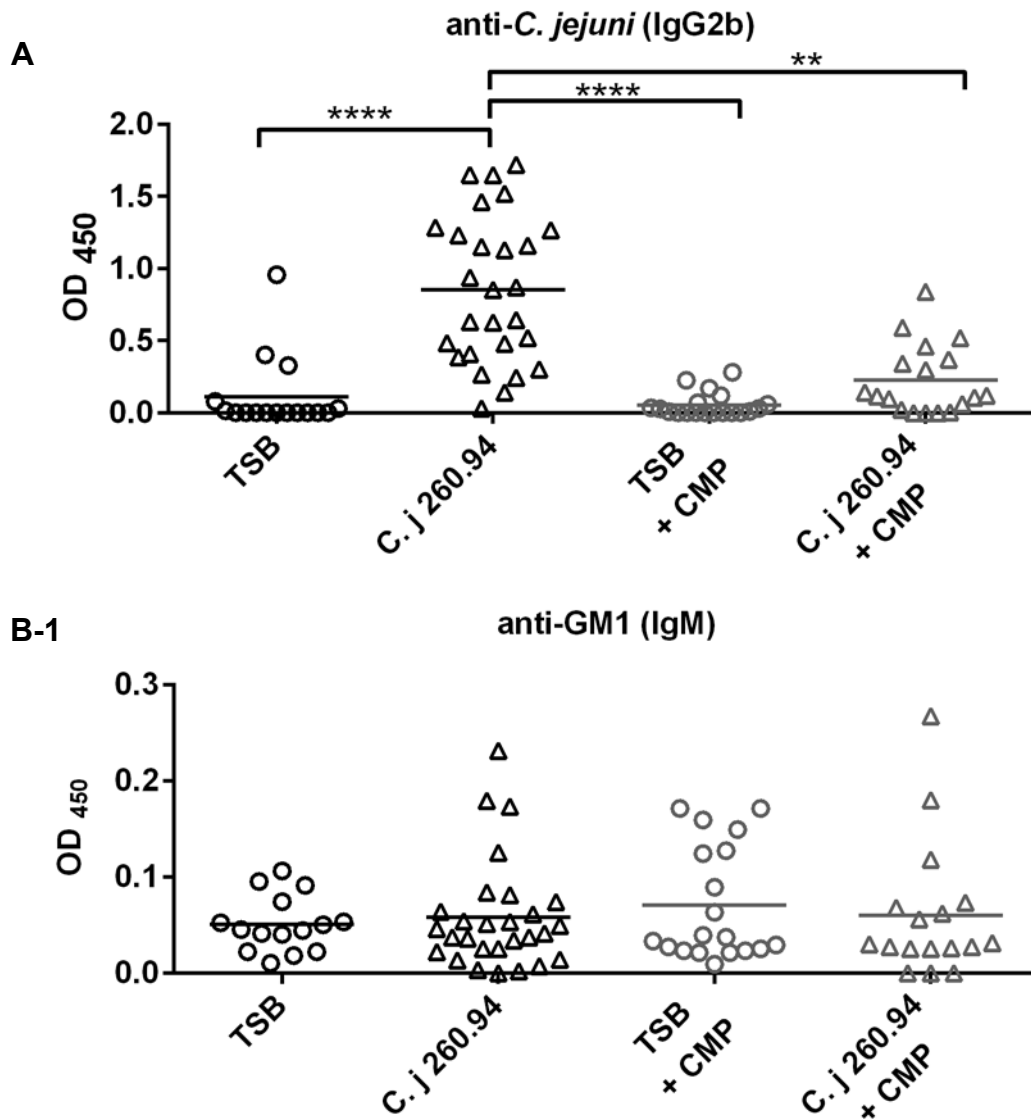


Figure C-2 (cont'd)

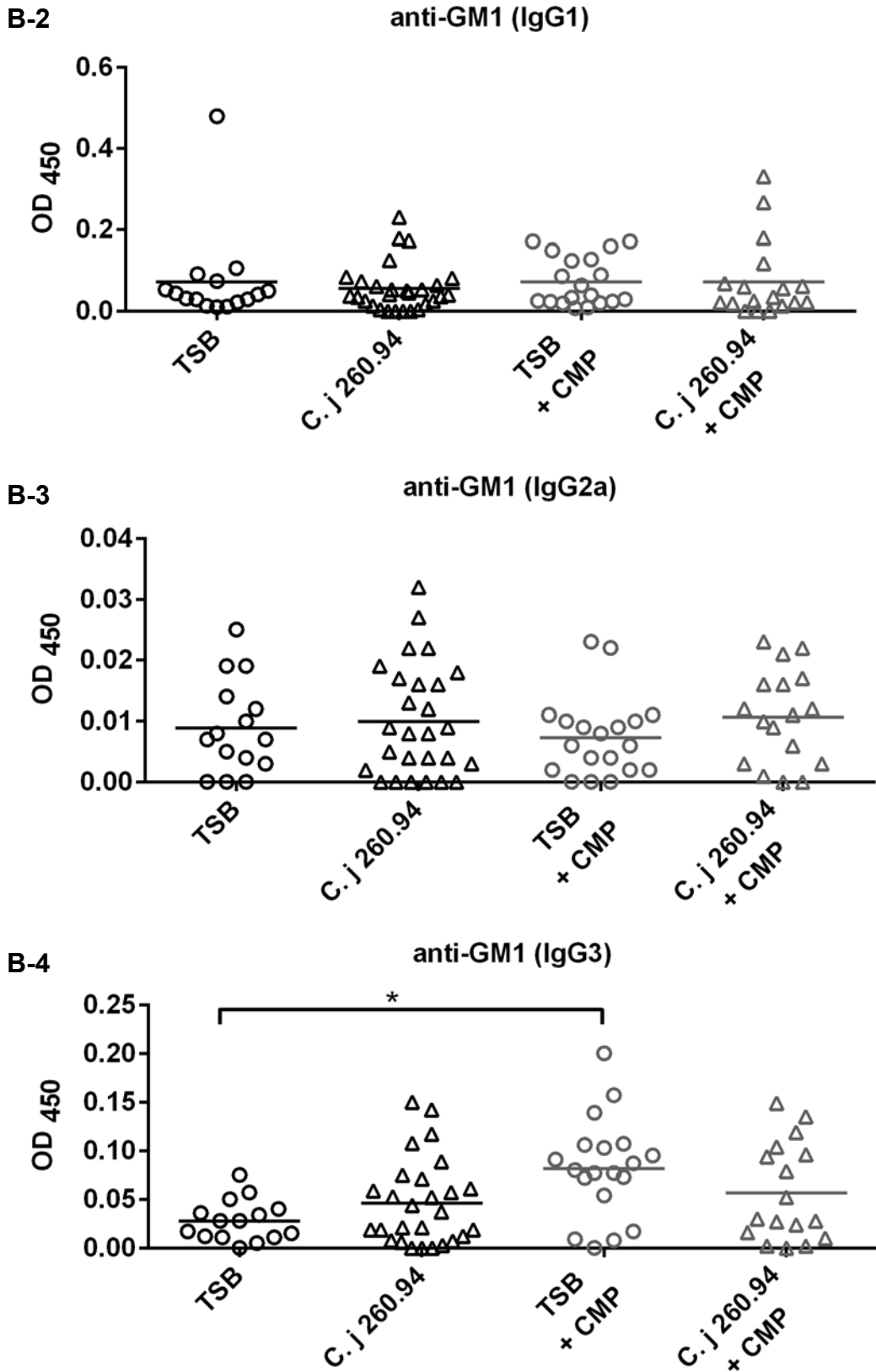


Figure C-2 (cont'd)

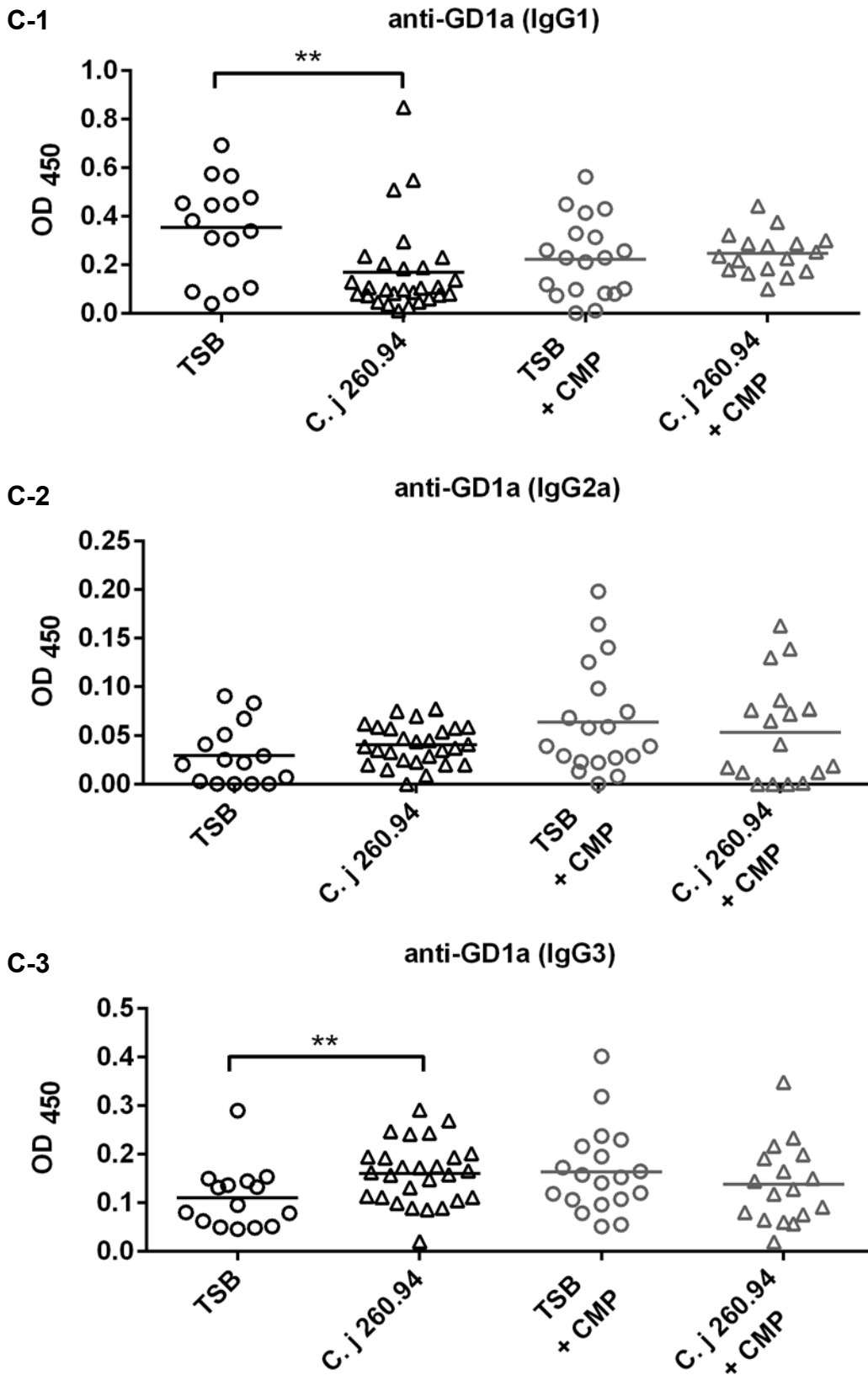
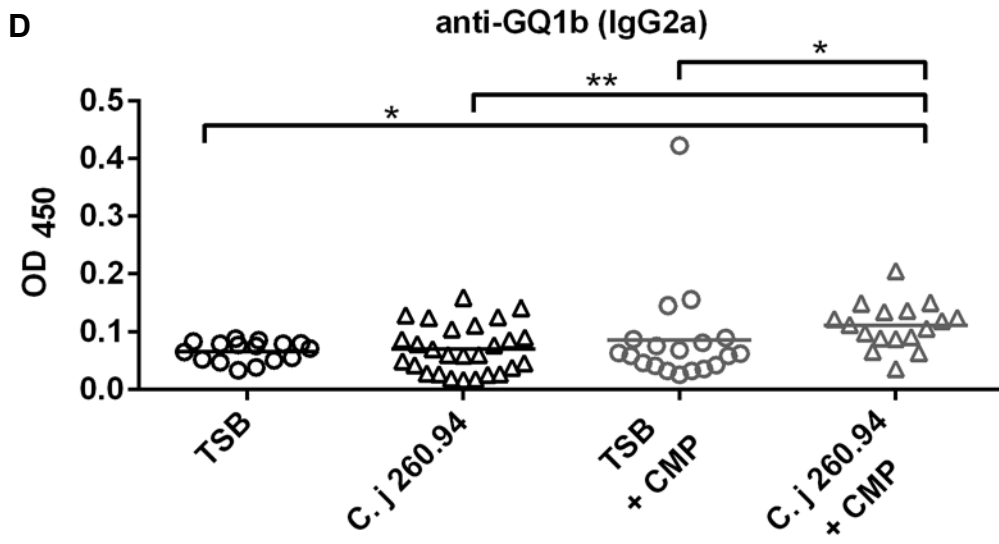


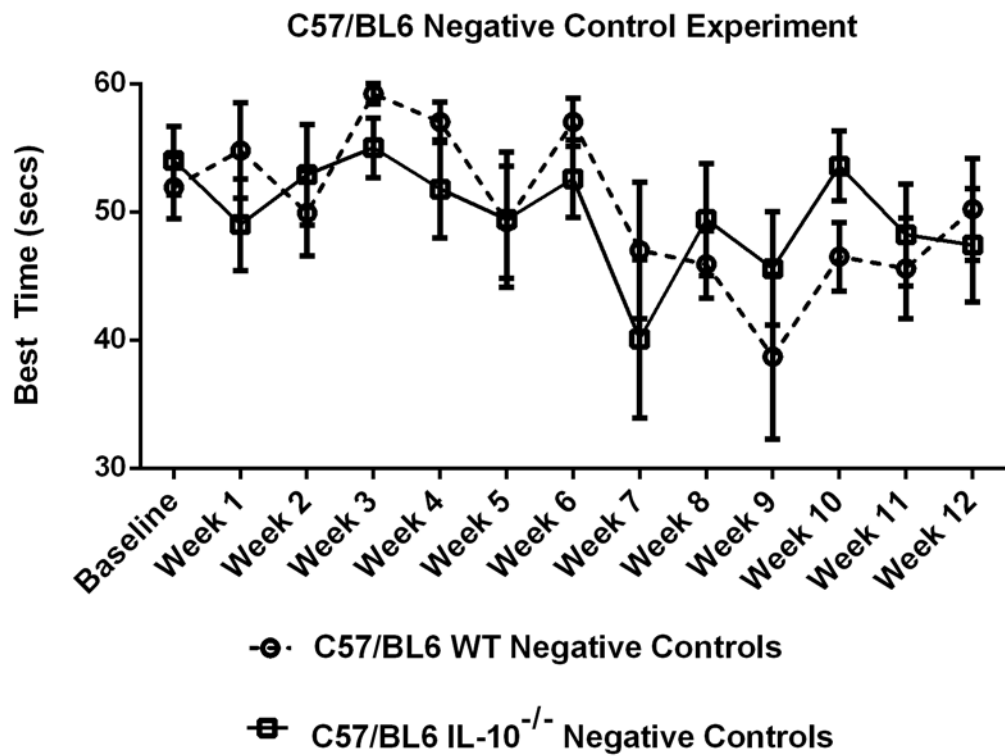
Figure C-2 (cont'd).



## **APPENDIX D**

### Chapter 2 Rotarod Controls

**Figure D-1: Rotarod Control Experiment with C57/BL6 mice.** This graph shows rotarod data for uninfected C57/BL6 WT mice and C57/BL6 IL-10<sup>-/-</sup> mice over time to determine whether if these mice experience a drop in time spent on the rotarod. The experiment was maintained for 84 days; these mice did display a decrease in time spent on the rotarod as the experiment progressed.



## REFERENCES

## REFERENCES

1. AVMA Guidelines for the Euthanasia of Animals, 2013 ed. American Veterinary Medical Association, Schaumburg, IL.
2. J. Craig Venter Institute 2012, posting date. Campylobacter Genome Project. <http://gsc.jcvi.org/projects/msc/campylobacter/index.shtml>. [Online.]
3. The Jackson Laboratory, posting date. Jax® Mice Database. <http://jaxmice.jax.org/query/> 6.1. [Online.]
4. **Allos, B. M.** 1997. Association between Campylobacter infection and Guillain-Barre syndrome. *J Infect Dis* **176 Suppl 2**:S125-8.
5. **Allos, B. M.** 2001. Campylobacter jejuni Infections: update on emerging issues and trends. *Clin Infect Dis* **32**:1201-6.
6. **Altekruse, S. F., N. J. Stern, P. I. Fields, and D. L. Swerdlow.** 1999. Campylobacter jejuni--an emerging foodborne pathogen. *Emerg Infect Dis* **5**:28-35.
7. **Ang, C. W., B. C. Jacobs, and J. D. Laman.** 2004. The Guillain-Barre syndrome: a true case of molecular mimicry. *Trends Immunol* **25**:61-6.
8. **Archelos, J. J., T. Fortwangler, and H. P. Hartung.** 1997. Attenuation of experimental autoimmune neuritis in the Lewis rat by treatment with an antibody to L-selectin. *Neurosci Lett* **235**:9-12.
9. **Asbury, A. K., and D. R. Cornblath.** 1990. Assessment of current diagnostic criteria for Guillain-Barre syndrome. *Ann Neurol* **27 Suppl**:S21-4.
10. **Bell, J. A., J. P. Jerome, A. E. Plovanich-Jones, E. J. Smith, J. R. Gettings, H. Y. Kim, J. R. Landgraf, T. Lefebure, J. J. Kopper, V. A. Rathinam, J. L. St Charles, B. A. Buffa, A. P. Brooks, S. A. Poe, K. A. Eaton, M. J. Stanhope, and L. S. Mansfield.** 2013. Outcome of infection of C57BL/6 IL-10(-/-) mice with

*Campylobacter jejuni* strains is correlated with genome content of open reading frames up- and down-regulated in vivo. *Microb Pathog* **54**:1-19.

11. **Bell, J. A., J. L. St Charles, A. J. Murphy, V. A. Rathinam, A. E. Plovanich-Jones, E. L. Stanley, J. E. Wolf, J. R. Gettings, T. S. Whittam, and L. S. Mansfield.** 2009. Multiple factors interact to produce responses resembling spectrum of human disease in *Campylobacter jejuni* infected C57BL/6 IL-10<sup>-/-</sup> mice. *BMC Microbiol* **9**:57.
12. **Blumstein, D. T., and J. C. Daniel.** 2007. *Quantifying Behavior the JWatcher Way*. Sinauer Associates, Inc., Sunderland, MA.
13. **Bour-Jordan, H., H. L. Thompson, and J. A. Bluestone.** 2005. Distinct effector mechanisms in the development of autoimmune neuropathy versus diabetes in nonobese diabetic mice. *J Immunol* **175**:5649-55.
14. **Brooks, S. P., and S. B. Dunnett.** 2009. Tests to assess motor phenotype in mice: a user's guide. *Nat Rev Neurosci* **10**:519-29.
15. **Bullens, R. W., G. M. O'Hanlon, E. Wagner, P. C. Molenaar, K. Furukawa, K. Furukawa, J. J. Plomp, and H. J. Willison.** 2002. Complex gangliosides at the neuromuscular junction are membrane receptors for autoantibodies and botulinum neurotoxin but redundant for normal synaptic function. *J Neurosci* **22**:6876-84.
16. **Bullens, R. W., G. M. O'Hanlon, E. Wagner, P. C. Molenaar, K. Furukawa, K. Furukawa, J. J. Plomp, and H. J. Willison.** 2003. Roles of complex gangliosides at the neuromuscular junction. *Ann N Y Acad Sci* **998**:401-3.
17. **Burns, T. M.** 2008. Guillain-Barre syndrome. *Semin Neurol* **28**:152-67.
18. **Busato, A., D. Hofer, T. Lentze, C. Gaillard, and A. Burnens.** 1999. Prevalence and infection risks of zoonotic enteropathogenic bacteria in Swiss cow-calf farms. *Vet Microbiol* **69**:251-63.
19. **Butzler, J. P.** 2004. *Campylobacter*, from obscurity to celebrity. *Clin Microbiol Infect* **10**:868-76.

20. **Calida, D. M., S. G. Kremlev, T. Fujioka, B. Hilliard, E. Ventura, C. S. Constantinescu, E. Lavi, and A. Rostami.** 2000. Experimental allergic neuritis in the SJL/J mouse: induction of severe and reproducible disease with bovine peripheral nerve myelin and pertussis toxin with or without interleukin-12. *J Neuroimmunol* **107**:1-7.
21. **Caporale, C. M., F. Papola, M. A. Fioroni, A. Aureli, A. Giovannini, F. Notturmo, D. Adorno, V. Caporale, and A. Uncini.** 2006. Susceptibility to Guillain-Barre syndrome is associated to polymorphisms of CD1 genes. *J Neuroimmunol* **177**:112-8.
22. **Carter, R. J., J. Morton, and S. B. Dunnett.** 2001. Motor coordination and balance in rodents. *Curr Protoc Neurosci* **Chapter 8**:Unit 8 12.
23. **Castresana, J.** 2000. Selection of conserved blocks from multiple alignments for their use in phylogenetic analysis. *Mol Biol Evol* **17**:540-52.
24. **Choleris, E., A. W. Thomas, M. Kavaliers, and F. S. Prato.** 2001. A detailed ethological analysis of the mouse open field test: effects of diazepam, chlordiazepoxide and an extremely low frequency pulsed magnetic field. *Neurosci Biobehav Rev* **25**:235-60.
25. **Church Potter, R., and J. B. Kaneene.** 2003. A descriptive study of Guillain-Barre syndrome in high and low *Campylobacter jejuni* incidence regions of Michigan: 1992-1999. *Neuroepidemiology* **22**:245-8.
26. **Cingoz, F., M. Tavlasoglu, M. Kurkluoglu, and M. A. Sahin.** 2012. Guillain-Barre syndrome after coronary artery bypass surgery. *Interact Cardiovasc Thorac Surg* **15**:918-9.
27. **Clark, C. G., A. Beeston, L. Bryden, G. Wang, C. Barton, W. Cuff, M. W. Gilmour, and L. K. Ng.** 2007. Phylogenetic relationships of *Campylobacter jejuni* based on *porA* sequences. *Can J Microbiol* **53**:27-38.
28. **Clark, C. G., E. Taboada, C. C. Grant, C. Blakeston, F. Pollari, B. Marshall, K. Rahn, J. Mackinnon, D. Daignault, D. Pillai, and L. K. Ng.** 2012. Comparison of molecular typing methods useful for detecting clusters of *Campylobacter jejuni* and *C. coli* isolates through routine surveillance. *J Clin Microbiol* **50**:798-809.

29. **Crawley, J. N.** 2007. What's wrong with my mouse? Behavioral phenotyping of transgenic and knockout mice, 2 ed. John Wiley & Sons.
30. **Crawley, J. N.** 1999. Behavioral phenotyping of transgenic and knockout mice: experimental design and evaluation of general health, sensory functions, motor abilities, and specific behavioral tests. *Brain Res* **835**:18-26.
31. **Cullen, T. W., J. P. O'Brien, D. R. Hendrixson, D. K. Giles, R. I. Hobb, S. A. Thompson, J. S. Brodbelt, and M. S. Trent.** 2013. EptC of *Campylobacter jejuni* mediates phenotypes involved in host interactions and virulence. *Infect Immun* **81**:430-40.
32. **de Haan, C. P., R. I. Kivisto, M. Hakkinen, J. Corander, and M. L. Hanninen.** 2010. Multilocus sequence types of Finnish bovine *Campylobacter jejuni* isolates and their attribution to human infections. *BMC Microbiol* **10**:200.
33. **Dereeper, A., V. Guignon, G. Blanc, S. Audic, S. Buffet, F. Chevenet, J. F. Dufayard, S. Guindon, V. Lefort, M. Lescot, J. M. Claverie, and O. Gascuel.** 2008. Phylogeny.fr: robust phylogenetic analysis for the non-specialist. *Nucleic Acids Res* **36**:W465-9.
34. **Dingle, K. E., F. M. Colles, D. R. Wareing, R. Ure, A. J. Fox, F. E. Bolton, H. J. Bootsma, R. J. Willems, R. Urwin, and M. C. Maiden.** 2001. Multilocus sequence typing system for *Campylobacter jejuni*. *J Clin Microbiol* **39**:14-23.
35. **Dingle, K. E., N. Van Den Braak, F. M. Colles, L. J. Price, D. L. Woodward, F. G. Rodgers, H. P. Endtz, A. Van Belkum, and M. C. Maiden.** 2001. Sequence typing confirms that *Campylobacter jejuni* strains associated with Guillain-Barre and Miller-Fisher syndromes are of diverse genetic lineage, serotype, and flagella type. *J Clin Microbiol* **39**:3346-9.
36. **Duim, B., P. C. Godschalk, N. van den Braak, K. E. Dingle, J. R. Dijkstra, E. Leyde, J. van der Plas, F. M. Colles, H. P. Endtz, J. A. Wagenaar, M. C. Maiden, and A. van Belkum.** 2003. Molecular evidence for dissemination of unique *Campylobacter jejuni* clones in Curacao, Netherlands Antilles. *J Clin Microbiol* **41**:5593-7.
37. **Duncan, R., and P. G. Kennedy.** 1987. Guillain-Barre syndrome following acute head trauma. *Postgrad Med J* **63**:479-80.

38. **Dzieciatkowska, M., X. Liu, A. P. Heikema, R. S. Houlston, A. van Belkum, E. K. Schweda, M. Gilbert, J. C. Richards, and J. Li.** 2008. Rapid method for sensitive screening of oligosaccharide epitopes in the lipooligosaccharide from *Campylobacter jejuni* strains isolated from Guillain-Barre syndrome and Miller Fisher syndrome patients. *J Clin Microbiol* **46**:3429-36.
39. **Edgar, R. C.** 2004. MUSCLE: multiple sequence alignment with high accuracy and high throughput. *Nucleic Acids Res* **32**:1792-7.
40. **Fearnhead, P., N. G. Smith, M. Barrigas, A. Fox, and N. French.** 2005. Analysis of recombination in *Campylobacter jejuni* from MLST population data. *J Mol Evol* **61**:333-40.
41. **Fitzgerald, C., K. Stanley, S. Andrew, and K. Jones.** 2001. Use of pulsed-field gel electrophoresis and flagellin gene typing in identifying clonal groups of *Campylobacter jejuni* and *Campylobacter coli* in farm and clinical environments. *Appl Environ Microbiol* **67**:1429-36.
42. **Fox, W. M.** 1965. Reflex-ontogeny and behavioural development of the mouse. *Anim Behav* **13**:234-41.
43. **French, N., M. Barrigas, P. Brown, P. Ribiero, N. Williams, H. Leatherbarrow, R. Birtles, E. Bolton, P. Fearnhead, and A. Fox.** 2005. Spatial epidemiology and natural population structure of *Campylobacter jejuni* colonizing a farmland ecosystem. *Environ Microbiol* **7**:1116-26.
44. **Friedman, C. R., R. M. Hoekstra, M. Samuel, R. Marcus, J. Bender, B. Shiferaw, S. Reddy, S. D. Ahuja, D. L. Helfrick, F. Hardnett, M. Carter, B. Anderson, and R. V. Tauxe.** 2004. Risk factors for sporadic *Campylobacter* infection in the United States: A case-control study in FoodNet sites. *Clin Infect Dis* **38 Suppl 3**:S285-96.
45. **Fry, B. N., V. Korolik, J. A. ten Brinke, M. T. Pennings, R. Zalm, B. J. Teunis, P. J. Coloe, and B. A. van der Zeijst.** 1998. The lipopolysaccharide biosynthesis locus of *Campylobacter jejuni* 81116. *Microbiology* **144 (Pt 8)**:2049-61.
46. **Gilbert, M., P. C. Godschalk, M. F. Karwaski, C. W. Ang, A. van Belkum, J. Li, W. W. Wakarchuk, and H. P. Endtz.** 2004. Evidence for acquisition of the lipooligosaccharide biosynthesis locus in *Campylobacter jejuni* GB11, a strain

isolated from a patient with Guillain-Barre syndrome, by horizontal exchange. *Infect Immun* **72**:1162-5.

47. **Gilbert, M., M. F. Karwaski, S. Bernatchez, N. M. Young, E. Taboada, J. Michniewicz, A. M. Cunningham, and W. W. Wakarchuk.** 2002. The genetic bases for the variation in the lipo-oligosaccharide of the mucosal pathogen, *Campylobacter jejuni*. Biosynthesis of sialylated ganglioside mimics in the core oligosaccharide. *J Biol Chem* **277**:327-37.
48. **Gilbert, M., C. T. Parker, and A. P. Moran.** 2008. *Campylobacter jejuni* lipooligosaccharides: structures and biosynthesis, *Campylobacter*, 3 ed. ASM Press, Washington D.C.
49. **Godschalk, P. C., A. P. Heikema, M. Gilbert, T. Komagamine, C. W. Ang, J. Glerum, D. Brochu, J. Li, N. Yuki, B. C. Jacobs, A. van Belkum, and H. P. Endtz.** 2004. The crucial role of *Campylobacter jejuni* genes in anti-ganglioside antibody induction in Guillain-Barre syndrome. *J Clin Invest* **114**:1659-65.
50. **Godschalk, P. C., M. L. Kuijf, J. Li, F. St Michael, C. W. Ang, B. C. Jacobs, M. F. Karwaski, D. Brochu, A. Moterassed, H. P. Endtz, A. van Belkum, and M. Gilbert.** 2007. Structural characterization of *Campylobacter jejuni* lipooligosaccharide outer cores associated with Guillain-Barre and Miller Fisher syndromes. *Infect Immun* **75**:1245-54.
51. **Godschalk, P. C., A. van Belkum, N. van den Braak, D. van Netten, C. W. Ang, B. C. Jacobs, M. Gilbert, and H. P. Endtz.** 2007. PCR-restriction fragment length polymorphism analysis of *Campylobacter jejuni* genes involved in lipooligosaccharide biosynthesis identifies putative molecular markers for Guillain-Barre syndrome. *J Clin Microbiol* **45**:2316-20.
52. **Gold, R., H. P. Hartung, and K. V. Toyka.** 2000. Animal models for autoimmune demyelinating disorders of the nervous system. *Mol Med Today* **6**:88-91.
53. **Gong, Y., Y. Tagawa, M. P. Lunn, W. Laroy, M. Heffer-Lauc, C. Y. Li, J. W. Griffin, R. L. Schnaar, and K. A. Sheikh.** 2002. Localization of major gangliosides in the PNS: implications for immune neuropathies. *Brain* **125**:2491-506.
54. **Goodyear, C. S., G. M. O'Hanlon, J. J. Plomp, E. R. Wagner, I. Morrison, J. Veitch, L. Cochrane, R. W. Bullens, P. C. Molenaar, J. Conner, and H. J. Willison.** 1999. Monoclonal antibodies raised against Guillain-Barre syndrome-

- associated *Campylobacter jejuni* lipopolysaccharides react with neuronal gangliosides and paralyze muscle-nerve preparations. *J Clin Invest* **104**:697-708.
55. **Govoni, V., E. Granieri, I. Casetta, M. R. Tola, E. Paolino, E. Fainardi, and V. C. Monetti.** 1996. The incidence of Guillain-Barre syndrome in Ferrara, Italy: is the disease really increasing? *J Neurol Sci* **137**:62-8.
  56. **Guerry, P., C. M. Szymanski, M. M. Prendergast, T. E. Hickey, C. P. Ewing, D. L. Pattarini, and A. P. Moran.** 2002. Phase variation of *Campylobacter jejuni* 81-176 lipooligosaccharide affects ganglioside mimicry and invasiveness in vitro. *Infect Immun* **70**:787-93.
  57. **Habib, I., R. Louwen, M. Uyttendaele, K. Houf, O. Vandenberg, E. E. Nieuwenhuis, W. G. Miller, A. van Belkum, and L. De Zutter.** 2009. Correlation between genotypic diversity, lipooligosaccharide gene locus class variation, and caco-2 cell invasion potential of *Campylobacter jejuni* isolates from chicken meat and humans: contribution to virulotyping. *Appl Environ Microbiol* **75**:4277-88.
  58. **Hadden, R. D., H. Karch, H. P. Hartung, J. Zielasek, B. Weissbrich, J. Schubert, A. Weishaupt, D. R. Cornblath, A. V. Swan, R. A. Hughes, and K. V. Toyka.** 2001. Preceding infections, immune factors, and outcome in Guillain-Barre syndrome. *Neurology* **56**:758-65.
  59. **Hafer-Macko, C., S. T. Hsieh, C. Y. Li, T. W. Ho, K. Sheikh, D. R. Cornblath, G. M. McKhann, A. K. Asbury, and J. W. Griffin.** 1996. Acute motor axonal neuropathy: an antibody-mediated attack on axolemma. *Ann Neurol* **40**:635-44.
  60. **Hafer-Macko, C. E., K. A. Sheikh, C. Y. Li, T. W. Ho, D. R. Cornblath, G. M. McKhann, A. K. Asbury, and J. W. Griffin.** 1996. Immune attack on the Schwann cell surface in acute inflammatory demyelinating polyneuropathy. *Ann Neurol* **39**:625-35.
  61. **Hahn, A. F.** 1996. Experimental allergic neuritis (EAN) as a model for the immune-mediated demyelinating neuropathies. *Rev Neurol (Paris)* **152**:328-32.
  62. **Halstead, S. K., G. M. O'Hanlon, P. D. Humphreys, D. B. Morrison, B. P. Morgan, A. J. Todd, J. J. Plomp, and H. J. Willison.** 2004. Anti-disialoside antibodies kill perisynaptic Schwann cells and damage motor nerve terminals via membrane attack complex in a murine model of neuropathy. *Brain* **127**:2109-23.

63. **Hardy, C. G., L. G. Lackey, J. Cannon, L. B. Price, and E. K. Silbergeld.** 2011. Prevalence of potentially neuropathic *Campylobacter jejuni* strains on commercial broiler chicken products. *Int J Food Microbiol* **145**:395-9.
64. **Harvey, R. B., R. E. Droleskey, C. L. Sheffield, T. S. Edrington, T. R. Callaway, R. C. Anderson, D. L. Drinnon, R. L. Ziprin, H. M. Scott, and D. J. Nisbet.** 2004. *Campylobacter* prevalence in lactating dairy cows in the United States. *J Food Prot* **67**:1476-9.
65. **Haubold, B., and R. R. Hudson.** 2000. LIAN 3.0: detecting linkage disequilibrium in multilocus data. *Linkage Analysis. Bioinformatics* **16**:847-8.
66. **Hayashi, T., and D. Faustman.** 1999. NOD mice are defective in proteasome production and activation of NF-kappaB. *Mol Cell Biol* **19**:8646-59.
67. **Ho, T. W., B. Mishu, C. Y. Li, C. Y. Gao, D. R. Cornblath, J. W. Griffin, A. K. Asbury, M. J. Blaser, and G. M. McKhann.** 1995. Guillain-Barre syndrome in northern China. Relationship to *Campylobacter jejuni* infection and anti-glycolipid antibodies. *Brain* **118 (Pt 3)**:597-605.
68. **Horrocks, S. M., R. C. Anderson, D. J. Nisbet, and S. C. Ricke.** 2009. Incidence and ecology of *Campylobacter jejuni* and coli in animals. *Anaerobe* **15**:18-25.
69. **Hotter, G. S., I. H. Li, and N. P. French.** 2010. Binary genotyping using lipooligosaccharide biosynthesis genes distinguishes between *Campylobacter jejuni* isolates within poultry-associated multilocus sequence types. *Epidemiol Infect* **138**:992-1003.
70. **Hughes, R. A., and D. R. Cornblath.** 2005. Guillain-Barre syndrome. *Lancet* **366**:1653-66.
71. **Hughes, R. A., R. D. Hadden, N. A. Gregson, and K. J. Smith.** 1999. Pathogenesis of Guillain-Barre syndrome. *J Neuroimmunol* **100**:74-97.
72. **Hughes, R. A., and J. H. Rees.** 1997. Clinical and epidemiologic features of Guillain-Barre syndrome. *J Infect Dis* **176 Suppl 2**:S92-8.

73. **Hughes, R. A., and J. H. Rees.** 1994. Guillain-Barre syndrome. *Curr Opin Neurol* **7**:386-92.
74. **Ilyas, A. A., H. J. Willison, R. H. Quarles, F. B. Jungalwala, D. R. Cornblath, B. D. Trapp, D. E. Griffin, J. W. Griffin, and G. M. McKhann.** 1988. Serum antibodies to gangliosides in Guillain-Barre syndrome. *Ann Neurol* **23**:440-7.
75. **Iovine, N. M.** 2013. Resistance mechanisms in *Campylobacter jejuni*. *Virulence* **4**.
76. **Islam, Z., M. Gilbert, Q. D. Mohammad, K. Klaij, J. Li, W. van Rijs, A. P. Tio-Gillen, K. A. Talukder, H. J. Willison, A. van Belkum, H. P. Endtz, and B. C. Jacobs.** 2012. Guillain-Barre Syndrome-Related *Campylobacter jejuni* in Bangladesh: Ganglioside Mimicry and Cross-Reactive Antibodies. *PLoS ONE* **7**:e43976.
77. **Islam, Z., A. van Belkum, A. J. Cody, H. Tabor, B. C. Jacobs, K. A. Talukder, and H. P. Endtz.** 2009. *Campylobacter jejuni* HS:23 and Guillain-Barre syndrome, Bangladesh. *Emerg Infect Dis* **15**:1315-7.
78. **Islam, Z., A. van Belkum, J. A. Wagenaar, A. J. Cody, A. G. de Boer, H. Tabor, B. C. Jacobs, K. A. Talukder, and H. P. Endtz.** 2009. Comparative genotyping of *Campylobacter jejuni* strains from patients with Guillain-Barre syndrome in Bangladesh. *PLoS One* **4**:e7257.
79. **Israeli, E., Agmon-Levin, Nancy.** 2012. Guillain-Barre Syndrome-A Classical Autoimmune Disease Triggered by Infection or Vaccination. *Clinical Reviews In Allergy and Immunology* **42**:121-130.
80. **Jacobs, B., A. van Belkum, and H. Endtz.** 2008. Guillain-Barre syndrome and *Campylobacter* Infection, p. 245-261, *Campylobacter*, 3 ed.
81. **Jay-Russell, M. T., R. E. Mandrell, J. Yuan, A. Bates, R. Manalac, J. Mohle-Boetani, A. Kimura, J. Lidgard, and W. G. Miller.** Using major outer membrane protein typing as an epidemiological tool to investigate outbreaks caused by milk-borne *Campylobacter jejuni* isolates in California. *J Clin Microbiol* **51**:195-201.
82. **Jin, T., L. S. Hu, M. Chang, J. Wu, B. Winblad, and J. Zhu.** 2007. Proteomic identification of potential protein markers in cerebrospinal fluid of GBS patients. *Eur J Neurol* **14**:563-8.

83. **Jolley, K. A., and M. C. Maiden.** BIGSdb: Scalable analysis of bacterial genome variation at the population level. *BMC Bioinformatics* **11**:595.
84. **Kaida, K., T. Ariga, and R. K. Yu.** 2009. Antiganglioside antibodies and their pathophysiological effects on Guillain-Barre syndrome and related disorders--a review. *Glycobiology* **19**:676-92.
85. **Kaida, K., D. Morita, M. Kanzaki, K. Kamakura, K. Motoyoshi, M. Hirakawa, and S. Kusunoki.** 2007. Anti-ganglioside complex antibodies associated with severe disability in GBS. *J Neuroimmunol* **182**:212-8.
86. **Kaida, K., D. Morita, M. Kanzaki, K. Kamakura, K. Motoyoshi, M. Hirakawa, and S. Kusunoki.** 2004. Ganglioside complexes as new target antigens in Guillain-Barre syndrome. *Ann Neurol* **56**:567-71.
87. **Kalischuk, L. D., and A. G. Buret.** 2010. A role for *Campylobacter jejuni*-induced enteritis in inflammatory bowel disease? *Am J Physiol Gastrointest Liver Physiol* **298**:G1-9.
88. **Kapperud, G., E. Skjerve, N. H. Bean, S. M. Ostroff, and J. Lassen.** 1992. Risk factors for sporadic *Campylobacter* infections: results of a case-control study in southeastern Norway. *J Clin Microbiol* **30**:3117-21.
89. **Kawamura, N., H. Piao, M. Minohara, T. Matsushita, S. Kusunoki, H. Matsumoto, K. Ikenaka, Y. Mizunoe, and J. Kira.** 2011. *Campylobacter jejuni* DNA-binding protein from starved cells in Guillain-Barre syndrome patients. *J Neuroimmunol* **240-241**:74-8.
90. **Koga, M., M. Gilbert, J. Li, S. Koike, M. Takahashi, K. Furukawa, K. Hirata, and N. Yuki.** 2005. Antecedent infections in Fisher syndrome: a common pathogenesis of molecular mimicry. *Neurology* **64**:1605-11.
91. **Konkel, M. E., M. R. Monteville, V. Rivera-Amill, and L. A. Joens.** 2001. The pathogenesis of *Campylobacter jejuni*-mediated enteritis. *Curr Issues Intest Microbiol* **2**:55-71.
92. **Kuroki, S., T. Saida, M. Nukina, T. Haruta, M. Yoshioka, Y. Kobayashi, and H. Nakanishi.** 1993. *Campylobacter jejuni* strains from patients with Guillain-Barre syndrome belong mostly to Penner serogroup 19 and contain beta-N-acetylglucosamine residues. *Ann Neurol* **33**:243-7.

93. **Lee, K. Y.** 2012. Anti-GQ1b-negative Miller Fisher syndrome after *Campylobacter jejuni* enteritis. *Pediatr Neurol* **47**:213-5.
94. **Li, C. Y., P. Xue, W. Q. Tian, R. C. Liu, and C. Yang.** 1996. Experimental *Campylobacter jejuni* infection in the chicken: an animal model of axonal Guillain-Barre syndrome. *J Neurol Neurosurg Psychiatry* **61**:279-84.
95. **Lin, T. M., S. S. Lee, R. T. Lin, C. S. Lai, and S. D. Lin.** 2006. Guillain-Barre syndrome following facial bone fracture. *J Plast Reconstr Aesthet Surg* **59**:543-6.
96. **Linton, D., R. J. Owen, and J. Stanley.** 1996. Rapid identification by PCR of the genus *Campylobacter* and of five *Campylobacter* species enteropathogenic for man and animals. *Res Microbiol* **147**:707-18.
97. **Lo, Y. L.** 2007. Clinical and immunological spectrum of the Miller Fisher syndrome. *Muscle Nerve* **36**:615-27.
98. **Mansfield, L. S., J. A. Bell, D. L. Wilson, A. J. Murphy, H. M. Elsheikha, V. A. Rathinam, B. R. Fierro, J. E. Linz, and V. B. Young.** 2007. C57BL/6 and congenic interleukin-10-deficient mice can serve as models of *Campylobacter jejuni* colonization and enteritis. *Infect Immun* **75**:1099-115.
99. **Mansfield, L. S., J. S. Patterson, B. R. Fierro, A. J. Murphy, V. A. Rathinam, J. J. Kopper, N. I. Barbu, T. J. Onifade, and J. A. Bell.** 2008. Genetic background of IL-10(-/-) mice alters host-pathogen interactions with *Campylobacter jejuni* and influences disease phenotype. *Microb Pathog* **45**:241-57.
100. **Markoula, S., S. Giannopoulos, I. Sarmas, S. Tzavidi, A. P. Kyritsis, and G. Lagos.** 2007. Guillain-Barre syndrome in northwest Greece. *Acta Neurol Scand* **115**:167-73.
101. **Meinersmann, R. J., L. O. Hessel, P. I. Fields, and K. L. Hiatt.** 1997. Discrimination of *Campylobacter jejuni* isolates by *fla* gene sequencing. *J Clin Microbiol* **35**:2810-4.
102. **Meinersmann, R. J., R. W. Phillips, K. L. Hiatt, and P. Fedorka-Cray.** 2005. Differentiation of *Campylobacter* populations as demonstrated by flagellin short variable region sequences. *Appl Environ Microbiol* **71**:6368-74.

103. **Moran, A. P., H. Annuk, and M. M. Prendergast.** 2005. Antibodies induced by ganglioside-mimicking *Campylobacter jejuni* lipooligosaccharides recognise epitopes at the nodes of Ranvier. *J Neuroimmunol* **165**:179-85.
104. **Murgatroyd, C., D. Bilko, and D. Spengler.** 2006. Isolation of high-quality DNA for genotyping from feces of rodents. *Anal Biochem* **348**:160-2.
105. **Nachamkin, I., B. M. Allos, and T. Ho.** 1998. *Campylobacter* species and Guillain-Barre syndrome. *Clin Microbiol Rev* **11**:555-67.
106. **Nye, T. M., P. Lio, and W. R. Gilks.** 2006. A novel algorithm and web-based tool for comparing two alternative phylogenetic trees. *Bioinformatics* **22**:117-9.
107. **O'Hanlon, G. M., G. J. Paterson, J. Veitch, G. Wilson, and H. J. Willison.** 1998. Mapping immunoreactive epitopes in the human peripheral nervous system using human monoclonal anti-GM1 ganglioside antibodies. *Acta Neuropathol* **95**:605-16.
108. **Oh, S. J., C. LaGanke, and G. C. Claussen.** 2001. Sensory Guillain-Barre syndrome. *Neurology* **56**:82-6.
109. **Overell, J. R., and H. J. Willison.** 2005. Recent developments in Miller Fisher syndrome and related disorders. *Curr Opin Neurol* **18**:562-6.
110. **Pandey, J. P., and C. A. Vedeler.** 2003. Immunoglobulin KM genes in Guillain-Barre syndrome. *Neurogenetics* **4**:147-9.
111. **Parker, C. T., M. Gilbert, N. Yuki, H. P. Endtz, and R. E. Mandrell.** 2008. Characterization of lipooligosaccharide-biosynthetic loci of *Campylobacter jejuni* reveals new lipooligosaccharide classes: evidence of mosaic organizations. *J Bacteriol* **190**:5681-9.
112. **Parker, C. T., S. T. Horn, M. Gilbert, W. G. Miller, D. L. Woodward, and R. E. Mandrell.** 2005. Comparison of *Campylobacter jejuni* lipooligosaccharide biosynthesis loci from a variety of sources. *J Clin Microbiol* **43**:2771-81.
113. **Phongsisay, V., V. N. Perera, and B. N. Fry.** 2006. Exchange of lipooligosaccharide synthesis genes creates potential Guillain-Barre syndrome-inducible strains of *Campylobacter jejuni*. *Infect Immun* **74**:1368-72.

114. **Piao, H., M. Minohara, N. Kawamura, W. Li, T. Matsushita, R. Yamasaki, Y. Mizunoe, and J. Kira.** 2011. Tissue binding patterns and in vitro effects of *Campylobacter jejuni* DNA-binding protein from starved cells. *Neurochem Res* **36**:58-66.
115. **Piao, H., M. Minohara, N. Kawamura, W. Li, Y. Mizunoe, F. Umehara, Y. Goto, S. Kusunoki, T. Matsushita, K. Ikenaka, T. Maejima, J. Nabekura, R. Yamasaki, and J. Kira.** 2010. Induction of paranodal myelin detachment and sodium channel loss in vivo by *Campylobacter jejuni* DNA-binding protein from starved cells (C-Dps) in myelinated nerve fibers. *J Neurol Sci* **288**:54-62.
116. **Pithadia, A. B., and N. Kakadia.** 2010. Guillain-Barre syndrome (GBS). *Pharmacol Rep* **62**:220-32.
117. **Plomp, J. J., P. C. Molenaar, G. M. O'Hanlon, B. C. Jacobs, J. Veitch, M. R. Daha, P. A. van Doorn, F. G. van der Meche, A. Vincent, B. P. Morgan, and H. J. Willison.** 1999. Miller Fisher anti-GQ1b antibodies: alpha-latrotoxin-like effects on motor end plates. *Ann Neurol* **45**:189-99.
118. **Porcelli, S. A., and R. L. Modlin.** 1999. The CD1 system: antigen-presenting molecules for T cell recognition of lipids and glycolipids. *Annu Rev Immunol* **17**:297-329.
119. **Poropatich, K. O., C. L. Walker, and R. E. Black.** 2010. Quantifying the association between *Campylobacter* infection and Guillain-Barre syndrome: a systematic review. *J Health Popul Nutr* **28**:545-52.
120. **Prendergast, M. M., A. J. Lastovica, and A. P. Moran.** 1998. Lipopolysaccharides from *Campylobacter jejuni* O:41 strains associated with Guillain-Barre syndrome exhibit mimicry of GM1 ganglioside. *Infect Immun* **66**:3649-55.
121. **Prendergast, M. M., D. R. Tribble, S. Baqar, D. A. Scott, J. A. Ferris, R. I. Walker, and A. P. Moran.** 2004. In vivo phase variation and serologic response to lipooligosaccharide of *Campylobacter jejuni* in experimental human infection. *Infect Immun* **72**:916-22.
122. **Price, L. B., A. Roess, J. P. Graham, S. Baqar, R. Vailes, K. A. Sheikh, and E. Silbergeld.** 2007. Neurologic symptoms and neuropathologic antibodies in poultry workers exposed to *Campylobacter jejuni*. *J Occup Environ Med* **49**:748-55.

123. **Quinones, B., M. R. Guilhabert, W. G. Miller, R. E. Mandrell, A. J. Lastovica, and C. T. Parker.** 2008. Comparative genomic analysis of clinical strains of *Campylobacter jejuni* from South Africa. *PLoS One* **3**:e2015.
124. **Revez, J., and M. L. Hanninen.** 2012. Lipooligosaccharide locus classes are associated with certain *Campylobacter jejuni* multilocus sequence types. *Eur J Clin Microbiol Infect Dis* **31**:2203-9.
125. **Richards, V. P., T. Lefebure, P. D. Pavinski Bitar, and M. J. Stanhope.** 2013. Comparative characterization of the virulence gene clusters (lipooligosaccharide [LOS] and capsular polysaccharide [CPS]) for *Campylobacter coli*, *Campylobacter jejuni* subsp. *jejuni* and related *Campylobacter* species. *Infect Genet Evol* **14**:200-13.
126. **Rostami, A. M.** 1997. P2-reactive T cells in inflammatory demyelination of the peripheral nerve. *J Infect Dis* **176 Suppl 2**:S160-3.
127. **Sahin, O., T. Y. Morishita, and Q. Zhang.** 2002. *Campylobacter* colonization in poultry: sources of infection and modes of transmission. *Anim Health Res Rev* **3**:95-105.
128. **Salloway, S., L. A. Mermel, M. Seamans, G. O. Aspinall, J. E. Nam Shin, L. A. Kurjanczyk, and J. L. Penner.** 1996. Miller-Fisher syndrome associated with *Campylobacter jejuni* bearing lipopolysaccharide molecules that mimic human ganglioside GD3. *Infect Immun* **64**:2945-9.
129. **Salmon, D. A., M. Proschan, R. Forshee, P. Gargiullo, W. Bleser, D. R. Burwen, F. Cunningham, P. Garman, S. K. Greene, G. M. Lee, C. Vellozzi, W. K. Yih, B. Gellin, and N. Lurie.** 2013. Association between Guillain-Barre syndrome and influenza A (H1N1) 2009 monovalent inactivated vaccines in the USA: a meta-analysis. *Lancet*.
130. **Salomon, B., L. Rhee, H. Bour-Jordan, H. Hsin, A. Montag, B. Soliven, J. Arcella, A. M. Girvin, J. Padilla, S. D. Miller, and J. A. Bluestone.** 2001. Development of spontaneous autoimmune peripheral polyneuropathy in B7-2-deficient NOD mice. *J Exp Med* **194**:677-84.
131. **Sanad, Y. M., G. Closs, Jr., A. Kumar, J. T. Lejeune, and G. Rajashekara.** 2013. Molecular epidemiology and public health relevance of *campylobacter* isolated from dairy cattle and European starlings in ohio, USA. *Foodborne Pathog Dis* **10**:229-36.

132. **Sellon, R. K., S. Tonkonogy, M. Schultz, L. A. Dieleman, W. Grenther, E. Balish, D. M. Rennick, and R. B. Sartor.** 1998. Resident enteric bacteria are necessary for development of spontaneous colitis and immune system activation in interleukin-10-deficient mice. *Infect Immun* **66**:5224-31.
133. **Semchenko, E. A., C. J. Day, J. C. Wilson, I. D. Grice, A. P. Moran, and V. Korolik.** 2010. Temperature-dependent phenotypic variation of *Campylobacter jejuni* lipooligosaccharides. *BMC Microbiol* **10**:305.
134. **Shahrizaila, N., and N. Yuki.** 2011. Antiganglioside antibodies in Guillain-Barre syndrome and its related conditions. *Expert Rev Neurother* **11**:1305-13.
135. **Shahrizaila, N., and N. Yuki.** 2010. Guillain-barre syndrome animal model: the first proof of molecular mimicry in human autoimmune disorder. *J Biomed Biotechnol* **2011**:829129.
136. **Shui, I. M., M. D. Rett, E. Weintraub, M. Marcy, A. A. Amato, S. I. Sheikh, D. Ho, G. M. Lee, and W. K. Yih.** 2012. Guillain-Barre syndrome incidence in a large United States cohort (2000-2009). *Neuroepidemiology* **39**:109-15.
137. **Snyder, L. A., V. Rismondo, and N. R. Miller.** 2009. The Fisher variant of Guillain-Barre syndrome (Fisher syndrome). *J Neuroophthalmol* **29**:312-24.
138. **Suerbaum, S., M. Lohrengel, A. Sonnevend, F. Ruberg, and M. Kist.** 2001. Allelic diversity and recombination in *Campylobacter jejuni*. *J Bacteriol* **183**:2553-9.
139. **Takahashi, M., M. Koga, K. Yokoyama, and N. Yuki.** 2005. Epidemiology of *Campylobacter jejuni* isolated from patients with Guillain-Barre and Fisher syndromes in Japan. *J Clin Microbiol* **43**:335-9.
140. **Tam, C. C., L. C. Rodrigues, and S. J. O'Brien.** 2003. Guillain-Barre syndrome associated with *Campylobacter jejuni* infection in England, 2000-2001. *Clin Infect Dis* **37**:307-10.
141. **Tam, C. C., L. C. Rodrigues, I. Petersen, A. Islam, A. Hayward, and S. J. O'Brien.** 2006. Incidence of Guillain-Barre syndrome among patients with *Campylobacter* infection: a general practice research database study. *J Infect Dis* **194**:95-7.

142. **Tan, I. L., T. Ng, and S. Vucic.** 2010. Severe Guillain-Barre syndrome following head trauma. *J Clin Neurosci* **17**:1452-4.
143. **Tribble, D. R., S. Baqar, M. P. Carmolli, C. Porter, K. K. Pierce, K. Sadigh, P. Guerry, C. J. Larsson, D. Rockabrand, C. H. Ventone, F. Poly, C. E. Lyon, S. Dakdouk, A. Fingar, T. Gilliland, P. Daunais, E. Jones, S. Rymarchyk, C. Huston, M. Darsley, and B. D. Kirkpatrick.** 2009. *Campylobacter jejuni* strain CG8421: a refined model for the study of *Campylobacteriosis* and evaluation of *Campylobacter* vaccines in human subjects. *Clin Infect Dis* **49**:1512-9.
144. **Tsang, R. S., G. Figueroa, L. Bryden, and L. Ng.** 2001. Flagella as a potential marker for *Campylobacter jejuni* strains associated with Guillain-Barre syndrome. *J Clin Microbiol* **39**:762-4.
145. **Van Koningsveld, R., P. I. Schmitz, C. W. Ang, J. Groen, A. D. Osterhaus, F. G. Van der Meche, and P. A. Van Doorn.** 2002. Infections and course of disease in mild forms of Guillain-Barre syndrome. *Neurology* **58**:610-4.
146. **Vegosen, L., M. F. Davis, E. Silbergeld, P. N. Breysse, J. Agnew, G. Gray, L. B. Freeman, and F. Kamel.** 2012. Neurologic symptoms associated with cattle farming in the agricultural health study. *J Occup Environ Med* **54**:1253-8.
147. **Vucic, S., M. C. Kiernan, and D. R. Cornblath.** 2009. Guillain-Barre syndrome: an update. *J Clin Neurosci* **16**:733-41.
148. **Walling, A. D., and G. Dickson.** 2013. Guillain-barre syndrome. *Am Fam Physician* **87**:191-7.
149. **Walsh, F. S., M. Cronin, S. Koblar, P. Doherty, J. Winer, A. Leon, and R. A. Hughes.** 1991. Association between glycoconjugate antibodies and *Campylobacter* infection in patients with Guillain-Barre syndrome. *J Neuroimmunol* **34**:43-51.
150. **Willison, H. J.** 2005. The immunobiology of Guillain-Barre syndromes. *J Peripher Nerv Syst* **10**:94-112.
151. **Willison, H. J., and G. M. O'Hanlon.** 1999. The immunopathogenesis of Miller Fisher syndrome. *J Neuroimmunol* **100**:3-12.

152. **Willison, H. J., and J. J. Plomp.** 2008. Anti-ganglioside antibodies and the presynaptic motor nerve terminal. *Ann N Y Acad Sci* **1132**:114-23.
153. **Winer, J. B.** 2011. Guillain-Barre syndrome: clinical variants and their pathogenesis. *J Neuroimmunol* **231**:70-2.
154. **Winer, J. B.** 2001. Guillain Barre syndrome. *Mol Pathol* **54**:381-5.
155. **Yazdanbakhsh, M., P. G. Kremsner, and R. van Ree.** 2002. Allergy, parasites, and the hygiene hypothesis. *Science* **296**:490-4.
156. **Young, K. T., L. M. Davis, and V. J. Dirita.** 2007. *Campylobacter jejuni*: molecular biology and pathogenesis. *Nat Rev Microbiol* **5**:665-79.
157. **Yu, R. K., T. Ariga, S. Usuki, and K. Kaida.** 2011. Pathological roles of ganglioside mimicry in Guillain-Barre syndrome and related neuropathies. *Adv Exp Med Biol* **705**:349-65.
158. **Yuki, N.** 2005. Carbohydrate mimicry: a new paradigm of autoimmune diseases. *Curr Opin Immunol* **17**:577-82.
159. **Yuki, N.** 2007. Ganglioside mimicry and peripheral nerve disease. *Muscle Nerve* **35**:691-711.
160. **Yuki, N.** 2010. Human gangliosides and bacterial lipo-oligosaccharides in the development of autoimmune neuropathies. *Methods Mol Biol* **600**:51-65.
161. **Yuki, N.** 2001. Infectious origins of, and molecular mimicry in, Guillain-Barre and Fisher syndromes. *Lancet Infect Dis* **1**:29-37.
162. **Yuki, N.** 1997. Molecular mimicry between gangliosides and lipopolysaccharides of *Campylobacter jejuni* isolated from patients with Guillain-Barre syndrome and Miller Fisher syndrome. *J Infect Dis* **176 Suppl 2**:S150-3.
163. **Yuki, N., and H. P. Hartung.** 2012. Guillain-Barre syndrome. *N Engl J Med* **366**:2294-304.

164. **Yuki, N., and S. Kuwabara.** 2007. Axonal Guillain-Barre syndrome: carbohydrate mimicry and pathophysiology. *J Peripher Nerv Syst* **12**:238-49.
165. **Yuki, N., K. Susuki, M. Koga, Y. Nishimoto, M. Odaka, K. Hirata, K. Taguchi, T. Miyatake, K. Furukawa, T. Kobata, and M. Yamada.** 2004. Carbohydrate mimicry between human ganglioside GM1 and *Campylobacter jejuni* lipooligosaccharide causes Guillain-Barre syndrome. *Proc Natl Acad Sci U S A* **101**:11404-9.
166. **Yuki, N., T. Taki, F. Inagaki, T. Kasama, M. Takahashi, K. Saito, S. Handa, and T. Miyatake.** 1993. A bacterium lipopolysaccharide that elicits Guillain-Barre syndrome has a GM1 ganglioside-like structure. *J Exp Med* **178**:1771-5.
167. **Yuki, N., M. Yamada, M. Koga, M. Odaka, K. Susuki, Y. Tagawa, S. Ueda, T. Kasama, A. Ohnishi, S. Hayashi, H. Takahashi, M. Kamijo, and K. Hirata.** 2001. Animal model of axonal Guillain-Barre syndrome induced by sensitization with GM1 ganglioside. *Ann Neurol* **49**:712-20.
168. **Yuki, N., H. Yoshino, S. Sato, and T. Miyatake.** 1990. Acute axonal polyneuropathy associated with anti-GM1 antibodies following *Campylobacter* enteritis. *Neurology* **40**:1900-2.
169. **Zhang, M., L. He, Q. Li, H. Sun, Y. Gu, Y. You, F. Meng, and J. Zhang.** 2010. Genomic characterization of the Guillain-Barre syndrome-associated *Campylobacter jejuni* ICDCCJ07001 Isolate. *PLoS One* **5**:e15060.